043
JAI
7525

INSTABILITIES IN IONOSPHERIC PLASMA

A THESIS
SUBMITTED FOR THE DEGREE OF
DOCTOR OF PHILOSOPHY
TO THE

GUJARAT UNIVERSITY

BY
RAJ KUMAR JAIN

MAY 1976

043
B7525

PHYSICAL RESEARCH LABORATORY
AHMEDABAD 380 009
INDIA

NATIONAL RESEARCH LABORATORY
LIBRARY
Cl. No.
Date
Acc. No.
Price

DEDICATED

TO

MY ELDEST BROTHER

RAJENDRA KUMAR

AND

MY SISTER-IN-LAW

SMT. BIMALA DEVI

CERTIFICATE

I hereby declare that the work presented in this thesis is original and has not formed the basis for the award of any degree or diploma by any University or Institution.

R K Jain

RAJ KUMAR JAIN

(Author)

Certified

A.C. Das

ANATH CHANDRA DAS

(Professor Incharge)

May 21, 1976

STATEMENT

The ionospheric plasma under different natural conditions, exhibits various natural perturbations, termed as 'irregularities', and associated irregular phenomena, such as sporadic-E, spread-F, etc.. All these phenomena seem to play an important role in long distance communication and broadcasting and this is why the study of ionospheric plasma has become more important. There is, of course, an academic interest in the understanding of physical processes of plasma in the ionosphere which can produce so many interesting and puzzling phenomena. In the present work we are interested only on those aspects of irregular phenomana observed within the equatorial ionosphere which manifest themselves as wave like perturbations (irregularities) of ionisation density and electric fields during the transmission of radio signals to or from the ground stations and spacecrafts.

A theoretical study of some of the instabilities related to ionospheric plasma has been made in this thesis, with a view to understand the generation mechanisms of the ionization density irregularities and associated phenomena. The ionospheric plasma which is a weakly ionized inhomogeneous plasma embedded in orthogonal d.c. electric and magnetic fields (at the equator), can become unstable against self-excitation of a large variety of waves and natural modes of oscillations. These natural modes may be driven unstable due to a number of plasma-instabilities operating individually or simultaneously.

It is widely recognized that the unstable plasma in nature

state arising due to preponderance of various modes under different conditions, in which the energy supply to a plasma may be in harmony with energy dissipation from it. An extensive study of linear and nonlinear theories of these instabilities is important from the point of view of not only gaining a clear understanding of the basic behaviour of plasma instabilities, but also of applying the results in understanding of detailed structures of the irregularities observed.

Our principal objective is to study the generation mechanisms of the irregularities which can satisfactorily explain some of their important basic characteristics observed during both day and night time in the E-and F-regions of the equatorial ionosphere. With the advent of backscatter radar and in-situ rocket and satellite measurements, the irregularities with various properties have been observed over a wide range of wavelengths. Based on their spectral characteristics, their spatial extents and the existing conditions in the ionosphere, the electrojet (E-region) irregularities are distinctly classified as (1) Type I or Types Ms and Ss and (2) Type II or Types Mc and Sc irregularities. The equatorial F-region irregularities which are observed at night only, show wavelike structures with scale sizes ranging from a few meters to a few kms or even more.

The author has studied mainly three kinds of low frequency electrostatic instabilities, namely (i) Cross-Field or Gradient-Drift, (ii) Two-Stream and (iii) Gravitation-induced Rayleigh-Taylor instabilities. The investigation of these instabilities

which case the amplitude of perturbation is sufficiently small and therefore, it does not deal with very large amplitude perturbations.

The first chapter contains a preliminary introduction to the ionospheric plasma and a summary of the related experimental observations of the irregularities in the equatorial E-and F-regions. This also includes a brief description of the specific physical mechanisms of the instabilities concerned, in terms of basic plasma physics concepts. The chapter is concluded with the motivation of the studies made in the thesis.

The second chapter deals with the investigation of the Cross-field ($\underline{E} \times \underline{B}$) instability which is believed to be the potential candidate as the source of the Types II, Mc and Sc irregularities occuring in the E-region. This work is, however, confined mainly to the linear treatment of the theory. This study was, in fact, completed a long time ago with a primary objective to consider, for the first time, the effects of both the primary horizontal and vertical polarization electric fields together (through a relation valid for equatorial ionosphere) which were not taken into account by any earlier workers. Furthermore, the treatment of the theory developed here, is more general because it includes the propagation of the waves along vertical direction also.

The dependence of growth rate and scale size on the variation in the horizontal electric field, background electron density and background density gradient is investigated further.

field in the formation of smaller wavelength and fastest growing irregularities. The theoretical results are then applied to the equatorial E-region by considering an observed electron density profile. The chapter ends with the comparison of the results of the theory with the observations of Types II, Mc and Sc irregularities.

In the third chapter, the author discusses a special class of coherent, weakly, nonlinear type I modes in the equatorial electrojet, which are believed to be excited by two-stream instability. Including ion viscous effects which are important for shorter wavelength modes and introducing a dimensionless independent variable in the wave frame, the partial differential equations describing one-dimensional Type I modes are converted into an ordinary differential equation. An amplitude dependent nonlinear dispersion relation for such nonlinear modes is found for weak nonlinearity. The stability of these nonlinear modes against long wavelength, slowly varying large amplitude perturbations is further examined. The study of the formation of modulational envelope solitons in the adiabatical non-stationary case is also carried out.

We have made further investigation in support of our analytical calculations by solving numerically the exact set of nonlinear basic equations of Type I modes which otherwise, are intractable by conventional analytical methods. Some observed features of Types I, Ms and Ss irregularities are found to be consistent and in good agreement with the predictions of the

Low frequency incompressible waves in the equatorial F-region, which seem to be responsible for equatorial spread-F, are studied in Chapter IV. In this chapter, the author has made an investigation of the nonlinear evolution of the gravitation-induced Rayleigh-Taylor (R-T) instability which may be one of the possible mechanisms for the generation of spread-F irregularities. Following the method similar to one that is described in Chapter III and retaining the complete ion inertial term, ion neutral collisions and ion finite Larmor radius corrections, we have looked for stabilization mechanism for R-T modes.

The linear theory is first briefly outlined in this chapter and the linear results are then compared with those obtained by earlier workers. The existence of coherent, weakly nonlinear, almost sinusoidal stationary solutions to the nonlinear equations describing R-T modes, the shapes in which these modes would travel in the F-region and the physical conditions satisfied by such nonlinear modes are discussed further in detail. The theoretical results in this chapter are then finally compared with the observations of equatorial spread-F irregularities in the ionosphere.

The last chapter presents a synoptic view of the whole work along with a short investigation of how the instability mechanisms discribed here, can support the formation of equatorial sporadic-E (E_{sq}) and spread-F, the disappearance of E_{sq} and its correlation with electrojet. The limitations of these investigations and the

scope for further work are pointed out towards the end of the thesis.

(Professor A.C. Das)

(R.K. Jain)

May 21, 1976

ACKNOWLEDGEMENTS

The author is sincerely grateful to his thesis adviser, Professor Anath C. Das, who introduced him to the subject of Plasma Physics and at various stages of the work presented here, offered constructive guidance. Countless discussions and close interaction with him were invaluable and of great help during all phases of this work. The author owes a special debt of thanks for his zeal in reading the manuscript critically and with the greatest care. His magnanimous attitude and stimulating counsel during the entire research period are profoundly appreciated.

I would like to express my sincere thanks to Professor S.P. Pandya for encouraging me to pursue this thesis topic. I also express my sincere and deep gratitude to Professor P.K. Kaw with whom I had the benefit of stimulating and close interaction. The invaluable discussions with him and his very helpful comments, during the course of the whole work, were of immense importance and are greately appreciated.

It is a great pleasure to thank the members of my advisory committee, Professor R.K. Varma, Professor K.H. Bhatt and Professor B.H. Subbaraya, for their helpful suggestions and useful discussions.

I wish to thank Professor S. Prakash and Dr. S.P. Gupta for supplying me the Thumba rocket data needed for computations.

The author wishes to acknowledge gratefully the considerable assistance of Dr. M.R. Shivaraman, Mr. B.G. Anandarao

manuscript carefully.

I gratefully acknowledge the useful and helpful discussions with Professor (Miss) B. Buti, Professor R. Pratap, Dr. A.K. Sundaram, Dr. Y.C. Saxena, Dr. V.H. Kulkarni, Dr. N. K. Vyas and Mr. P.K. Chaturvedi, during the different stages of the thesis work. I also appreciate the enthusiastic cooperation and long support that graduate students of Plasma Physics Group have given me in some way or the other.

The help of Dr. Koneru S. Rao and Dr. D.R. Kulkarni in solving computational problems, was invaluable. I express my sincere thanks to them. I also acknowledge the general cooperation of the personnel, especially of Mr. P.S. Shah, of the PRL Computer Centre.

I am very much thankful to Dr. Dinesh M. Patel for his general helpful attitude during the entire period of research work.

The author is greately indebted to Dr.V.R. Rao, Dr. M.S. Narayanan, Dr. M.R. Shivaraman, Mr. P.S. Sehra and Mr. S.M. Bhandari for their inspiration throughout the period of this thesis work. I wish to express my deep sense of gratitude, especially to Dr. V.R. Rao, Dr. M.R. Shivaraman and Mr. P.S. Sehra who consistently encouraged and consoled me in my efforts and often turned despair into renewed hope.

I sincerely thank Mr. P.P. Narayanan for his neat, excellent and prompt typing of this thesis. I also thank Mr.K. Venugopalan for designing the first page of the thesis. My thanks are also due to Mr. Ganshyam Patel for speedy cyclostyling of

The assistance of Drafting Section, Photography Section and Library is appreciated.

It would be impossible to acknowledge adequately all my friends and other persons who have taken keen interest and have helped me directly or indirectly during my tenure as a Ph.D. student. They all deserve at least my explicit sincere thanks.

Whatever value this work may have, however, must be attributed in large part to my parents, brothers and cousins, who right from the beginning helped me in cultivating an interest for learning. Last, but not the least, I greately appreciate the enthusiastic cooperation, consistent encouragement, remarkable patience and moral support of my wife, Urmi R. Jain.

R K Jain

(R.K. JAIN)

TABLE OF CONTENTS

	Page
STATEMENT	i
ACKNOWLEDGEMENTS	vii
CHAPTER I INTRODUCTION	1-70
1.1 Objectives	1
1.11 Importance of Ionospheric Plasma Research	2
1.12 Main Purpose of the Investigation	6
1.2 A Short Description of Ionospheric Plasma, its Structure and Dynamics of its Constituents	7
1.21 Ionosphere as a Plasma Medium	7
1.22 Motion of the Charged Particles in Ionospheric Regions of Interest	9
a) Transport Processes	11
b) The Mean Drift Velocities of the Particles	13
c) Currents and Conductivities	15
d) Collision Frequencies of Charged Particles	18
1.23 Importance of Equatorial Ionospheric studies with the Emphasis Mainly on the E-and F-Regions	20
a) Equatorial Electrojet	22
b) Equatorial Sporadic-E (E_{sq})	24
c) Equatorial Spread-F	26
1.3 Observations of Ionization Density Irregularities in the Equatorial E-and F-Regions	29
1.31 E-Region Irregularities	30
a) Type I Irregularities	32
b) Type II Irregularities	35

c) In-Situ Rocket Irregularity Observations 39

1.32 F-Region Irregularities 42

1.4 Possible Instability Mechanisms Associated with the E-and F-Regions Irregularities 49

a) Cross-Field or Gradient-Drift Instability 53

b) Two-Stream Instability 57

c) Rayleigh-Taylor Instability 60

1.5 Statement of the Present Work 64

CHAPTER II LOW FREQUENCY LINEAR GRADIENT-DRIFT OR CROSS-FIELD INSTABILITY IN THE EQUATORIAL E-REGION 71-138

2.1 Introduction 71

2.2 Basic Equations and Assumptions 83

2.3 Zeroth Order Equilibrium Model 87

2.4 Instability Analysis-Dispersion Relation 92

2.5 Growth Rates and Scale Sizes of the Perturbations 99

2.6 Application to an Equatorial Ionospheric E-Region 108

2.7 The Effect of the Electric-Field Strength and the Background Electron Density Gradient on the Formation of Irregularities at a Particular Height 117

a) The Effect of the Electric Field Strength 117

b) The Effect of the Background Electron Gradient or Density Gradient (i.e. 'a') 118

2.8 Discussions of the Results and their Comparison with the Observations 122

2.9 Conclusions 136

CHAPTER III NONLINEAR TWO-STREAM INSTABILITY MECHANISM ASSOCIATED WITH TYPE I IRREGULARITIES 139-184

3.1 Introduction 139

3.2 Basic Equations and Quasilinear Modification of Polarization Electric Field 158

3.3 Wave Equation for Nonlinear Type I Modes 162

3.4 Solutions of the Nonlinear Wave Equation and Nonlinear Dispersion Relation 163

3.41 Linear Type I Modes 163

3.42 Nonlinear Type I Modes 165

3.5 Stability Criteria of Nonlinear Stationary Waves 167

3.6 Numerical Calculations and Results 170

a) Numerical solutions of the Exact (Full) Nonlinear Wave Equation 171

b) Space and Time Dependences of Solutions of the Exact Set of Basic Equations 173

3.7 Discussions and Conclusions 177

CHAPTER IV LOW FREQUENCY RAYLEIGH-TAYLOR INSTABILITY AND THE EQUATORIAL SPREAD-F 185-222

4.1 Introduction 185

4.2 Basic Equations 195

4.21 Assumptions and Approximations Used 196

4.22 Equilibrium Configuration of Equatorial F-Region Plasma 197

4.3 Linear Theory 199

4.4 Wave Equation for Nonlinear R-T Modes 203

4.5 Nonlinear Solutions of the Wave Equation Describing Nonlinear R-T Modes 208

4.6 Discussions of Results and Their Relevance to the Observations of Spread-F Irregularities 214

4.7 Conclusions 221

CHAPTER V SUMMARY, LIMITATIONS AND SCOPE FOR FURTHER WORK 223-235

5.1 A Synoptic View (Summary) of the Work Done 224

5.2 Limitations and Scope for Further Studies 231

BIBILIOGRAPHY 236

CHAPTER I

INTRODUCTION

1.1 Objectives:

The physics of plasma is an extremely important discipline for understanding the different processes of the universe, because 99.9% of the apparent universe exists in the plasma state. However, there is very little in the state of natural plasma on the earth, as the low temperature and high density of the earth and its near atmosphere preclude the existence of plasma. This only means that the plasma must be created in the laboratory by experimental means so as to study its property and different physical processes occuring in it. However, the study of space plasma phenomena is difficult in a laboratory where the simulation of such plasmas is not always possible because of small dimensions of plasma system in the laboratory.

The direct experimentation wherever possible, with naturally occuring space plasmas and the investigation of the associated phenomena appear to be a more justifiable approach to the study of plasma physics, in particular and to the understanding of nature, in general. The earth's upper atmosphere known as ionosphere, is one of such natural plasma laboratories which is easily accessible to a plasma physicist.

1.11 Importance of Ionospheric Plasma Research:

Throughout the history, every advance of mankind in the extension of his world has brought with it problems of communication. Today, more than ever, man's exploration of unknown territories depends upon communication. Each advance of man into space must be preceded by remotely operated unmanned probes and by the transmission of a vast quantities of informations concerning the space environments. With the development of rockets, satellites and other space probes, our knowledge of space environment in the immediate vicinity of the sun and its planets has progressed by leaps and bounds. Our knowledge of plasma physics, in general and the atmospheric phenomena, in particular, have played a major and important role in radio communication studies.

The earth's upper atmosphere is the region wherein the ionizing radiations from the sun have caused sufficient ionization for the reason to be termed as partially ionized plasma. This naturally occuring partially ionized plasma which is embedded in earth's magnetic field, is termed as 'ionosphere' which can be defined as a conglomeration or mixture of neutral, positive and negative charged particles in a state of dynamic equilibrium such that the loss of charged particles by recombination is balanced by the creation of new ones via some energy input mechanism. It goes through periods of relative calm as well as through stormy and turbulent phases, but never actually settles down to perfectly calm or static state.

The ionosphere has entered into the everyday life of

most persons because of its role played in long distance communication and broadcasting. The ionosphere modifies the propagation characteristics of radio waves in transit. Waves of certain frequencies can be bent sufficiently by the ionosphere to make long distance communication possible between different earth and space stations. Although microwave communication via satellites is becoming increasingly popular in recent years, short wave communication is restricted to the ionosphere and is largely controlled by the ionospheric plasma conditions. Anyone who has ever listened to a short wave radio broadcast has experienced the effects of the dynamic ionosphere in the form of apparently random fading of radio signals; time variation in received signals strength must reflect time variation in the propagation medium. Clearly, then an understanding of the ionospheric plasma as a telecommunication medium would be incomplete without the study of its dynamic behaviour and its associated phenomena. Besides communications, the ionosphere is also relied upon as an indicator of surveillence activities.

A weakly ionized plasma immersed in magnetic and electric fields is susceptible to various kinds of instabilities which manifest themselves as wavelike perturbations of electron density and electric field. The ionospheric plasma under different conditions, therefore, exhibits these natural perturbations termed as 'irregularities'. HF radio waves undergo rather easily measurable perturbations and distortions

their dynamic characteristics can affect every characteristics by which a radio wave is specified; its amplitude, phase, frequency, polarization, direction of arrival, etc.. Fluctuations (which are almost wavelike or nearly random in character) in these quantities occur because of these wavelike or some other types of ionospheric motions or irregularities.

It is quite well understood how the various radio propagation effects, such as scattering and fading of HF radio signals, refraction and oscillations in the intensity of solar and galactic radio emissions, radio star and satellite scintillations, can arise if irregularities in ionization densities which are mostly aligned with earth's magnetic field, are present in the ionosphere. In view of the important role played by the ionosphere throughout a wide range of wavelengths (from short waves right upto the wavelength of tens of kms or more), it is impossible to understand the propagation of radio waves without a thorough study of the irregularities generated in the ionospheric plasma. Consequently, the investigation of the ionospheric irregularities and their associated generation mechanisms, which influence greatly the radio wave propagation, is interesting and vitally necessary for a proper functioning of radio communication and other networks.

In the last decade or so, there has been a great upsurge in interest and activity on both the experimental and theoretical sides. There are still many fundamental gaps and contradictions about the explanation of the irregularities,

experimental means have been employed having accumulated a huge quantity of data some of which are confusing and conflicting. Theories are yet to be developed to explain satisfactorily the existence and the production of these irregularities and their associated phenomena. The difficulty lies in the fact that so many factors and parameters exist in the study of ionosphere that it becomes almost impossible to take them all into account simultaneously. Observations show that these irregularities are generated at various heights at different times of the day in different geographic regions and over a wide range of wavelengths under a wide variety of circumstances. Because of the complex nature of the phenomena, it seems reasonable to believe that there are many different physical processes that are responsible for the cause of ionospheric irregularities. Some of the irregularities are certainly caused by plasma instabilities, but in most cases the instabilities operate only at the wavelengths longer than the gyroradius of the particles.

Some features of the different phenomena associated with these irregularities have become clearer, a few of them have been explained and others have apparently become more complicated by new observations. Various theoretical approaches have been tried, but a satisfactory instability theory is yet to be developed. The more fundamental task, however, is to explain the generation of the irregularities themselves in different regions of the ionosphere. The investigation

different features associated with irregularities would not only be helpful to us in developing a deeper understanding of nature, but would also provide us with an insight towards an excellent HF radio wave communication and satellite navigation with very little possibility of interception by unwanted parties (irregularities) in the ionosphere.

1.12 Main Purpose of the Investigation:

The principal goal of the work presented here is concerned with the theoretical investigation of different plasma instability mechanisms which are responsible for the generation of ionization density irregularities observed in different regions of ionosphere and which could explain some of their observed characteristics satisfactorily. An attempt has been made to study these processes in both the linear and nonlinear regimes. Emphasis has been given to the relevance of these mechanisms to the equatorial ionospheric regions only.

Linear plasma instability theory appears to account only for the presence or absence of irregularities. The ionospheric plasma may develop a nonlinear state due to preponderance of various instabilities under different conditions. Thus, a nonlinear theory of the instabilities is essential to understand their development in details. A nonlinear instability theory is capable not only of explaining the nonlinear phenomena such as instability saturation, irregularities amplitude, the wavelength distribution, the propagation velocity, etc., but also of attaching considerable

of plasma instabilities and in turn, to the physical investigation of the real states of plasma in which it is most likely to be encountered in nature. In the present study, a modest attempt has been made to develop, separately for the equatorial E- and F-regions, the nonlinear instability theories which seem to be capable of explaining most of the features of irregularities observed and their associated phenomena such as equatorial sporadic-E and spread-F. These investigations may, therefore, be quite helpful in deducing much about the structure of the equatorial ionosphere, an important medium for HF radio wave communication.

1.2 A Short Description of Ionospheric Plasma, Its Structure and Dynamics of its Constituents:

1.21 Ionosphere as a Plasma Medium and its Structure:

From what has been said above, one feels that the knowledge of basic ionospheric plasma is fundamental to any radio communication studies. Communication involves the propagation of radio waves (electromagnetic waves) in a plasma medium (ionosphere) at different frequencies and the interaction of these waves with the medium. In the physics of a plasma, waves occupy an important position and the concept of a wave in the medium is quite familiar. The waves are generated in the plasma medium because of instabilities excited and may be considered as perturbations on the slowly changing background. These waves in the medium, which are known as 'irregularities', have two basic properties associated with them: firstly, energy is being propagated from one point to another; secondly, the

disturbances (irregularities) travel through the medium without giving it, as a whole, any permanent displacement.

Ionospheric plasma is susceptible to a number of instabilities. Because of their excitation under different conditions prevailing in the medium, it is capable of sustaining a large number of irregularities (wave-like perturbations). This thesis deals with the type of irregularities that are most important in a particular compressible medium, such as ionosphere, that is permeated by density gradients, temperature gradients and electric fields.

As the plasma medium responds to disturbances (irregularities) originating in it, their characteristics give considerable insight into the properties of ionospheric plasma. Conversely, the ionospheric plasma must be thoroughly understood to predict the character of its waves which interact with the propagating radio waves and modify the ionosphere affecting the communication.

Ionosphere is that part of the earth's upper atmosphere where ions and electrons equal in number are present in quantities sufficient to affect the propagation of radio waves. It is usually extends from about 50 km upto great heights, far our in space. Ionosphere is divided into regions called D, E and F, defined such that the part below 80 km is called D-region, that between 80 km and 140 km, the E-region and that above 140 km the F-region. These regions may be distinct layers of electrons, named D, E and F layers according to the level at which their peak occurs. However, these are not strictly demarcated layers but as described, rather regions which overlap. Sometimes these

There may occur more than one layer or ledge inside the single region, for example, F_1 ledge (with maximum around 150 km) below F_2 layer (with maxima around 400 km).

The charged particles in the ionosphere are embedded in a neutral gas. At some levels the neutral gas is moved by the gravitational forces of sun and moon (tidal motion of the earth's atmosphere), and probably also by the forces of thermal origins. The charged particles share this motion to some extent and since they behave like a conductor moving through earth's magnetic field, a current is induced, as in dynamo. The region of the ionosphere where this current is induced is given the name 'Atmospheric Dynamo'. Its flow is accompanied by a electrostatic field, the dynamo field (Baker and Martyn, 1953; Fejer, 1953), which reaching the other parts of the ionosphere, causes currents to flow there also. The earth's magnetic field, acting on these currents, then causes the electron-ion plasma at these distant places to move bodily. This part of the ionosphere is given the name 'Atmospheric Motor'. To a first approximation, the 'dynamo' is believed to be situated in the E-region and the 'motor' in the F-region.

1.22 Motion of the Charged Particles in Ionospheric Regions of Interest:

In the E-and F-regions, the motions of charged particles are more or less controlled by the earth's magnetic field $\underline{B}$. The plasma in these regions is subject mainly to electromagnetic, collisional, gravity and density gradient

construct separate equations for the ions and electrons as they apply to ionospheric environment; that is, a partially ionized, collision dominated plasma moving in a neutral atmosphere under the forces of gravity, electric and magnetic fields. With some reasonable assumptions, the plasma drift velocity can then be found out. Negative ions are scarce in parts of the ionosphere where transport processes have any importance (except perhaps in the nighttime E-region). To a good approximation, the concentrations of positive ions and electrons can then be equated, since neutrality must be very nearly preserved. Even when electric polarization charges are developed, the difference between negative and positive charged particle densities is only one part in 10^{10}. The rate of change of these charges is also insignificant so that if an electric current flows, it must be nondivergent. This leads to the following condition for ionospheric current densities $\underline{j}$:

$$\nabla \cdot \underline{j} = e \nabla \cdot [N_0 (\underline{v}_i^0 - \underline{v}_e^0)] = 0 \qquad ..(1.1)$$

where e is electric charge, N_0 the number density of the charges and $\underline{v}^0$ the mean drift velocity with subscripts i and e respectively for ions and electrons. This condition is obtained by using the continuity equations for electrons and ions.

Collisions between particles are so frequent that ions and electrons can both be treated as fluids. This implies that the random thermal velocities (about 1 km S^{-1} for ions and

their existence can be ignored. Normally, this assumption is very well justified for thermal particles in the ionosphere. Collisions between charged particles themselves (i - e) are negligible, because collisions of charged particles with neutral particles predominate over collisions between charged particles in a weakly ionized plasma.

a) Transport Processes:

The important transport processes taking place in the ionosphere are enumerated as follows:

1) The electrons and ions are greatly subject to electric fields. The resulting motions and the electric currents depend upon the magnetic field and the collision frequencies, which determine the mobility and the electrical conductivity of the charged particles.
2) The charged particles can have motions by neutral winds. These produce forces proportional to differences between the wind velocity $\underline{U}$ and the charged particles velocities $\underline{v}_i$, $\underline{v}_e$ and to the relevant collision frequencies. In the E-region, the winds are normally associated with the tidal motions. Since these winds also produce the dynamo action, the physical situation is quite complicated.
3) The daily temperature changes in the thermosphere affect the charged particles as well as the neutral air.
4) Plasma tends to diffuse under the action of gravity and of gradients in its own partial pressure. The electrical

together, so that both kinds of particles diffuse at same speed. This ambipolar diffusion is impeded by collisions of charged particles with neutral particles and tends to be constrained by earth's magnetic field. Diffusion proceeds more rapidly in the F-region where motions due to d.c. electric fields are insignificant to that due to diffusion, but more slowly in the lower ionosphere where collisions are more frequent and the effects due to d.c. electric and magnetic fields are significantly large.

In the ionosphere there are large scale motions in which changes take place very slowly. In this quasiequilibrium, the inertial term (representing acceleration) in the equations of motion for the charged particles may be neglected (they might not be negligible for small-scale wavelike motions). Under these conditions which exist in the ionosphere, one can write the equations of motion for the charged particles as

$$m_j \frac{d\underline{C}_j}{dt} = 0 = q_j(\underline{E} + \underline{C}_j \times \underline{B}) + m_j \underline{g} - m_j \nu_j (\underline{C}_j - \underline{U}) - N^{-1} \nabla p_j \quad ..(1.2)$$

where $\underline{C}_j$ is the local mean velocity of the charged particles; ν_j, the effective collision frequency and is often termed as 'collision frequency', p_j the partial pressure given by $p_j = NKT_j$ and other symbols have their conventional meanings. The subscript j denotes i for ions and e for electrons. It is sometimes convenient to introduce the relative velocity $\underline{v}_j = \underline{C}_j - \underline{U}$ of the charged particles with respect to the neutral gss. Then equation (1.2) assumes the form as

$$0 = q_j(\underline{E} + \underline{U} \times \underline{B}) + q_j(\underline{v}_j \times \underline{B}) + \ldots - m_j \nu_j \underline{v}_j - N^{-1} \nabla p_j \quad \ldots(\ldots)$$

The first term q_j ($\underline{E} + \frac{1}{c}\underline{U} \times \underline{B}$) is the force exerted on a charged particle by the total applied electric field $\underline{E}_o = (\underline{E} + \frac{1}{c}\underline{U} \times \underline{B})$ that would be seen by an observer moving with the neutral gas. The field $\underline{E}$ is the electrostatic field (due to polarization charges) and the field $\underline{U} \times \underline{B}$ is often called 'dynamo field' since it corresponds to the field seen by the armature of a dynamo moving at velocity $\underline{U}$ in a magnetic field of a induction $\underline{B}$. The term $m_j \underline{g}$ is the gravity force acting on the particles and the term $(N^{-1} \nabla p_j)$ represents the partial pressure gradient force which may be quite important in 'ambipolar diffusion' process (in the upper F-region where electromagnetic forces are significantly smaller). The gravity and the pressure gradient forces are usually very much smaller than the electromagnetic forces and are thus neglected to a first approximation (except when considering the motions in the upper F-region where the reverse is true). Thus the equation of motion (1.3) for a charged particle becomes,

$$m_j \nu_j \underline{v}_j - q_j \left(\frac{\underline{v}_j \times \underline{B}}{c}\right) = q_j \underline{E}_o \qquad \ldots(1.4)$$

where $\underline{v}_j$ is the mean relative drift velocity of a charged particle.

b) <u>The Mean Drift Velocities of the Particles</u>:

Knowing applied electric field $\underline{E}_o$, one can determine $\underline{v}_j$ from the equation (1.4). The mean relative drift velocity, $\underline{v}_j$ can then be obtained as

$$\underline{v}_j = \frac{q_j}{m_j}\cdot\frac{\nu_j}{\nu_j^2+\Omega_j^2}\,\underline{E}_0 + \frac{q_j}{m_j}\cdot\frac{\Omega_j}{\nu_j^2+\Omega_j^2}\cdot\frac{\underline{E}_0\times\underline{B}}{B}$$

$$= \frac{c}{B}\cdot\frac{\Omega_j\nu_j}{\nu_j^2+\Omega_j^2}\,\underline{E}_0 + \frac{c}{B}\cdot\frac{\Omega_j^2}{\nu_j^2+\Omega_j^2}\cdot\frac{\underline{E}_0\times\underline{B}}{B} \qquad ..(1.5)$$

where $\Omega_j = q_j B/m_j c$ is the gyrofrequency of the particles, including the sign (i.e., Ω_e is negative as $q_e = -e$).

It is often convenient to employ a cartesian coordinate system (ξ, η, ζ), whose positive ζ axis is directed along $\underline{B}$ and whose η axis is perpendicular to $\underline{E}_0$. Then, three components of the mean relative drift velocity are given by

$$v_{j\xi} = \frac{q_j}{m_j}\cdot\frac{\nu_j}{\nu_j^2+\Omega_j^2}\cdot E_{0\xi} = \frac{c}{B}\cdot\frac{\nu_j\Omega_j}{\nu_j^2+\Omega_j^2}\cdot E_{0\xi} \qquad ..(1.6)$$

$$v_{j\eta} = -\frac{q_j}{m_j}\cdot\frac{\Omega_j}{\nu_j^2+\Omega_j^2}\cdot E_{0\xi} = -\frac{c}{B}\cdot\frac{\Omega_j^2}{\nu_j^2+\Omega_j^2}\,E_{0\xi} \qquad ..(1.7)$$

$$v_{j\zeta} = \frac{q_j}{m_j\nu_j}\,E_{0\zeta} = \frac{c}{B}\,\frac{\Omega_j}{\nu_j}\,E_{0\zeta} \qquad ..(1.8)$$

The comparison of collision and gyro-frequencies of the charged particles divide the ionosphere into three regions I, II and III as shown in Fig.1.0. These regions are separated by the height $h_e \approx 75$ Km for which $\nu_e \approx |\Omega_e|$ and the height $h_i \approx 140$ Km for which $\nu_i = \Omega_i$. The heights, h_e and h_i represent transitions for the motion of the electrons and ions respectively. Below and above these critical heights, the relations between ν_j and Ω_j have been shown in the Fig.1.0. Below the critical height h_e, the ions move relative to the neutral gas at the velocity $E_0 q_i/m_i\nu_i$ in the direction of

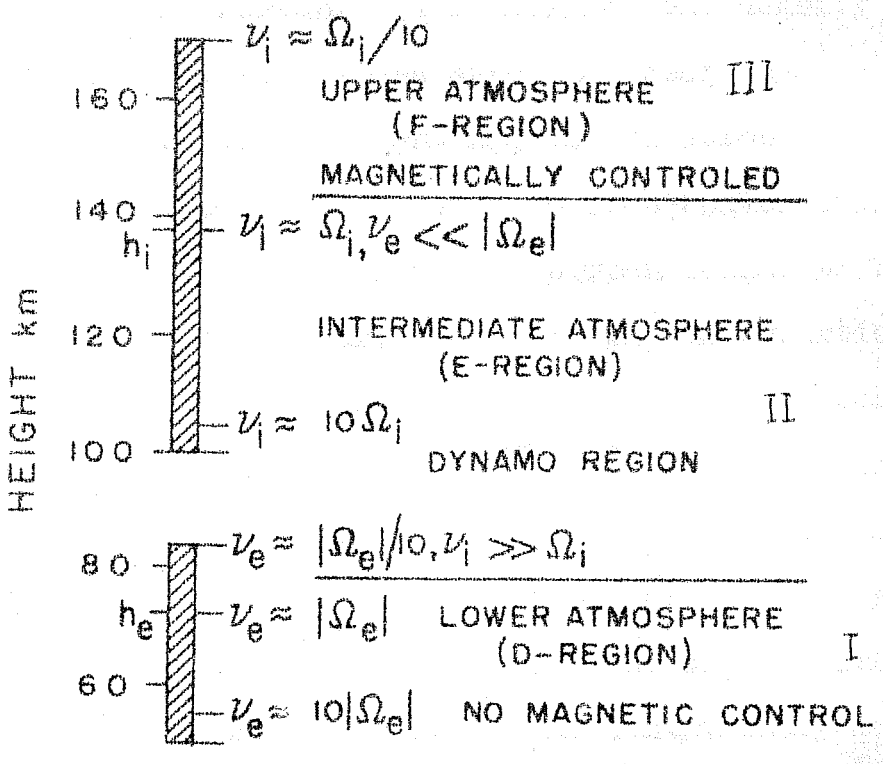


Fig.1.0. Schematic representation of ionospheric regions. Also shown is the variation of electron and ion collision frequencies (ν_e and ν_i) with altitude.

velocity $E_o q_e/m_e \nu_e$ in the opposite direction. In this approximation ($\nu_j >> \Omega_j$), the magnetic field has no influence on the mobility of the particles beyond that already included in $\underline{E}_o$. For constant $\underline{E}_o$, the ion and electron drift velocities will increase with increasing height since the density of the neutral particles decreases and hence ν_j decreases.

Above the critical height h_i, the electrons and ions move with a common drift speed cE_o/B or a common drift velocity $c\underline{E}_o \times \underline{B}/B^2$, in a direction perpendicular to both the electric and magnetic fields. In addition, the particles move parallel to the magnetic field at velocities which are independent of that field and which, for a given parallel component of the electric field, continue to increase with height as ν_j decreases. In the intermediate regions between h_e and h_i, only the electrons move with the drift velocity $c\underline{E}_o \times \underline{B}/B^2$, whereas the ions remain almost stationary in comparison with the electrons. Consequently, the resulting current which flows in a direction perpendicular to both the electric and the magnetic fields, is called 'Hall current'.

c) Currents and Conductivities:

The presence of electrons and ions in the ionosphere makes this region electrically conducting. The concentrations of the charged particles and of the neutral particles govern the electrical conductivity, because collisions of charged particles restrict their movement under the action of any impressed electric field, for example, $\underline{E}$. The presence of

restricts the motion of the charged particles across $\underline{B}$ and therefore, makes the conductivity anisotropic. Hence, several different conductivities must be defined for use in the different physical situations occuring in the ionosphere, and these are defined in the following.

The current density $\underline{J}$ in the medium is given by

$$\underline{J} = N_0 \left(q_e \underline{v}_e + q_i \underline{v}_i \right) \qquad ..(1.9)$$

After substitution of $\underline{v}_e$ and $\underline{v}_i$ from corresponding equations (1.6), (1.7) and (1.8) for ions and electrons, the components of current density $\underline{J}$ are given by

$$J_\xi = \frac{N_0 e c}{B} \left[\frac{\nu_i \Omega_i}{\nu_i^2 + \Omega_i^2} - \frac{\nu_e \Omega_e}{\nu_e^2 + \Omega_e^2} \right] E_{0\xi} \qquad ..(1.10a)$$

$$J_\eta = \frac{N_0 e c}{B} \left[\frac{\Omega_e^2}{\nu_e^2 + \Omega_e^2} - \frac{\Omega_i^2}{\nu_i^2 + \Omega_i^2} \right] E_{0\xi} \qquad ..(1.10b)$$

$$J_\zeta = \frac{N_0 e c}{B} \left[\frac{\Omega_i}{\nu_i} - \frac{\Omega_e}{\nu_e} \right] E_{0\zeta} \qquad ..(1.10c)$$

where $e = q_i = -q_e$ is assumed and as before gyrofrequencies Ω_i and Ω_e differ in sign. These equations may be written in a somewhat more general form which permits the inclusion of η- component of electric field $\underline{E}_0$ as

$$\underline{J} = \underline{\underline{\sigma}} \cdot \underline{E}_0 \qquad ..(1.11)$$

where $\underline{\underline{\sigma}}$ is conductivity tensor given by

$$\sigma \equiv \begin{bmatrix} \sigma_1 & -\sigma_2 & 0 \\ \sigma_2 & \sigma_1 & 0 \\ 0 & 0 & \sigma_0 \end{bmatrix} \qquad ..(1.12)$$

in a coordinate system whose third axis is aligned in the direction of $\underline{B}$. Equations (1.10) or equations (1.11) and (1.12) determine the current that flows in presence of a known total applied electric field $\underline{E}_o$. σ_o is the longitudinal conductivity, which determines the current parallel to the magnetic lines of force and would exist for all directions in the absence of magnetic field. The conductivity σ_1 is called the 'Pedersen Conductivity' which is used to calculate the current parallel to that component of electric field which is normal to the magnetic field. σ_2 is the 'Hall conductivity' which determines the current ('Hall current') flowing in a direction perpendicular to both the electric and magnetic fields. In the F-region and above, σ_o becomes very large and also $\sigma_o >> \sigma_1, \sigma_2$ (which become vanishingly small), as ν_e and ν_i are quite smaller there than $|\Omega_e|$ and Ω_i. Therefore, $\underline{E}_o$ can not be maintained with any substantial component along the magnetic field lines, and hence the latter are very nearly lines of constant potentials. These conductivities, σ_o, σ_1 and σ_2 can be defined as

$$\sigma_o = \frac{N_o e c}{B}\left(\frac{\Omega_i}{\nu_i} - \frac{\Omega_e}{\nu_e}\right) \qquad ..(1.13a)$$

$$\sigma_1 = \frac{N_o e c}{B}\left(\frac{\nu_i \Omega_i}{\nu_i^2 + \Omega_i^2} - \frac{\nu_e \Omega_e}{\nu_e^2 + \Omega_e^2}\right) \qquad ..(1.13b)$$

$$\sigma_2 = \frac{N_o e c}{B}\left(\frac{\Omega_e^2}{\nu_e^2 + \Omega_e^2} - \frac{\Omega_i^2}{\nu_i^2 + \Omega_i^2}\right) \qquad ..(1.13c)$$

Since the current is strongly inhibited across the field lines, in the F-region and above whatever current is poured

must consequently pour out of it at opposite end in the southern hemisphere. Hence, a horizontal current system flows in a relatively thin spherical shell in the E- and D-regions.

Near the geomagnetic equator, the Cowling conductivity σ_3 which is defined by

$$\sigma_3 = \sigma_1 + \sigma_2^2/\sigma_1 \approx \sigma_1 \left(1 + \sigma_2^2/\sigma_1^2\right) \approx \sigma_1 \left(\sigma_2/\sigma_1\right)^2 \quad ..(1.14)$$

is the most important and is about 10 to 25 times as great as that elsewhere, within a comparatively narrow range of height near 100 Km (since σ_2 is greater than σ_1 by that factor). For this reason, it is permissible, in a first approximation, to consider that the dynamo region, near the equator, consists of a bounded slab near these heights. The dynamo e.m.f. (given by $\underline{U} \times \underline{B}$) varies over the surface of the earth. Therefore, a horizontal distribution of space charges is built up before the current can flow. The electric field of this horizontally distributed space charges will modify the tensor conductivity $\underline{\underline{\sigma}}$ and influences the F-region. In the simple slab picture, this field has to reach that region through the intervening weakly ionized region where it may be supposed that the tensor conductivity is predominantly along the magnetic lines of force and has large amplitude, σ_0. In the F-region, therefore, there is an e.m.f. conducted up along these lines of force from the horizontal space-charge in the E-region. This e.m.f. then produces horizontal currents in the (supposed) slab-like F-layer, as determined by the horizontal layer conductivity. These currents, acted on by

moves bodily, constituting the 'atmospheric motors'.

d) Collision Frequencies of Charged Particles:

Nicolet (1953) has given expressions for the collision frequencies of electrons with ions and with neutral particles. The collision frequency of electrons with neutral particles is given by the expression

$$\nu_{en} = 5.4 \times 10^{-10} n_n T_e^{1/2} \qquad ..(1.15a)$$

where n_n is the number density of neutral particles. The collision frequency of electrons with ions is represented by the expression

$$\nu_{ei} = \left[34 + 4.18 \log\left(T_e^3/n_e\right)\right] n_e T_e^{-3/2} \qquad ..(1.15b)$$

The electron-ion collision frequency, ν_{ei} is much more temperature dependent than the electron-neutral collision frequency, ν_{en}. The sum of these two collision frequencies ν_{ei} and ν_{en}, is termed as the effective electron collision frequency or simply electron collision frequency, $\nu_e (= \nu_{ei} + \nu_{en})$.

An expression for the collision frequency of ions with neutral particles is given (Chapman, 1956) as

$$\nu_i = 2.6 \times 10^{-9} (n_n + N) M^{-1/2} \qquad ..(1.16)$$

where M is the molecular weight of the ions and neutral particles, which are assumed to have the same mass. One does not need to consider ion collisions with electrons, because the electrons are so light that the ions are, essentially,

electrons are, of course, greatly affected by their encounters with ions, which are represented by eq.1.15b).

1.23 Importance of Equatorial Ionospheric Studies, with the Emphasis Mainly on the E-and F-Regions:

At the magnetic equator, the earth's magnetic field is totally horizontal, due to which a variety of most interesting phenomena originate in the equatorial ionosphere. One of the topics of great interest has been that of observations of density irregularities of various scale sizes. It is quite well known that most of the irregularities are generated in the equatorial ionosphere. The dip equatorial region is particularly interesting in this respect as the electric and magnetic field configurations and the electron density gradients existing there, which are difficult to obtain elsewhere, are most suited for providing simplicity to understanding of generation mechanisms of these irregularities and in turn, in giving the reasonably good explanations for associated equatorial ionospheric phenomena.

The equatorial ionospheric E-and F-regions have, over the years, provided a variety of perplexing yet interesting problems to the radio communications. The practical importance of studying the equatorial ionosphere was emphasized by the observations of radio amateurs who were able to communicate, primarily during nighttime, on frequencies near 50 MHz (far above the maximum value of plasma frequency, $\omega_p = 4\pi N_e e^2/m_e \simeq 10$ MHz) between points on either side of magnetic equator (Southworth, 1960). This occurred in spite of the fact that MUF (maximum usable frequency)

be impossible. These amateur contacts which were most prevalent around the equinoxes, were aimed to see the relationship between echostructure and the rapid fading of HF radio signals, known as equatorial flutter fading which is known to be closely associated with the equatorial spread-F, an irregular phenomena occuring in F-region.

Of interest to the present work are those aspects of irregular phenomena observed within the equatorial ionosphere that manifest themselves as wavelike perturbations (irregularities) of electron densities and electric fields, when ccnsidering the transmission of radio signals to or from the ground stations and spacecrafts, for such investigations as ionospheric sounding and cosmic or ionospheric noise. These irregularities may be of a localized or resonant nature.

The lower ionospheric regions (below 1000 Km) are, in some respects, the most interesting of the whole upper atmosphere, for they support a wide range of physical phenomena than any other regions do. They are not understood in detail partly because of the complexity of their processes and partly because of observational limitations. It has been recognized that a certain feature of radar scatter returns (radar echoes) on a conventional ionogram (essentially the out put of a swept frequency h.f. radar) is closely associated with changes in the equatorial magnetic field and hence the electrojet current (Matsushita, 1951). This H.F. scatter is generally called as equatorial sporadic-E (E_{sq}), as shown

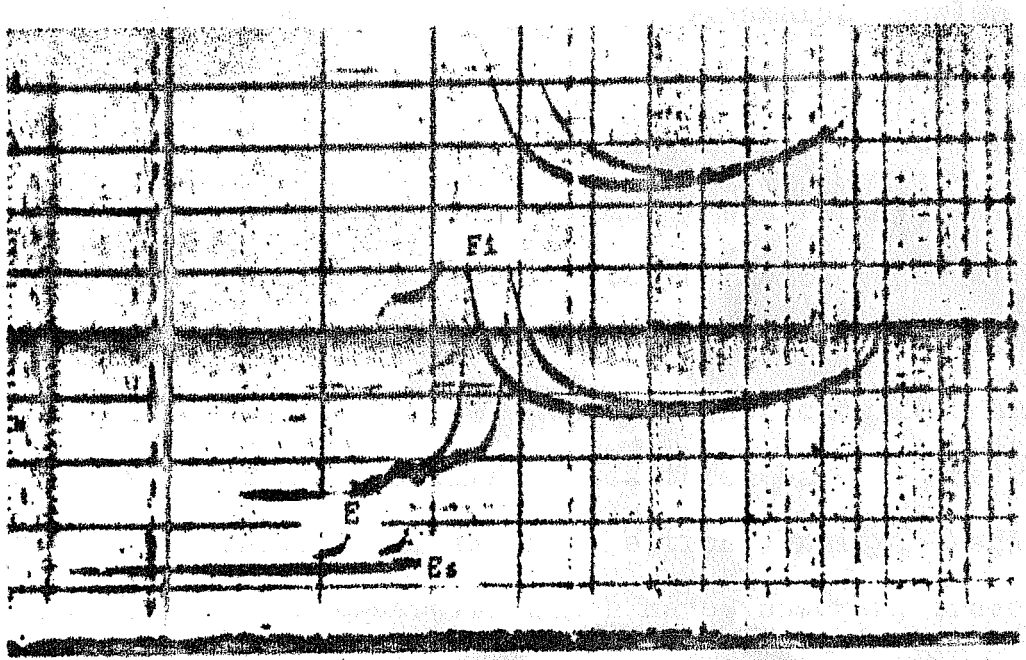


Fig.1.1. Ionogram showing sporadic-E
(After D'Angelo, 1969)

However, the real progress which has been made recently in our understanding of the physics of the scatter returns is primarily the results of the VHF and HF scatter radar observations ($\sim$50 MHz and greater) carried out in Peru (close to magnetic equator) at Jicamarca (Bowles and Cohen, 1957, 1962; Bowles et al., 1960, 1963; Cohen and Bowles, 1963a,b, 1967; Cohen et al., 1962; Balsley, 1965, 1969a,b, 1973a; Farley, 1971; Balsley and Farley, 1971, 1973; Farley and Balsley, 1972, 1973; Cohen, 1973; Fejer et al., 1973, 1975a,b). At such frequencies, most of the transmitted energy of radio waves passes through the ionosphere and is lost; only a small fraction is scattered back to the receiver from small fluctuations in the electron density. Radio signals at such frequencies which have, however, travelled the lower equatorial ionosphere uninterrupted, are found to have rapid fluctuations in amplitude and phase, causing fading of the waves. As has been pointed out already (page 21), the irregularities such as spread-F occuring in upper equatorial ionospheric regions (F-region), may be responsible for causing such variations in the HF radio signals.

a) Equatorial Electrojet (E-Region):

Observations of the enhancement of diurnal range of horizontal component H of geomagnetic field could be accounted for by the enhancement in the horizontal conductivity in the region near magnetic equator (Cowling, 1932; Martyn, 1947; Cowling and Borger, 1948). Cowling (1932) showed that the

vertical Hall currents are inhibited by the polarization electric field built up in vertical direction in the conductive region where $\nu_i / \Omega_i >> 1$ and $\nu_e / |\Omega_e| << 1$. The suppression of these vertical currents is consistent with the idea of a belt of high current density (i.e., the vertical polarization field enhances the horizontal current flow considerably) which accounts for the enhanced horizontal conductivity, in the equatorial ionosphere at E-region heights. The high concentration of electric currents flowing from west to east in a narrow belt flanking the dip equator, on the sunward hemisphere, was named the 'equatorial electrojet' by Chapman (1951).

The equatorial electrojet has been a subject of extensive study both observationally and theoretically. The in-situ rocket-borne experiments have established the vertical and latitudinal extent of the equatorial electrojet and have provided approximate values of electron and current densities. The electrojet occupying a narrow height range of 10 to 15 Kms, is centered at an altitude of about 105 Km and it appears in the areas within two to three degrees of latitude of magnetic dip equator. The positive daytime electrojet consists of essentially a flow of electrons toward the west. The positive ions have no appreciable ordered motion because of their relatively greater mass and greater collision frequency with neutral particles in this region. This westward day-time electrojet flow reverses during nighttime and flows toward

E-region ionization, along with that in the D-region, tends to disappear. However, certain electron density irregularities in the electrojet region can somehow exist at night in the midst of reduced electron density.

Electrojet models based on latest evidences have been described from time to time (Maeda, 1955; Zmuda, 1960; Sugiura and Cain, 1966; Sugiura and Poros, 1969). The latest of these models is proposed by Sugiura and Poros (1969) which is necessarily idealized model. In this, they made the assumptions that the primary electrostatic field is uniform and that the vertical Hall current is completely inhibited within approximately $\pm 2^{o}$ around the magnetic dip equator. Although these assumptions can not be true, in practice, they are certainly reasonable and necessary for the first order theory. Therefore, the use will be made of this idealized model along with the assumptions made in the present analysis of the instability theories for the equatorial electrojet region.

b) Equatorial Sporadic-E (E_{sq}):

Superimposed on the normal E-layer and sometimes obscuring it in conventional ionograms, may be one, or more dense layers of ionization. Ionosonde often detects such dense layers, patches or ledges of ionization (layers of enhanced ionization) at heights of 100 - 120 km which is known as 'sporadic-E or E_s' (Fig.1.1) because of their rather random appearances. Generally, E_s appears as a patchy and partially

which completely blankets the overlying F-layer and is known as 'blanketing' type E_s. While the morphology of E_s has been studied almost since the beginning of systematic ionospheric observations, the theoretical approach has been extremely difficult. There is no doubt that the E_s is the most irregular phenomena in the ionosphere, because of both its random appearance in time and space and its structure.

Several distinct categories of E_s are now identified emperically. Some of these appear on normal days and are probably associated with the dynamic processes. Whitehead (1970a) has given an excellent summary of all types of E_s (temporal, auroral and equatorial), reviewing briefly the earlier theories of formation of sporadic-E irregularities. Near the magnetic equator, a distinct type of 'equatorial E_s' (E_{sq}) is observed which is patchy and transparent to waves reflected from higher level. It is predominantly daytime phenomena and is strongly correlated with the equatorial electrojet current (Matsushita, 1951).

E_{sq} occurances are negatively correlated with the geomagnetic disturbances (Matsushita, 1957). It has been found that even on quiet days there are occasional disappearance of E_{sq} for short periods associated with abnormally low values of horizontal magnetic field intensity (Matsushita, 1957; Cohen et al., 1962; Gouin and Mayaud, 1967; Rastogi et al., 1971; Krishnamurthy and Sengupta, 1972). This disappearance of E_{sq} is attributed to the reversal of electrojet

electrojet' (Gouin and Mayaud, 1967).

The highly transparent E_{sq} is now mostly attributed to a rather inhomogeneous plasma structure believed to be produced due to plasma instabilities, e.g., Two-stream and Cross-field instabilities. Transparent echoes can be accounted for due to partial reflections from either sharp gradient in electron concentration or small-scale weak irregularities occuring in the equatorial sporadic-E layer. The cross-field plasma instability is found to be responsible for some diffuse non-blanketing type E_{sq} (Tsuda et al., 1966, 1969).

c) Equatorial Spread-F:

It is now established that F-region reveals itself in diverse forms and regular and irregular shapes on ionograms obtained from ionosondes. One of these mysterious irregular forms is a phenomenon which shows a diffuse character called 'spread-F' which is attributed to scattering by irregularities of ionization embedded in the surrounding region. The term 'spread-F' is derived from the spread, smeared or fuzzy appearance of the F-layer-reflected echo traces, seen on the ionograms; that is, the reflection of a vertically incident electromagnetic wave appears to occur at a continuum of altitudes. In common usage, the phenomenon of spread-F is, generally, associated with the actual ionospheric conditions causing the spread echo traces. The gradual and vast accumulation of knowledge about the spread-F for many years has, certainly, revealed that it is one of major and important

distance communications.

There are two main classes of spread-F; 'frequency-spreading' and 'range-spreading' which are shown in Fig.1.2. The high and temporate latitude ones are usually characterized by frequency-spreading type in which the frequencies of the reflected signals appear to be shifted by varying amount. At equatorial latitudes, the spread-F is mainly of the range-spreading type in which apparent variations in the reflection heights 'smear out' the traces. Basically, both types of spread-F have been described for equatorial ionospheric regions (Cohen and Bowles, 1961; Calvert and Cohen, 1961; Pitteway and Cohen 1961; Krishnamurthy and Rao 1964; Huang, 1970; Skinner and Kelleher, 1971; Nielson and Crochet, 1972).

Equatorial spread-F occurs in the evening and at night. It is most prevalent before mid-night and occurs more frequently in sunspot minimum years than sunspot maximum. A brief comparison of the characteristics of the equatorial and high latitude spread-F is shown in the Table 1.1.

Moreover, the morphology of equatorial spread-F is so different from that of high latitude spread-F and also, the experimental evidence suggests that the cause may not necessarily be the same for the spread-F in both regions. It is wellknown and now believed, on the basis of correlations made between the occurrence of spread-F and other recent ionospheric observations, such as radio star scintillations and angular distribution of radiations scattered, that the

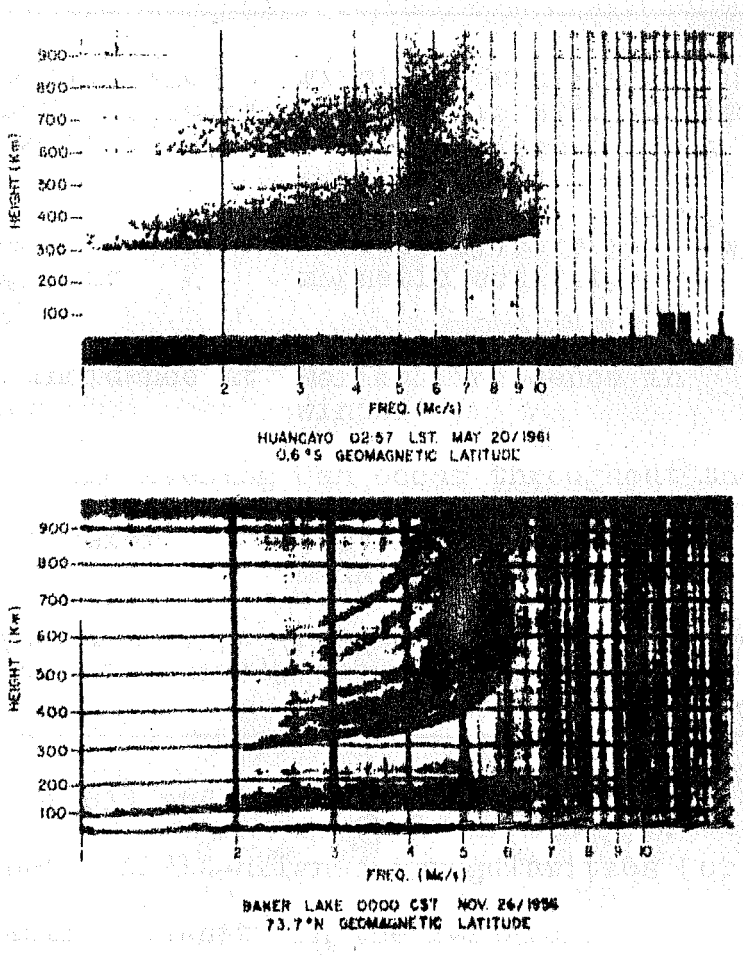


Fig.1.2. Two types of spread-F. The upper ionogram shows the type commonly called in the equatorial region. The lower one shows the type usually observed at middle to high latitudes (After Hines et al., 1965)

Table 1.1 : Characteristics of Spread-F

Equatorial Spread-F	High Latitude Spread-F
1. Occurs within the geomagnetic latitude zone from 0^{o} to 30^{o}	First evident at latitude from 40^{o} to 60^{o}. Maximum occurrence occurs just above auroral zone
2. Negatively correlated with magnetic activity	Positively correlated with magnetic activity
3. Maximum incidence at equinoxes	Maximum incidence in winter
4. Occurs in the evening and night only. Most prevalent before midnight	Can occur throughout the day but usually at night. Most frequent between midnight and sunrise.
5. Range-spreading type occurs most frequently	Frequency-spreading type occurs most frequently

and Bowles, 1961) and on the top side of the layers, is caused by the magnetic field-aligned irregularities (or inhomogenities) in electron density in the F-region.

Some of the important and burning questions in a complete theory of spread-F which need to be answered are (i) why such field-aligned irregularities cause spread-echoes (spread-F) ? ; (ii) how are they produced ? and (iii) how can their important observed characteristics be reasonably understood ? The specific physical processes causing the development of spread-F are not well understood. Among the proposed causes for spread-F irregularities are (i) atmospheric

transport due mainly to an irregular polarization field in the E-region, which is communicated to F-region along the highly conductiving lines of the geomagnetic field; (iv) hydromagnetic waves arriving from outer space; (v) charge particles' penetrations; (vi) the gravitation-induced Rayleigh-Taylor instability. A brief review on the existing theories of occurance of spread-F irregularities has been given by Cole (1973) and Farley (1974).

1.3. Observations of Ionization Density Irregularities in the Equatorial E-and F-regions:

The equatorial ionosphere has, over the years, provided a wide variety of perplexing and yet interesting problems to radio communicators. The phenomena, occuring in equatorial ionosphere such as E_{sq}, spread-F, Barium cloud striations, fading of HF radio waves, radio star scintillations, fluctuations in signal strength of satellite transmissions, HF and VHF scatter, etc., are familiar manifestations of the ionization density irregularities. Therefore, the study of the irregularities generated in the equatorial ionosphere has been a scientific endeavour for several decades. A great deal of effort, both experimentally and theoretically, has gone into investigating these ionospheric E-and F-region irregularities for last one and half decade or so.

During recent years, experimental studies of the equatorial E-and F-regions made by a variety of ground-based and space techniques have revealed the presence of an assortment of irregularities in electron density under a wide

These observations have shown the existence of several types of the irregularities, based on their scale sizes, shapes, spectral measurements and other characteristics which depend upon the local conditions and other important parameters of ionospheric regions of interest such as electron density, electric fields and plasma streaming velocity.

In order to clarify the objective of the present studies, we first present the important observed results of the electron density irregularities in both the equatorial E-, in particular, the electrojet and F-regions. Their types and most important features which are of interest to the present studies, will be briefly discussed in the following.

1.31 E-region Irregularities:

The presence of an anomalous scattering region in the equatorial E-region was indicated in the earliest (Circa, 1937; Berkner and Wells, 1937) low magnetic latitude ionosonde records. Examination of some of the features of this region seen on the ionosonde records and now in recent rocket and radar observations, clearly indicate that the equatorial E-region is embedded with both the weak and strong electron density irregularities (i.e., small and large amplitude fluctuations in ionization density). During the last decade or so, the equatorial E-region irregularities, particularly the equatorial electrojet irregularities have been becoming

HF and VHF backscatter radar investigations (between 1 MHz and 150 MHz) made at the Jicamarca radar observatory (magnetic dip 2^{o}N) in Peru (Bowles and Cohen, 1957, 1962; Bowles, et al., 1960, 1963; Egan, 1960; Cohen and Bowles, 1963a,b, 1967; Cohen et al, 1968; Balsley, 1965, 1969a,b, 1973a; Farley, 1971; Balsley and Farley, 1971, 1973; Farley and Balsley, 1972, 1973; Cohen, 1973; Fejer et al., 1973, 1975a,b) and in-situ rocket measurements at Thumba (magnetic dip $0^{o}47'$S) in India (Prakash et al., 1969, 1970, 1971a,b, 1972, 1973) have yielded a large body of information on the characteristics and structure of these irregularities in the equatorial E-region.

It is now certain that much of our elucidation and understanding of the physical processes responsible for the generation of the equatorial E-region irregularities depends upon the VHF radar and in-situ rocket observations. From these observations, it is well established that these irregularities are mostly associated with the electrojet region, a range that agreed well with the limits of the electrojet current system determined by Singer et al. (1951). Although their main characteristic features are now well known and have been briefly reviewed by Farley (1974), for the sake of totality of the studies concerned here we shall draw below an overall picture of the important characteristics of the electrojet electron density irregularities of our present interest.

There are various kinds of electron density irregularities observed in the equatorial electrojet (Balsley, 1969b;

the earth's magnetic field (Bowles and Cohen, 1957; Egan, 1960). On the basis of the spectral observations of VHF radar echoes returned from the irregularities, there are two distinct types of irregularities in the electrojet; type I irregularities (Bowles et al., 1963; Cohen and Bowles, 1963a,b, 1967; Balsley, 1969a,b) and type II irregularities (Balsley, 1969b). The echoes returned from these two groups are classified as type I and type II echoes respectively. The major characteristics of these types of irregularities in context to the present studies are briefly enumerated as follows (Balsley, 1969b, 1973a, Fejer et al., 1973, 1975a,b).

a) Type I Irregularities:

Type I irregularities are those which are thought to be directly excited, at the observed wavelengths, by the two-stream instability in a collisional plasma (Farley, 1963a,b; Buneman, 1963). They are distinguished from the other types by the following observed characteristics.

1. These irregularities are produced when the relative electron-ion drift velocity (i.e., streaming velocity of electrons) is large enough and exceeds the threshold velocity which is ion-acoustic velocity (supersonic) in the electrojet (approximately equal to 360 m/sec.).

2. These are plane-wave structures. The lines of force of earth's magnetic field are always very nearly in the plane of the waves. The deviation is seldom more than 1^{o}, i.e., they are highly field-aligned (Bowles and Cohen, 1957; Egan, 1960).

3. They only appear when the electrojet current exceeds some

to 1 meter wavelength irregularities) is somewhat higher than the the threshold for echoes at 50 MHz (3 meter wavelength). That is, threshold is higher for smaller wavelength which means that strong current is required for the formation of such irregularities.

4. Type I irregularities travel in directions most nearly parallel to the directions of mean flow of electrons. They have a relatively constant Doppler shift corresponding approximately to ion-acoustic speed in the medium, i.e., they travel with the phase velocity V_p, equal to the ion-acoustic speed C_s, in marginally stable state in the electrojet.

5. They are generated during day and at times at night.

6. Type I echo strength, i.e., the irregularity amplitude generally varies as electrojet current strength which varies with altitude. But however, they have a nearly constant amplitude between 15 and 1 m wavelengths (Prakash et al.,1973).

7. When they occur, they propagate in a wide range of angles, including 90° (vertical incidence), relative to the horizontal, at wavelengths as short as 1 meter, i.e., type I echoes appear more or less simultaneously over a substantial range of radar elevation angles.

8. These have a narrow, sharp and nearly marginally stable spectrum, with a distinct maximum at a constant Doppler shift that corresponds at least approximately to C_s of the medium, which is independent of the elevation angles of radar beam, and is symmetrical about zero Doppler shift (i.e., about C_s).

7529.

14. The upgoing type I waves reach a larger amplitude than the down going waves (Fejer et al., 1973).

b) Type II Irregularities:

They are generally considered to be generated due to a gradient drift instability (Simon, 1963; Hoh, 1963; Rogister and D'Angelo, 1970 and references therein) and can be easily excited than type I, for wavelengths longer than a few meters (> 10 m). The following are the major features of the type II irregularities in view of the present interest.

1. These irregularities, having smaller (3-15 meter) and larger (30-300 meters and more) scale sizes, are observed even when the mean V_D is quite small and below C_s (subsonic), whereas 1 meter type II are too weak to be detected. In fact, this class is never observed at the equator for wavelength of 1 meter or less.

2. These are practically always present, during both the day and night times, at least at long wavelengths, and at short wavelengths when type I are absent.

3. They have a rather much broader spectrum, with the variable width often greater than the mean Doppler shift which is approximately proportional to the cosine of elevation angle.

4. These are generally weaker and have a variable smaller mean Doppler shift which is greater for echoes returned at more oblique angles.

5. They propagate at all angles, including 90°, relative to the horizontal, with the electron drift velocities. Although the mean motion is, generally, in horizontal directions, their

shift indicates that they are not just drifting horizontally at some particular velocity, but rather that the motion is more complex.

6. Drift velocities of these irregularities range from 50 m/sec. to at least 360 m/sec (Balsley, 1969a,b). For velocities above 360 m/sec, the spectra become contaminated by type I echoes, showing the appearance of type I only. But at times, however, the type II spectra also show the velocities greater than 360 m/sec (the ion-acoustic speed), when the type I contamination is least (Balsley, 1969b; Cohen, 1973). Type II irregularities in the electrojet can, therefore, exist independently of the type I which means that type II can not arise from type I as postulated by Dougherty and Farley (1967).

7. During nighttime they travel eastward (Balsley, 1969a,b) in contrast to their daytime westward motion (Balsley, 1966), implying a close relation between type II irregularity motion and the electron flow obtained from dynamo theory of electrojet. Drift of these irregularities reverses, during both evening and morning hours, at the time that is reversal time of V_D, showing that the electron drift velocity and type II irregularity drift are zero at nearly the same time. Therefore these features along with those of (6) lead to conclude the fact that the type II drift velocity is linearly related to the true electron drift velocity (Balsley, 1967, 1969b; Fejer et al., 1975a,b).

8. They exhibit roughly isotropic structure of east-west/vertical velocity distribution of the random velocity

spreading about the mean drift velocity) (Balsley, 1969b).

9. Type II echo power is proportional to the square of the type II drift velocity (Balsley, 1969b).

10. A marked splitting (bifurcation) of the echoing region occurs at times well away from midday, when the electrojet intensity (i.e., V_D) is considerably much less than its normal midday value when the type I are produced (Bowles and Cohen, 1962; Balsley, 1965, 1969b; Fejer et al., 1975b). This implies that the type II are the only ones present when the electrojet is bifurcated; the type I appearing only when the two layers are well merged.

11. The irregularities appear only near the top and bottom edges of the electrojet under marginal conditions (Balsley, 1969b).

Radar observations (Balsley and Farley, 1971), at 16.25 and 49.92 MHz, corresponding to 10 and 3 meters irregularity wavelengths respectively, revealed that the enhanced backscatter return is a mixture of type I and type II. The type II irregularity amplitude falls off rapidly with the increasing backscatter radar frequency, so that enhanced backscatters at 146.25 MHz (1 meter wavelength) only have a type I spectrum with a definite threshold V_D. They (in 1973) further reported that (a) the spectra of the irregularities are usually still smeared and sometimes have two distinct peaks, showing the fact that the long wavelength irregularities are present; (b) the velocities corresponding to the spectral peaks at higher

vertical ones being comparable (Cohen and Bowles, 1967); (c) the fading times or lifetimes of the echoes in the lower region (below 105 km) are of the order of 0.03 sec or longer, and in the upper layer, the lifetimes are much shorter, often less than 0.01 sec.

Very recently, Fejer et al., (1973, 1975a,b) report the Jicamarca radar observations taken at a frequency of 49.92 MHz and deduce from them the following features of the irregularities. The phase velocity of the obliquely travelling waves varies drastically with the altitude and the velocity is very small in the lowest part of echoing region and then increases with height. The Doppler shift (phase velocity) and the irregularity strength vary rapidly in time at a given altitude and can even change sign (Balsley and Farley, 1973). During the day, echoes are observed only in a narrow altitude region about 20 kms wide (between 93 and 113 kms) with a single maximum in the echo strength at approximately 103 km, but sometimes, the maximum being at altitudes as low as 100 kms. At night, the echoes exhibit strongly layered structures and are concentrated in many (sometimes five or more) discrete thin layers, which can be at altitudes as high as 130 kms. The altitude of echoing region(s) changes when the electrojet reverses an hour or two after sunset (reversal time was found to be 2048 hr), i.e., there was an interchange in the altitudes of the echoing regions, The nighttime echoes can sometimes be nearly as strong as those observed during the day, even though the nighttime electron densities are 1-2

the observations show highly variable type I (as well as type II) echoes with both positive and negative Doppler shifts.

c) In-Situ Rocket Irregularity Observations:

With the advent of rocket and satellites, a new dimension has been added to the scope of radar observations discussed above. Using in-situ rocket-borne Langmuir (Prakash and Subbaraya, 1967) and resonance (Prakash et al., 1972) probes, many important characteristics of ionization density irregularities have been, further, obtained. While in-situ results support the radio and radar observations to some extent, many new exciting and important features have been revealed. We shall now briefly outline below the important properties and characteristics of those equatorial E-region irregularities which are of interest to our present studies, based on in-situ rocket observations at Thumba, India (Prakash et al., 1969, 1970, 1971a,b, 1972, 1973). Prakash et al. (1973) have recently summarized their rocket-borne measurements, and based on their scale sizes or spectral analysis (or both) and other characteristics, they have classified the irregularities into following types:

1. Larger Scale, Type L, Irregularities:

These irregularities have larger scale sizes of a few kilometers in the vertical direction and more than 40 kms in the east-west (horizontal) direction. These are observed only during nighttime flight (Prakash et al., 1970). The large scale structures of the irregularities are very prominently observed

in these structures is found to vary by a factor lying between 4 and 25, thereby giving them the appearance of distinct layers. These are found to appear randomly and in the form of discrete bursts in the regions of density profile which shows a large downward (negative) gradient (Fig.2.2), while the regions with an upward (positive) gradient are smooth and almost free of irregularities.

2. Medium Scale, Type M, Irregularities:

They have scale sizes ranging from 30 to 300 meters and can be classified into following types:

i) Type M_c: These irregularities, with scale sizes in the range of 30-300 meters, are observed only in the regions where the background electron density profile exhibits a positive gradient (density increasing with height) during daytime and evening twilight hours and a negative gradient during nighttime (Fig.2.2). They have amplitudes varying from a few percent to about 30 percent. From radar observations, these are identified as type II irregularities. They are observed in altitude region of about 90 to 130 kms. During daytime, these have large amplitudes (more than 20 percent) around 85 kms. The amplitudes decrease with increasing height, reaching a value of about 5 percent around 95 kms and showing a rapid decrease above about 95 kms. During nighttime also, the irregularities with amplitudes as large as 30 percent are observed, but however, they are confined to an extended height region from 90 to 130 kms. During evening hours, these are observed both

in the upper region, are smaller.

The amplitude and the size of the irregularities are found to decrease with increase in electron density. They are found to have a definite shape in the medium and exhibit a saw-tooth type structure, with a steeper rise than fall in electron density during the ascent of the rocket and with a steeper fall than rise during the descent of the rocket. On an average, as one moves along the directions of the positive gradients, the increase in the electron density is sharper than decrease.

ii) Type M_S: These irregularities have small amplitudes (only a few percent) and are observed to occur along with type S_S which are described below.

3. Smaller Scale, Type S, Irregularities:

The type S irregularities with amplitudes varying from 0.1% to a few percent, have scale sizes lying between 1 and 15 meters, and can be categorized into following types:

i) Type Sc: This type of irregularities with the scale sizes in the range of 1-15 meters, is observed to occur in the same height region where type Mc (with amplitudes as high as 30 per cent) are produced, but with much smaller amplitudes (from 0.1 percent to a few percent). They occur in the form of discrete bursts and the amplitudes of the higher scale sizes are greater than those of lower scale sizes. Using a power law, $E(k) = ck^n$ (where E is the power in wave number k and c is a constant),

(the spectral index n being -4 below 100 kms and -3 in the 110-140 kms region during evening time, between -2 and -4 around 90 kms during daytime and -4 around 95 kms and -3 around 120 kms during nighttime). Because of their occurrence on most of the rocket flights and their observed steep spectra in contrast to the type I flatter spectrum, the type Sc are identified as type II irregularities.

ii) Type Ss: They occur nearly continuously during midday only, in the altitude region of 100-120 kms where V_D is higher, with a peak intensity (maximum amplitude which is of the order of 1-2 percent) near 105 km. Even though the type Ss occur in the same scale sizes as type Sc, their nature is quite different. They are observed in all scale sizes ranging from 1 to 15 meters with nearly a constant amplitude at a given altitude and have a flat spectrum with spectral index zero, which is consistent with the flat type I spectrum observed at 16, 49.92 and 146.25 MHz (Balsley and Farley, 1971). Unlike type Sc (i.e., short wavelength type II), their amplitudes show no correlation with the electron density profile. The amplitudes of the irregularities are found to increase with the detector frequency. Based on the comparison between the profiles of the type Ss irregularity amplitudes and the profile of the electrojet current (Sastry, 1970) with a maximum around 105 km, the type Ss have been identified as type I irregularities.

1.32 F-Region Irregularities:

The irregularities in the equatorial F-region have been

since they were first observed with ionosonde measurements by Berkner and Wells in 1934. Till to-day, using a wide variety of observational techniques, several types of irregularities, such as large scale irregularities or large patches (~ several hundred kilometers in size), small scale field aligned irregularities (scale sizes ranging from a few meters to several kilometers) and travelling ionospheric disturbances (tens of kilometer and more in size), have been reported in the literature. Of these, small scale irregularities (scale sizes of the order of a few kilometers down to a few meters) are most intensively investigated and are, however, of fundamental importance to the phenomena of spread-F, first detected by Booker and Wells (1938). Larger patches (Large scale irregularities) are, in actuality, a collection of small scale irregularities, and spread-F will be seen as long as the patch is over an observing station. These irregularities have been thought to be manifestations of spread-F and therefore, the equatorial spread-F has been attributed to the irregularities (or inhomogeneities) in electron concentration (or density) in the F-region of the equatorial ionosphere.

Experimental observations on equatorial spread-F irregularities are obtained employing various techniques, e.g., ground-based ionosondes (a review on recent ionosonde work has been given by Rastogi, 1973), HF and VHF back-scatter as well as forward-scatter radars (Farley et al., 1970; Woodman, 1973), in-situ rocket-and satellite-borne probes (a review by Kelley, 1973), scintillations of satellite radio transmissions (Huang,

scintillation records (Koster, 1963), etc..Herman (1966) and Clemesha and Wright (1966) have comprehensively reviewed the earlier experimental observations on spread-F irregularities. The other reviews of work on spread-F irregularities and their associated phenomena have also been given by Kent and Wright (1968), Kent (1970), King (1970) and Nielson and Crochet (1972). Farley et al. (1970) have, recently, given a critical review on the VHF backscatter radar observations of equatorial spread-F irregularities and brought out difficulties that existing theories have in explaining many of the observations. Recent observations with HF and VHF backscatter radar (Farley et. al., 1970; Kelleher and Skinner, 1971; Kelleher and Rottger, 1972; Woodman, 1972, 1973; Balsley et al., 1972), in-situ rocket-and satellite measurements (Hanson and Sanatani, 1971; Hanson et al., 1972, 1973; McClure, 1973; McClure and Hanson, 1973; Dyson, 1971, 1973; Kelley, 1973; Dyson et al., 1974; Kelley et al., 1975) and other measurements like scintillations, have revealed a vast amount of new informations about the equatorial spread-F irregularities and their characteristics.

Although very recently, Farley (1974) has summarized their most important basic characteristics, we shall in the following catalogue those features which are mostly related to the interest of our present studies, made in the thesis: (1) The spread-F irregularities are highly field-aligned ionization density irregularities (Spencer (1955) who seems to have been

observed only at night (Martyn, 1959). They have never been observed during the day except that at times they may persist for a short period after sunrise (Farley et al., 1970); (3) Most of the irregularities have generally wavelike structures with both the 'noiselike' and the 'sinusoidal' appearances (McClure, 1973; Dyson et al., 1974). However, sometimes coherent non-sinusoidal structures of the irregularities are also observed (McClure, 1973; Dyson et al., 1974; Kelley et al., 1975); (4) The wavelengths are observed more or less simultaneously in a range from a few meters ($\sim$ 3 m) or less ($\lambda_\perp < \rho_i$ ion Larmour radius) to a few kilometers ($\sim$ 20 kms) or more ($\lambda_\perp >> \rho_i$) transverse to the magnetic field. Scintillation observations (Koster, 1963; Huang, 1970; Wernik and Liu, 1973) show that the most effective wavelengths are of the order of 200-300 m; (5) Generally, the irregularity amplitude is very nearly proportional to the irregularity scale size over the range 70 m to 7 km, i.e., the gradient in ion concentration are independent of wavelength (Dyson et al., 1974). In this wavelength range, they observed their power spectrum to be often approximately proportional to k^{-2} (k is wave number); (6) The irregularity amplitudes are observed in the range from 0.01 - .03 percent to less than 0.1 percent relative to the background electron density. However, at times they have amplitudes comparable to the largest auroral amplitude values. There are evidences that 'sinusoidal' structures with wavelengths from approximately 1 to 20 kms

percent are also observed (McClure, 1973; Dyson et al., 1974; Kelley et al., 1975); (7) Field-aligned irregularities usually appear in rather large patches; that is, when the irregularity structures do appear and are well developed, an extended region of the ionosphere is affected. This extent in the east-west direction has been observed from 100-400 meters to 1000 kms (Cohen and Bowles, 1961; Clemesha, 1964), in the north-south upto 1000 kms (Koster, 1963) and in vertical direction to heights a few hundred kilometers above 1000 kms (Woodman, 1972, 1973). The thickness of the patches appears to vary from 10-200 kms (Calvert and Cohen, 1961; Yerukhimov, 1962); (8) The irregularities are observed to have often very sharply (thin) layered structures (Woodman, 1972, 1973) as well as coherent, steepened wavelike structures (Dyson et al., 1974; Kelley et al., 1975) exhibiting an asymmetric east-west gradient on either side of the irregularity patch observed at HF frequencies, but more symmetric at the higher frequencies (Nielson and Crochet, 1972; Kelley et al., 1975); (9) The irregularities occur over a wide range of altitudes from as low as 250 kms to 1000 kms (well above the F_2 layer peak) at times. They are most often observed below F_2 peak (bottomside or underside of the layer) and are identified as bottomside spread-F. They can appear essentially simultaneously above, below and at the peak (Farley et al., 1970; Woodman, 1972, 1973; Balsley et al., 1972); (10) They usually appear first within an hour or two after sunset, only

minimum threshold altitude (~ 300 kms or more) exists which the bottom of the layer must lie above. At times they are generated almost anywhere in the F-region, no matter which way the region is moving. They persist often for several hours as the layer moves downward and then are eventually quenched. In a period before sunrise when the electron densities are small, they are also observed even if the layer is at fairly low altitudes (Farley et al., 1970; Woodman, 1972, 1973; Balsley et al., 1972); (11) The drift velocities of the irregularities are comparable to those of F-layer. Their drifts range from 10 to 500 m/sec. The most probable speed is 60-100 m/sec. The drift direction is predominantly east-west (Kelleher and Rottger, 1972), being east by day and west by night, and north-south component is zero (Cohen and Bowles, 1961; Calvert and Cohen, 1961). The vertical drift velocities often are 100 m/sec (3 to 4 times greater than that of normal undisturbed region) with mean downward velocity being ~ 25 m/sec and the mean upward velocity being as large as 50-60 m/sec, whereas the mean eastward velocity is ~110 m/sec (Balsley and Woodman, 1969; McClure and Woodman, 1972; Balsley and Haerendel, 1972; Rottger, 1972), implying that the drift velocity varies rapidly with the altitudes. Small(weak) perturbations are observed to travel with an apparent slower speed than the large (strong) perturbations which produce strong echoes returning from the regions close to F-region peak (Farley et al., 1970); (12) Growth times of the irregularities range from a few seconds or less to a few tens of minutes (~ 30 min) or more (Farley et

regions, two types; (a) a range-spreading occuring mainly before midnight and (b) a frequency-spreading occuring later in the night, have been observed (see sec.1.23a). Recent VHF radar studies indicate, further, that there may be two (or even more) different classes for each type of spread-F irregularities, at short wavelength at least, just as there are two types (Type I and Type II - sec. 1.31a and b) of E-region irregularities. One class of F-region irregularities is weak and produces a very narrow Doppler spectrum (Farley et al., 1970), whereas the second corresponds to much stronger spread-F echoes, with a wide spectrum and the turbulent drift velocities (electric fields) with fluctuations larger than their mean (Balsley et al., 1972).

These density irregularities which serve as a means of studying the ionospheric plasma, have also been observed and investigated by artificial means, for example, in artificially generated ion plasma clouds related at the equatorial E-and F-region heights (Rieger, 1969, 1971, Haerendel et al., 1970; Davis and Moore, 1970; Davis and Althouse, 1970; Davis, 1971; Valenzuela et al., 1973; Raghavarao et al., 1976), in a reflex arc plasma produced in the laboratory (Hooper, 1970; Hooper and Girvin, 1971) and in other recent laboratory experiments simulating the certain essential characteristics of the equatorial electrojet (D'Angelo et al., 1974, 1975; John and Saxena, 1975a,b, 1976a,b; Saxena and John, 1975). The observations of local conditions favouring the formation of the field-aligned striations (irregularities) in the plasma

their observed features, such as growth, spectrum, propagation, scale sizes, evolution, etc., provide a valuable source of information regarding the nature of ionospheric irregularities. Such observations are quite helpful and provide a better insight into the understanding more clearly of the source (instability) mechanisms which are responsible for the generation of the irregularities described above.

By virtue of their observed features, dispersion characteristics and the conditions of their occurrence, these artificially created irregularities have been identified as the naturally occuring Type I (D'Angelo et al., 1974; 1975; John and Saxena, 1975a, 1976b) and Type II (Davis and Moore, 1970; Davis and Althouse, 1970; Davis, 1971; Hooper, 1970; Hooper and Girvin, 1971; Ogawa, 1972; Saxena and John, 1975; John and Saxena, 1976b) irregularities. In view of the present studies, the author is interested in understanding the instability mechanisms which could explain the formation of naturally occuring ionospheric irregularities. We will not therefore, be describing the observations of artificially produced irregularities.

1.4 Possible Instability Mechanisms Associated with the E- and F-Region Irregularities:

The main concern of the work done in this thesis is a theoretical study most relevant to the above-mentioned plasmawave irregularities of ionization density occuring in equatorial ionosphere. In recent years, although a large

been advanced in accounting their production and many of the observed features, there are a few other important basic characteristics whose explanation is still uncertain and the detailed agreement between the theory and these observations is not wholly established. Therefore, more theoretical work is, further needed as suitable theories are not yet developed. The difficulty lies in the fact that so many parameters exist in the study of ionospheric plasma that it becomes very much cumbersome to consider them all simultaneously. Because of this complexity, it is almost likely that there are many different physical processes (instablity mechanisms) which may be responsible, individually or collectively, for the occurrence of ionospheric irregularities.

In the preceding section, we laid out the observational features and properties of the density irregularities. Now we turn our attention to the investigation of the sources of their origin. It is now certain that the ionospheric irregularities have been identified as some kinds of waves or oscillations or fluctuations or perturbations occuring in ionospheric plasma. The ionospheric plasma which is, as has already been mentioned, a weakly ionized inhomogeneous plasma embedded in orthogonal d.c. electric and magnetic fields (at the equator), can become unstable against self excitation of a large variety of waves and natural modes of oscillations. At any frequency, these oscillations or fluctuations can, in general, be grouped into two classes: essentially the electromagnetic transverse

somewhat like sound waves (acoustic waves). While both these types of modes, appearing as plane wave irregularities, may be present in the E-and F-regions, there are experimental evidences that the irregularities are, in general, of electrostatic types because the longitudinal electrostatic waves which exist only in matter, are most sensitive to the properties of plasma. The electrostatic modes, therefore, represent the principal subject of interest of our present studies and will, thus, be explored in the present theoretical investigation made in the following chapters. However, we shall restrict ourselves to those perturbations (i.e., modes of oscillations) which occur only in the ionization density, as these are more relevant to the observations of ionospheric irregularities.

The source of the origin of these density fluctuations (waves) may, naturally, be identified with one of the plasma instabilities or more than one operating simultaneously. Several instability mechanisms, by a number of workers, have been suggested so far, as the source of the above-discussed different types of irregularities, e.g., Type I and Type II in E-region and F-region irregularities. A number of reviews has been given by various authors on the instability theories of equatorial E-region irregularities (Whitehead, 1970a; Kato, 1972; Tsuda, 1973; Farley, 1974) and of equatorial spread-F irregularities (Farley et al., 1970; Cole, 1973; Farley, 1974). As being the most successful mechanisms for

which have attracted considerable interest soon after they were proposed to be operating in the ionosphere and have been most extensively investigated theoretically by several workers, are classified, according to their source of driving energy, mainly,into three kinds: (i) The Cross-Field ($\underline{E} \times \underline{B}$) or Gradient-Drift instability; (ii) The Two-Stream instability, both being applied to E-region and (iii) The Gravitation-induced Rayleigh-Taylor instability having relevance to F-region. These all are generally low frequency instabilities, the frequency of oscillations, ω being less than or comparable with the ion cyclotron frequency, Ω_i (sometimes ω may have values greater than Ω_i, for example, in the case of two-stream instability). An attempt has been made here to present the theoretical treatment of these three kinds of low frequency electrostatic instabilities, in both linear and nonlinear regimes, which are capable of giving rise to growing irregularities and appear to explain satisfactorily some of their important basic features observed during both day and night time in the E-and F-regions of equatorial ionosphere.

It is not intended that this chapter should outline the development of existing theories of the instabilities just mentioned, especially within the context of ionospheric irregularities, but rather that it should at least provide, for reasons of completeness, basic need and unity, their specific physical mechanisms describing how they are produced in terms of basic plasma physics concepts. The theories of

in the different chapters of the thesis (Chapters II, III and IV). However, a physical description on how the instabilities operate, is necessary to study the properties of modes (irregularities). Therefore, before concluding this chapter, we shall give below the definitions and a pictorial view of these three instabilities to have a physical insight into their driving mechanisms and to understand their formation, in the equatorial ionospheric regions of interest.

a) The Cross-Field or Gradient-Drift Instability:

In the presence of orthogonal d.c. electric and magnetic fields, an inhomogeneous weakly ionized plasma, such as equatorial ionospheric plasma, is subject to an electrostatic instability commonly called 'Gradient-drift instability' if there exists an appreciable gradient in plasma density. While the name 'gradient-drift' is assigned because of the fact that the charged particles drifts are involved in the instability excitation in presence of density gradient acting as the energy source of the instability, it has also been known as 'Cross-Field (or $\underline{E} \times \underline{B}$) instability' (because the crossed electric and magnetic fields act as driving forces of the instability) or 'Drift-resistive instability (because of an important role played by the neutral particles in the form of collisions with the charged particles, giving rise to finite resistivity). The instability produces, in general, low frequency electrostatic charge density oscillations having characteristic drift frequency, ω small compared with Ω_i.

with the phase velocity $V_p(\omega/k)$ which coincides with the drift velocity of the plasma particles caused due to the combined effects of pressure gradient and electric field with $\underline{B}_o$. This instability, under specific suitable conditions, can give rise to the growing irregularities in ionization density that are aligned along the direction of magnetic field.

The basic physical picture of this instability of the charge density perturbation can be understood on the basis of Rosenbluth-Longmire picture taking into account the fact that the ions and electrons do not drift equally in crossed electric and magnetic fields when finite resistivity is included (Rosenbluth and Longmire, 1957). One of the modes in which this instability can operate has been given by Tsuda et al., (1966), Sato and Tsuda (1967), Reid (1968), Sato et al. (1968), and McDonald et al. (1975) for E-region and by Williams and Weinstock (1970) for F-region and is illustrated here in the Fig.1.3. Its mechanism is solely due to the difference between electron and ion mobilities versus neutral particles. Suppose that the steady background density gradient, ∇n_o and an applied d.c. electric field, $\underline{E}_o$ both acting vertically upward (in x-direction) exist, together with the ambient magnetic field, $\underline{B}_o$ directed into the paper (in z-direction), as shown in Fig.1.3. The horizontal line represents an unperturbed contour of constant electron concentration. If now the density is perturbed by small-amplitude sinusoidal (a plane wave) variation with wave-front parallel to the

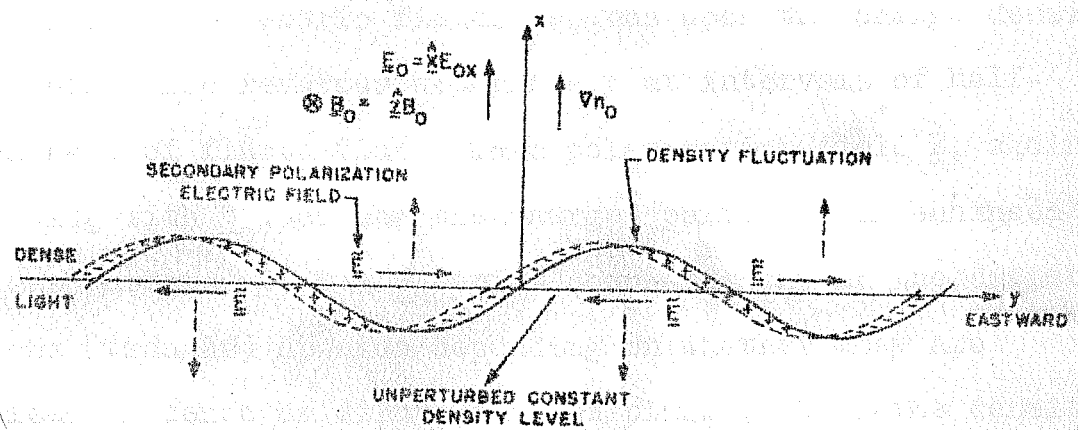


Fig.1.3. Simplified schematic physical picture showing irregularity formation process. Secondary polarization fields $\underline{E}$ (solid arrows) and the magnetic field $\underline{B}_o$ force the ionization along the vertical directions (broken arrows), causing the density fluctuation shown to enhance if the background density increases with increasing x(height).

make them move to the left (in y-direction). Since the Hall mobility of the ions is always less than that of electrons, the medium will be polarized. The space charges will then appear as a result of the electron and ion density profiles being somewhat out of phase, which in turn, gives rise to small scale secondary polarization electric fields, $\tilde{E}$ as shown by solid curves in Fig.1.3. Since the intensity of induced (polarization) electric fields depends upon the charge density, their direction reverses alternately at intervals of half-wavelength of fluctuations. This polarization field $\tilde{E}$, again operating with B_o, causes the charged particles in enhanced regions (crests) to $\tilde{E} \times B_o$ drift downwards and in the depleted regions (troughs) upwards depending on whether they are immersed in dense or dilute ambient plasma. Thus the density perturbation develops getting enhanced in the region of crests and reduced at the troughs, so that the mode is unstable and appears to grow in amplitude, making clearer contrast against the background density.

One can easily realize from the picture that if either the electric field, E_o or the density gradient, ∇n_o were reversed in direction, the perturbations would tend to disappear, giving rise to stable situation. Thus the perturbations amplify in amplitude only when the electric field, E_o and the background density, ∇n_o are appreciable and in proper directions. For small amplitude waves, the effect of classical diffusion counteracts this growth process

instability beyond which the diffusion is not sufficient to smooth out the disturbance.

In Fig.1.3, we have demonstrated a mere schematic representation of the case when $\underline{E}_o$ is directed straight upward so that the difference of the ion and electron Hall mobilities is important. Similarly, we can have another mode of operation of the gradient-drift instability even when the applied electric field is directed toward right (in y-direction) instead of upward, but then the difference of the ion and electron Pedersen mobilities is more important. And their opposite directions now tend to produce a similar periodic space-charge potential which leads to similar results. But, however, this latter mode generates larger wavelength irregularities at greater altitudes in the ionosphere than the former mode (Reid, 1968).

b) Two-Stream Instability:

The two-stream instability is perhaps the most extensively investigated in plasma physics and appears to be the first plasma instability to be treated theoretically and/or observed experimentally. It can certainly be traced back at least 25 years (Bohm and Gross, 1949) and with some generosity all the way back to Langmuir in 1925 (which is the year zero in plasma physics calender). If the plasma contains particles with directed energy due, for example, to the electron drift velocity (giving rise to the electron streaming) of the current carrying electrons, another

can be excited. When the current (or drift velocity) reaches a certain threshold level, the plasma becomes unstable and strong electrostatic type waves with phase-fronts aligned with the magnetic field are generated by the excitation of the two-stream instability (Buneman,1959).

In general, the two-stream instability develops due to the interaction of two groups of plasma particles drifting with respect to each other. This instability leads to growing longitudinal electrostatic waves, which derive their energy from the kinetic energy associated with the relative drift velocity of the particles (i.e.,relative electron streaming). These waves which are high frequency oscillations with frequency, ω, greater or equal to Ω_i and have smaller wavelengths compared to those produced by the gradient-drift instability, are of mainly two types: electron oscillations at a frequency of the order of $\omega_{p.e}$, excited when the drift velocities of the electron (V_D) relative to the ions exceeds the mean electron thermal velocity (V_e); and ion-acoustic oscillations at about ω_{pi} when $V_e > V_D > C_s$ (where C_s is the ion-acoustic speed). The first type is excited with $V_p = V_D$, while the second one with $V_p = C_s$ (slightly greater than the mean thermal velocity of ions), and the latter have smaller growth rates (Buneman, 1959).

In the equatorial electrojet, one of such conditions on the electron drift velocity, namely $V_D > C_s$ is easily satisfied at least during the day time. Such longitudinal

therefore, be excited in the electrojet by the two-stream instability driven due to cross-field streaming electrons relative to ions. These smaller wavelengths waves growing in amplitude, propagate in the direction exactly normal to earth's magnetic field and are those which manifest themselves as the ionization density irregularities associated with Type I backscatter echoes (as shown independently by Farley (1963a,b) and Buneman (1963)).

The two-stream instability which is also known as 'Farley-Buneman instability' as they first developed it independently for equatorial electrojet, has had considerable success and has been well received as a possible mechanism for the formation of Type I irregularities. Basically, its physical mechanism describing how it operates, is similar to that of cross-field instability just discussed, with the difference that there is no vertical density gradient in the present case of the two-stream instability and is briefly described below.

We know that the equatorial electrojet is characterized by magnetized electrons ($\nu_e << \Omega_e$) and collisional ions ($\nu_i >> \Omega_i$). The crossed ambient vertical polarization electric field and the horizontal (south-north) earth's magnetic field, then lead to a cross-field streaming of electrons with respect to ions in y-direction (Fig.1.3) as the ions are tied up with the neutrals because they are highly collisional. Suppose that the horizontal density

(sinusoidal) oscillation as shown in Fig.1.3, the secondary polarization electric field $\underline{\tilde{E}}$ is then produced, alternately in directions at the interval of half wavelengths because of the phase difference between electron and ion density profiles which arises due to the ions lagging behind the electrons as the ions are much heavier than the electrons. This secondary field $\underline{\tilde{E}}$ crossed with $\underline{B}_o$ makes crests (troughs) of the perturbation to move downwards (upwards). Now if initially, the magnitude of relative electron-ion streaming drift velocity is greater than C_s, the given perturbations become unstable and in turn, they will continue to grow in amplitudes giving rise to a form of spectrum of longitudinal electrostatic plane waves, called ion-acoustic waves, with wave-front parallel to ambient magnetic field.

c) Rayleigh-Taylor Instability:

It is well known that an interface dividing the heavy incompressible fluid on the top from the supporting lighter incompressible fluid at the bottom in a gravitational force field, is unstable. Such an instability is called Rayleigh-Taylor (R-T) instability investigated first by Rayleigh (1916) for the case of hydrodynamic fluids. This instability is, in fact, the fundamental magnetohydrodynamic instability of an incompressible fluid interface experiencing an acceleration, g which may be due to either real gravitational force or equivalent effective gravitational force due to different plasma configurations (Chandrasekhar 1961)

In analogy with this instability of a fluid interface, the plasma interfaces in different given plasma situations also become unstable to the small amplitude perturbations. For example, in the situation where the plasma (regarded as heavy fluid) is supported against gravity by the magnetic field (lighter fluid), the plasma-vacuum interface is one which is unstable. In another example, which is of our interest, the plasma-plasma interface in the situation where an inhomogeneous incompressible plasma is supported against gravity by a magnetic field, is prone to this R-T instability. In this latter situation, the upper plasma region with higher density above the interface can be regarded as the heavy fluid, while the lower region with smaller density below the interface as the lighter fluid, thereby fulfilling the R-T instability criteria.

In the ionosphere, a number of competing processes, such as production, recombination, and transport of electrons and ions, exist. These processes cause the ionosphere to form a layer (e.g., a layer in the F-region) whose underside has a positive density gradient and hence fulfills broadly the light fluid-supporting-heavy fluid description and therefore, is susceptible to the instabilities of R-T type. The physical description of how the R-T instability operates or is driven in the plasma situation of our interest, can be understood, on the basis of following two principles.

i) Drift Analysis: This instability is physically under-

caused by the gravitational drifts of ions and electrons arising due to the effect of gravity, $\underline{g}$ and the magnetic field, $\underline{B}$. The charge seperation so produced, which in turn, results in a polarization electric field, is able to overcome exactly the restraining influence of the magnetic field.

To understand how the instability is, basically, caused, consider the situation depicted schematically in Fig.1.4, where an incompressible inhomogeneous plasma with density increasing in the direction opposite to the direction of gravitational force, is supported against a z-directed gravitational force ($\underline{g} = -\hat{z}\, g$) by a x-directed magnetic field ($B_x = \hat{x}\, B$). Imagine that the plasma-plasma interface (a solid horizontal line) is perturbed by a small-amplitude electrostatic plane-wave perturbation as shown in Fig.1.4. The ions and electrons initially drift parallel to y-axis as a result of $\underline{g}$ and $\underline{B}_o$, with the drift velocities.

$$V_j^{\alpha} = c\,\frac{m_\alpha}{q_\alpha}\,\frac{\underline{g}\times\underline{B}}{B^2} \qquad ..(1.17)$$

Since the drift velocity is inversely proportional to the charge-to-mass ratio, the ions and electrons will have drift in opposite directions and the ions have a velocity that is m_i/m_e times greater than the electrons. Thus the ions drift from the electrons, both getting accumulated on the interface and consequently, a charge seperation is developed, resulting in a space-charge potential and hence an electric field $\underline{E}'$, as shown in Fig.1.4. Now the ions and electrons will drift in the z-direction as a result of this electric field $\underline{E}'$ and the

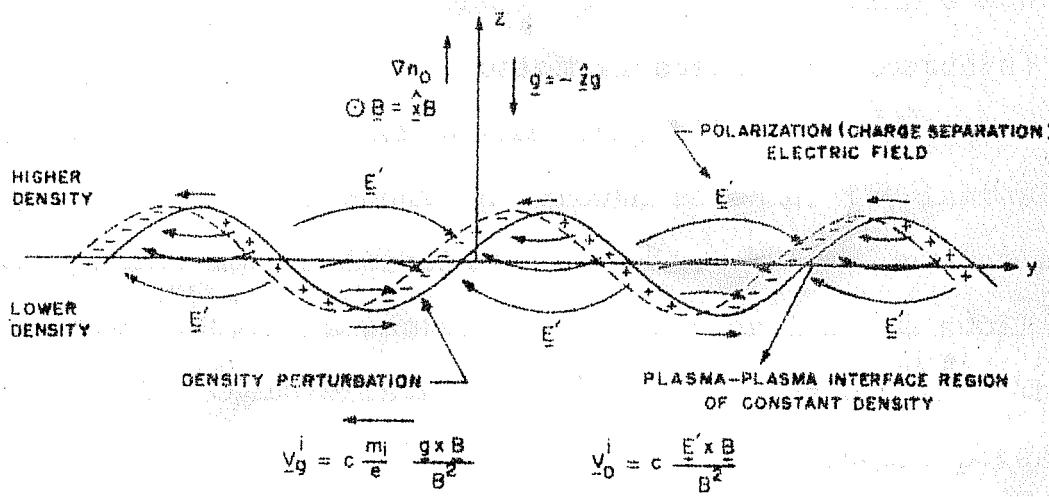


Fig.1.4. Simplified schematic physical view of perturbation of the plasma-plasma interface region in an inhomogeneous incompressible plasma supported against gravity $\underline{g}$ by a magnetic field $\underline{B}$, showing the development of the charge separation electric field $\underline{E}'$ caused by the $\underline{g} \times \underline{B}$ drift motion.

and electrons, because of this drift, move in such a way so as to increase the amplitude of the initial perturbation and thereby, making the system unstable as the perturbation grows.

ii) Energy Analysis: The energy principle determines whether or not a given plasma equilibrium is stable (or unstable) as a function of equilibrium parameters, but in general it does not give information about the growth rates of the instability or the plasma motion associated with it. Thermodynamically, an isolated system is unstable if, after applying a small perturbation, there exists a state of lower potential. The system itself will seek out, if possible, the lowest potential energy. As a consequence of conservation of energy, the extra energy goes into the kinetic energy of the instability. Hence such a plasma system will be unstable.

Now consider an ionosphere layer, in particular the underside of the F-layer, at a given time as sketched in Fig.1.5. Suppose an arbitrary small amplitude perturbation is introduced, as shown by the dotted line in the figure, to the underside of the F-layer in the ionosphere. To know the stability of the layer, one has to find out whether the system has increased or decreased its total energy. The difference in total energy is, essentially, due to interchange of fluid marked 1 with the fluid marked 2 in the Fig.1.5. Since the interchange is taking place in a direction parallel to both gravity and pressure force, the perturbed ionosphere

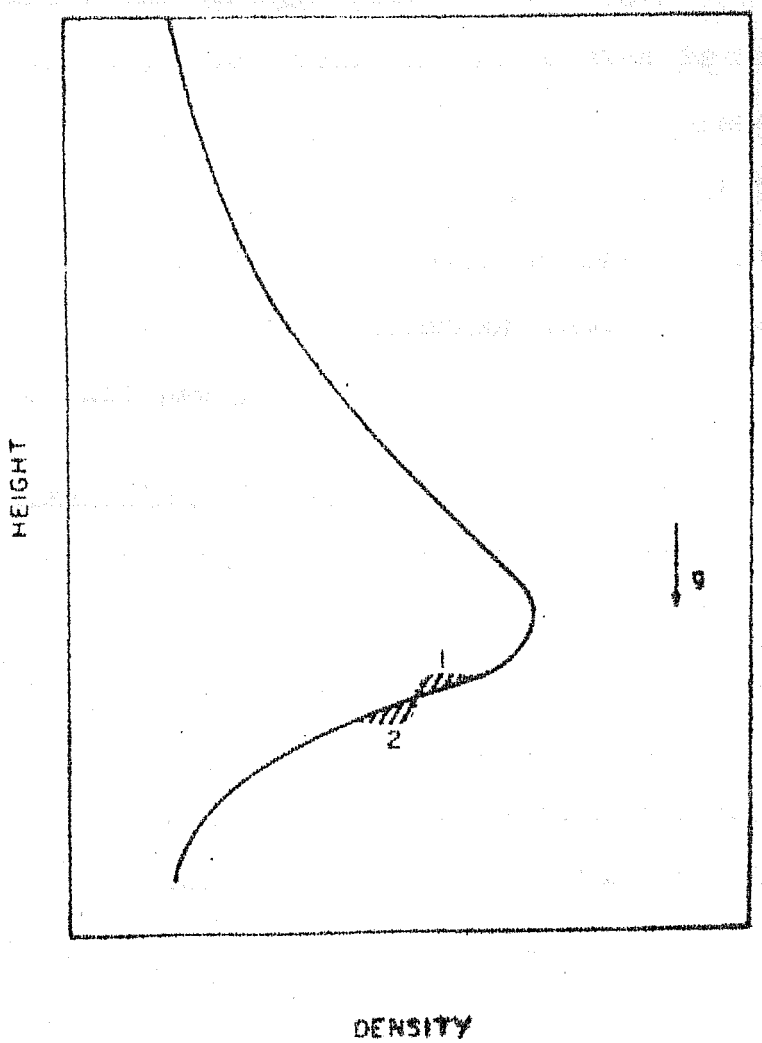


Fig.1.5. Sketch of ionospheric F-layer showing possibility for instability.

is unstable.

Of course, the energy-conservation arguments for instability to occur, are valid if the system is isolated and this is, in general, not the case here due to presence of production and recombination. Intuitively, it is then expected that the growth rate of such an instability must be able to compete with the recombination rate in order that instability should prevail.

1.5 Statement of the Present Work:

The prime goal of the investigation presented in the thesis is to make a detailed theoretical study of the above-discussed three instabilities which seem to have relevance to the subject of equatorial ionospheric plasma and hence, to the density irregularities observed during both day and night time conditions in the E- and F-regions. Waves (irregularities) under certain specific conditions discussed in the preceding sections, grow both with distance traversed and time. Conditions for the occurrence of such unstable modes, and their characteristics, such as the phase velocities, frequencies, amplitudes, structures, etc., are some of the major points in the investigation of the instabilities. Since the irregularities with a broad range of amplitude, wavelengths, etc., are observed under a wide variety of circumstances, both the linear and nonlinear theories of the instabilities have been developed in the thesis so as to account for most of the

There has been a considerable progress in the linear analysis of the instabilities in last decade or so. However, the linear analysis can predict only the existence or non-existence of the instability without a description of its subsequent development. Also it can yield only the critical (threshold) conditions on the parareters which are either responsible for the onset of the instability or related to the characteristic properties of the instability. Although many observational aspects of laboratory plasma, ionospheric irregularities and plasma cloud experiments in the ionosphere are brought into light on the basis of the linear dispersion relation, it fails to decide the ultimate fate of an initial perturbation which grows indefinitely in amplitude in the linear limit. One essentially demands that the wave amplitude should not grow indefinitely so as to have some stable configuration of the system.

It is widely recognized that the unstable plasma in nature is destined to result into after a long time of development, a state known as turbulent or nonlinear state arising due to preponderances of various unstable modes under different conditions, in which the energy supply to a plasma system may be in harmony with energy dissipation from it. This limits the amplitude of indefinitely growing perturbation as a result of some damping mechanism operating, which enables the wave to get saturated at some finite value of amplitude. The nonlinear treatment of the instability is thus mandatory so as to decide an appropriate instability saturation mechanism

the amplitude, frequency shift of the finite modes which grow linearly above the critical point and later saturate at some finite amplitudes. The nonlinear analysis is not only helpful in the study of long time behaviour of the instability, but it can also unravel many new basic phenomena which can never be recognized at the linear stage. This should clearly provide us with a clearer understanding of the existence and the basic mechanisms of the irregularities and some of their observed features. In this thesis the author has, therefore, tried to make a modest attempt on the nonlinear theories of the instabilities concerned.

Since the analytical treatment of the 'full nonlinear' development is too difficult to handle due to complexities both in the physical as well as mathematical concepts, our attention will be devoted mainly to the case of weak nonlinearity in which the assumption of sufficiently small amplitude perturbation can be made, in consistent with the observed amplitudes of the irregularities. With this assumption, the terms of the order higher than cube of the amplitude of the perturbation are considered negligibly small in the nonlinear set of ordinary and differential equations describing the unstable modes.

A plasma and its dynamics can be described in many possible ways. In the fluid approach which is valid when the collision mean free-path of the particles is small compared with the macroscopic scale lengths involved, the plasma can be treated as being composed of an electron-fluid

The macroscopic lengths in this study are the wavelengths of perturbations. We shall, therefore, use the two-fluid model as the basis of our studies in the following chapters.

The author starts with the investigation of the gradient-drift or Cross-field instability in Chapter II, which is the potential candidate, as is widely accepted, for type II irregularities in the E-region. This study was, in fact, completed a long time ago with a primary objective to consider the effect of both the primary horizontal (E_{oy}) and vertical polarization (E_{ox}) electric field together, which was not taken into account by any earlier workers. The present study has included, for the first time, the combined effects of E_{ox} and E_{oy} through an approximate relation $E_{ox} = (\sigma_2/\sigma_1) E_{oy}$, which is valid for equatorial ionosphere. Furthermore, the treatment of the theory has been more general because it includes the propagation of the waves in the vertical direction also.

The characteristics of the irregularities, such as the growth rate (ω_i), the minimum unstable wavelength (λ_{min}), etc., for a number of situations prevailing in the ionospheric region of interest and their variation with altitude have been studied in detail. The dependence of ω_i and λ_{min} on the variations in the horizontal electric field, background electron density and the background density gradient is investigated. The author also discusses the importance of vertical polarization field in the formation of smaller wavelength and fastest growing irregularities. The theoretical results so obtained, are then applied to the equatorial

density profile. The chapter ends with the comparison of results of the theory with the observations of Type II irregularities associated with the Type II backscatter echoes in the equatorial E-region.

In the third chapter, the author discusses a special class of coherent, weakly, nonlinear Type I modes in the equatorial electrojet, which are believed to be excited by two-stream instability. Introducing a dimensionless independent variable ξ in the wave frame, the partial differential equations describing one-dimensional Type I modes are converted into an ordinary differential equation. Having retained the quasilinear modification of E_{ox} (which provides quasilinear saturation mechanism) and ion viscosity, an amplitude dependent nonlinear dispersion relation for such nonlinear modes is found for weak nonlinearity. A study of the stability of these nonlinear modes against long wavelength, slowly varying amplitude perturbations is carried out both analytically and numerically.

We have made further investigation in support of our analytical calculations by solving numerically the exact set of basic nonlinear equations of Type I modes which otherwise, are intractable by conventional analytical methods. It is very encouraging that there is a reasonable agreement between the analytical and numerical results. This is also interesting to note that these results seem to explain the existence as well as some of the observed features of Type I irregul-

Low frequency incompressible waves in the equatorial F-region, that seem to be responsible for equatorial spread-F, are studied in Chapter IV. In this chapter, the author has made an investigation of the nonlinear evolution of the gravitation-induced Rayleigh-Taylor instability which may be one of the possible mechanisms for the generation of equatorial spread-F irregularities.

Following the method similar to one that is described in chapter III, and including the finite Larmor radius (FLR) corrections, we have looked for a stabilization mechanism for Rayleigh-Taylor modes. The finite larmor radius corrections are found to be responsible for the existence of nonlinearity in the wave-equation and therefore, may have an important role to play in connection with nonlinear interactions of waves. The existence of coherent, weakly nonlinear, almost sinusoidal stationary solutions of the nonlinear equations describing R-T modes has thus been investigated. The final structure of the R-T modes and the shapes in which these would travel in the F-region are discussed in details. Finally, the theoretical results obtained in this chapter are also compared with the observations of equatorial spread-F irregularities made by in-situ rocket and satellite measurements.

The principal results of the investigations presented in this thesis are then summarized in the last chapter. It also includes discussions on the relevance of the theoretical studies made in the thesis [illegible]

of the ionization irregularities occuring in the equatorial E-and F-regions of the ionosphere. In addition, a short investigation has been made to explain how the instability mechanism discussed here, can also support the formation of equatorial sporadic E(E_{sq}), the disappearance of E_{sq} with sudden decrease in the magnetic field value and their correlation with the equatorial electrojet and the equatorial spread-F. Lastly, the limitation of the work and the scope for further work have also been discussed.

CHAPTER II

LOW FREQUENCY LINEAR GRADIENT-DRIFT OR CROSS-FIELD INSTABILITY IN THE EQUATORIAL E-REGION

2.1. Introduction:

In recent years, considerable attention has been focussed on the low-frequency electrostatic drift instabilities in the inhomogeneous weakly ionized plasma existing under various situations. Of particular interest to us here is one in which an inhomogeneous weakly ionized plasma is immersed in crossed electric and magnetic fields. It is well established now that under suitable conditions such a plasma configuration is driven unstable against small amplitude perturbations by the zero-order drifts and density gradients. The concerned instability which is directly excited for wavelengths greater than a few meters ($>$ 10 meter at least) is known as gradient drift instability or cross-field ($\underline{E} \times \underline{B}$) instability. This instability is now widely believed to be the potential candidate as the source of many of the ionization density irregularities observed in the equatorial E-region, for example, type II, Mc and Sc irregularities discussed in sections 1.31(b) and (c). There exists a number of theoretical and experimental investigations on this instability.

The drift instabilities in an inhomogeneous fully ionized plasma in the presence of a uniform magnetic field have been discussed by Tserkovnikov (1957) and Rudakov and Sagdeev (1961). The theory of this instability has been

(1957) on the stabilization of flute-like instability in a low density plasma where the collisions between the charged particles could be neglected. The drift waves are, however, obtained in the investigation of the weakly ionized plasma where the collisions between the charged particles and neutral gas atoms are dominent and an external electric field is applied normal to the magnetic field. When an appropriate density gradient across the magnetic field exists in the plasma, such drift waves are excited by the so called cross-field or gradient-drift instability (or 'drift-resistive instability' as collisions giving rise to resistivity, take part). This instability is driven by the density gradient in the presence of particle drift due to the crossed electric and magnetic fields ($\underline{E}_o \times \underline{B}_o$ drifts), that is, the energy which is poured into the growing electrostatic waves is extracted from the sources such as the density gradients, particle drifts and ambient electric fields.

In the ionospheric E-region plasma which is collision-dominated and satisfies all the conditions that are necessary for onset of the instability, this $\underline{E} \times \underline{B}$ instability can give rise to the growing irregularities in ionization density observed at wavelengths greater than a few meters (> 10 meters), e.g., Type II (Jicamarea HF back-scatter radar observations) and Type Mc and Sc (in-situ rocket measurements in India) whose characteristics have already been discussed in details in sections 1.31 (b) and 1.31 (c). This instability is similar to the hydromagnetic negative drift instability and the

physical process that explains how $\underline{E} \times \underline{B}$ drift in presence of a density gradient leads to this type of instability, can be understood on the basis of the work of Rosenbluth and Longmire (1957) and has been demonstrated in section 1.4 (a). It has been shown that this instability results from the Hall or Pedersen drift of the charged particles in the presence of a plasma density gradient. In the lower ionosphere where the Hall mobility is much higher than the Pedersen mobility, the instability is determined by the (electron) Hall motion (Hall mode). On the other hand, the Pedersen mobility dominates in the upper E-layer and consequently, the instability is controlled by the (ion) Pedersen motion (Pedersen mode). Since, we have no remarkable density gradient in the upper layer in normal equilibrium state, the Pedersen mode does not seem so essential for irregularity formation as the Hall mode in the lower E-layer.

In fact, the gradient drift instability is very similar to the well-known gravitational flute instability (Rosenbluth and Longmire, 1957). The gravitational potential is replaced by the electric potential, ϕ_o which drives the electrojet drifts. Instability arises when the electron density increases in the same direction as the electron potential energy ($-e\phi_o$) increases, in analogy to the situation of a dense-fluid supported by a lighter-fluid. The actual mechanisms by which the potential energy is released, relies on unequal drift of the electrons and ions. In the gravitational instability, the drifts are proportional to the electron and ion masses, whereas

essential role in producing unequal drifts in the presence of an electric field.

Originally, the gradient drift instability was first derived by Simon (1963) and Hoh (1963), independently, in an attempt to explain the instability observed in the laboratory plasma (bounded along the ambient density gradient) of Penning-type discharge (Chen et al., 1962). Following Kadomtsev and Nedospasov (1960), these authors predicted that such a plasma will be unstable to the gradient drift instability if the applied electric field exceeds a critical value (threshold) and the sign of the product of the electric field and the density gradient, both perpendicular to the magnetic field, be positive. They showed that under such conditions, the instability grows as the collisional damping is overcome. Later, Morse (1965) extended the analysis to a more generalized form, i.e., two-dimensional linear analysis, giving an exact mathematical solution for an exponential layer of the plasma.

As regards to its application to the ionosphere, the basic idea of the cross-field instability seems to have originated first from Martyn (1959) who inferred that the ionization density irregularity in ionosphere might grow in the presence of a gradient of the ambient ionization density. Soon afterward, such intuitive arguments met with an objection by Fejer (1959) who showed that a magnetic field-aligned slab irregularity is not unstable. Note that these two studies concerned only the F-region where the Hall conductivity σ_2 is much smaller than the Pedersen conductivity σ_1. Kato (1972)

$\nu_i >> \Omega_i$ ($\sigma_2 >> \sigma_1$) as in the electrojet.

Maeda et al. (1963a,b) appear to have been the first to develop the linear theory of this instability for the conditions prevailing in the equatorial E-region where $\sigma_2 >> \sigma_1$. Making some particular modifications to the analysis of Simon (1963) so as to make the theory applicable to the present ionospheric model and taking the background density scale length of $\sim$ 1 km, they suggested that this instability with wavelength of $\sim$ 100 meters could give rise to the formation of the inhomogeneity (irregularity) in charge density responsible for the equatorial sporadic E-layer and is well correlated with the electrojet. Later, Knox (1964) applying the instability specifically to the equatorial ionospheric E-region, showed that with an electron drift velocity of $\sim$ 1 km/sec and background density scale height of $\sim$ 2 km, instabilities of wavelengths of 10-600 meters would develop and could be the cause of the formation of E_{sq}, whereas Whitehead (1967) showed that a rather thicker E-region and lower electron velocity could give rise to the instabilities with wavelengths of 20 meters to 6 kms. Tsuda et al. (1966), however, followed closely the analysis of Simon (1963) and explained the formation of sporadic-E, inferring that large amplitude irregularities have structures very different between east-west and north-south directions. Several other linear theories of this instability (e.g., Kato and Hirata, 1967; Whitehead, 1968; Sato et al., 1968, etc.) have also been

observed features more satisfactorily.

All of these linear analysis have, however, suffered from artificialities which have been necessary from the point of view of mathematical tractability. For example, in all these cases a special (sinusoidal) shape suitable for bounded laboratory plasma, has been postulated for both the background density and the perturbed quantities, which are not immediately applicable to the unbounded plasma of ionosphere. There are observations (Prakash et al., 1970, 1973) that the background density scale height is of the order of 3 km, below the altitude of 100 km and it is usually a factor of 2 larger above this height. Thus the magnitudes of the parameters (e.g., the background density scale length and electric field E_o) used in these analysis so as to apply them to the observations are also not comparable with their observed values and thus do not represent a realistic model ionosphere. Hence, it was still an open question whether the equatorial ionosphere E-region is unstable and if so, what are the conditions for such instability.

Taking into account the altitude variation of neutral gas density, physically more realistic boundary conditions and an appropriate electron density profile, Reid (1968) performed a one-dimensional linear analysis of the cross-field instability. He showed that the dynamo region is likely to be unstable to the growth of the irregularities with the scale sizes in the range from a few tens of meters to a few kms. However, in his model the electric field (horizontal) needed to obtain the

observed scale sizes of $\sim$ 30 meters and less, is very high ($\gtrsim$ 30 mV/m). The Reid's model is highly idealized because such a strong horizontal electric field is neither observed nor expected to exist in the equatorial ionosphere. Whitehead (1970b) obtained the numerical solutions of the linear differential equations describing the perturbations in a bounded ionospheric layer, which indicated that this instability does not occur in a horizontally stratified ionosphere except perhaps in the equatorial E-region. Later, having allowed the height variation of collision frequency and considering an arbitrary electron density distribution, Whitehead (1971) obtained the approximate solutions to the complicated equations, which showed that the equatorial electrojet is unstable to the gradient drift instability. He tentatively suggested that the electron density irregularities are those which give rise to HF equatorial sporadic-E echoes and to VHF non-two-stream echoes.

The irregularity observations (Balsley, 1969b) indicate that the type II irregularities are observed even when the current density in the electrojet is much below its threshold value required for excitation of two-stream instability (Farley, 1963; Buneman, 1963). At such low current densities, the ion inertia gives rise to the dissipation effects by a mechanism opposite to that which leads to the two-stream instability. Having taken into account the ion inertia which was neglected by earlier workers, Rogister and D'Angelo (1970) made an attempt to explain the main features of the type II

authors who first examined several other possible instabilities, found that only density-gradient-driven instability could occur in the equatorial electrojet. They also noted that this instability appears in the analysis as high frequency version ($\omega > \Omega_i$; $\omega > \nu_i$) of Simon-Hoh instability ($\nu_i >> \Omega_i >> \omega$) developed for bounded plasma without the inclusion of ion inertia. They showed that their theory could account for Balsley's type II irregularities and some of their main features observed and that the instability disappears only at the reversal time when d.c. electric field vanishes.

Recently, a three-dimensional linear analysis of the cross-field instability, for a geometry in which the magnetic field lines make an arbitrary angle with the direction of density gradient, has been made by Sato and Tsuda (1972). They inferred that as a special case, this instability is a potential source of small-scale irregularities in the equatorial E-region, but the threshold d.c. electric field obtained by them for instability is very small compared with the observed or expected electric field in the ionosphere.

In an attempt to improve the understanding of the generation mechanism and of the features of type II, Mc, Sc and other types of irregularities a number of other authors have studied this instability for equatorial conditions on the basis of one-and two-dimensional linear theories (Tsuda et al., 1969; Chimonas, 1969; Whitehead, 1970a, Jain and Das, 1971; Sudan et al., 1973). Whitehead (1970a) has made an excellent brief survey of the earlier cross-field instability theories

and associated irregularities, summarizing the current ideas of the physical basis of sporadic-E irregularities. In other two short reviews, Kato (1972) and Tusda (1973) have also summarized some of these works, showing clearly the differences between their results and pointing out the limitations and difficulties met in these theories.

It is now well accepted that the cross-field instability is capable of explaining the formation and development of striations in relatively sharply bounded alkali ion plasma clouds (Reid, 1970; Linson and Workman, 1970; Linson, 1970; Simon, 1970; Rao and Russel, 1971; Davis, 1971; Ossakow, 1974) released in the equatorial ionosphere for the measurements of electric field $\underline{E}_o$. Besides the above-mentioned applicability of this instability to the electrojet density irregularities, it has, widely, been applied for the explanation of other ionospheric phenomena, such as the formation and deformation of auroral arcs (Wescott et al., 1963; Hooper and Walker, 1971; Ogawa and Sato, 1971) and pulsation and features of type B_2 and B_3 (Short and long disorete) radio aurora (Unwin and Knox, 1968, 1970, 1971; Unwin and Baggaley, 1972; Knox, 1972; Oksman, 1974; Greenwald, 1974; Greenwald et al., 1975). This instability has also, recently, been recognized to have a satisfactory application to the phenomena observed in artificially created plasma, for example, the irregularities and their characteristics observed in reflex arc plasma in laboratory (Hooper, 1970; Hooper and Girvin, 1971) and the instability observed in the laboratory experiments simulating essential

John and Saxena, 1975a,b; 1976a,b; Saxena and John, 1975).

It is to be noted that the case for the existence of the gradient drift instability in the equatorial electrojet has been strengthened considerably by recent rocket, radar and ionosondes studies (Section 1.31). The results indicate either directly or indirectly, that (i) when the vertical electron density gradient and the mean horizontal electron drift velocity are of the proper sense, the irregularities are generated; (ii) if the sense of one is reversed, the irregularities disappear; (iii) if the sense of both is reversed, they reappear, all in agreement with theory.

Since the present instability, in association with ionospheric and laboratory phenomena (as mentioned above) other than sporadic-E, has attached the interest of many ionospheric and plasma physicists, it is now timely as well as necessary to verify further whether this instability can generate all the observed ionospheric irregularities in more detail. It has become quite obvious now that a lot of work has been done and is, further, needed in linear and nonlinear regimes, both analytically and numerically, for the development of the theory of this instability so as to have a proper saturation mechanism and a better explanation for the observed features of the irregularities concerned. We will not, however, consider the nonlinear treatment of the problem here, in this chapter, and confine our discussions only to the linear two-dimensional evolution of the instability for the conditions prevailing in the equatorial E-region. The linear analysis of the gradient

new support to the conjucture of this instability and reinforces the criteria for onset of the instability, but it could also explain many of the observed basic features of the irregularities satisfactorily.

However, all the workers earlier to the present analysis described in this chapter, have allowed the horizontal (E_{oy}) and the vertical (E_{ox}) components of electric field ($\underline{E}_o$) to vary independently, though the component E_{ox} is connected with E_{oy} through the relation, $E_{ox} = (\sigma_2/\sigma_1) E_{oy}$ (Baker and Martyn, 1953) which, we think, might make the study of the formation of small scale irregularities more interesting. In the present work, we considered, for the first time, the combined effect of both the components E_{ox} and E_{oy} and allowed E_{ox} to vary with height according to above relation as σ_2/σ_1, i.e., collision frequencies ν_i and ν_e, change with height, while E_{oy} is assumed to be constant (though it is shown to vary with height by Subbaraya et al., 1972). Instead of considering an arbitrary electron density profile as was adopted by Whitehead (1971) and many others, in our model we shall consider an average nighttime realistic electron density profile (Fig.2.2) observed by Prakash et al., (1970) for our studies of the instability to explain some of the features of the type Mc and Sc irregularities detected by them.

The assumption made by all the previous authors that the electron temperature, T_e is equal to the neutral or ion temperature T_i, does not seem to be appropriate, because one

lack of equality between T_e and T_i in the ionosphere. It has been reported, on the basis of strong experimental evidences from rocket and satellite measurements (Aono et al., 1962; Brace et al., 1963; Nagy et al., 1963; Spencer et al., 1965; Prakash et al., 1968, 1969, 1970; Gupta, 1970; Subbaraya et al., 1973; Sagalyn et al., 1964; Brace et al., 1965) as well as from theoretical calculations (Hanson and Jonhson, 1961; Bourdeau, 1964; Geiser and Bowhill, 1965) that the electron temperature exceeds the neutral (and ion) temperature by a considerable amount during day and by a lesser, but still a significant amount at night. Therefore, an observed electron temperature profile (Fig.2.3) different from the ion or neutral temperature has also been considered in the analysis as T_e can be seen to possess a value higher than that of T_i, approximately by factor varying from 1.8 to 5.5.

The present investigation in the chapter of the linear cross-field instability, which not only determines the growth rates and minimum wavelengths of the perturbations likely to become unstable but also includes discussions of the effects on them of the background quantities (e.g., $\underline{E}_o$ and ∇n_o), is different from that of other works in one or more than one, of the following ways: (1) The analysis is essentially two-dimensional, taking into account the propagation of perturbation in horizontal as well as vertical directions, that is, all the parameters vary in both the horizontal and vertical directions; (2) T_e has been taken different from T_i in

horizontal (E_{oy}) and vertical (E_{ox}) component of equilibrium electric field ($\underline{E}_o$) are considered at the same instant by a relation (2.11) which is appropriately valid in the equatorial E-region; (4) A realistic observed nighttime electron density profile (Fig.2.2) is used to calculate collision frequencies and other parameters so that the theoretical results obtained here could be compared with the observations; (5) The calculations are made for a number of different plasma situations; (6) A detailed study is made to show how the variation in E_o and ∇n_o affect the growth rate and minimum unstable wavelengths.

What will now follow is the investigation of the linear theory of the low frequency gradient drift instability by deriving an appropriate linear dispersion relation and then the expressions of the growth rates and scale sizes of the marginal unstable waves. This essentially will involve in finding out the thresholds and the conditions for the onset of the instability under different physical situations prevailing in the equatorial E-region of the ionosphere. Finally, the author speculates on the possible relevance of the theoretical calculations to the ionospheric irregularities of interest.

2.2 Basic Equations and Assumptions:

We consider an inhomogeneous weakly ionized low-β plasma immersed in a uniform and steady magnetic field, $\underline{B}_o$ and a steady electric field, $\underline{E}_o$. Our treatment of the problem starts with the use of 'two fluid' equations which, for wavelengths of a few meters or more, are adequate to describe equatorial E region

continuity and momentum transfer for the ion and electron components of a three-fluid model of plasma, where it is assumed that ion and electron motions are controlled by their collisions with the neutral gas atoms and that the neutrals are taken as a stationary background which only affect the electrons and ions through the collisional drag forces. The basic set of equations governing the motions of electrons and singly charged ions in the frame of neutrals are then

$$\frac{\partial n^{\pm}}{\partial t} + \nabla \cdot (n^{\pm} \underline{v}^{\pm}) = \Gamma^{\pm} \qquad ..(2.1)$$

$$n^{\pm} m^{\pm} \frac{d\underline{v}^{\pm}}{dt} = n^{\pm} q^{\pm} \left(\underline{E} + \frac{\underline{v}^{\pm} \times \underline{B}_0}{c} \right) - \nabla p^{\pm} - n^{\pm} m^{\pm} \nu^{\pm} \underline{v}^{\pm} + \underline{Q}^{\pm} \qquad ..(2.2)$$

where the subscript '+' and '−' are referred to the quantities appropriate to the ions and electrons respectively. The symbols in these equations are defined as follows: n is the number density of the particles; $\underline{v}$ is their macroscopic velocity; ν_i is the collision frequency of the charged particles with neutrals; q, m, p are the charge, mass and pressure of the particles respectively; $\underline{E} = -\nabla\phi$ is the electrostatic electric field, ϕ being the potential, while $\underline{B}_0$ is earth's magnetic field assumed to be uniform and steady; the terms such as Γ and $\underline{Q}$ represent the ionization and recombination processes. In fact, Γ represents both the ionization and recombination, while $\underline{Q}$, on the other hand, accounts for the momentum change brought by new ions created with a momentum generally different from the average ion momentum. If we wish to account for the

these terms must be retained in equations (2.1) and (2.2). All other symbols in (2.1) and (2.2) have their usual conventional meanings.

These equations (2.1) and (2.2) can be simplified for the low frequency gradient drift instability in the equatorial E-region by making the following assumptions:

1. Since we are interested in wavelengths (λ) much larger than Debye length (λ_D), i.e., the space charges that arise are sufficiently small in the distances of interest ($\lambda_D/\lambda \approx 10^{-5}$ for $\lambda = 5$ meters), we assume plasma to be quasi-neutral, that is, the electron and ion number densities can safely be treated as identical ($n^+ \approx n^- = n$ is assumed).

2. The electron and ion inertial terms on the left-hand side of (2.2) are neglected, because the collision frequencies of electrons and ions (ν^+ and ν^-) are much larger than the wave frequency Doppler-shifted to the electrojet drift frame ($\omega << \nu$) so that the inertial forces are small compared to those applied to the particles by collisions and gradients of density and potential.

3. The electrons and ions are isothermal (the electrons may, in fact, not be isothermal, but this will not alter the results significantly), that is, there are no temperature gradients present ($\nabla T = 0$) and $p^{\pm} = nKT^{\pm}$. With a different pressure law usually amounts to a renormalization of the Boltzman constant, K.

4. The wave electric field is essentially electrostatic ($E = -\nabla\phi$) since the plasma pressure

5. The waves are assumed to propagate in a plane exactly perpendicular to the magnetic field, $\underline{B}_0$, since these waves suffer least damping due to diffusion and are highly damped at small angles away from perpendicularity to $\underline{B}_0$ ($k_{\parallel} = 0$).

6. The fluctuations in the magnetic field arising from the presence of the waves are neglected.

7. The finite Larmor radius effects are neglected.

8. We neglect the production and loss of the charged particles, since these processes are much slower than that of instability. That is, the ionization and recombination processes are very slow (of the order of minutes) compared to the period of waves that have been observed ($\sim 10^{-2}$ sec) and are thus unlikely to play any role in the linear stability analysis (T and Q are neglected).

With these restrictions and assumptions, the basic governing set of fluid equations (2.1) and (2.2) describing equatorial E-region plasma, are then written as follows:

$$\frac{\partial n}{\partial t} + \nabla \cdot (n \underline{v}^{\pm}) = 0 \qquad ..(2.3)$$

$$n q^{\pm}\left(-\nabla\phi + \underline{v}^{\pm} \times \underline{B}_0/c\right) - kT^{\pm} \nabla n - n m^{\pm} \nu^{\pm} \underline{v}^{\pm} = 0 \qquad ..(2.4)$$

The coordinate system we have adopted, is shown in Fig.(2.1). The steady density gradient, ∇n_0 is along the x-axis, while the steady electric field, $\underline{E}_0$ lies in the x-y plane and the magnetic field, $\underline{B}_0$ is taken along the z-axis. Thus the potential and density gradients along $\underline{B}_0$ are not considered in our model, i.e., $\underline{E}_0 \parallel \underline{B}_0$ is assumed to be zero due to large conductivity of electrons along $\underline{B}_0$. The x, y and z directions of this coordinate system then represent vertically upward, eastward

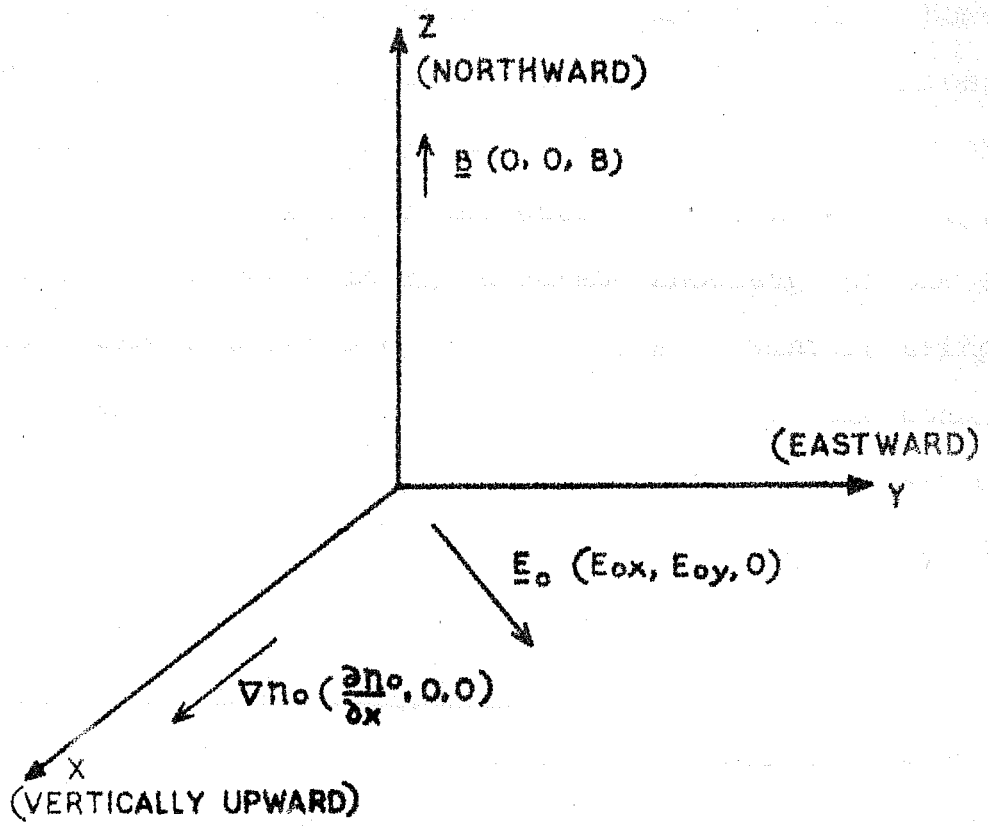


Fig.2.1. The coordinate system used

ionosphere.

Plasma instability occurs due to the departure of the velocity and the spatial distribution of the charged particles from the thermodynamic equilibrium distribution. However, a convincing identification of the instability requires a careful linear stability analysis and determination of the threshold conditions for the onset of the instability. This, in turn, requires a fairly accurate knowledge of the equilibrium state (zeroth order model) of the system that is being perturbed. Therefore, before we investigate the stability of the equatorial E-region, it becomes essential to set up a zeroth order equilibrium model which is described in the next section.

2.3 Zeroth Order Equilibrium Model:

In this section, we shall devote our attention to the discussion of an equilibrium model for unperturbed equatorial E-region. The model can thus describe the variation with altitude of zero order equilibrium quantities (e.g., $\underline{E}_o$, n_o and $\underline{v}_o$) which are to be perturbed. These quantities satisfy the eqs.(2.3) and (2.4) that are to be linearized. Qualitatively, the equilibrium steady state solution applicable to equatorial electrojet can be understood in the following way. The electric field component, E_{oy} which arises from world-wide dynamo action, drives the electrojet, and the electrons and ions are then drifted with velocity cE_{oy}/B_o in vertical

compared to that of ions, a charged separation is produced. This sets up a secondary polarization electric field, E_{ox}, the so called Hall electric field, in the vertical direction, which in turn inhibits the vertical currents. Therefore, it is assumed that the ambient vertical current is zero, i.e., $J_{ox}=0$ (Baker, 1953; Sugiura and Cain, 1966; Lee and Kennel, 1973a). This assumption of complete vertical polarization or suppression of vertical currents is, in fact, valid within approximately $\pm 2^{o}$ around the magnetic dip equator (Sugiura and Poros, 1969).

In zeroth order approximations, equations (2.3) and (2.4) for the steady state of the system, can be written as

$$\nabla\cdot(n_0 \underline{v}_0^{\pm}) = 0 \qquad ..(2.5)$$

$$\mu^{\pm}\left(\underline{E}_0 + \frac{\underline{v}_0^{\pm}\times\underline{B}_0}{c}\right) - D^{\pm}\,\underline{a} - \underline{v}_0^{\pm} = 0 \qquad ..(2.6)$$

where $\underline{a}$ is the inverse density scale length defined by $\underline{a} = \nabla \log n_0$, and the subscript '0' denotes the equilibrium values. μ's and D's are respectively the longitudinal mobilities and diffusion coefficients which are identical to the mobilities and diffusion coefficients in the absence of $\underline{B}_0$ and are defined as

$$\mu^{\pm} = q^{\pm}/m^{\pm}\nu^{\pm} \;;\; D^{\pm} = KT^{\pm}/m^{\pm}\nu^{\pm} \qquad ..(2.7)$$

The equation (2.4) can be solved for zeroth order equilibrium drift velocity $\underline{v}_0$ in the ionosphere to give us

$$\underline{v}_0^{\pm} = \mu_P^{\pm}\,\underline{E}_0 + \mu_H^{\pm}\,\frac{\underline{E}_0\times\underline{B}_0}{B_0} - D_P^{\pm}\,\underline{a} - D_H^{\pm}\,\frac{\underline{a}\times\underline{B}_0}{B_0} \qquad ..(2.8)$$

where the quantities subscripted by 'P' and 'H' refer to

Pedersen and Hall mobilities (μ's) and diffusion coefficients (D's) respectively. These quantities are defined as

$$\mu_P^{\pm}\,(D_P^{\pm}) = \mu^{\pm}(D^{\pm})\cdot(\nu^{\pm})^2/\{(\nu^{\pm})^2+(\Omega^{\pm})^2\} \qquad ..(2.9a)$$

$$\mu_H^{\pm}\,(D_H^{\pm}) = \mu^{\pm}(D^{\pm})\cdot\Omega^{\pm}\nu^{\pm}/\{(\nu^{\pm})^2+(\Omega^{\pm})^2\} \qquad ..(2.9b)$$

where Ω's are gyrofrequencies, given by $\Omega^{\pm} = q^{\pm}B_0/m^{\pm}c$. These expressions for electron and ion drift velocities reduce to those obtained by Linson and Workman (1970) if one assumes that $\nu^- = 0$ and to those obtained by Rogister and D'Angelo (1970) if ν^- and n_0 are both neglected. The assumption that the magnetic field $\underline{B}_0$ is steady, gives $\nabla \times \underline{E}_0 = 0$ which, considering the variation in x-direction, yields that E_{oy} is constant and E_{ox} varies with height. Though, recently it has been qualitatively shown by rocket measurements (Subbaraya et al., 1972) that in the electrojet region, the horizontal electric field, E_{oy} is not a constant and most probably increases with height, even then we shall assume E_{oy} to be constant for the sake of simplicity and for the reason that there are not sufficient observational evidence. Following Baker and Martyn (1953), the radio K_o of Hall (σ_2) and Pedersen (σ_1) conductivities in the equatorial region is

$$K_0 = \frac{\sigma_2}{\sigma_1} = \frac{\alpha^- + \alpha^+}{\alpha^+\alpha^- - 1}\;;\quad \alpha^{\pm} = \Omega^{\pm}/\nu^{\pm} \qquad ..(2.10)$$

Considering that $|\alpha^-| >> \alpha^+$ through out the region, $K_0 = \alpha^-/(\alpha^+\alpha^- - 1)$ $= \nu^+/\Omega^+(1 - \nu^+\nu^-/\Omega^+\Omega^-)$ and the vertical polarization field, E_{ox} in equatorial ionospheric region is related to a spatially constant horizontal driving field, E_{oy} (Baker and

Martyn, 1953) by the relation

$$E_{ox} = K_0 E_{oy} = \frac{\alpha^-}{\alpha^+\alpha^- - 1} E_{oy} \qquad ..(2.11)$$

Using (2.11), the electron and ion drift velocities in the x-and y-directions are then given by

$$v_{ox}^+ = \mu_0 V_0 - D^+ a \qquad ..(2.12)$$

$$v_{ox}^- = (\nu^-/\Omega^-)^2 \left[\mu_0 (\Omega^-/\nu^-)^2 V_0 - D^- a\right] \qquad ..(2.13)$$

$$v_{oy}^+ = -(\Omega^+/\nu^+)\left[\mu_0 \psi V_0 - D^+ a\right] \qquad ..(2.14)$$

$$v_{oy}^- = -(\nu^-/\Omega^-)\left[\mu_0 \psi (\Omega^-/\nu^-)^2 V_0 - D^- a\right] \qquad ..(2.15)$$

where $\psi = \nu^+\nu^-/\Omega^+\Omega^-$, $\mu_0 = 1/(1-\psi)$, and $\alpha^+ = \Omega^+/\nu^+ \ll 1$ and $\alpha^- = \Omega^-/\nu^- \gg 1$ have been assumed. V_0 is the zero-order drift velocity of the particles in the vertical direction, which is the same as that due to the electric and magnetic fields in the absence of collisions and diffusion and is equal to cE_{oy}/B_0.

It is seen that throughout the region under consideration, the first term in (2.12), (2.13) and (2.15) is much larger than the second term. Therefore, the electron and ion drift velocities in vertical direction reduce to

$$v_{ox}^{\pm} = v_{ox} = \mu_0 V_0 = \frac{cE_{oy}/B_0}{1 - \nu^+\nu^-/\Omega^+\Omega^-} \qquad ..(2.16)$$

which is exactly equal to the drift of irregularities in the vertical direction (Clemmov and Johnson, 1959). As a consequence of (2.16), the vertical current, $J_{ox}\left[= n_0 e (v_{ox}^+ - v_{ox}^-)\right]$ at all altitudes of interest is, therefore, zero in the steady state, i.e., the assumption of complete inhibition of vertical current

same as obtained by Linson and Workman (1970), Linson (1970), Whitehead (1971) and Lee and Kennel (1973a). However, in deriving (2.16), small ambipolar effects caused by vertical density gradients, i.e., the contribution to the motions due to diffusion of particles are neglected, which are more important at the altitudes higher than about 130 km. Hence in the actual ionosphere the assumption of complete inhibition of vertical currents is not strictly valid everywhere and is only an approximation in the region considered (Untiedt, 1967; Sugiura and Poros, 1969). Nevertheless, it is reasonably valid within the equatorial E-region heights as the diffusion plays an insignificant role and the effect of the vertical current may not be so significant to change the above arguments (Sugiura and Poros, 1969).

It can easily be seen that the vertical drift velocity v_{ox} (eq.2.16) increases monotonically with altitude upto 120 km or so and then it attains almost a constant value equal to V_o because μ_o increases upto that height ($|\psi|$ being decreased in magnitude) and then it becomes unity ($|\psi| \ll 1$). For E_{oy} = 0.5 mv/m, the computed v_{ox} is approximately equal to 1.0 m/s at 90 km and its maximum value is around 20.0 m/s at 120 km.

For negligible diffusion, the equations (2.14) and (2.15) yield the ion and electron horizontal drift velocities in y-direction as

$$v_{oy}^{+} \equiv - \mu_o V_o \nu^- / \Omega^- \qquad \text{(for altitudes } < 120 \text{ km)} \quad ..(2.17a)$$

$$= D^+ \alpha \nu^+ / \omega^+ \qquad \text{(for altitudes } > 120 \text{ km)} \quad ..(2.17b)$$

$$v_{oy}^{-} \approx -\mu_0 V_0 \nu^{+}/\Omega^{+} \qquad ..(2.18)$$

These results are exactly similar to those obtained by Whitehead (1971). It is obvious from (2.17a) and (2.18) that $v_{oy}^{+} = |\alpha^{+}/\alpha^{-}| v_{oy}^{-}$. For parameters appropriate to the regions of interest, $|\alpha^{+}/\alpha^{-}| = |\Omega^{+}\nu^{-}/\Omega^{-}\nu^{+}|$ is approximately of the order of 10^{-4}. Therefore, the ion horizontal drift velocity is four order of magnitude less than the electron horizontal drift velocity in the electrojet region. It is easy to show with the help of (2.10) and (2.18) that $|v_{oy}^{-}| = K_0 V_0$. Therefore, both the ion and electron horizontal drift velocities vary as the ratio $K_0 (= \sigma_2/\sigma_1)$ does, with a maximum around 100 km. Considering $E_{oy} = .5$ mV/m, this maximum value of v_{oy}^{-} is approximately equal to 450 m/s and its value around 90 km is approximately 170 m/s.

The horizontal driving field, E_{oy}, remains constant with altitude while the altitude variation of the vertical polarization field, E_{ox} is, as is obvious from (2.10), similar to that of the ratio K_0. The variation of E_{ox} has actually been computed and shown by Sugiura and Poros (1969) and Lee and Kennel (1973a). Subbaraya et al. (1972) have shown, however, that in the electrojet region, E_{oy} does not remain constant and most probably increases with increase in height. But, to a good approximation, E_{oy} is assumed to be a constant in the analysis made in this chapter.

2.4 Instability Analysis - Dispersion Relation:

Following the linear theory, the stability of the

in this section. Our next step is to solve equations (2.3) and (2.4) by using the first order perturbation theory, in consistent with (i) the zeroth order steady state equilibrium model obtained in the previous section, (ii) the coordinate system adopted and (iii) the assumptions made in sec.2.2. All the perturbed quantities, the density n_1, the potential ϕ defined by $\underline{E} = -\nabla \phi$ and the velocity $\underline{v}$ are, therefore, assumed to have the form

$$n = n_0(x) + n_1 \; ; \; \phi = \phi_0(x,y) + \phi_1 \; ; \qquad \underline{v}^{\pm} = \underline{v}_0^{\pm}(x,y) + \underline{v}_1^{\pm} \qquad ..(2.19)$$

where n_0, ϕ_0 and $\underline{v}_0$'s are equilibrium steady state values (discussed in previous section) of the electron density, potential and drift velocities respectively; the quantities, n_1, ϕ_1 and $\underline{v}_1$'s are small first order perturbations in n_0, ϕ_0 and $\underline{v}_0$'s. We assume that n_1 and ϕ_1 have the sinusoidal forms given by

$$n_1(\phi_1) = N_1(\Phi_1)\, e^{i(\omega t - \underline{k}.\underline{r})} \qquad ..(2.20)$$

where N_1 and Φ_1 are the amplitudes of perturbations. The space and time dependence of both the perturbations are periodic, the former being in the direction of the vector $\underline{r}(x,y)$ with real wave number $\underline{k}(x,y)$, while the latter varies with time constant ω, the angular frequency of the perturbations. We assume ω to be a complex quantity given by $\omega = \omega_r + i\omega_i$. Thus, we have the perturbations varying as

$$n_1(\phi_1) = N'(\Phi')\, e^{i(\omega_r t - \underline{k}.\underline{r})} \qquad ..(2.21)$$

It is thus obvious from their shapes that the amplitude of perturbations either grows or damps out with time according as the sign of ω_i, the imaginary part of ω, is negative or positive respectively. The physical conditions for the instability to occur, are therefore, those for which ω_i is negative.

Our aim will thus be to determine those physical conditions which make ω_i negative and as a result, allow the waves to grow. To do this, the continuity and momentum transfer equations (2.3) and (2.4) for electrons and ions are first linearized and then solved together, yielding a dispersion relation for the waves. Substituting (2.19) into (2.4) and using (2.8), we get the linear perturbations in velocities $\underline{v}_1^{\pm}$ as

$$\underline{v}_1^{\pm} = \mu_p^{\pm} \underline{E}_1 + \mu_H^{\pm} \frac{\underline{E}_1 \times \underline{B}_0}{B_0} - D_p^{\pm} \frac{\nabla n_1 - n_1 \underline{a}}{n_0} - D_H^{\pm} \frac{(\nabla n_1 - n_1 \underline{a}) \times \underline{B}_0}{n_0 B_0} \quad ..(2.22)$$

which obviously depend upon ω and $\underline{k}$ in the same manner as $\underline{E}_1$ $(= -\nabla \phi_1)$ and n_1 defined by (2.20) depend on ω and $\underline{k}$. The linearized continuity equation (2.3), together with (2.8) and (2.22) gives a set of second order partial differential equations in n_1 and ϕ_1, one for ions (+ sign) and another for electrons (- sign), as

$$\frac{\partial n_1}{\partial t} - \mu_p^{\pm} \left\{ n_0 a \left(\frac{\partial \phi_1}{\partial x} + \alpha^{\pm} \frac{\partial \phi_1}{\partial y} \right) - \left(E_{0x} + \alpha^{\pm} E_{0y} \right) \frac{\partial n_1}{\partial x} - \left(E_{0y} - \alpha^{\pm} E_{0x} \right) \frac{\partial n_1}{\partial y} \right\} - D_p^{\pm} \left(\frac{\partial^2 n_1}{\partial x^2} + \frac{\partial^2 n_1}{\partial y^2} \right) - \mu_p^{\pm} n_0 \left(\frac{\partial^2 \phi_1}{\partial x^2} + \frac{\partial^2 \phi_1}{\partial y^2} \right) = 0 \quad ..(2.23)$$

where $E_{ox} = -\partial\phi_o/\partial x$, $E_{oy} = -\partial\phi_o/\partial y$ and 'a' is the inverse scale height defined by 'a' $= \frac{1}{n_o}\frac{\partial n_o}{\partial x}$; all the transport coefficients have been chosen to be constant; and $\mu_H^{\pm}(D_H^{\pm})$ have been replaced by $\alpha^{\pm}\mu_p^{\pm}(D_p^{\pm})$ by definitions (2.9b). The equations (2.23) without any adhoc approximations is so complicated that no conclusive analysis could be made. Therefore, for the sake of simplicity and a clear physical understanding of the solutions, it was necessary to make the following approximations: firstly, the terms involving the product $k_x k_y$ have been neglected, i.e., the propagation of the perturbation in either x or y direction at a time is assumed; secondly, it has been considered that there is negligible deformation of background steady gradient so that $\partial^2 n_o/\partial x^2 = 0$; thirdly, the electric field induced by the deformation of steady density gradient has also not been included.

Equation (2.23) represents a coupled pair of linear second order partial differential equations in n_1 and ϕ_1. Substituting the values of n_1 and ϕ_1 from (2.20), the equations(2.23) can be converted into a pair of algebraic equations in amplitudes, N_1 and $\bar{\phi}_1$, one for ions (upper sign, +) and another for electrons (lower sign, -). We will now consider two cases: (A) when the amplitudes (N_1, $\bar{\phi}_1$) of the perturbations are constants with height; and (B) when these are functions of x.

CASE (A): Amplitudes of Perturbations are Constant, i.e., $N_1(\Phi_1) = N(\Phi)$:

Substituting $N_1(\Phi_1) = N(\Phi) \exp i(\omega t - \underline{k}.\underline{r})$ into (2.23), we obtain the following pair of algebraic equations:

$$N\left[D_p^{\pm} k^2 + i\left\{\omega - \mu_p^{\pm}\left(\underline{k}.\underline{E}_0 + \alpha^{\pm}(\underline{k}\times\underline{E}_0)_z\right)\right\}\right] + n_0 \mu_p^{\pm}\left(k^2 + i\, k_\alpha^{\pm} a\right)\Phi_1 = 0 \qquad ..(2.24)$$

where $k = (k_x^2 + k_y^2)^{1/2}$ is the magnitude of the wave number perpendicular to $\underline{B}_0$ and

$$k_\alpha^{\pm} = k_x + \alpha^{\pm} k_y \qquad ..(2.25)$$

The non-trivial solution to eqs.(2.24) can be obtained by putting their determinent equal to zero which then gives the following dispersion relation:

$$\omega = \frac{A k^4 + \beta\alpha_1\left(2 E_{ox} k_x k_y - (k_x^2 - k_y^2) E_{oy}\right) a - \left\{\left(\beta\alpha_1 E_{ox} - L_2 a\right) k_y - \left(\beta\alpha_1 E_{oy} + A a\right) k_x\right\} k^2}{\left(\beta_1 k_x + L_1 k_y\right) a - i\,\beta_1 k^2} \qquad ..(2.26)$$

where

$$A = \mu_p^- D_p^+ - \mu_p^+ D_p^- \;;\; \beta = \mu_p^- \mu_p^+ \;;\; \beta_1 = \mu_p^- - \mu_p^+$$
$$L_1 = \mu_H^- - \mu_H^+ \;;\; L_2 = \mu_H^- D_p^+ - \mu_H^+ D_p^- \;;\; \alpha_1 = \alpha^- - \alpha^+ \qquad ..(2.27)$$

The growth rate of the perturbations can now be decided by the imaginary part of ω, which can be derived from (2.26) and is given by

$$A\beta_1\left(k^4 + a^2 k_x^2\right) k^2 + \left[\left\{\beta\alpha_1\left(\beta_1 E_{ox} + L_1 E_{oy}\right) a + \left(A L_1 + \beta_1 L_2\right) a^2\right\} k_x k_y + \left\{\beta\alpha_1\left(\beta_1 E_{oy} - L_1 E_{ox}\right) a + L_1 L_2 a^2\right\} k_y^2\right] k^2 \qquad ..(2.28)$$

If this is negative, the perturbations grow exponentially with time and ω_i is called as the growth rate of the perturbations. If it is positive, they are damped out and ω_i is known as the damping rate. The physical conditions of the onset of the growth are discussed in next section.

CASE (B): Amplitudes of Perturbations are Functions of x, i.e., $N_1(\Phi_1) = N_1(x)$ $(\Phi_1(x))$:

In this case, amplitudes of the perturbations are assumed as the varying functions of x. We will here adopt the procedure, first used by Kadomtsev and Nedospasov (1960) and then by Simon (1963) and Hoh (1963), to solve eqs.(2.23) by choosing the physically reasonable and realistic functional forms for the amplitudes N_1 and Φ_1. In all these papers and most of the theories by earlier workers, a sinusoidal form of half wave length L is used with the assumptions that the amplitudes of the perturbations vanish at x = 0 and x = L and that the density gradient and electric field over the distance L are taken in terms of the spatial averages. They made series expansion for the variables in terms of eigen functions and retained only the first fundamental terms satisfying the boundary conditions. Their particular form is probably valid for bounded laboratory plasma and does not apply to ionospheric plasma because of variation in the ionosphere of the physical quantities in a complex way with height (x). Later, Morse (1965), Reid (1968) and Williams and Weinstock (1970) assumed the form of N_1 and Φ_1 as exponentially varying functions of

the scale height 1/a, which seems to be valid for ionospheric plasma. Hence, having considered the exponential functional forms, of N_1 and Φ_1, we have

$$N_1(\Phi_1) = N(\Phi)\, e^{ax} \; ; \; n_1(\Phi_1) = N(\Phi)\, e^{i(\omega t - \underline{k}.\underline{r}) + ax} \qquad ..(2.29)$$

On substituting these into (2.23) and following the same procedure as before in the case (A), we get the following dispersion relation:

$$\omega = \frac{\begin{aligned} & A k^4 - (\beta\alpha_1 E_{oy} + 3Aa) a k^2 - 2(Ak_x + L_2 k_y) a^2 k_x \\ & + \beta\alpha_1 (2E_{ox} k_x k_y - (k_x^2 - k_y^2) E_{oy}) a - i\Big[\{(\beta\alpha_1 E_{ox} - L_2^2) k_y \\ & - (\beta\alpha_1 E_{oy} + 3Aa) k_x\} k^2 + 3\beta\alpha_1 (k_x E_{oy} - E_{ox} k_y) a^2\Big] \end{aligned}}{(\beta_1 k_x + L_1 k_y) a - i\beta_1 (k^2 - 2a)} \qquad ..(2.30)$$

The imaginary part of ω which describes the instability criterion can again be derived from this equation and is given below for the case when the amplitudes have functional forms, as

$$\frac{A\beta_1 k_1^2 k^4 + (\beta_L P_1 k_1^2 + \beta_k P_2 a) a k^2 + (\beta_1 P_3 k_1^2 + \beta\beta_k P_4) a}{\beta_k^2 a^2 + \beta_1^2 k_1^4} \qquad ..(2.31)$$

where

$$k_1^2 = k^2 - 2a^2 \; ; \; \beta_k = 3\beta_1 k_x + L_1 k_y \; ; \; P_1 = -(\beta\alpha_1 E_{oy} + 3Aa)$$
$$P_2 = 5Ak_x + L_2 k_y \; ; \; P_3 = \beta\alpha_1 (4E_{ox} k_x k_y - (3k_x^2 - k_y^2) E_{oy} - 2(3Ak_x + L_2 k_y) a k_x$$
$$P_4 = \alpha_1 [(k_x E_{oy} - k_y E_{ox}) k^2 - (5k_x E_{oy} - 3k_y E_{ox}) a^2] \qquad ..(2.32)$$

and other symbols are similar as those in (2.27). For instability to grow, we demand that ω_i should be negative.

In order to complete the discussions for instability it is essential to find out the conditions for which the

which in turn would provide a fairly good estimate of the scale sizes likely to grow and growth rates of the irregularities. This, we will discuss in the next section by considering the different physically possible electric fields and directions of propagation.

2.5 Growth Rates and Scale Sizes of the Perturbations:

In this section, we pay our attention to determine the conditions for instability and to obtain the expressions for growth rates and scale sizes of irregularities for cases (A) and (B) discussed in the previous section. This will be done for the cases when steady field component either E_{ox} or E_{oy} or both are present at a given time. We will, for the reason given in preceding section, first consider k_x with $k_y = 0$ and then k_y with $k_x = 0$ in all the cases.

CASE (A): In this case the amplitudes of perturbations are constants and the imaginary part of ω is given by (2.28) considering first the case $k_y = 0$, the expression for ω_i given by (2.28), becomes

$$\omega_i = D_a k_x^2 = \frac{4\pi^2}{\lambda_x^2} D_a \; ; \; D_a = \frac{K(T^+ + T^-)}{m^+ \nu^+ (1 - \alpha^+ \alpha^-)} = - \frac{C_s^2}{\nu^+} \frac{K_a}{\alpha^-} \qquad ..(2.33)$$

where D_a is classical ambipolar diffusion coefficient perpendicular to $\underline{B}_o$, $C_s = (K(T^+ + T^-)/m^+)^{1/2}$ is the ion acoustic speed in the medium and $\lambda = 2\pi/k$ is the wavelength of the perturbation which represents the scale size of the irregularities. The use of the fact that $(\alpha^+)^2 << |\alpha^+ \alpha^-|$ throughout the ionospheric region has been made in obtaining equation

It is quite obvious from (2.33) that ω_i, for the waves having wave number in x-direction (vertically upward), depends neither on the electron density gradient nor on the electric field. It is positive for any value of λ_x or k_x, because D_a is a positive quantity. This clearly shows that the perturbations propagating in the vertical direction are completely damped out because of the damping by diffusion. However, if the medium is perturbed by sinusoidal waves propagating in the vertical direction, the waves with larger wavelengths are damped out slower than those with smaller wavelengths. It is thus inferred that when the amplitudes of perturbations are assumed to be having nonfunctional forms and constant, the ionospheric E-region plasma is stable to vertically excited perturbations.

We consider now the case when $k_x = 0$, i.e., the perturbations are assumed to propagate in y-direction (horizontally eastward). Using eqs.(2.9) and (2.27), and then simplifying, the expression (2.28) for ω_i in this case reduces to

$$\omega_i = -\frac{\alpha^+(\alpha^-)^2}{(1-\alpha^+\alpha^-)^2}\left\{\frac{c}{B_0}\left(E_{0x} - \frac{1-\alpha^+\alpha^-}{\alpha^-}E_{0y}\right)a - \left(\frac{V_i^2}{\Omega^+} - \frac{V_e^2}{\Omega^-}\frac{\alpha^+}{\alpha^-}\right)\frac{a^2}{2}\right\} + D_a k_y^2 \qquad ..(2.34)$$

where V_i and V_e are ion and electron thermal velocities respectively. In deriving (2.34) we have assumed that $|\alpha^-| >> \alpha^+$ and $|a| << k_y$ which are valid throughout the ionospheric region of interest. Equation (2.34) determines the wave growth rate. If $\omega_i << 0$, then the waves grow with time and the medium is unstable to the perturbations given

right side contains the quantity $(c/B_o)\,(E_{ox}-E_{oy}(1-\alpha^+\alpha^-)/\alpha^-)\,a$, which, with the use of (2.10), (2.11), (2.18) and the fact that $\sigma_1 << \sigma_2$ in electrojet region, can be approximated to $V_D\,a$, where $V_D(=cE_{ox}/B_o)$ is the horizontal electron drift velocity. (Note that V_D is positive for electrons drifting towards the west, the usual daytime conditions, whereas it is towards the east at night). When this quantity is sufficiently large and positive, then $\omega_i < 0$ for some k_y and the waves will grow. Since it involves the gradient 'a' and drift V_D, it is referred to as the gradient-drift instability; (b) the second term in (2.34) gives rise to damping, for all wavelengths excited, due to collisional diffusion of mainly ions (as it can be seen by comparing two quantities in this term), though the magnitude of this term involving a^2, is smaller than others and can be assumed to be negligible; (c) the last term in (2.34) is another damping term which is wavelength dependent and is seen to be due to collisional diffusion of both electrons and ions (ambipolar diffusion). Obviously, this term dominates for smaller wavelengths. This essentially means that only horizontally propagating large wavelength waves are linearly excited by the gradient drift instability.

It can be noted that these results are more or less similar to those obtained by earlier workers (Rogister and D'Angelo, 1970; see also Sato, 1971; 1973; Sudan et al., 1973) except for the second term which, containing a^2 and hence being smaller, can be neglected here ($a \cong 5$ km in region of

which $|\alpha^+ \alpha^-| >> 1$ and using (2.11), the growth rate ω_i given by (2.34) reduces to that obtained for plasma cloud striations in the ionosphere by Linson and Workman (1970) except for both the damping terms and later by Linson (1970) except for the wavelength independent term (second term) which is the function of ion and electron temperatures and the inverse scale height, a. For a given constant value of k/a, they have maximised the growth rate with respect to angle of propagation, θ = arc tan (k_y/k_x) which depends upon the altitude and density gradient. In this model, we have, however, obtained the growth rate for the fixed angle of propagation either $\theta = 90^o$ (horizontal direction) or $\theta = 0^o$ (vertical direction) and it has not been maximized.

If an arbitrary choice for an electric field is permissible then the three different cases can be studied as follows.

Case (i). $E_{ox} \neq 0$ and $E_{oy} \neq 0$: Since the quantities α^- and Ω^- are negative and D_a is positive, the second and third terms in (2.34) are positive and are thus, diffusional damping terms. Therefore, the sign of ω_i is determined by the first term in (2.34), which should be negative for the instability. Hence, if $\omega_i < 0$, then (1) the sign of $\underline{a}(\nabla n_o)$ and that of E_{ox} and E_{oy} must be same, i.e.,

either (a) $(\underline{E}_o \times \underline{B}_o)$. $\nabla n_o > 0$ or (b) $\underline{E}_o$, $\nabla n_o > 0$ ..(2.35)

must be satisfied and (2) the absolute value of the first [illegible] must be larger than the sum of the

The minimum wavelength, λy_{min} of the instability in horizontal direction can then be obtained immediately by using condition (2) and is given by

$$\lambda^2_{y_{min}} = 4\pi^2 \left(\frac{1-\alpha^+\alpha^-}{\alpha^-}\right)^2 \left[\frac{-\left(U_{oy} + \frac{1-\alpha^+\alpha^-}{\alpha^-} U_{ox}\right) a - \left(\frac{V_i^2}{\Omega^+} - \frac{V_e^2}{\Omega^-}\cdot\frac{\alpha^+}{\alpha^-}\right)\frac{a^2}{2}}{D_\alpha / \alpha^+}\right]^{-1} \quad ..(2.36)$$

where

$$\underline{U}_o = c(\underline{E}_o \times \underline{B}_o)/B_o^2 \quad ..(2.37)$$

is the drift velocity due to the crossed electric and magnetic fields. It is easily seen from (2.36) that for a real value of λy_{min}, the relation (2.35) must be satisfied, i.e., the electric field has to be of the same sign as the density gradient ∇n_o, and the drift term in (2.36) must be greater than the other terms of (2.36). For ionospheric region of interest, these conditions together with (2.11) then give rise to the threshold conditions on the electric field and the drift velocity for instability as

$$|U_{ox}| \geq \frac{V_i^2 a}{2\nu^+} \equiv U_{ox}^c \; ; \; E_{oy} \geq \frac{B_o}{c}\cdot\frac{V_i^2 a}{2\nu^+} \equiv E_{oy}^c \quad ..(2.38)$$

$$|U_{oy}| \geq \frac{V_i^2 a}{2\Omega^+} \equiv U_{oy}^c \; ; \; E_{ox} \geq \frac{B_o}{c}\cdot\frac{V_i^2 a}{2\Omega^+} \equiv E_{ox}^c \quad ..(2.39)$$

where $|\alpha^+ \alpha^-| >> 1$ has been assumed and $V_i^2 \Omega^- \alpha^- >> V_e^2 \Omega^+ \alpha^+$ has been used. At the base of E-region (90 km) with $|\underline{a}| \approx 10^{-5}$ cm^{-1} ($|\underline{a}|$ may be smaller at higher heights reaching a value of $\sim .16 \times 10^{-5}$ cm^{-1} corresponding to density scale height of 6-7 km; Prakash et al., 1973), the threshold electron drift velocities and threshold electric fields required for the growth of the instability are given by

$$U^c_{oy} = 45.0 \text{ m/sec} \quad ; \quad E^c_{ox} = 1.35 \text{ mV/m} \qquad ..(2.41)$$

The values of drift velocities observed in (and also calculated in sec.2.3) the equatorial E-region are much higher than these threshold velocities, U_{ox} and U_{oy}. It can also be noticed from (2.40) and (2.41) that the threshold fields (E^c_{oy} and E^c_{ox}) for instability are quite smaller compared with the usual estimated or observed horizontal ($E_{oy} \sim 0.1 - 1$ mV/m) and vertical ($E_{ox} \sim$ 10-30 mV/m) electric fields in the electrojet region. Hence, above 90 km, the ionospheric region must be unstable to the growth of the low frequency gradient drift instability discussed in the chapter, which may give rise to the growing irregularities observed in the electron concentration. Note that these threshold values are higher than those obtained by Sato (1971).

Case (ii). $E_{ox} \neq 0$ and $E_{oy} = 0$: In this case, the minimum wavelength for instability to grow is (by putting $E_{oy} = 0$ in (2.36)) given by

$$\lambda_{y_{min}} = 4\pi^2 \left(\frac{1-\alpha^+\alpha^-}{\alpha^-}\right)^2 \left[\frac{-U_{oy}a - \left\{\frac{V_i^2}{\Omega^+} - \frac{V_e^2}{\Omega^-}\cdot\frac{\alpha^+}{\alpha^-}\right\}\frac{a^2}{2}}{Da\,|\alpha^+}\right]^{-1} \qquad ..(2.42)$$

where U_{oy} is horizontal electron drift velocity defined by (2.37) and is equal to $-cE_{ox}/B_o$. For $\lambda_{y_{min}}$ to be real, we have again two conditions: (1) 'a' and E_{ox} must be in the same direction i.e., $a.E_{ox} > 0$; (2) the first term which drives the instability, must be larger than the other term in denominator of (2.42). The second condition leads to threshold for instability as those given in (2.41).

Case (iii). $E_{ox} = 0$ and $E_{oy} \neq 0$: For this situation, we obtain the minimum wavelength for the growth of the instability (by putting $E_{ox} = 0$ in (2.36)) as

$$\lambda_{y_{min}} = 4\pi^2\left(\frac{1-\alpha^+\alpha^-}{\alpha^-}\right)^2\left[\frac{-U_{ox}a(1-\alpha^+\alpha^-)/\alpha^- - \left\{\frac{V_i^2}{\Omega^+} - \frac{V_e^2}{\Omega^-}\cdot\frac{\alpha^+}{\alpha^-}\right\}\frac{a^2}{2}}{Da/\alpha^+}\right]^{-1} \quad ..(2.43)$$

where U_{ox} is vertical electron drift velocity given by (2.37) and is equal to cE_{oy}/B_o. As α^- is a negative quantity, $\lambda_{y_{min}}$ will be a real quantity if the two conditions given below are satisfied; (i) 'a' and E_{oy} must be of the same sign, i.e., $a.E_{oy} > 0$; (2) the instability driving term which depends upon drift and density gradient, must be larger than the damping term (second term in denominator of eq. 2.43) and this condition, in turn, yields thresholds for instability as those represented in (2.40).

Thus, it is quite obvious from above discussions of eqs.(2.34), (2.36), (2.43) that the conditions (2.35) must be satisfied in order to allow the waves to grow, i.e., for the growth of the instability the ambient electric field has to be of the same sign as the inverse scale height (the steady density gradient, ∇n_o). This first condition supports the result obtained previously by Kadomtsev and Nadospasov (1960), Simon (1963), Hoh (1963), Tsuda et al., (1966), Reid (1968) and others. Note, however, that if $a(= \nabla \log n_o) = 0$, the growth rate, ω_i given by (2.34) reduces to $D_a k_y^2$, a damping term, i.e., the instability disappears and the waves are damped by ambipolar diffusion. The same is true when both the

gradient may be present. The gradient drift instability in the ionosphere is thus operative only when the density gradient, ∇n_o and either of the ambient electric field components of proper sign act together so as to drive the waves unstable in horizontal direction. Under the situations, such as (a) when 'a' and E_{ox} are of the same sign, and 'a' and E_{oy} are of the opposite sign; (b) 'a' and E_{oy} are of the same sign, and 'a' and E_{ox} are of the opposite sign (the former combination leads to driving term, while latter gives rise to damping contribution), the instabilities are, however, also possible provided that the driving term is larger than the sum of damping terms. The scale sizes of the waves for such cases may be deduced from (2.36). This implies that there may be instabilities even when the steady density gradient, ∇n_o is opposite to either E_{ox} or E_{oy}, but not to both.

CASE (B): In this case, amplitudes of perturbations have functional forms as assumed in eqs.(2.29). The growth rate ω_i in this case, is given by (2.31). We will first consider the case when $k_y = 0$, i.e., the waves are assumed to propagate in vertical direction only. Using equations (2.9), (2.27) and (2.32), the expression (2.31) for ω_i is reduced to

$$\omega_i = -\frac{\psi}{\nu^+} C_s^2 k_x^2 - \frac{e}{B_o} E_{oy} a \equiv -\frac{\psi}{\nu^+} C_s^2 k_x^2 - U_{ox} a \quad ..(2.44)$$

where the use of the fact that $\alpha^+ << 1$ and $|\alpha^-| >> 1$ has been made. We have assumed $|a| << k_x$ in order to simplify eq.(2.44) and hence, $(a/k_x)^2$ and such higher order terms have been neglected in comparison with other terms, which is valid

for ω_i to be negative we have the conditions: (1) a and E_{oy} must be of same sign satisfying the condition (2.35); (2) $U_{ox}\, a > -\psi C_s^2 k_x^2/\nu^+$. The second condition determines the minimum wavelength for instability to grow, which is given by

$$\lambda^2_{x_{min}} = -4\pi^2 \psi (\nu^+ U_{ox} a)^{-1} C_s^2 \qquad ..(2.45)$$

Thus, it is interesting to note that the dependence of the growth rate and wavelength (along x-direction) on density gradient and electric field appears only through the functional form of the perturbation amplitude. It is also seen that the growth rate and the scale sizes of the perturbations in the vertical direction (x-direction) are governed by the horizontal component of electric field, E_{oy} and thus by the vertical electron drift, U_{ox}. This means that horizontal electric field is the only energy source responsible for sustaining the instability for the case being discussed. We consider now the case when $k_x = 0$, i.e., the propagation is assumed to be in horizontal direction (y-direction) only. Similar to the above discussed case when $k_y = 0$, we now obtain the expression for growth rate, ω_i from (2.31) as

$$\omega_i = -\frac{\psi}{\nu^+} C_s^2 k_y^2 + \frac{\nu^+}{\Omega^+}\left(\frac{V_i^2}{\Omega^+} - \frac{V_e^2}{\Omega^-}\frac{\alpha^+}{\alpha^-}\right) a^2 + \frac{\nu^+}{\Omega^+} U_{oy}\, a \qquad ..(2.46)$$

where U_{oy} is horizontal electron drift velocity (eq.2.37) equal to $-cE_{ox}/B_o$ and $a/k_y \ll 1$ has been used. It can again easily be shown that the instability can occur, i.e., the perturbations in horizontal direction are likely to grow, only if (1)

instability criteria (2.35), and (2) the magnitude of last term in (2.46) which is driving source for the instability, is greater than the sum of other two terms in (2.46) arising due to diffusion across the magnetic field. The second condition then gives us the minimum wavelength of the disturbances as

$$\lambda_{y_{min}}^2 = -4\pi^2 \frac{\nu^-}{\Omega^-} \frac{C_s^2}{\nu^+} \left[-U_{oy} a - \left(\frac{V_i^2}{\Omega^+} - \frac{V_e^2}{\Omega^-} \frac{\alpha^+}{\alpha^-} \right) a^2 \right]^{-1} \quad ..(2.47)$$

One can easily see from (2.46) that the growth rate of the disturbance (ω_i) along the horizontal direction (y-direction) in the case of the functional form of the amplitude of the disturbance does not explicitly depend on the magnitude or direction of horizontal electric field, E_{oy} which may, however, give rise to a field, E_{ox} in vertical direction (see relation 2.11). We find from (2.47) that the thresholds on vertical electric field and horizontal drift are now as large as twice the thresholds (given by eqs.2.39 and 2.41) for the case of nonfunctional forms of perturbation amplitudes. Nevertheless, they are smaller than the observed or estimated values of corresponding electric fields and electron drifts, implying that the instability can occur in the ionospheric region of interest. Contrary to the case when $k_y = 0$, the vertical electric field, E_{ox}, producing horizontal electron drift, drives now the instability and is thus the energy source for the growth of the waves.

Note that the condition (2.35) that the gradient and the field must be of the same sign for the growth will have to be satisfied both for functional and non functional forms of the

all the above-discussed cases of instability, the absence of inhomogeneity in the plasma (a = 0) leads only to the positive values of $(\omega)_i$ which means that waves are damped, i.e., in the absence of ambient density gradient ($\nabla n_o = 0$) in the plasma the model shows the complete stability due to the damping of the perturbation by classical diffusion across to the magnetic field.

2.6 Application to an Equatorial Ionospheric E-Region:

In this section, we apply the results obtained in the previous section to the E-region of the equatorial ionosphere in 87-175 km altitude region and compute the scale sizes and the growth rates of irregularities occuring in the electron concentration. In Figs. 2.2 and 2.3 are shown respectively the observed electron density and temperature profiles used for computation of ionospheric parameters which determine the instability criteria. The dashed curve in Fig.2.2 represents the average fit to the profile (continuous curve) measured by Prakash et al., (1970) at 2300 hr IST on 29th August, 1968 using a rocket borne Langmuir probe at Thumba (India) near the magnetic equator. Fig.2.3 represents a seventh degree orthogonal polynomial fit (dashed curve) to their data (solid curves) measured simultaneously with the electron density profile in Fig.2.2 (Gupta, 1970). In the present calculation we shall use the electron density (n_o) and temperature (T^-) read by the fitted curves (dashed curves) in Figs.2.2 and 2.3, while other authors have assumed the electron temperature, T^- to be

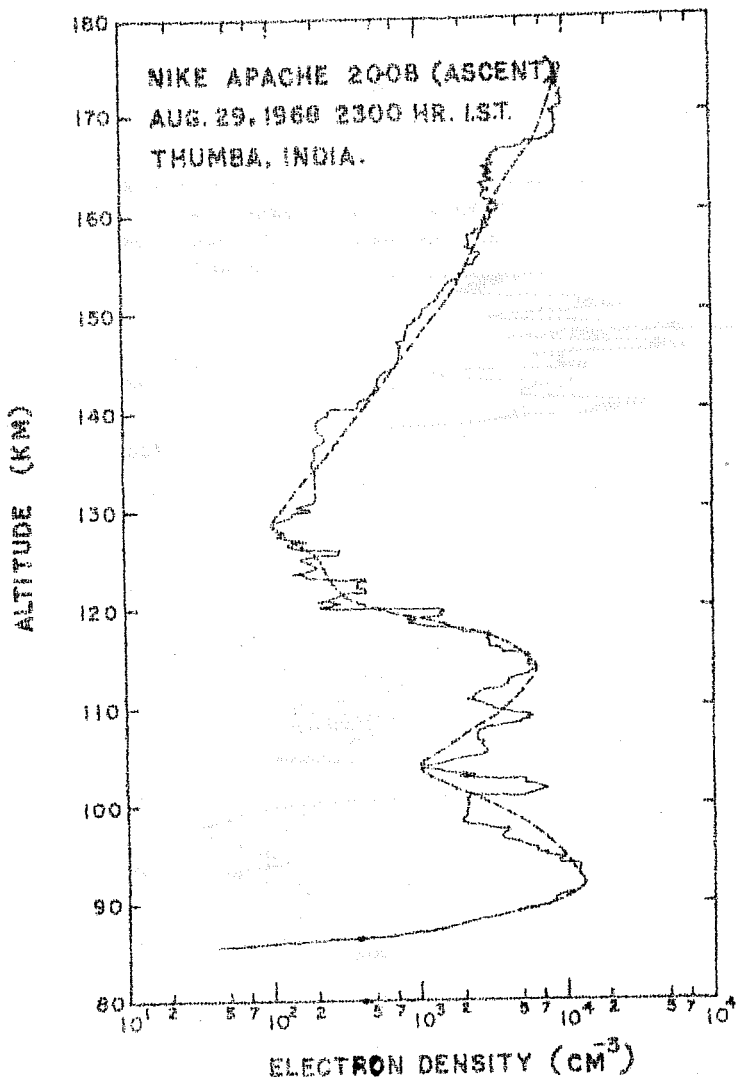


Fig.2.2. Electron density profile (The dashed curve represents smoothed profile used for computation and the solid curve represents the actual observed profile).

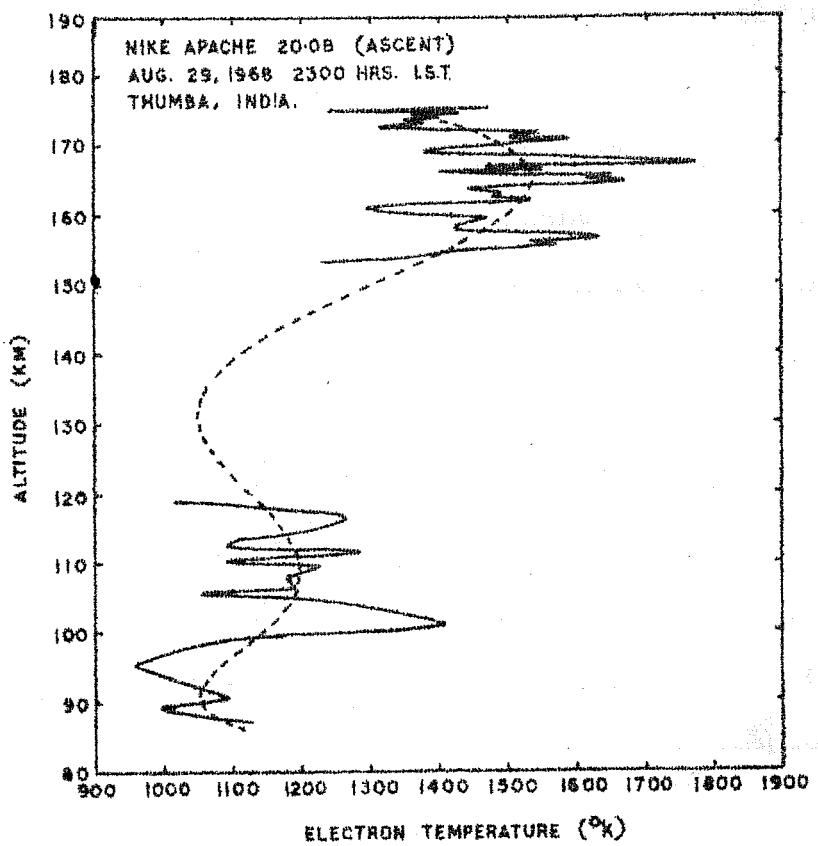


Fig.2.3. Electron temperature profile (Legend same as for Fig.2.2).

temperature, T^+), which is not reasonable because the observed magnitude of T^- is much higher than that of T_N or T^+ (see introduction for references).

The collision frequency of electrons with the neutral particles, ν_e is calculated using the expression given by Nicolet (1953), where the collision frequency of the electrons with the ions is neglected because it is much smaller than that of the electrons with the neutrals in the region under consideration (eq.1.15). The collision frequency of the ions with the neutrals is calculated using the expression derived by Chapman (1956), where the ion collision frequency with the electrons is neglected because the motions of ions are not at all affected by the electrons (eq. 1.16). CIRA model of atmosphere (1965) is adopted to compute the collision frquencies. The temperature of ions, T^+ will be assumed identical to the temperature of the neutral particles, T_N taken from CIRA model atmosphere (1965). These values of the collision frequencies are different from the values obtained by Sugiura and Cain (1966), because here the nighttime profiles of the electron density and temperature have been used. These values are used extensively in the present calculations.

The scale sizes, λy_{min} and the growth rate, ω_i of the irregularities are now computed for the two cases (A) and (B) for which the amplitudes of perturbations are either constant or a varying function of altitude. It is well known that the horizontal electric field, E_{oy} is westward during nighttime, and E_{ox} (see eq. 2.11) will, therefore be vertically downward

Balsley, 1969a,b). We are interested here in explaining the features of the observed nighttime electron density irregularities, but the components, E_{ox} and E_{oy} are directed in Fig.2.1 (valid for day time conditions) respectively vertically upward (along positive x-axis) and horizontally eastward (along positive y-axis). Therefore, E_{ox} and E_{oy} for nighttime conditions are taken with negative sign for the computations.

CASE (A): It is obvious from (2.33) that in the vertical direction, ω_1 is independent of both $\underline{E}_o$ and ∇n_o and is a positive quantity depending upon D_a. This implies that if medium is perturbed by some perturbations having wave number in the vertical direction, the perturbations are immediately damped out due to diffusion of the particles across the magnetic field, and as a result, there are no irregularities produced in the vertical direction. It can also be seen from (2.33) that the sinusoidal disturbances with larger vertical wavelengths if they are somehow excited, die out slower than those with smaller wavelengths. Therefore, in the situation when the amplitudes of the perturbations remain constant with altitude, the present model predicts the complete stability of the ionospheric E-region plasma in the vertical direction because of classical ambipolar diffusion across the magnetic field.

The minimum horizontal scale sizes and the growth rates are now computed using (2.36) and (2.34) and are plotted with

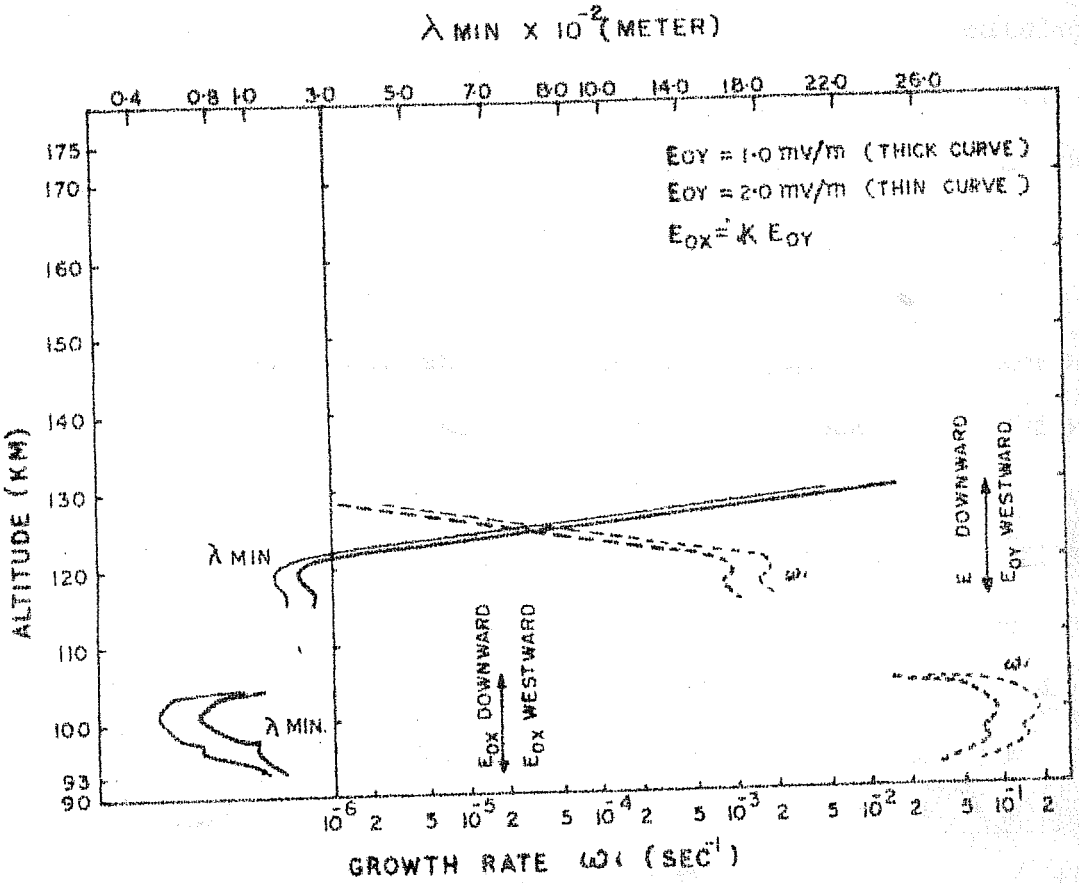


Fig.2.4. Growth rate and minimum scale sizes in the horizontal direction as function of altitude for Case (A) and when both the components E_{ox} and E_{oy} are present together at the same instant. The arrows indicate the region of occurrence of irregularities for appropriate directions of E_{ox} and E_{oy}. Thick curves represent the values for E_{oy} = 1.0 mV/m and thin ones for E_{oy} = 2.0 mV/m.

field E_{oy} taken equal to 1.0 and 2.0 mV/m which are reasonable to assume in the region of the ionosphere under consideration because such fields have been both estimated and observed (Sugiura and Cain, 1966; Balsley and Woodman, 1971; Balsley, 1973a; Haerendel et al., 1970; Davis, 1971; Valenzuela et al., 1973; Raghavarao et al., 1976). The relation (2.11) is used to calculate corresponding vertical electric field, E_{ox}. It is clearly seen from Fig.2.4 that the irregularities are predicted in 93-104 kms and 115-129 kms regions. The lowest scale size occurs at the altitude around 100 kms and it is 70 meters for E_{oy} = 1.0 mV/m and 50 meters for E_{oy} = 2.0 mV/m. These results which are obtained using the smoothed profile (dashed curve of Fig.2.2), are however, very much subjected to the actual background electron density (solid curve) and the strength of the electric field. We will discuss this in the next section.

It is shown in Fig.2.4 that the irregularities in the altitude range from 105 to 115 kms and above 130 km do not exist because of the positive density gradient in the density ($a > 0$) in the smoothed profile of Fig.2.2 and it is even obvious from the instability criteria (2.35) which requires that $a < 0$. This supports the experimental results obtained by Prakash et al. (1970), that the irregularities during nighttime are, in general, not obtained in the region of positive density gradient.

The variation of growth rate, ω_i, with the altitude

equal to 1.0 and 2.0 mV/m. In order to calculate the growth rate we have considered the value of k_y which is 0.1 percent less than the value of k_{ymax} as we are interested in finding out the minimum wavelength which can be unstable. The use of relation (2.11) is again made to estimate E_{ox}. It can clearly be seen from Fig.2.4 that the growth rate, ω_i, first increases, becomes maximum around 100 km and then decreases with altitude. This means that the amplitude of the irregularities first increases upto 100 km and then decreases with altitude, i.e., larger amplitude (strong) irregularities are produced around 100 km. This behaviour of the irregularity amplitude with altitude can be found by using the relation (2.11). Substituting (2.10) and (2.11) in the first term of (2.33) which, as has already been shown in the previous section, is responsible for the growth of the irregularities and is thus instability driving term, we get

$$\text{Instability driving term} = -\mu_o(K_o^2 + 1)\,\underline{U}_o.a \qquad ..(2.48)$$

Since $K_o > 1$ (upto 125 kms approximately), the instability driving term and hence, the growth rate, ω_i (amplitude) are proportional to $\mu_o K_o^2$ if 'a' is taken more or less a constant, where $\mu_o = \alpha^+ K_o = (1-\psi)^{-1}$ being less than 1 far below 100 km, increases slowly with altitude and becomes unity above approximately 100 km. It has, therefore, maximum value around 100 km where the ratio $K_o (= \sigma_2/\sigma_1)$ is maximum, and thus behaves with altitude as K_o^2 does, implying that the irregularity amplitude (i.e., the growth rate) is proportional to K_o^2 provided 'a' remains more or less constant. Similarly, the behaviour of

(2.36), and neglecting the a^2 term (a small diffusion term) compared to other terms in (2.36), we find the minimum unstable horizontal scale size as

$$\lambda_{y\min} = 2\pi \left(-\psi C_s^2/\nu^+\right)^{1/2} K_o^{-1/2} \left(\underline{U}_o \cdot \underline{a}\right)^{-1/2} \quad ..(2.49)$$

where D_a has been substituted for by eq.(2.33). As both $|\psi|$ and ν^+ decrease with altitude, the irregularity wavelength is inversely proportional to $K_o^{1/2}$. Thus the small wavelength irregularities, as illustrated in Fig.2.4, are produced in the region where K_o is maximum. It is also obvious from Fig.2.4 that the waves of smaller wavelengths have larger growth rate (larger amplitude) and are mainly formed in the region of strongest electrojet (93-104 kms), which implies that more intense (fastest growing) irregularities with smaller scale sizes are observed in this region because of larger values of K_o and hence the vertical electric field, E_{ox}.

The effect of either E_{ox} or E_{oy} alone on $\lambda_{y\min}$ in the present case can, however, also be studied by expressions (2.42) and (2.43) and the computed scale sizes as a function of altitude are depicted respectively in Figs.2.5 and 2.6. It can clearly be seen from these figures that the irregularities occur only in 93-104 kms and 115-129 kms regions where the electron density has negative gradients in the profile of Fig.2.2 and the instability criteria (2.35) is satisfied. In the case when $E_{oy} = 0$ and $E_{ox} = 1.0$ mV/m (Fig.2.5), their scale sizes in horizontal direction lie from 394-700 m and

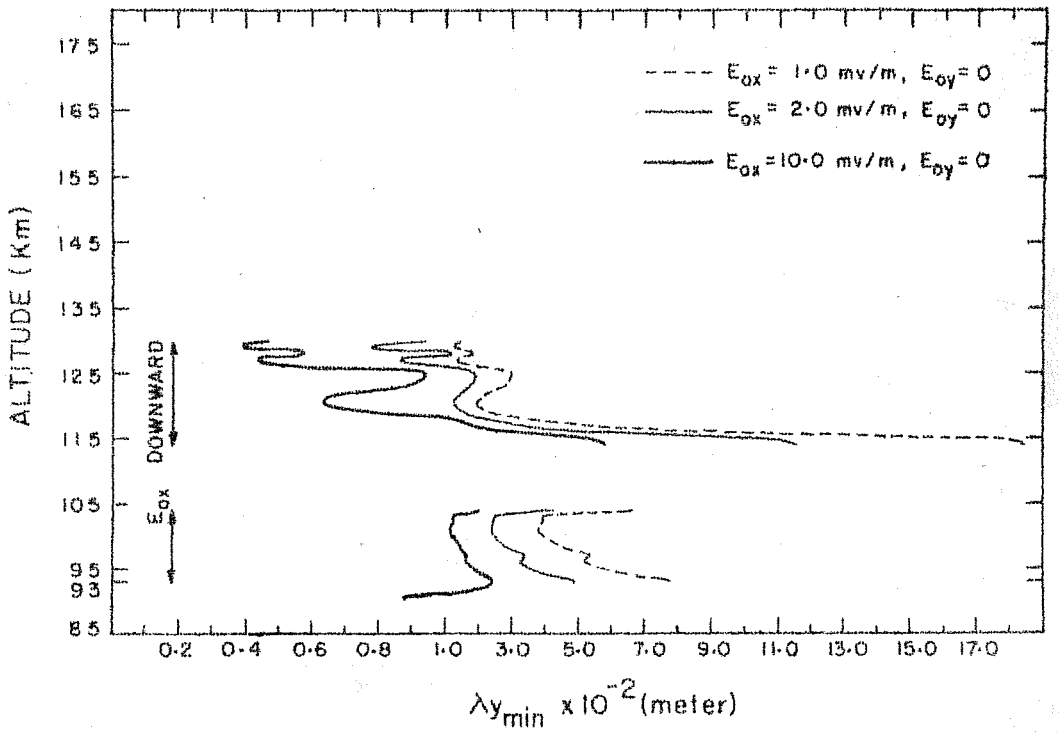


Fig.2.5. Minimum horizontal scale sizes as function of altitude for three values of E_{ox} and $E_{oy} = 0$ (Case A). The arrows indicate the regions of occurrence of irregularities for appropriate direction of E_{ox}. These curves also represent the scale sizes in horizontal direction for Case (B) but now the values are higher by the quantity Ω^+/ν^+ (see the text of Case B).

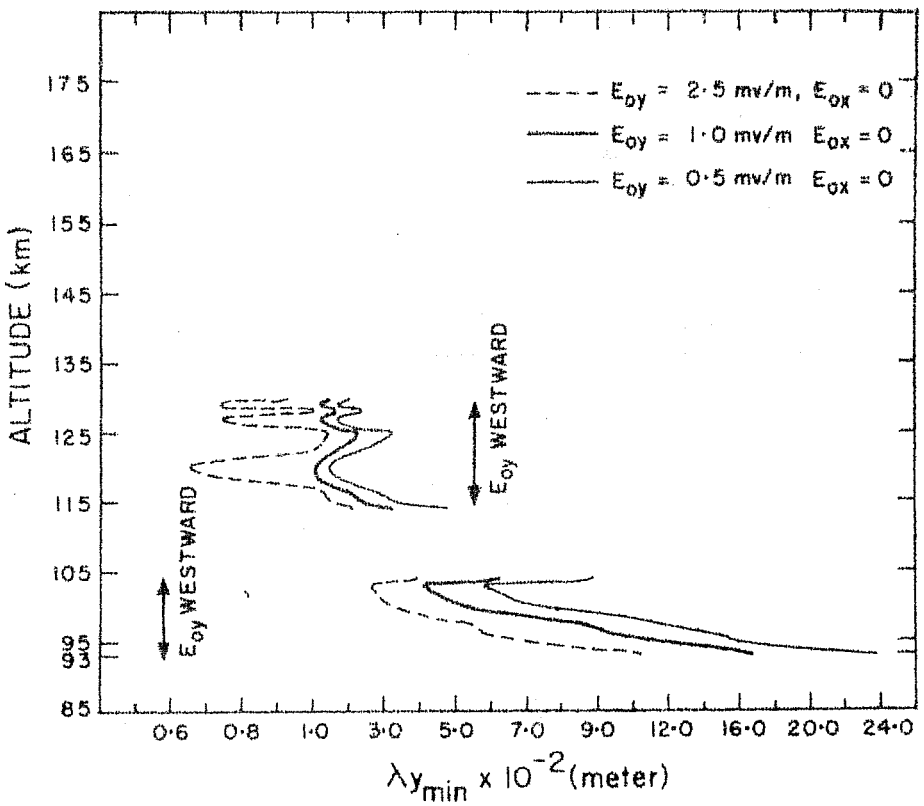


Fig.2.6. Minimum horizontal scale sizes as functions of altitude for three values of E_{oy} and $E_{ox} = 0$ (Case A). The arrows indicate the regions of occurrence of irregularities for appropriate direction of E_{oy}.

at 129 km for two regions respectively. On the other hand, for the case when $E_{ox} = 0$ and $E_{oy} = 1.0$ mV/m chosen as a constant value throughout the ionosphere region (Fig.2.6), the irregularities are obtained with the horizontal scale sizes ranging from 1.7 km to 409 m and from 237 to 102.6 m, the minimum being 409 m at 103 km and 102.6 m at 120 km for two regions respectively. For higher values of electric fields, these ranges of scale sizes are reduced and have been plotted in the Figures 2.5 and 2.6 for two more values of E_{ox} or E_{oy}.

CASE (B): In this case when amplitudes of perturbations are considered as the exponential function of altitude (eq. 2.29), the scale sizes of the irregularities occuring in the vertical and horizontal directions can be estimated by eqs.(2.45) and (2.47) respectively. The minimum scale sizes in the vertical and horizontal directions, at which the irregularities occur, are not dependent on both the components E_{ox} and E_{oy} together. The vertical scale sizes, λ_{xmin} depend upon the horizontal component, E_{oy} which leads to the vertical electron drift, whereas the horizontal scale sizes, λ_{ymin} depend on the vertical component, E_{ox} which gives rise to the horizontal electron drift. In this case also, the irregularities are formed in 93-104 kms and 115-129 kms regions which are the regions of 'valley' in electron density (Fig.2.2), as can be seen from the scale sizes versus altitudes plots in Figs.2.7 and 2.5 respectively for irregularities in vertical and horizontal directions. The minimum unstable vertical scale

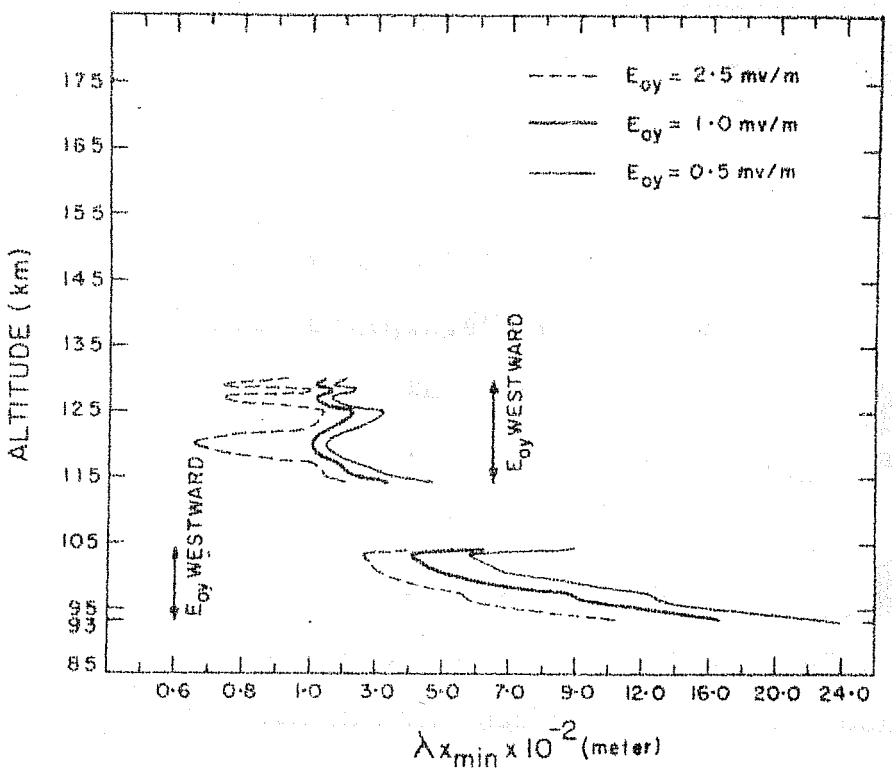


Fig.2.7. Minimum vertical scale sizes as function of altitude for three values of E_{oy} (Case B). The arrows indicate the regions of occurrence of irregularities for appropriate direction of E_{oy}.

for three values of E_{oy}. These scale sizes for E_{oy} = 1.0 mV/m have the values ranging from 1.68 to 0.41 kms with a minimum value of 410 m at 103 km and from 370 to 100 m with a minimum equal to 100 m at 120 km in two regions of valley respectively, whereas for E_{oy} = 2.5 mV/m these range from 1.06 km - 260 m, with the minimum equal to 260 m at 103 km and from 210 - 65 m with the minimum equal to 65 m at 120 km.

The variation with altitude of the horizontal scale sizes, λ_{ymin} (given by eq.2.47) which depend upon E_{ox} only, is found to be similar to that shown in Fig.2.5 for Case (A), except the difference that the values of λ_{ymin} are now higher by the quantity α^+. This difference can easily be found out by using (2.11) in (2.47). The quantity α^+ increases rapidly with altitude as ν^+ is decreasing. Hence, it is concluded that the horizontal scale sizes in the case when the amplitudes of perturbations have functional form, are seen to have larger values than those shown in Fig.2.5 by a variable factor increasing rapidly with altitude. This implies that small scale irregularities are produced in lower altitude regions (electrojet) only.

All the above results have, however, been obtained by using the smoothed electron density (dashed curve) profile of Fig.2.2, while the actual observed electron density (solid curve) is seen to vary with the altitude in a manner very much different from the smoothed profile. These results are also highly dependent on the electric field strength. Hence, the

the electric fields and the variation in the background density which, in turn, corresponds to the variation in back ground density gradient 'a', is made in the next section with a view to explain the features of the irregularities more accurately.

2.7 The Effect of the Electric-Field Strength and the Electron Density Gradient on the Formation of Irregularities at a Particular Height:

So far, we have studied above the irregularities for some typical values of electric field strength (E_{oy} = .5, 1, 2 or 2.5 mV/m) and for smoothed profile of electron density (Fig.2.2). In the ionosphere, the electric field strength can have the values even higher than 2 or 2.5 mV/m, which have been both estimated theoretically (Sugiura and Jain, 1966; Matsushita, 1969; Balsley and Woodman, 1969, 1971; Woodman, 1970; Balsley, 1973a) and measured experimentally (Haerendel et al., 1970; Rieger, 1971; Davis, 1971; Valenzuela et al., 1973; Raghavarao et al., 1976). Under magnetically disturbed conditions, the electric field strength and the electron density distribution in the ionosphere change very dramatically. It is, therefore, very important to examine the effect of the electric field strength and the electron density on the growth rates and scale sizes and as a result, on the occurrence of the irregularities in the ionosphere.

a) The Effect of the Electric Field Strength: The dependence of the growth rate and the scale sizes on the strength of the electric field is studied at one altitude of the electron

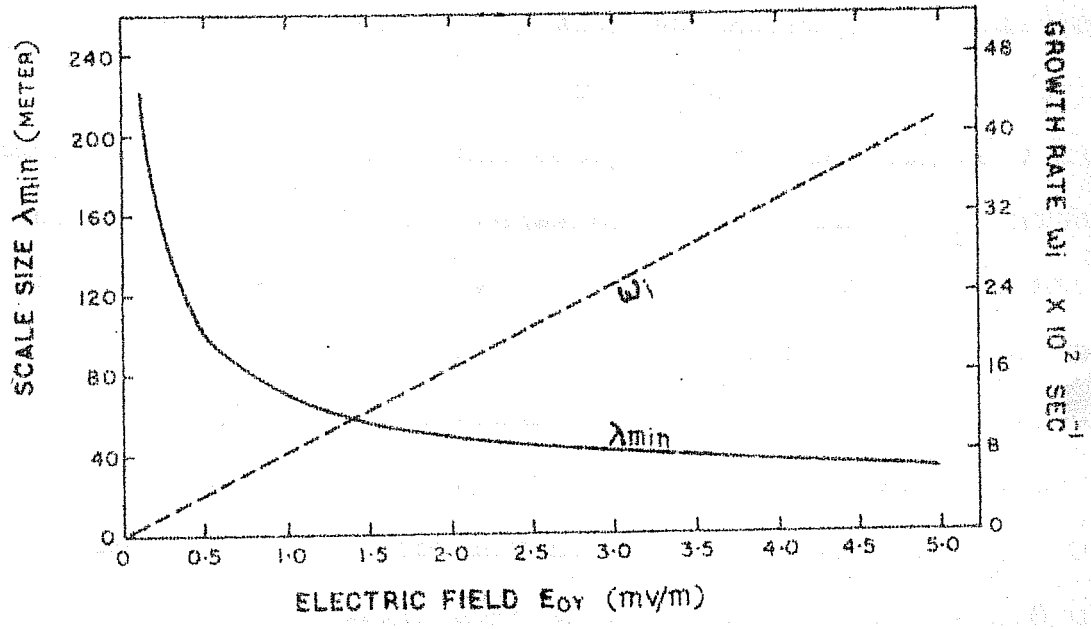


Fig.2.8. The effect of east-west electric field on the scale size (solid curve) and the growth rate (dashed curve) at a particular altitude of 101 km.

The dashed curve represents the growth rate, ω_i, while the solid curve shows the minimum scale sizes, λ_{min}, with the increase of east-west electric field, E_{oy} at an altitude of 101 km. The effect of electric field on ω_i and λ_{min} can also be seen in all the Figs. 2.4 - 2.9 which show that the growth rate increases linearly with the increasing values of the field, while λ_{min} shows a rapid fall between the field values of 0.1 to 2.0 mV/m and decays slowly for higher values of the field. To know the behaviour of ω_i and λ_{min} with electric field, we have, however, chosen here the horizontal scale size calculated by (2.36) at an arbitrary altitude of 101 km, and shown its behaviour as well as that of corresponding growth rate estimated by (2.34), in the Fig.2.8. The scale size of 221 m in the horizontal direction for E_{oy} = 0.1 mV/m at 101 km is reduced down to 30 meters for E_{oy} = 5.0 mV/m. One can, however, also show from (2.45) that the vertical scale size λ_{xmin} of 410 m for E_{oy} = 1.0 mV/m at 103 km is reduced to 180 meter for E_{oy} = 5.0 mV/m.

b) <u>The Effect of the Background Electron Density or Density Gradient (i.e., 'a'):</u>

We have already seen that the gradient of the background electron density has a considerable effect on the growth rate and the scale sizes of the irregularities. In the ionosphere, the electron density is a highly variable parameter, at least during night, having sharper gradients. There are some observations also by rocket measurements at night (Prakash

density gradient scale height in the E-region can be as small as a few hundred meters and as large as few kms (~ 6-7 km). Our intention in this section is thus to explain the observed scale sizes of the irregularities on the basis of exact observed profiles. On the other hand, it is very laborious to read data from the actual profile and in fact, we have used only a mathematically fitted curve for our analysis. We would like to do here a simple calculation to show how the departure of the electron density from the smooth curve affects the scale sizes of the irregularities so that looking at the actual and smoothed profiles, one would get the approximate scale size.

Suppose n_o and n_o' are the electron densities of the smoothed profile at heights $x-\Delta x$ and x respectively. The inverse scale height is then $a = (n_o' - n_o)/n_o \Delta x$. Let $n_o''(= n_o' + \Delta n_o')$ be the actual density at x, then the inverse scale height becomes $a' = (n_o'' - n_o)/n_o \Delta x$ ($\Delta n_o'$ is the departure from the smoothed curve). The percentage change or departure in the electron density to be termed as the 'variation in the background electron density', $\delta n_o(= \Delta n_o' \times 100/n_o')$ at x is given by

$$\delta n_o = n_o \delta a . \Delta x . 100/n_o' \qquad ..(2.50)$$

where $\delta a = a' - a = (\Delta n_o'/n_o) \Delta x$ is the change in the inverse scale height at x. Thus the variation in 'a' represented by δa is related with that of the background electron density through (2.50).

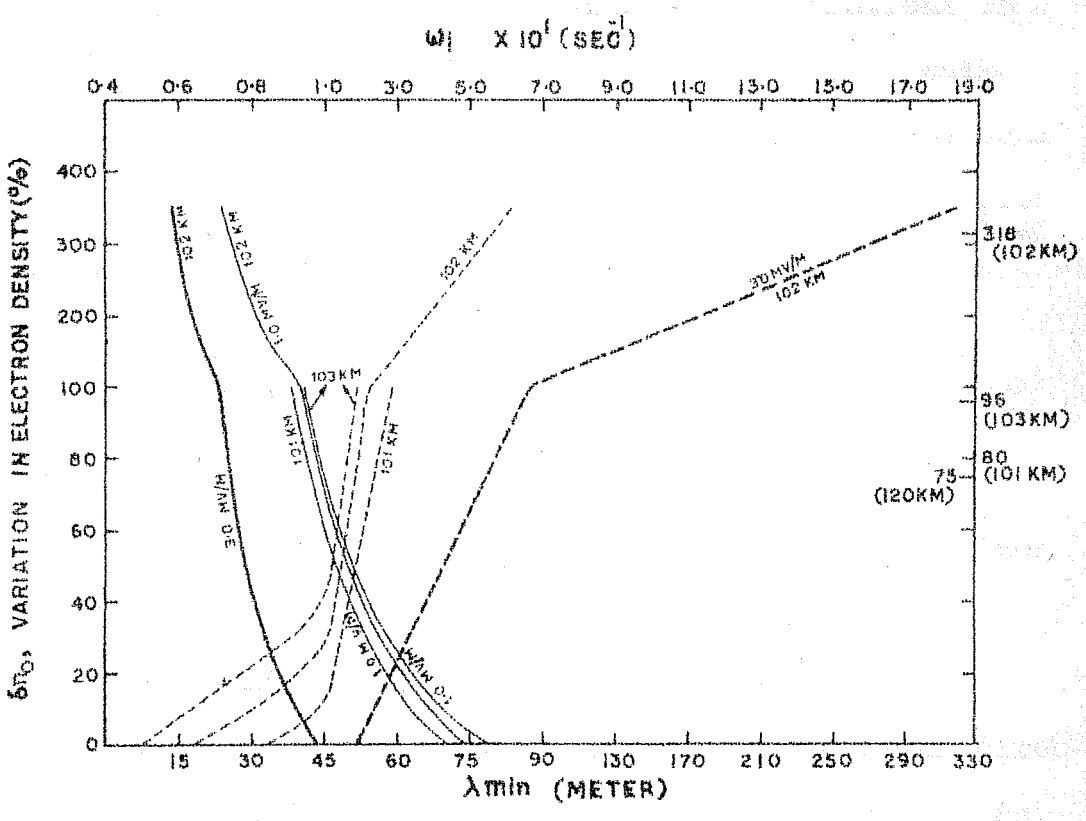


Fig.2.9. The scale size (solid curves) and the growth rate (dashed curves) at a particular altitude with the arbitrary change in the background electron density. The values on the right hand scale represent the percentage departure (δn_o) of actual observed electron density from the smoothed electron density profile (dashed curve in Fig.2.2) at the height mentioned in the bracket.

102 and 103 kms by assuming the east-west electric field, E_{oy} equal to 1 mV/m and at 102 km these are also plotted for E_{oy} = 3 mV/m. The values shown on the left-hand vertical scale of the Fig.2.9 are arbitrary percentage variations in the background electron density, estimated by (2.50), while those, on the right-hand vertical scale, represent the actual percentage departures in the background electron density from the smoothed profile calculated by using the electron densities on smoothed and observed profiles of Fig.2.2 at the height mentioned within the bracket.

Though we have, studied in the Fig.2.9 the effect of varying the background electron density n_o on the scale sizes and growth rates (given by eqs. 2.36 and 2.34 respectively) of the irregularities in the horizontal direction only, the effect on the scale sizes of the irregularities in the vertical direction can also be found out using the equation (2.45). It is, in general, seen that the scale sizes of the irregularities are diminished and the growth rate and hence, amplitude is enhanced with the enhancement in the background electron density at a particular height (Prakash et al., 1970, 1971a,b, 1973). Having accounted for the departure of the background electron density measured from the smoothed profile of Fig.2.2 from that measured from observed profile in Fig.2.2, the minimum horizontal scale sizes are reduced to 38 meters at 101 km, 25 meters at 102 km and 40 meters at 103 km for E_{oy} = 1.0 mV/m. The growth times (inverse of the growth rate, $1/\omega_i$) for

are seen to reduce to 4, 2 and 5 sec. respectively. For the field E_{oy} = 3.0 mV/m and having accounted for the difference between the smoothed and actual observed background densities, the scale size at 102 km in the horizontal direction is further reduced to 14 meters and the growth time is also further lowered down to 0.6 sec. This clearly points out that the smaller scale sizes irregularities grow faster in amplitude. In the vertical direction, the minimum scale size of 410 m at 103 km for E_{oy} = 1.0 mV/m is found to be equal to 290 m when the actual observed variation in the background density is accounted for, and it is further reduced to 168 m when E_{oy} is also increased to 3 mV/m.

The irregularities in the electron density with a wide range of scale sizes are, therefore, more often generated in the E-region of ionosphere particularly in the altitude range of 93 - 104 kms and they are seen to grow faster in the region around 100 km. The growth rate is found to be inversely related to the scale sizes as can be seen in all the Figs.2.4, 2.8 and 2.9. This, therefore, suggests that the amplitude of small scale irregularities in both the horizontal and vertical directions may increase with decreasing scale sizes although there is a limitation on the lower scale sizes. This is in agreement with rocket measurements of Type Mc and Sc irregularities (Prakash et al., 1969, 1970, 1971a,b, 1973).

2.8 Discussions of the Results and Their Comparison with the Observations:

Various results obtained herein are now discussed and compared with the radar and in-situ rocket observations of Types II, L, Mc and Sc irregularities occuring in the equatorial E-region of the ionosphere that have been described in secs. 1.31(b) and (c). As we have used the observed nighttime profiles of electron density and temperature (Prakash et al., 1970; Gupta, 1970) in the calculations, our attention will be devoted mainly to the comparison of our results with the nighttime observations of Type L, Mc and Sc irregularities reported by Prakash et al.,(1969, 1970, 1971a,b, 1973). Nevertheless, some attention will also be focussed on the discussion of the comparison with other irregularities observations, e.g., Type II, Mc and Sc irregularities during day as well as night times.

An effort has been made to show how the simple physical mechanism of the low frequency gradient drift instability developed in this chapter, can lead to the formation of the field aligned irregularities in the electron concentration in the equatorial E-region, if the magnitude and the direction of background electric field are appropriately considered and the appropriate electron density and temperature profiles are chosen. It has clearly been shown that the density irregularities are, in general, more often developed in the regions of nighttime equatorial E-regions, where the electron density exhibits the negative gradients (Fig.2.2) in the altitude ranges of 93-104 kms and 115-129 kms, as has been observed

and Farley, 1973; Fejer et al., 1975a,b).

We would like to point out here one important result why the instability model discussed has not revealed the formation of any irregularities between 105 and 114 kms while these have actually been observed (Prakash et al., 1970). The smoothed density profile used for computation, shows in this region a positive gradient (a condition for stability (2.35) at night), whereas observed density profile exhibits both the positive and negative gradients (Fig.2.2) and as such the irregularities are likely to be possible in this region. The minimum scale sizes (likely to grow)of the irregularities derived herein for the appropriate values of the parameters in the E-region are found to range from as small as 14 meters to as large as 2.4 kms. Thus, in particular, it is explained why both the small (30-300 meters or more) and smaller (< 15 meters) scale size irregularities (Types Mc and Sc respectively) are observed in the height region of 93-129 kms, in an agreement with the nighttime rocket observations (Prakash et al., 1969 , 1970, 1971a,b, 1973) and radar observations (Balsley, 1969; Balsley and Farley, 1973; Fejer et al., 1975a,b). It can be seen from Fig.2.4 that the growth rate of the irregularities in the horizontal direction is very low ($\sim 2 \times 10^{-3} - 3 \times 10^{-1}$ sec^{-1}) in the region of 120-129 kms compared to the lower region (< 120 km). Therefore, it suggests that the irregularities are mainly generated in the region of 93-120 kms, as has been inferred from observations (Prakash et al., 1970, 1973).

E_{ox}, with height can be neglected. It is well known fact that the ratio K_o of the Hall and Pedersen conductivities varies rapidly with height (Subbaraya et al., 1972; Richmond, 1973), the vertical field E_{ox} will, therefore, as it is clear from (2.11), vary with height (Sugiura and Poros, 1969) even when E_{oy} does remain constant. Hence, the variation of E_{ox} with height can not be ignored, as was done by almost all the earlier workers. A careful comparison of Fig.2.4 with Fig.2.5 which illustrates the behaviour of scale sizes with height for the Case A (ii) when $E_{ox} = 0$ and the instability can arise in view of eq. (2.35a), reveals that the irregularities in the horizontal direction occur in the regions of 93-104 kms and 115-129 kms for both the cases when $E_{ox} = 0$ (Case A (ii)) and when both E_{ox} and E_{oy} are present (Case A (i)). But it is to be noted that the scale sizes are larger and hence, the growth rate will be smaller in the former case A (ii) than those in the latter case A (i). This shows that the vertical polarization electric field E_{ox} satisfying (2.11) plays an important role in the formation of smaller scale and fastest growing irregularities in the electrojet region.

We have demonstrated that in the case of non-functional forms of the perturbation amplitude, the irregularities are observed only in the horizontal direction, and that their development depends upon both the vertical and horizontal components of elecrtic fields connected through (2.11). The scale sizes are found to vary inversely with $K_o^{1/2}$, whereas the

in the E-region. Thus, the growth rates are highest and the scale sizes are smallest around 100 km (Fig.2.4) where K_o is maximum and a strong electrojet current flows (Subbaraya et al., 1972; Richmond, 1973), implying that larger amplitude and smaller scale irregularities are mainly formed within and thus correlated with the strongest electrojet region (Balsley, 1969a, b; Prakash et al., 1970; Balsley and Farley, 1973; Fejer et al., 1975,a,b). Though the perturbation amplitude is assumed to be independent of altitude in the present case, this altitude dependence of the features of irregularities arises because of the fact that we have considered the variation of collision frequencies and other atmospheric parameters with altitude. The collision frequencies vary with altitude, since they depend upon the particular profiles of electron density and temperature and other ionospheric parameters, which we have used in the analysis in order to apply our results to the observations. Note, however, that the altitude variation of collision frequencies and atmospheric parameters has been implicitly taken into account throughout the calculations.

The theory predicts that in the vertical direction, the irregularities are seen to be produced only for the Case (B) when the amplitudes of perturbations are assumed to be a function of altitude in the same manner as the background density n_o varies with height (eq. 2.29), which is an appropriate assumption valid in the ionosphere. The theory predicts further, that in this case, the formation of irregularities in the horizontal

horizontal (E_{oy}) and vertical (E_{ox}) electric fields together. In the vertical direction, only E_{oy} is responsible for excitation of the perturbation, while in the horizontal direction, only E_{ox} is found to excite the instability. Thus, we infer that the vertical echoes as well as horizontal echoes should be observed in the equatorial E-region. This agrees with the observations of Types L, Mc and Sc irregularities (Prakash et. al., 1969, 1970, 1971a,b, 1973) and Type II irregularities (Balsley, 1969; Balsley and Farley, 1973; Fejer et al., 1975a,b).

The scale sizes of the irregularities predicted by the present computations are comparable to those measured by observations. It has clearly been shown that the scale sizes and the growth rate depend upon both the electric field and the variation in the background electron density in such a way that the growth rate enhances with the electric field and the variation in the background electron density, while the scale size diminishes (Prakash et al., 1970, 1972, 1973). The scale sizes of the order of 14 meters (even lower with higher electric field) are obtained by considering an electric field of 3 mV/m and including the actual observed variation in the background electron density from the smoothed profile. The irregularities with the scale sizes as large as 2.4 km (even higher with observed lower electric field) are found to be present for the electric field E_{oy} = 0.5 mV/m. This range (14 m - 2.4 km) of the scale sizes predicted herein agrees fairly well with the observed values of scale sizes of types L, Mc, Sc (Prakash et.

irregularities.

The above results are different from those obtained by Reid (1968) in the sense that the electric field E_{oy} needed to obtain the scale sizes in the observed range ($\leq$ 30 m) in his model is very high ($\geq$ 30 mV/m). This is highly idealized because such a strong electric field E_{oy} has not been observed in the ionosphere. In the present model, however, an electric field E_{oy} of the order of 3 mV/m (an order of magnitude less than that required by Reid's model) is adequate to produce smaller scale ($\sim$14 m) irregularities (Type Sc) because there exists a corresponding E_{ox} by virtue of (2.11), while in Reid's model it is assumed to be zero. Furthermore, we need to know only E_{oy} which is available from present observations. Hence, the present model of the gradient drift instability described here seems to be more realistic and applicable to the equatorial E-region irregularities.

However, the typical values of the growth rate at different altitudes in this model appear to be smaller than those obtained by Linson and Workman (1970) and Linson (1970). This descripancy may probably arise because in their model the calculations were made for mid-latitudes and during the twilight period, whereas this model is confined to the equatorial region and to the mid-night electron density profile. Furthermore, the growth rate expressions in this model contain an extra damping term (wavelength independent) which may be considerable during nighttime because of low electron density. We also note, however, that the values of the growth rate obtained by

those in this model.

The structures of the irregularities (as seen in Figs. 2.4-2.7) at least at night, seem to have somewhat complex nature with altitude, as is observed (Balsley, 1969a,b; Prakash et al., 1970; Fejer et al., 1975a,b). It is, therefore, pointed out that such a complex structure may give rise to smeared spectra of irregularities observed, i.e., the spectra may change drastically with altitude (Balsley and Farley, 1973; Fejer et al., 1975a,b).

A general comparison of Figs. 2.4-2.7 indicates that the characteristics of the irregularities are such that there are two distinct regions in the equatorial electrojet, the lower region below around 100 km in which the scale sizes can be seen to decrease with height (Prakash et al., 1970, 1973) and the upper region above around 100 km ($\sim$ 100-105 km) in which the scale sizes show opposite behaviour. As it has already been inferred that the growth rate (hence, amplitude) is inversely related to the scale size and hence it is larger for smaller scale size, the strongest echoes are observed from the region centered around 100 km (Balsley, 1969a,b; Balsley and Farley, 1973).

It can also be seen from Figs. 2.5-2.7 that the E-region irregularities have many small and large peaks in the regions of their occurrence, particularly, in 115-129 kms region, indicating that they have layered structures. This feature is in agreement with the observations that the echoes exhibit strongly layered structures and are concentrated in

many (upto five or sometimes more) thin layers which can be at altitudes as high as 130 km (Prakash et al., 1969, 1970, 1971a, b; Fejer et al., 1975a,b).

As can be seen from the growth rate expressions obtained herein, the growth rate and hence, the amplitude of the instability are directly proportional to the electron drift velocity in the electrojet region. Now it is an observed fact that type II irregularity drift velocity is linearly related to the electron drift velocity in the electrojet (Balsley, 1969; Fejer et al., 1975a,b). It can, therefore, be inferred from the present theory that the type II echo power (the square of the irregularity amplitude) is proportional to the square of the type II irregularity drift velocity, in an agreement with the observations (Balsley, 1969b).

Under daytime equatorial conditions (E_{oy} being eastward and E_{ox} vertically upward), the irregularities generated by the mechanism of the gradient drift instability that we have described here, could also be identified for a daytime electron density profile which shows only the positive density gradients (Prakash et al., 1972; 1973), as the criteria (2.35) for the instability are satisfied. But no definite theoretical predictions could be possible without a precise knowledge of the observed daytime density profile so as to apply them to the irregularity observations during daytime.

We have shown that the intense growing irregularities in the electron concentration with the smaller wavelengths occur

electrojet. These irregularities can, therefore, give rise to the enhanced radio-wave scattering in the equatorial region, commonly called the equatorial sporadic E-layer, E_{sq}. Matsushita's (1951) suggestion that the occurrence of E_{sq} is predominent in the equatorial electrojet is thus supported by the present model. It has been observed that during the period when the magnetic field value suddenly decreases below the nighttime mean value, the E_{sq} vanishes (Matsushita, 1957; Cohen et al., 1962; Rastogi et al., 1971; Krishnamurthy and Sengupta, 1972). These observations are, however, made during the daytime when the density profile shows only the positive gradients. It was suggested (Rastogi et al., 1971) that the disappearance of E_{sq} is due to the temporary reversal of equatorial electrojet currents. This supports the present theory because if sudden decrease in the magnetic field value can be attributed to the sudden reversal of equatorial electrojet currents which may be caused due to the temporary reversal of the electric fields satisfying now the nighttime conditions, then the criteria (2.35) of the occurrence of the instability discussed here will not be valid because a density gradient of opposite direction does not exist in the daytime and hence no irregularities could be formed.

Very recently, Fejer et al., (1975a,b) have observed that the altitudes of echoing regions change before and after the normal electrojet current reversal (reversal time is around 2048 hr). Though, no quantitative estimates of altitudes of

form of the instability model described herein, a qualitative explanation of this phenomenon in view of present model can be given as follows: Before sunset, i.e., during daytime, the density profile shows only the positive gradients, while after sunset, particularly at somewhat later time (2048 hr) when the current reverses (electric fields also reverse, satisfying nighttime conditions), it starts developing sharper and sharper negative gradients than those during day time. It is very likely that at reversal time, the sharp gradients satisfying the instability criteria (2.35) for night conditions, may be formed in the altitude regions different than those in which the irregularities exist before reversal time. Thus, the echoes (irregularities) may be observed as coming from two different altitude regions, implying that there is an interchange of altitudes of echoing regions, before and after normal electrojet current reversal.

As has been shown, the irregularities at night are generated in the electrojet in two different height regions (with a marked separation): (a) the lower region from 93 to 104 kms; and (b) the upper region from 114 to 129 kms, with their scale sizes, generally, being smaller in the lower region than those in the upper one. Though, we have seen that the growth rates (hence the amplitudes) of the irregularities are smaller in upper region, these may be sufficient to produce type II echoes as observed by radar when the electrojet intensity (i.e., the electron drift velocity) is considerably

value (Balsley, 1969b). We therefore, surmise that at night, the type II echoes can be received by radar from two distinctly separate regions (93-104 kms and 114-129 kms) of electrojet, embedded in them with type II irregularities. Nothing definite can be said at present about the type II echoing region, during daytime, without the knowledge of the daytime density profile. It is thus suggested that at least at night, there is marked splitting (bifurcation) of the echoing region in the electrojet, as observed by Bowles and Cohen (1962), Balsley (1965, 1969b, 1973) and Fejer et al. (1975b).

For simplicity, the author has restricted here himself to the discussion of the generation of pure horizontally or vertically propagating irregularities. It should be obvious, however, that irregularities travelling at all oblique angles will also be produced by the same linear mechanism. Though it is desirable to include both the propagation directions together (oblique propagation) for completeness of the theory presented, the conclusions will still qualitatively be valid. Nevertheless, the mechanism seems to be in quite satisfactory agreement with the radar and rocket observations of the ionization density irregularities and their features in the equatorial ionosphere.

However, the linear theory can not account for observed shorter wavelengths type II ($\sim$3 m) and type Sc ($<$ 14 m) irregularities (Prakash et al., 1970, 1971a,b, 1973; Balsley and Farley, 1973). Indeed, a linear analysis of the gradient drift instability for parameters applicable to the equatorial

have wavelengths of a few tens of meters or longer (Jain and Das, 1971; Sudan et al., 1973). Shorter wavelength (< 10 meters) irregularities are heavily damped by electron thermal diffusion across the magnetic field. In fact, for electron drift velocity less than ion acoustic velocity, there appears to be no other linear instability that can directly excite these shorter wavelength irregularities in the E-region. Consequently, the shorter wavelengths (3-10 m) are shown to be generated through some nonlinear process, e.g., the so called 'cascade mechanism' (Sudan et al., 1973) that transfers energy from the long wavelength linearly unstable modes to the shorter wavelengths linearly stable modes which, in turn, are stabilized by linear damping (classical diffusion), in an analogy to hydromagnetic turbulence.

In order to improve the understanding of the generation and saturation mechanisms of shorter wavelength (types II and Sc) as well as longer wavelength (type II, Mc, L, etc.) irregularities, many authors have investigated into this instability by using one-and two-dimensional quasilinear and nonlinear theories (Dougherty and Farley, 1967; Sato, 1968, 1971, 1972, 1973, 1974; Kim and Simon, 1969; Sleeper and Simon, 1970; Kamenetskaya, 1971; Rogister, 1972; Rogister and D'Angelo, 1972; Sleeper and Weinstock, 1972; Sudan et al., 1973; Balsley and Farley, 1973; Rognlien and Weinstock, 1973, 1974a,b, 1975; Ott and Farley, 1974; Weinstock and Rognlien, 1975). Whitehead (1970a), Kato (1972) and Tsuda (1973) have briefly

(1974) has given an another excellent brief review on some of these nonlinear theories, pointing out their limitations and difficulties encountered.

The nonlinear set of electrojet equations is highly complex and therefore, intractable analytically, but it can be solved numerically without much difficulty. Also, due to inability of the linear theory to explain the shorter wavelength type II and other types of irregularities and the controversy existing between the two basic nonlinear mechanisms of one-dimensional steepening (Sato, 1971, 1973; Rogister, 1972) and a two-dimensional turbulent cascade process (Sudan et al., 1973; Balsley and Farley, 1973), a number of extensive numerical studies of this instabilities have been performed (Sato and Tsuda, 1967; Tsuda and Sato, 1968; Tsuda et al., 1969). These authors concluded that small scale irregularities with the transverse wavelength $\lambda_\perp << (\sigma_1/\sigma_0)^{1/2}\lambda_{||}$, parallel wavelength to $\underline{B}_0$ (definition of field-alignment), could grow in the lower-E-region. These studies were made on perturbations very restricted in extent in dynamo region. The model of perturbation in all these works was one-dimensional in which it is assumed that all the variables vary along one direction, i.e., along the direction of wave propagation. However, the cross-field instability is, in fact, two-dimensional process, as can be seen in its physical picture and has been considered in the present analysis made in this chapter.

Ogawa (1972) has, recently, done extensive numerical

dimensional cross-field instability in nonlinear regime. He found the cyclic growth and decay with time of unstable waves, and inferred that the background density gradient and applied vertical electric field (potential) both acting as energy reservoirs for sustaining the instability, deform with time (i.e., flattening of both the profiles occurs) so as to quench the instability (providing a quasilinear saturation mechanism). He also pointed out that the wave forms become sawtooth or soliton like as the time passes. Very recently, the two-dimensional turbulent development of the $\underline{E} \times \underline{B}$ instability has been investigated numerically by Sato and Ogawa (1974) who interpreted the stabilization mechanism in a sharply bounded system as due to quasilinear density flattening, and by Ronglien and Weinstock (1974a, 1975) who invoked that the stabilization mechanism for each unstable mode is due to a nonlinear wave-enhanced flux of electrons which acts to deplete the growing perturbations. However, these two interpretations are not in conflict with one another, but they are simply two ways of viewing the same process. Further, McDonald et al. (1974, 1975) have performed the numerical studies of the nonlinear set of the electrojet equations describing short wavelength (< 28 meters) type II irregularities by a two-dimensional computer simulation and surmised that these irregularities are indirectly generated as a result of nonlinear two-dimensional turbulent-like process over one-dimensional steepening.

2.9 Conclusions:

In summary, the author has shown that the mechanism of the linear low frequency gradient drift (also called cross-field or drift-resistive) instability investigated in the chapter, seems to be quite satisfactory responsible for the creation of the field-aligned ionization density irregularities in the equatorial E-region. It has been further shown that the results of the theory are in fairly good agreement with their radar and rocket observations and account for many of their observed features, satisfactorily. The principal conclusions of the linear analysis of the instability that we have performed are as follows, in view of the observations explained here: (1) The mechanism appears to be quite capable of generating larger scale as well as smaller scale irregularities propagating both in the horizontal and vertical directions in the equatorial E-region of 90-130 kms, in presence of the appropriate ambient electron density and temperature profiles and electric field. The scale sizes range from a few meters ($\gtrsim$ 14 meters) to a few kms ($<$ 3 kms). (2) The calculations have shown that the theory discussed is likely to be more competent in the regions of electrojet where there are pronounced 'valleys' (93-105 kms and 115-129 kms in the smoothed profile of Fig.2.2) in the nighttime electron concentration. However, the generation of intense growing irregularities is predicted in the region of 93-120 kms (an observational fact), as in the upper valley (115-129) the growth rates are seen to be smaller than in the

(93-105 kms). (3) The vertical polarization electric field is necessarily found to play an important role in the formation of smaller scale and fastest growing irregularities. (4) The characteristics of the irregularities are such that the growth rate is proportional to K_o^2 and its behaviour with altitude is similar to that of K_o, while the scale sizes show the contrary behaviour, varying inversely with $K_o^{1/2}$. This implies that larger amplitude and smaller scale irregularities are formed within and thus correlated with the strongest electrojet region. (5) The theory predicts that in the vertical direction the irregularities are seen to be produced only for the case when the amplitudes of perturbations are assumed to be a function of altitude, as they are found observationally. It is thus pointed out here that the altitude dependence of the perturbation amplitude must be taken into account while developing any realistic and complete theory. (6) It has been shown that the characteristics of the irregularities depend upon both the electric field and the ambient electron density in such a way that the growth rate enhances with the electric field and the ambient electron density, while scale size diminishes. (7) Two distinct regions in the electrojet of occurrence of intense irregularities are predicted, in which their behaviour with altitude is quite opposite; the lower region (below 100 km) in which the scale sizes (growth rate) can be seen to decrease (increase), and the upper region (100-105 kms) in which the behaviour is reversed, with the

observed from the region centred around 100 km. (8) We have shown that E-region irregularities appear to have layered structure with many thin layers in the regions of their occurrence. (9) It has been inferred, qualitatively, that the type II echo power is proportional to square of the type II irregularity drift velocity. (10) The two suggestions that the occurrence of E_{sq} is predominent in the equatorial electrojet region (Matsushita, 1951) and that E_{sq} disappears where there is sudden reversal of electrojet current seems to be explained reasonably satisfactory by the present model. (11) It is suggested that marked splitting (bifurcation) of the echoing region in the electrojet may be caused, at least at night, by the irregularities produced in two different height regions.

CHAPTER III

NONLINEAR TWO-STREAM INSTABILITY MECHANISM ASSOCIATED WITH TYPE I IRREGULARITIES

3.1 Introduction:

In recent years, the type I irregularities in the equatorial electrojet have been extensively studied observationally by HF and VHF backscatter radar and in-situ rocket measurements (see secs. 1.31(a) and (c) for the detailed observations). These were first observed by Bowles and Cohen (1957) and Bowles et al. (1960, 1963). Although a substantial theoretical research in both linear and nonlinear regimes has been advanced in accounting their production and observed features discussed in sec.1.31, there remain a few other important basic characteristics whose explanation is still uncertain and the detailed agreement between the theories and these observations is not wholly established. Because of highly complex nature of the ionospheric plasma and its parameters, it is most likely that there are many different instability mechanisms which may be operating at a time individually or simultaneously, so as to give rise to the occurrence of type I irregularities over a wide range of wavelengths observed (from 1 meter or less to a few tens of meters). Of these mechanisms, the one, so-called two-stream instability, which is believed to be the most successful physical process as the source of the origin of the electrojet type I irregularities, will be the topic of our present investigation to be done below in this chapter.

in electric and magnetic fields, contains two groups of particles drifting with respect to each other with directed energy due, for example, to the electron drift velocity (giving rise to the relative electron streaming) of the current carrying electrons, a high frequency ($\omega \gtrsim \Omega_i$) electrostatic instability, termed as the 'two-stream instability' can be excited. When the current (or relative drift velocity) reaches a certain critical threshold level, the plasma becomes unstable and the growing electrostatic type modes with phase-fronts aligned with the magnetic field are generated by the excitation of the two-stream instability. These growing modes which derive their energy from the kinetic energy associated with the relative drift velocity of the particles (relative electron streaming), have their phase velocity, V_p equal to ion acoustic speed, C_s and are favoured at short wavelengths. Such a plasma situation and threshold condition on the electron drift velocity are easily visualized in the equatorial electrojet, at least during daytime, and such ion acoustic electrostatic plasma waves can, therefore, be excited in the electrojet due to streaming electrons by the two-stream instability. This instability was first developed independently by Farley (1963a,b) and Buneman (1963) for the electrojet conditions. These authors showed that these waves travelling normal to the magnetic field, would grow when $\underline{k}.\underline{v}_o/|\underline{k}|$, the component of streaming electron drift velocity in the wave direction exceeds a critical threshold value, the ion acoustic velocity, C_s. If the orthogonal condition for k x B is

is increased substantially.

As has been discussed in the Chapter I, the equatorial electrojet is characterized by a weakly ionized plasma with magnetized electrons ($\nu_e << \Omega_e$), collisional ions ($\nu_i >> \Omega_i$) and the vertical density gradients. The crossed ambient vertical polarization electric field and the horizontal northward earth's magnetic field, then leads to the streaming of electrons with respect to the ions in east-west direction due to the disparity in the electron-neutral (ν_e) and ion-neutral (ν_i) collision frequencies (see secs. 1.4(b) and 2.3). It is now, generally, agreed that this relative electron-ion streaming drift velocity when it exceeds the above discussed threshold (the ion acoustic velocity, C_s), excites the two-stream instability giving rise to a form of spectrum of longitudinal electrostatic waves, known as ion acoustic waves, with the wave-fronts parallel to the ambient magnetic field. These ion acoustic waves have been associated, in the literature, with the type I irregularities (Farley, 1963a,b; Buneman, 1963; Kato and Hirata, 1967; Balsley, 1969b; Rogister and D'Angelo, 1970; etc.). On the other hand, the combined influence of the vertical electron density gradient and the polarization electric field (i.e., east-west electron drift) excites the gradient-drift (or $\underline{E}$ x $\underline{B}$) instability generating low-frequency, long-wavelength modes (Type II irregularities) at very low threshold (Rogister and D'Angelo, 1970; Jain and Das, 1971), which has been discussed by the author in the previous chapter.

The physical nature of this instability is purely

particular, as is obvious from its linear dispersion relation) which provide resistivity to the medium, extract energy from the relative electron drift (electron streaming current) and transfer to the waves which then grow. That is, the plasma electrons in the perturbation given to the medium, exhibit oscillations as a result of their being excited by electron streaming, and these oscillating plasma electrons, in turn, interact back on the streaming due to their collisions. Thus, the amplitude of the waves increases exponentially along the streaming. The physical mechanism of this resistive type instability has already been demonstrated in details in sec. 1.4(b). It has, very recently, been shown, however, that the physical nature of this instability changes from resistive to reactive for off angle propagation of the waves ($k_{\parallel} \neq 0$, $k_{\parallel}/k_{\perp} << 1$), being probably resistive-inductive rather than purely resistive or purely reactive, for a large range of parameters applicable to the electrojet (Ossakow et al.,1975). There is general agreement that the so-called two-stream instability favours the excitation of high-frequency shorter-wavelength modes, while the gradient-drift instability favours the excitation of low-frequency long-wavelength modes.

The linear analysis of the two-stream instability applicable to the equatorial ionospheric conditions was first performed independently by Farley (1963a,b) considering the kinetic equations of the plasma and by Buneman (1963) in the fluid approximations. These authors predicted that the

the observational features of the type I irregularities show. It has now become apparent that many of the observed features of type I irregularities discussed in sec. 1.3(a), are more or less consistent with the linear Farley-Buneman instability theory. Since their prediction, a number of authors have studied this instability using linear theory (Waldteufel,1965); Kato and Hirata, 1967; Rogister and D'Angelo, 1970; Lee et al., 1971; Kaw, 1972; Lee and Kennel, 1973a,b; Sudan et al., 1973; Ossakow et al., 1975; Fejer et al., 1975b; Farley and Fejer, 1975).

All these linear analyses except a few (for example, Lee and Kennel, 1973a,b; Ossakow et al., 1975, etc.) as well as a host of linear analyses predict mostly the highly field aligned nature of the growing waves, consistent with the observations of the equatorial electrojet type I irregularities. Also, since $k_{\parallel} \neq 0$ modes have large group velocity $\parallel$ to $\underline{B}_o$, they should be weakly convectively amplified, and if they are at all important, they would appear with largest amplitudes at northern and southern extremities of the electrojet, where the assumption of complete suppression of vertical currents (i.e., complete vertical polarization) made here in the investigation fails. Until good convective amplification studies (see below for such studies) of the $k_{\parallel} \neq 0$ modes in a more realistic electrojet model are completed, it is difficult to evaluate their significance, as pointed out by Lee et al. (1974). Henceforth, with these facts in mind, we will assume the waves to propagate in the plane orthogonal to $\underline{B}_o$ in the

Rogister and D'Angelo (1970) and Sudan et al. (1973) gave a unified interpretation of both the type I and type II irregularities and derived a unified linear dispersion relation for the instabilities associated with them. These authors obtained a unified linear growth rate expression for the unstable waves, which contains two main driving terms: one involving ion inertia and referred to as the two-stream term and the other involving the electron density gradient identified as the gradient-drift term. In the literature, these two terms have been attributed respectively to the two-stream instability giving rise to the type I irregularities and the gradient drift instability associated with the type II irregularities. The type II irregularities, which are directly generated at long wavelengths even when the mean electron drift velocity is much smaller than C_s (i.e., the two-stream term is weak) and can not be produced directly at shorter wavelengths, but indirectly through some nonlinear processes (Farley and Balsley, 1973; Sudan et al., 1973; Sato, 1968, 1973; Rognlien and Weinstock, 1973, 1975b; Schmidt and Gary, 1973; McDonald et al., 1974; Ott and Farley, 1974; Rognlien and Weinstock, 1974, etc.), have been discussed in the Chapter II. Here the author devotes to the discussions of the type I irregularities associated with the two-stream term which is strong enough, at least during daytime, to produce direct generation of shorter wavelengths irregularities (the gradient-drift term being negligible for short wavelength modes) at the threshold

In Farley's (1963a,b) kinetic description which neglected finite Debye length effects ($k\lambda_D \to 0$), important for shorter wavelengths (comparable with ion or electron gyroradius), it was shown that most unstable modes were more or less exactly perpendicular to the magnetic field. He inferred that if the orthogonality condition for $\underline{k} \times \underline{B}_o$ is violated by more than 1^o or so, the threshold drift velocity for very small but nonzero $k_{\parallel}$ modes is substantially enhanced which may not be observable in the electrojet and hence the waves would not grow. Lee et al. (1971) have extended Farley's (1963a,b) analysis by including finite Debye length effects and found higher-frequency shorter-wavelength instabilities to be excited. Their calculation was restricted to modes propagating exactly perpendicular to $\underline{B}_o$ ($k_{\parallel} = 0$). Recently, Lee and Kennel (1973b) have performed a simple parallel propagation effect ($k_{\parallel} \neq 0$) analysis on type I instabilities in the fluid limit, and noted that even within the fluid theory, these modes may be more unstable and have larger growth rates than those with $k_{\parallel} = 0$, when $\nu_i \nu_e / \Omega_i \Omega_e$ is sufficiently small, as it is at the top of the electrojet.

Very recently, Ossakow et al. (1975) reexamined the linear theory of the resistive-type Farley-Buneman instability by considering finite Debye length effects (ion gyroradius is assumed to be large) for higher-frequency shorter wavelength modes having small but finite $k_{\parallel}$ ($k_{\parallel}/k_{\perp} \sim (m_e/m_i)^{1/2}$). They showed that when the current is driven sufficiently hard [illegible] times the ion thermal velocity),

perpendicular to $\underline{B}_0$, grow more unstable as these are found to have maximum growth slightly away from the perpendicular to $\underline{B}_0$, showing the importance of $k_{||} \neq 0$. That is, the off angle ($k_{||} \neq 0$) modes might actually dominate the linear stage in the higher drift velocity regimes. These authors suggested that the physical nature of the instability changes for off angle ($k_{||} \neq 0$) modes from 'resistive' to 'reactive' type, usually called a 'modified two-stream instability' strongly excited (strong growth) even in a collisionless plasma with $T_e \sim T_i$ (Krall and Liewer, 1971; McBride et al., 1972), and that for a large range of the electrojet paarameters, the instability is probably 'resistive-inductive' rather than purely resistive or purely reactive. They inferred, further, that V_p is rapidly decreasing function of angle for such modes as one moves away from pure perpendicular direction. Although this higher-frequency shorter-wavelength resistive-inductive type two-stream instability, could be applied to explain some of radar backscatter observations, it is felt by us that the ion viscosity effects play an important role in the development of unstable shorter wavelength modes. As these effects are significantly noticeable for the wavelengths comparable to ion mean free path or ion or electrons gyroradius, they are likely to contribute towards the stabilization of such modes. It is, therefore, important to examine the instability both linearly and nonlinearly by including the ion viscosity and this is what has been done in the investigation made in this chapter.

An idea was proposed by Kaw (1972) that since all waves have the vertical group velocity component, $\partial\omega/\partial k_z = v_0 \Big/ \left(1+\frac{\nu_i \nu_e}{\Omega_i \Omega_e}\right)$ being upward during the day and downward at night, the electrojet Farley-Buneman instability is undeniably convective. He argued that the linear convective amplification and refraction of plasma waves propagating through the horizontally stratified electrojet medium, might account for several of the puzzling features of type I irregularities and for their marginal stable spectra when the waves reach their largest amplitudes (hence spectral peak) near the end of their propagation path. Kaw, however, based his arguments on linear rather than nonlinear theory. Although this refraction certainly takes place, it can not consistently be included in the linear theory, as pointed out by Lee and Kennel (1973a) who subjected Kaw's suggestion to quantitative tests. They concluded that there are several difficulties with his idea and consequently, it fails on several counts and that only a nonlinear refraction and convective amplification theory could produce a constant Doppler spectrum and account for the type I observations in much better way. The major difficulty is that typical growth rates are so large that nonlinear effects must become important before the wave has travelled far enough to make refraction, significant. Furthermore, the refraction rate is weakest where the growth rate is strongest (i.e., at the spectral peak near the altitude of 102.5 km where $\nu_i \nu_e / \Omega_i \Omega_e = 1/3$ (Lee and Kennel, 1973a)) and refraction can not account for the vertically and very

difficulties have been enumerated in the works of Lee and Kennel (1973a) and Lee et al. (1974) and in a short review article by Farley (1974).

Kaw et al. (1974), recently, stressed upon the possible importance of the electromagnetic (EM) effects in the linear electrostatic (ES) streaming instability theory and examined the excitation of mixed EM-ES linear (two-stream) instability (especially in the long wavelength range) by the cross-field electron current. It was inferred by these authors that the retention of the finite EM corrections ($ck/\omega_{pe} < 1$, where $c/\omega_{pe} = 20$ m is the collisionless skin depth) for both the cases of $k_{||} = 0$ and $k_{||}/k_{\perp} << 1$ modes, contributes the additional (rather small) destabilizing terms that could excite the new cross-field streaming instability of mixed EM-ES waves, even when the electron streaming velocity (~ 200 ms^{-1}) is below the two-stream threshold and the electron density gradient is absent. But it is not yet clear, however, whether or not this new instability is of much importance in the equatorial electrojet, as the present measurements do not show the existence of such mixed type irregularities. Also it apparently operates at long wavelengths (> 500 meters) and has a slow growth rate (typical growth time $\sim$ 1 min).

Very recently, Farley and Fejer (1975) studied in details, the effect on the linear type I instability of the gradient drift term, the importance of which was first pointed out by Lee et al. (1974). It was shown by Lee et al. (1974) that the

instability theory are significant only when $v_o/v_c \approx 1$ and the density gradient scale length, L << 1 km. But the parameter L has been observed in the unstable electrojet plasma to range from 3 km to about 6 km or more (Prakash et al., 1969, 1972, 1973). Hence they concluded that for short wavelength type I modes ($kC_s/\gamma_i \approx 1$), the density gradient corrections are a negligible correction to the linear theory. This problem was reexamined by Farley and Fejer (1975) and hypothesized on the basis of strong observations that the phase velocity of the unstable type I modes always remain very close to that which corresponds to the marginal excitation (i.e., to instability threshold condition), even when the destabilizing terms (electron drift and plasma density gradient) exceed the thresholds. It was clearly shown by these authors that this constant threshold velocity of unstable waves can be affected appreciably by gradient drift term even at short wavelengths, particularly at night when the density gradient are much sharper and highly variable than they are during the day. At night, this phase velocity may differ significantly and vary over a considerable range from the usual constant threshold acoustic velocity, in consistent with the existing nighttime equatorial radar observations of considerable variability in the type I velocity. However, this hypothesis does not have strong convincing footing, as adequate measurements of type I irregularities at nighttime are, unfortunately, not yet available.

The linear theory of the instability can merely decide

propagation it will grow more. The ultimate (saturation) level of the linearly growing modes, energy spectrum, phase velocity and many other characteristics can only be found from a satisfactory nonlinear theory. The nonlinear evolution of the instability is used most frequently to unravel its long time behaviour and several detailed features which are otherwise not possible from the linear theory. It is well conceived fact that all the observational features of the concerned irregularities occuring in the electrojet arise from a final saturated or marginally stable nonlinear state. The biggest question is thus a nonlinear saturation mechanism for the two-stream instability so as to know about the detailed properties of the instability and have a closer agreement between the theory and the observations. Therefore, in this chapter a nonlinear analysis of two-stream instability associated with type I modes is presented which, including ion viscosity and some quasilinear stabilization effects, discusses a special class of coherent nonlinear harmonic stationary type I modes observed to exist in such a nonlinear state in the equatorial electrojet (Balsley, 1973a,b; Farley and Balsley, 1973).

Several nonlinear theories of the two-stream instability have been attempted by a number of authors so as to decide a proper nonlinear mechanism to explain the marginally stable saturation spectrum of unstable type I modes and their observed features (Skadron and Weinstock, 1969; Kamenetskaya, 1971; Rogister, 1971; Weinstock and Williams, 1971; Sato, 1972,

Sleeper, 1972; Farley and Balsley, 1973; Sudan et al., 1973; Weinstock, 1973; Lee et al., 1974; Weinstock and Rognlien, 1975; Rogister and Jamin, 1975).

All of these studies of nonlinear saturation mechanisms of type I modes can, in general, be viewed from four different angles. In one approach, Skadron and Weinstock (1969) and Weinstock and Sleeper (1972, 1973) using the Kinetic theory description (developed by Weinstock, 1968, 1969, 1970) and Weinstock and Williams (1971) and Sleeper and Weinstock (1972, 1973) based on the fluid theory description, followed the Dupree-Weinstock nonlinear perturbed electron orbit diffusion theory (Dupree, 1966, 1967, 1968; Weinstock, 1968, 1969, 1970). These authors have suggested various nonlinear modifications for the form of the growth rate, when a turbulent wave spectrum is excited. The saturation is referred to perturbed or diffusing orbits, since the transfer of energy from waves to electrons (at the rate at which the unstable waves gain from the electrojet) is associated with the perturbation (heating) of the electron orbits by the waves. In other words, the balance of energy takes place when the configuration and velocity orbits of electrons supporting the waves, diffuse away from their unperturbed orbits as a result of heating. However, these authors have estimated only the integrated saturated amplitude, ignoring the actual detailed structure of the saturation spectrum of the instability.

A second approach (quasi-linear) was proposed by Kamenetskaya (1971), Rogister (1971) and Sato (1972, 1973) who

polarization electric field in obtaining marginally stable spectrum of type I modes. They concluded that the form of the growth rate remains unchanged, but enhanced electron scattering (flux) across the magnetic field lines by irregularities could increase the vertical component of the average electron Pedersen current and thereby short out the polarization field. In turn, this reduces down the electron streaming drift driving the instability to its marginal stable value or below, thereby quenching the instability, and thus provides a marginal stable state for the type I modes.

The third approach to the study of marginal stable spectrum of the type I modes is based on the Kaw's (1972) idea, but as has been discussed earlier, he, however, based his arguments on linear rather than nonlinear theory, which was subjected to quantitative tests by Lee and Kennel (1973a) and Lee et al. (1974). These authors noted that there are several difficulties with the Kaw's idea and inferred that it fails to explain the observations on several counts. In fourth approach, Farley and Balsley (1973), Sundan et al. (1973) and Sato (1973) put forward the turbulent mode coupling mechanism in which they suggested that gradient drift instability first generates large scale ($\gtrsim 10^2$ m) irregularities propagating primarily in horizontal direction. When these grow to sufficiently large amplitudes ($n/n_o \sim$ a few percent), the first-order gradient and velocity perturbations associated with the wave are large enough (comparable to zero-order equilibrium values) to generate short [illegible] which can easily travel

However, this theory can perhaps be thought as the combination of the two linear theories rather than a nonlinear theory, since the mechanisms that limit the growth and thus account for the constant spectral shape, are not considered.

Although all the above approaches are very interesting and physically sound, it has been made clear by Lee et al. (1974) that none of them is individually sufficient enough in explaining all aspects of observations. They showed, however, that a combination of all of them seems to be capable of doing so. These authors argued that since both quasi-linear polarization reduction and nonlinear perturbed electron orbits diffusion damping arise from spatial electron diffusion, they can not be considered seperately. They, further, argued that since many modes are required for diffusion approximations to be valid, these nonlinear mechanisms are incomplete and do not give the detailed structure of the saturation spectrum, without the inclusion of other nonlinear mechanisms, such as wave-wave coupling (mode coupling). They stressed clearly upon the importance of Kaw's (1972) idea that it not only provides a natural way to produce a marginal stable spectrum, but also forces reformulation of the above nonlinear theories which were carried out for a homogeneous plasma. Therefore, Lee et al. (1974) investigated into all of the above-discussed nonlinear limiting mechanisms by incorporating the Kaw's idea of convective effects and then formulated a rather elaborate self-consistent convective nonlinear theory of type I irregularities in the electrojet. They concluded that this self-consistent nonlinear theory, combining wave refraction and convect-

reduction and nonlinear perturbed electron orbit diffusion damping, could account for the radar backscatter observations of ubiquitous marginally stable or 'constant ion acoustic Doppler shift' - saturation spectrum better than any of these mechanisms separately. But it can not explain the presence of vertical type I echoes, however, and appears to be very hard put to account for the very oblique echoes and east-west symmetry.

Very recently, Weinstock and Rognlien (1975) developed a nonlinear theory and derived a unified nonlinear dispersion relation for the electrojet two-stream and gradient drift instabilities, by generalizing the unified linear dispersion relation (Rogister and D'Angelo, 1970; Sudan et al. 1973; Sato, 1973) and using the perturbed electron orbit diffusion damping theory (Weinstock and Williams 1971; Sleeper and Weinstock, 1972). Basically, the saturation mechanism can be viewed as arising due to slowing down of electrons by turbulent unstable waves to their marginal velocity, i.e., essentially it is equivalent to quasilinear theory of Rogister (1971), since the electrons experience the enhanced friction (viscosity) as they travel through the linearly growing waves approaching turbulent level. This friction is caused by the scattering of electrons by the turbulent unstable waves. Though, Weinstock and Rognlien's theory could account only for the observations of saturation level, frequency shift and asymmetrical angular spectrum about the horizontal plane of the vertically propagat-

marginally stable saturation spectrum of type I modes propagating both horizontally and vertically.

Simultaneously, Rogister and Jamin (1975) also studied the two-dimensional nonlinear theory of the turbulence in a uniform electrojet, based on the strong turbulence theory of Weinstock and Sleeper (1972). They invoked in their analysis both the one-dimensional quasi-linear modification of the vertical polarization field (Rogister, 1971; Sato, 1972) resulting into quasi-linear enhancement of vertical Pedersen conductivity and the two-dimensional nonlinear wave coupling processes which transfer energy from the linearly growing short wavelength modes to linearly damped long wavelength ones. It was concluded by these authors that their theory could provide a plausibly better interpretation of some of the yet puzzling observations and account for the detailed stabilization over the entire spectrum of type I irregularities. However, the definiteness of their conclusions and of the agreement of their predictions with observations are not yet fully established, which can, as they remarked, only be achieved by numerical calculations.

One of the basic features of VHF radar backscatter observations of type I irregularities in the equatorial electrojet, which has not yet been explained, is that short wavelength (1-3 m) irregularities travel in fairly discrete packets, i.e., in the shape of fairly sharp isolated pulses (Balsley, 1969a,b; 1973a,b; Farley and Balsley, 1973). This feature of the irregularities certainly suggests that in the

particular structures must be caused by some nonlinear mechanism.

One of the stabilization mechanisms suggested so far is, a quasilinear theory (referred above as second approach of attempts in developing nonlinear saturation theories) proposed by Kamenetskaya (1971), Rogister (1971) and Sato (1972). These authors indicated, as has been discussed above, that quasilinear effects undeniably play a significant role in stabilization of the unstable modes growing linearly to large amplitudes. Though a few limitations of this quasilinear saturation theory were pointed out by Lee and Kennel (1973a) and Lee et al. (1974), even then its importance and reality cannot be denied, as they confessed that quasi-linear effects are remarkably efficient and are most favoured at least within the electrojet region where $\nu_i \nu_e/\Omega_i \Omega_e \lesssim 1/3$ (low altitude regions < 105 km), but with some modifications (i.e., including convective effects) within $\nu_i \nu_e/\Omega_i \Omega_e > 1/3$ regions where the efficiency of quasilinear effects decreases with increasing altitudes.

In this chapter, the author discusses a special class of coherent weakly nonlinear type I modes excited by two-stream instability in the equatorial electrojet. Having admitted the importance of quasilinear effects (discussed above and in sec. 3.2 here), we have included them in our nonlinear treatment of the two-stream instability. Introducing $\xi = (\omega t - \underline{k}.\underline{r})$ as the only independent variable, the nonlinear partial differential equations describing one-dimensional type I modes

wave equation (sec. 3.3). Having retained the quasilinear modification of the vertical polarization field (quasilinear effects), the author has shown that in the weakly nonlinear limit, almost harmonic nonlinear stationary waves exist as special solutions. An amplitude dependent dispersion relation for these nonlinear modes is obtained in sec.3.4. To get the nonlinear stationary modes, we have to retain dispersion of type I irregularities. For wavelengths comparable to ion mean free path or ion gyroradius ($\lambda \gtrsim$ a few meters), this dispersion arises due to kinetic effects (Lee et al., 1971). A simplified way of taking into account of the dispersion, which produces qualitatively identical effects, is to introduce ion viscosity in the fluid equations: this is what we have done here.

A study of stability of the nonlinear stationary modes made in sec. 3.5, shows that they are stable against long wavelength slowly varying amplitude perturbations. However, as shown by Karpman and Krushkal (1969), generally for such waves, a large amplitude perturbation has a tendency to break-up the nonlinear stationary modes into envelope solitons. Thus we suspect that nonlinear type I modes might exist in the form of wave-packets with soliton shaped envelopes (fairly sharp isolated pulses). There seems to be some evidence from the VHF radar backscatter experiments for such a nonlinear state that the short wavelength irregularities do in fact travel in fairly discrete packets (Balsley, 1969a,b; 1973a,b; Farley and Balsley, 1973). Finally, as the complexity of 'full nonlinear' equat-

calculations (in sec. 3.6) to verify some of the conclusions of the present theory and to establish their definiteness.

3.2 Basic Equations and Quasilinear Modification of Polarization Electric Field:

For wavelengths of a few meters or more (longer than either iongyroradius or ion-mean free path), the fluid equations are adequate to describe the E-region plasma. In the frame work of a two fluid theory, the E-region plasma, in the presence of a steady electric field $\vec{E}_o$ and a uniform and steady magnetic field $\vec{B}_o$, is considered to be governed by continuity and momentum transfer equations for electrons and ions, where the collisions of the charged particles with a neutral background are dominant. The following assumptions are made to simplify these equations.

1. The ions are considered to be unmagnetized since their gyrofrequency $\Omega_i (= eB_o/Mc)$ is much smaller than the ion-neutral collision frequency ν_i.

2. The electron inertia is neglected, because the electron-neutral collision frequency ν_e is much larger than the wave frequency Doppler-shifted to the electrojet drift frame.

3. The wave electric field is essentially electrostatic ($\vec{E} = - \vec{\nabla} \phi$), since the plasma pressure is much smaller than the ambient magnetic energy density and $ck/\omega_{pe} >> 1$ for wavelengths of interest (ω_{pe} is the electron plasma frequency).

4. The waves are assumed to propagate exactly perpendicular to the magnetic field, since these waves experience least damping

5. The ions and electrons are assumed to be isothermal.

In the nonlinear regime, higher harmonics are produced and steepening occurs for waves of short wavelengths (Sudan et al., 1973) for which case, the ion viscosity effects become significantly important, which in turn, lead to dispersion of the waves (sec. 3.1-9th and 22rd para). Therefore, the ion viscosity term must be included into the ion momentum transfer equation. This has been ignored by most of the previous authors, although these effects might compete with the non-linear effects and then lead to a steady state solution. However, the ion viscosity term ($\propto k^2 \mu$, where μ is the coefficient of viscosity and k is wave number) becomes more significant when $k^2 \mu / \nu_i \approx 1$, i.e., when wavelength is comparable to ion-mean free path and for such cases, one must use the kinetic theory for ions (Lee et al., 1971).

With the inclusion of ion viscosity to take account of dispersive effects, the governing equations for electrons (3.1 and 3.2) and singly charged ions (3.3 and 3.4) are given by

$$\frac{\partial n}{\partial t} + \vec{\nabla}.(n\vec{v}) = 0 \qquad ..(3.1)$$

$$-\frac{e\vec{E}}{m} - \vec{v}\times\vec{B}_e - \frac{S_e^2}{n}\vec{\nabla} n - \nu_e \vec{v} = 0 \qquad ..(3.2)$$

$$\frac{\partial N}{\partial t} + \vec{\nabla}.(N\vec{V}) = 0 \qquad ..(3.3)$$

$$\frac{\partial \vec{V}}{\partial t} + (\vec{V}.\vec{\nabla})\vec{V} = \frac{e\vec{E}}{M} - \frac{S_i^2}{N}\vec{\nabla} N - \nu_i \vec{V} + \mu \nabla^2 \vec{V} \qquad ..(3.4)$$

The Poisson equation is

Where $\vec{E} = -\vec{\nabla}\phi$ is the electric field, n and N are the number densities of electrons and ions respectively, M and m denote the ion and electron masses, $\vec{v}$ and $\vec{V}$ represent the electron and ion velocities, $\vec{\Omega}_e$ is the gyrofrequency of the electrons ($\vec{\Omega}_e = e\vec{B}_o/mc$) and μ is the coefficient of ion viscosity. S_e and S_i are respectively electron and ion thermal velocities. All other symbols have their conventional meaning.

We choose a rectangular coordinate system (Fig.3.1) with x-axis pointing(magnetic) southward, y-axis eastward and z-axis vertically upward. Before solving the equations (3.1) - (3.5) describing the type I modes for the nonlinear analytical solutions, let us briefly describe how the equilibrium conditions in the equatorial electrojet get modified in nonlinear state due to quasi-linear effects (Kamenetskaya, 1971; Rogister, 1971; Sato, 1972). In the simplified model of equatorial electrojet (Sugiura and Cain, 1966; Lee and Kennel, 1973), the primary eastward electric field $\vec{E}_p$ and the vertical polarization field E_{oz} are such as to cause complete superssion of vertical currents, i.e.,

$$J_z = e n_o (V_{oz} - v_{oz}) = 0 \qquad .. (3.6)$$

which yields the equation (Baker and Martyn, 1953)

$$E_{oz} = (\sigma_2/\sigma_1) E_p \qquad .. (3.7)$$

where σ_1 and σ_2 are respectively the Pedersen and Hall conductivities (Chapman, 1956). The horizontal electron drift velocity is then given by

$$v_o \approx -\frac{c}{B_o} E_{oz} = -\frac{c}{B_o}\cdot\frac{\sigma_2}{\sigma_1} E_p \qquad .. (3.8)$$

Rogister (1971) and Sato (1972) have argued that in the

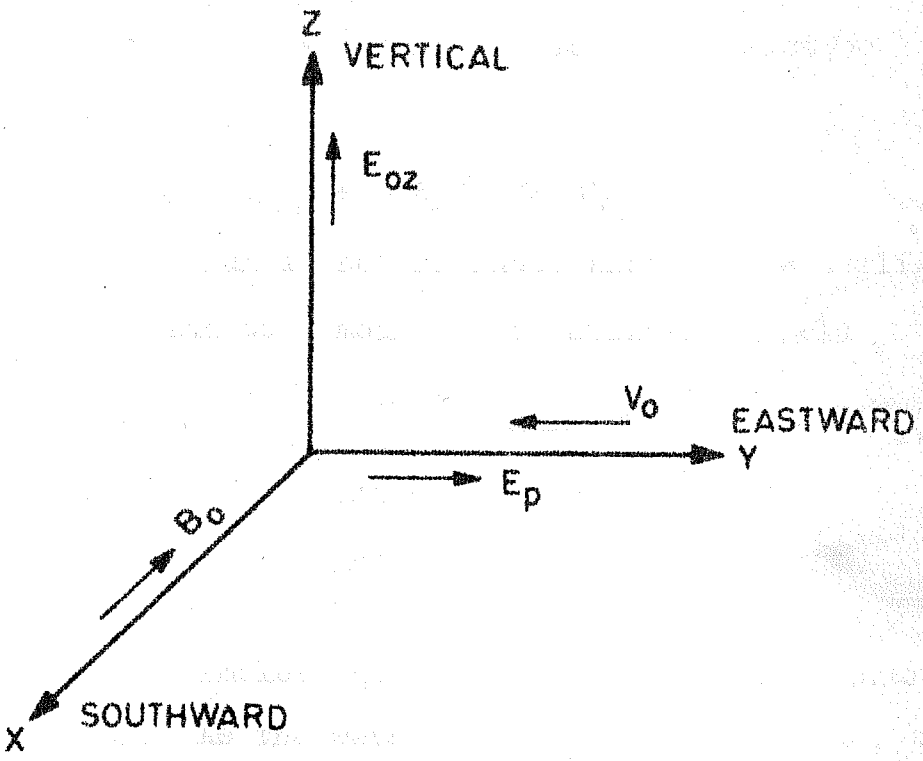


Fig.3.1. The coordinate system used.

presence of type I instability, the polarization electric field E_{oz} is reduced. Physically, the fully developed instability, however, produces a net negative nonlinear vertical electron flux $< \tilde{n}\, \tilde{v}_z >$ in the direction opposite to that of the primary flux $n_o\, v_{oz}$ so that equation (3.6) must be modified as

$$J_z = e n_o \left(v_{oz} - v_{oz} \right) + (-e) < \tilde{n}\, \tilde{v}_z > = 0 \qquad ..(3.9)$$

The nonlinear ion flux is not included since it is negligible. Equation (3.9) leads to a modified polarization field

$$E'_{oz} = E_p \frac{\sigma_2}{\sigma_1} \left[1 + \left(\frac{\sigma_2}{\sigma_1} \right)^2 \frac{< \tilde{n}\, \tilde{n} >}{n_o^2} \right]^{-1} \qquad ..(3.10)$$

and a modified electron drift velocity

$$v_{om} = v_o \left[1 + \left(\frac{\sigma_2}{\sigma_1} \right)^2 \frac{< \tilde{n}\, \tilde{n} >}{n_o^2} \right]^{-1} \qquad ..(3.11)$$

This produces the simplest quasi-linear saturation mechanism for type I modes. As the waves attain large amplitude, the electron drift v_{om} decreases reducing the growth rate of the wave until marginal stability is reached. In other words, the turbulence level inhibits the formation of large current and thereby maintains the plasma in a state relatively close to linear marginal instability. In fact, irregularities at turbulence level scatter the electrons across the magnetic fields, and thereby lead to an enhancement of the vertical Pedersen conductivity of the medium, increasing the vertical component of the average electron Pedersen current. This increase, in turn, tends to short out the polarization electric field and the electrojet current which drive the instability,

down by the unstable wave to their marginally stable value of the drift velocity, i.e., to the threshold value (Rogister, 1971; Sato, 1972; Lee et al., 1974; Weinstock and Rognlien, 1975; Rogister and Jamin, 1975). We shall now use above results in deriving an equation describing coherent nonlinear type I modes.

3.3 Wave Equation for Nonlinear Type I Modes:

Because we are interested in wavelengths much larger than the Debye length, we shall assume quasi-neutrality, i.e.,

$$n \approx N \qquad ..(3.12)$$

We are interested to look for nonlinear stationary waves by which we mean those waves in which all the oscillating quantities are functions of only s-ut, where s is the coordinate along the direction of wave propagation and $u = \omega/k$ is the phase velocity of the wave. In case of periodic stationary waves, it is therefore, convenient to introduce the phase of oscillation as

$$\xi = \omega t - \vec{k}.\vec{r} \qquad ..(3.13)$$

where $k = 2\pi/\lambda$ and λ is the wavelength, then all the oscillating quantities can be represented as periodic functions of ξ (with period 2π). We define each variable q as

$$q = q_o + \tilde{q} \qquad ..(3.14)$$

where q_o is the equilibrium value and $\tilde{q}$ is the perturbation. Including the modified quasilinear electron drift $\vec{v}_{om}$ instead of linear electron drift $\vec{v}_o$, the equations (3.1) to (3.4) may be combined to give

$$\mu\omega k^2 \frac{d^2(n_o/n)}{d\xi^2} - \frac{1}{2}\omega^2 \frac{d}{d\xi}\left(\frac{n_o}{n}\right)^2 + \nu_i \omega\left(1 - \frac{n_o}{n}\right) = k^2\left[\frac{e}{m}\frac{d\varphi}{d\xi} + \frac{S_i^2}{n}\frac{dn}{d\xi}\right] \quad ..(3.15)$$

for ions and

$$\left(1 - \frac{n_o}{n}\right)\omega = -\frac{\nu_e k^2}{\Omega_e}\left[\frac{e}{m}\frac{d\varphi}{d\xi} - \frac{S_e^2}{n}\frac{dn}{d\xi}\right] \quad ..(3.16)$$

for electrons, where $n = n_o + \tilde{n}$ and Ω_e ($= |\vec{\Omega}_e|$) $>> \nu_e$ has been considered. Eliminating $d\varphi/d\xi$ from (3.15) and (3.16), we obtain the wave equation for nonlinear type I modes as

$$\frac{d^2\eta}{d\xi^2} - \frac{2}{1+\eta}\left(\frac{d\eta}{d\xi}\right)^2 - \frac{u}{k\mu}\left\{1 - \frac{C_s^2}{u^2}(1+\eta)^2\right\}\frac{1}{1+\eta}\cdot\frac{d\eta}{d\xi} + \frac{\nu_i}{k^2\mu}\left\{\frac{1}{\psi}\left(\frac{\vec{k}\cdot\vec{v}_{om}}{\omega} - 1\right) - 1\right\}(1+\eta)\eta = 0 \quad ..(3.17)$$

where $\eta = \tilde{n}/n_o$, $\psi = \nu_i\nu_e/\Omega_i\Omega_e$ and $C_s^2 = S_i^2 + (\Omega_i/\Omega_e)S_e^2$ where C_s is the acoustic velocity. The first two terms in (3.7) arise because of the ion viscosity.

3.4 Solutions of the Nonlinear Wave Equation and Nonlinear Dispersion Relation:

3.41 Linear Type I Modes:

In the linear limit, we may assume that $\eta = \tilde{n}/n_o \to 0$ so that the wave equation (3.17) can be written as

$$\frac{d^2\eta}{d\xi^2} - \frac{u}{k\mu}\left(1 - \frac{C_s^2}{u^2}\right)\frac{d\eta}{d\xi} + \frac{\nu_i}{k^2\mu}\left(\frac{1}{4}\left(\frac{\vec{k}\cdot\vec{v}_o}{\omega} - 1\right) - 1\right)\eta = 0 \quad ..(3.18)$$

where $\vec{v}_{om}$, in the linear limit, has been replaced by $\vec{v}_o$ (eq.3.11). The stationary solution of the form

$$\eta = A\cos(\omega t - \vec{k}\cdot\vec{x} + \Phi) \quad ..(3.19)$$

$$\omega = \vec{k}.\vec{v_o}\left\{1+\psi\left(1+k^2\mu/\nu_i\right)\right\}^{-1} \qquad ..(3.20)$$

and

$$u = C_s \qquad ..(3.21)$$

The condition (3.21) is obtained by equating the coefficient of first derivative of η in (3.18) to zero, which gives the condition of marginal instability (no growth). The critical electron drift velocity for instability to occur can thus be determined by combining (3.20) and (3.21) and is given by the magnitude of v_o, say v_c;

$$v_c = C_s\left[1+\psi\left(1+k^2\mu/\nu_i\right)\right] \qquad ..(3.22)$$

These results are essentially the same as obtained by earlier workers in the linear case (Farley, 1963a,b; Buneman, 1963; Rogister and D'Angelo, 1970). The following differences arise because of inclusion of ion viscosity effects: (a) it effectively changes the ion collision frequency from ν_i to $(\nu_i+k^2\mu)$ and thus introduces dispersion of the waves: (b) the threshold v_c is increased. Note that the ion viscosity term becomes important when $k^2\mu/\nu_i \simeq 1$, i.e., when the wavelength is comparable to ion-mean free path. For such cases, a kinetic theory for ions (Lee et al., 1971) would be more appropriate. However, since inclusion of ion viscosity gives qualitatively similar results, we have chosen that for simplicity.

An important result to be noted here, which differs from earlier results obtained from fluid theory, is that in the linear limit, our analysis of the instability leads to the

wavelength dependent threshold electron drift velocity, v_c (3.22) for marginally stable waves (described by the condition (3.21)). This agrees with the result predicted by marginal stability calculations from kinetic theory (Farley, 1963a,b) that the phase velocity of the marginally stable waves are wavelength dependent. The phase velocities of type I irregularities are, in fact, wavelength dependent; yet they still correspond to marginally stable waves (Cohen and Bowles, 1967; Balsley and Farley, 1971).

3.42 Nonlinear Type I Modes:

It is obvious that the analytical treatment of the nonlinear wave equation (3.17) is too difficult to handle mathematically and to obtain the physical real solutions. Our attention will, therefore, be devoted mainly to the case of weak nonlinearities, in which case we assume sufficiently small amplitude perturbation ($\eta << 1$), in consistent with the observations. Thus, in the case of weakly nonlinear modes for which $\eta << 1$, the wave equation (3.17) can be written as (neglecting terms of order higher than η^3).

$$\frac{d^2\eta}{d\xi^2} + K_0^2(1+\eta)\eta = \frac{u}{k\mu}\left[1-\eta+\eta^2-\frac{c_s^2}{u^2}(1+\eta)\right]\frac{d\eta}{d\xi} + 2(1-\eta)\left(\frac{d\eta}{d\xi}\right)^2 \quad ..(3.23)$$

where

$$K_0^2 = \frac{\nu_i}{k^2\mu}\left[\frac{1}{\psi}\left(\frac{\vec{k}\cdot\vec{v}_0}{\omega}\cdot\frac{1}{1+(\sigma_2/\sigma_1)^2\langle\eta\eta\rangle}-1\right)-1\right] \quad ..(3.23a)$$

In the weakly nonlinear regime, the amplitude and the

averaging (Bogoliubov and Mitropolsky, 1961) to solve equation (3.23). Let the solution be

$$\eta = A \cos\left(K_0 \xi + \Phi\right) \qquad ..(3.24)$$

where the amplitude A and the phase Φ are slowly varying functions of ξ . Following Bogoliubov and Mitropolsky (1961), we obtain the dependence of A and Φ on ξ as

$$\frac{dA}{d\xi} = \frac{u}{k\mu}\left(1 - \frac{c_s^2}{u^2}\right)\frac{A}{2} - \frac{c_s^2}{4k\mu u} A^3 \qquad ..(3.25)$$

$$\frac{d\Phi}{d\xi} = 0 \qquad ..(3.26)$$

The equation (3.26) shows that the waves travel with constant phase in the wave frame.

In nonlinear stationary regime, the amplitude gets saturated and does not vary with ξ , i.e., the saturated amplitude is given by

$$\frac{dA}{d\xi} = 0 \qquad ..(3.27)$$

This condition and the wave-equation (3.23) are satisfied by the solution with stationary amplitude (A = constant, say A_0) of the type

$$\eta = A_0 \cos\left(\omega t - \vec{k}.\vec{x} + \Phi\right) \qquad ..(3.28)$$

if

$$\omega = \frac{\vec{k}.\vec{v}_0}{1 + 4\left(1 + k^2\mu/\nu_1\right)} \cdot \frac{1}{1 + \left(\sigma_2/\sigma_1\right)^2 A_0^2/2} \qquad ..(3.29)$$

and

$$u^2 = c_s^2\left(1 + A_0^2/2\right) \qquad ..(3.30)$$

where in equation (3.29) the value of $\langle \eta\eta \rangle$ has been put

Equation (3.29) shows that the phase velocity of the nonlinear wave is a function of the amplitude A_o. This dependence arises because of the quasilinear reduction of vertical polarization field. From equation (3.30), we note that the critical condition for marginal stability is also modified. The amplitude dependent term here can be traced back to $(\vec{V} \cdot \vec{\nabla})\vec{V}$ term in the ion equation of motion (i.e., like an ion ponderomotive force).

It is, therefore, concluded that nonlinear stationary sinusoidal solutions exist for coherent type I modes in equatorial electrojet. Now the question arises whether these nonlinear stationary wave propagating in the electrojet are stable to long wavelength slowly varying large amplitude perturbations or not. This is discussed in the next section.

3.5 Stability Criteria of Nonlinear Stationary Waves:

It is obvious from the nonlinear dispersion relation that the frequency of the wave ω depends not only on the wave number k, but also on the nonlinear parameter, the amplitude A which is assumed small in linear approximation. The dependence of ω on k and A is called nonlinear dispersion relation and is given by (3.29). In general, the nonlinear dispersion relation can be expressed as

$$\omega = \omega(k^2, A^2) \qquad ..(3.31)$$

Considering the waves of sufficiently small (but finite) amplitude, we can restrict ourselves to the first two terms of the expansion of the dispersion equation (3.31) in powers of A^2,

$$\omega = \omega^{0}(k^{2}) + (\partial\omega/\partial A^{2})_{0}\, A^{2} \qquad ..(3.32)$$

where $\omega^{0}(k^{2})$ determines the dispersion law in the linear approximation.

For studying the stability of these nonlinear periodic stationary solutions obtained in earlier section, we consider a nonlinear non-stationary wave where the amplitude, the wavelength, etc. change sufficiently slowly at a distance of the order of wavelength and over a time of the order of the period of oscillations and which differs from the stationary wave (the latter has the parameter k_0, ω_0, A_0) satisfying the dispersion equation (3.31), the phase of the wave can be represented in the form

$$\xi(\vec{r},t) = \omega_0 t - k_0 y + \Phi(\vec{r},t) \qquad ..(3.33)$$

where $\Phi(\vec{r},t)$ is the contribution to the phase made by the non-stationarity. Karpman and Krushkal (1969) have investigated the modulation of nonlinear stationary waves in nonlinear dispersive media. By comparing the set of equations with the hydrodynamic equations they found that the 'adiabatic compressibility' is determined by

$$\alpha = -\frac{A_0^2}{u_0'}\left(\frac{\partial\omega}{\partial A^2}\right)_0 \qquad ..(3.34)$$

where $u_0' = (\partial^2\omega/\partial k^2)_{k=k_0,\, A=0}$ and the square of the velocity of sound is given by

$$C_s^2 = -\alpha \qquad ..(3.35)$$

It follows from this that for a plane wave to be stable against the changes in phase and amplitude, it is necessary that

$$\alpha < 0 \qquad ..(3.36)$$

For $\alpha > 0$, the plane waves considered will be unstable. This result was first obtained by Lighthill (1967). To apply this criteria, we have to know only the dispersion equation in the form (3.32). Karpman and Krushkal (1969) found the following dispersion equation for the perturbations

$$\Omega = \frac{(\chi^2 - 4\alpha)^{1/2}}{2}\chi \qquad ..(3.37)$$

where Ω is the frequency and χ is the wave number of the amplitude and phase perturbations. Using the linear and nonlinear dispersion relations (eqs. (3.20) and (3.29)), we obtain the expression for α as

$$\alpha = -\frac{A_0^2}{2}\left(\frac{\sigma_2}{\sigma_1}\right)^2 \frac{\nu_i}{\psi\mu}\cdot\frac{\left[1+\psi(1+k_0^2\mu/\nu_i)\right]^3}{k_0\left[1+\psi(1-\mu_0)\right]}\cdot\frac{k}{1+\psi(1+k^2\mu/\nu_i)} \qquad ..(3.38)$$

where $\mu_0 = k_0^2\mu/\nu_i$. For the parameters appropriate to the equatorial electrojet and for the wavelength of interest, it can be shown that the quantity $\mu_0 << 1$ and hence $\alpha < 0$. This means that the frequency Ω is real leading to nongrowing waves. For not too large $A - A_0$, the set of equations obtained by Karpman and Kruskal (1969) reduces to the Korteweg de Vries equation (an equation of hydrodynamics with dispersion, in which the role of density is played by A^2). As is well known the profile of the solution of the Korteweg de Vries equation decays for large time into solitary waves (solitons) and small oscillations. Thus, modulational envelopes of nonstationary waves distort into solitons or soliton-like shapes (fairly sharp isolated pulses)

It may thus be concluded that the nonlinear and dispersive properties of type I modes are such that nonlinear stationary solutions are modulationally stable but at the same time large perturbations in the amplitude tend to develop into envelop solitons. Balsley (1973b) has pointed out that some backscatter observations at Jicamarca are consistent with the propagation of fairly isolated wave-packets of short wavelength (e.g., 3 m) type I modes (Balsley, 1969a,b, 1973a; Farley and Balsley, 1973), an experimental observation, which may be of relevance to this result.

3.6 Numerical Calculations and Results:

The above analytical results have been derived for weak nonlinearities by using Bogoliubov-Mitropolsky method. The approach followed above is approximate one, as this method is valid only for sufficiently small (but finite) amplitude perturbation and the terms of order higher than the cube of amplitude were neglected. In order to establish the definiteness of these results obtained in secs. 3.4 and 3.5, they need to be verified by some other method. An accurate and simplest method of verification of the results is one which involves solving either the full nonlinear wave equation (3.17) or the exact set of the basic equations (3.1)-(3.4) or both, numerically on computer, and then comparing the numerical solutions so obtained with the analytical ones. And this is done below in this section. The parameters appropriate to equatorial electrojet were chosen as; $\Omega_e = 5 \times 10^6$ cps; $\nu_e = 8 \times 10^4$ cps; $\Omega_i = 1.3 \times 10^2$ cps;

a) Numerical Solutions of the Exact (Full) Nonlinear Wave Equation (3.17):

As a check on our analytical results, for the reasons mentioned above, we have therefore, solved the exact nonlinear wave equation (3.17) on the computer. The numerical procedure adopted is briefly laid out as follows: The wave equation (3.17) is solved as a system of two first order differential equations by the unconditionally stable trapezoidal rule. The initial values of the amplitude A of the perturbation η and $d\eta/d\xi$ at $\xi = 0$, are arbitrarily chosen. For taking η forward with ξ, one needs the values of v_{om} and u, both of which depend upon $\langle \eta\eta \rangle$. Since η is a periodic function of ξ, for each cycle $\langle \eta\eta \rangle$ is calculated from the one preceding cycle. Fig.3.2 shows an example of such a numerical calculation.

In the Fig.3.2 is depicted the numerical solution of the exact nonlinear wave equation (3.17) for $A(\xi = 0)$ equal to 0.005 (which is 0.5/ of the equilibrium density, n_o), wherein the wavelength chosen is of the order of a meter. One finds from this figure that for large ξ, the amplitude does not seem to grow any more and a periodic stationary solution with a constant amplitude, say A_o, which is nearly equal to 1.38%, is finally achieved, whereas initially the perturbation is found to grow with linear growth. This initial linear growth arises because of the fact that at the initial stage, the amplitude is not sufficiently large so as to make quasilinear effects (quasilinear reduction of v_{om}) play an efficient role. When the amplitude increases to sufficiently high value, i.e., when

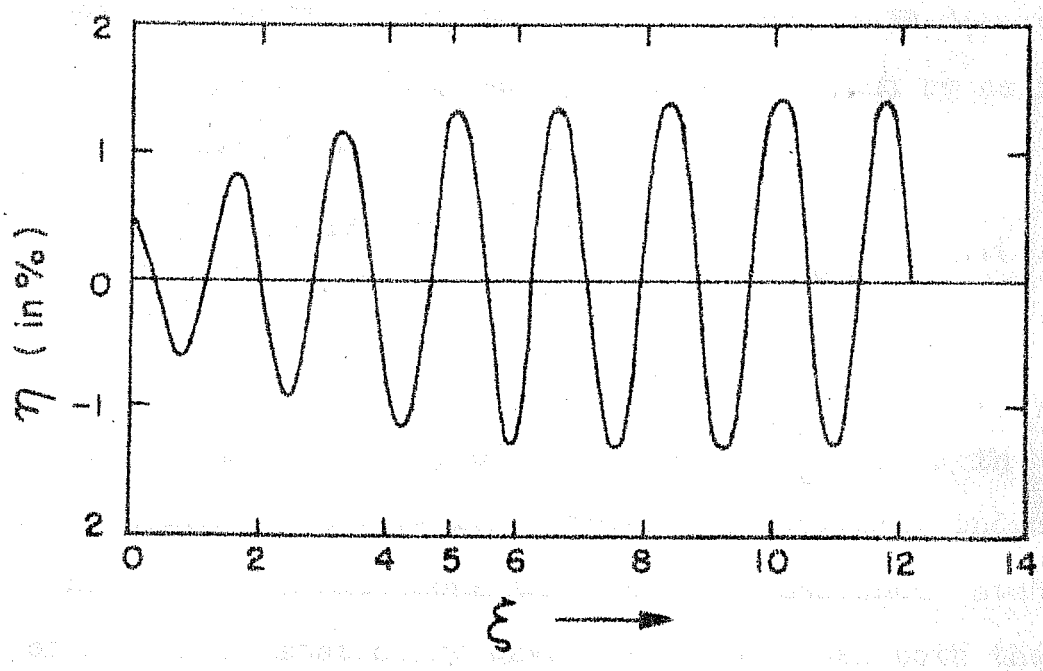


Fig. 3.2. A plot of η versus ξ showing nonlinear stationary state followed by linear growth and later characterized by steady amplitude of the perturbation η.

reduces down to its threshold value for marginal instability due to quasilinear effects and consequently, saturates the nonlinear perturbation at some finite level, A_o. In this nonlinear saturation regime, the electron drift velocity v_{om} and the phase velocity u(computed by 3.11 and 3.29), are found to satisfy respectively the relation (obtained by using 3.11 , 3.29 and 3.30)

$$v_{os} = -C_s \left\{1 + \psi\left(1 + k^2\mu/\nu_i\right)\right\}\left(1 + A_o^2/2\right)^{1/2} \qquad ..(3.39)$$

and the relation

$$u_o^2 = C_s^2\left(1 + A_o^2/2\right) \qquad ..(3.40)$$

where v_{os} and u_o are the respective values of v_{om} and u in nonlinear stationary (saturation) state. This clearly indicates that the numerical calculations show that the nonlinear stabilization of nonlinear stationary wave will occur when both the expressions (3.29) and (3.30) for the phase velocity are satisfied, a fact which was found analytically in earlier sections.

However, all these above results have been derived by solving the nonlinear wave equation (3.17) which resulted in after the assumption of a single independent variable ξ was made, and hence, do not describe the nonlinear state of type I modes with respect to time and space variations separately. This kind of information can be achieved by solving further the set of basic equations numerically which is done below.

b) Space and Time Dependences of Solutions of the Exact Set of Basic Equations:

The above numerical computation was made on the nonlinear ordinary differential equation which resulted after the assumption of a single independent variable $\xi = (\omega t - \vec{k}.\vec{r})$ had already been made. As a further check of the above theory in the general case where dependences on $\vec{r}$ and t are independent of each other we, therefore, carried out a numerical computation using the exact set of partial differential equations (3.42) to (3.46) which are derived as follows.

Substitution of $\vec{E}$ from (3.2) into (3.4) and taking the components of resulting equation in y-and z-directions give us two equations. The z-component of equation (3.2) gives the third equation. The assumption of quasineutrality(equation 3.12) and combination of electron and ion continuity equations (3.1) and and (3.3) lead to fourth equation which is, in fact, $\vec{\nabla}.j = 0$. The fifth equation is the ion continuity equation (3.3) itself. Thus these are the five basic equations to be solved for five unknowns η, $\tilde{v}_y$, $\tilde{v}_z$, $\tilde{V}_y$, $\tilde{V}_z$. We define the following dimensionless parameters

$$\tau = \omega_o t \; ; \; k y = \lambda \; ; \; \vec{\tilde{v}} = U_o \vec{\tilde{v}}' \; ; \; \vec{\tilde{V}} = U_o \vec{\tilde{V}}' \qquad ..(3.41)$$

where ω_o is the wave frequency at time t = 0 (calculated by 3.20) and $U_o = \omega_o/k$. Thus the set of basic equations to be solved numerically for five unknowns η, $\tilde{v}_y'$, $\tilde{v}_z'$, $\tilde{V}_y'$ and $\tilde{V}_z'$ is written in the dimensionless parameters as

$$\left(\frac{\partial}{\partial t} + (V_{oy}' + \tilde{V}_y')\frac{\partial}{\partial \lambda}\right)\tilde{V}_y' = \frac{\Omega_i}{\Omega_e}\left(\tilde{v}_z' - \tilde{V}_z' - \frac{\nu_e}{\Omega_e}\tilde{v}_y' - \frac{\nu_i}{\Omega_i}\tilde{V}_y'\right)$$

$$\left(\frac{\partial}{\partial t}+\left(v'_{oy}+\tilde{v}'_{y}\right)\frac{\partial}{\partial \lambda}\right)\tilde{v}'_{z}=-\frac{\nu_i}{\omega_o}\tilde{v}'_{z}+\frac{k\mu}{U_o}\cdot\frac{\partial^2\tilde{v}'_{z}}{\partial\lambda^2} \qquad ..(3.43)$$

$$\frac{\partial\eta}{\partial t}+\frac{\partial}{\partial\lambda}\left[(1+\eta)\tilde{v}'_{y}+\eta\, v'_{oy}\right]=0 \qquad ..(3.44)$$

$$-\Omega_e\tilde{v}'_{y}+\nu_e\tilde{v}'_{z}=0 \qquad ..(3.45)$$

$$\frac{\partial}{\partial\lambda}\left[(1+\eta)\left(\tilde{v}'_{y}-\tilde{v}'_{y}\right)+\eta\, v'_{om}\right]=0 \qquad ..(3.46)$$

Where, we have made use of the quasilinear modification v_{om} instead of v_o and V'_{oy} is dimensionless equilibrium (zero order) ion drift velocity in y-direction given by

$$U_o V'_{oy}=V_{oy}=\frac{e}{M\nu_i}E_p \qquad ..(3.47)$$

The equation (3.46) can easily be integrated analytically and others are integrated by the numerical procedure given below. At $\tau = 0$, we start with an initial density perturbation, with the space dependence

$$\eta=A\cos ky=A\cos\lambda \qquad ..(3.48)$$

Since A is assumed small, the initial values of variables $\tilde{v}'_y$, $\tilde{v}'_y$, $\tilde{v}'_z$ and $\tilde{v}'_z$ are calculated respectively from the linearized set of equations (3.1), (3.3) and (3.45) where $\tilde{v}'_z$ is obtained by z-component of linearized equation (3.4) and are given by

$$\tilde{v}'_{y}=\left(\omega/kU_o-v'_o\right)\eta\;;\quad \tilde{v}'_{y}=\left(\omega/kU_o\right)\eta \qquad ..(3.49)$$

$$\tilde{v}'_{z}=-\left(\Omega_e/\nu_e\right)\tilde{v}'_{y}\;;\quad \tilde{v}'_{z}=0 \qquad ..(3.50)$$

For simplicity, we will consider the monochromatic disturbance (defined by 3.48) to be of one fundamental

dimensionless fundamental wavelength λ. The range of λ from 0 to 2π is divided into M equal parts with M + 1 points. All the spatial derivatives are replaced by central differences of secondorder at all the (M + 1) points. The finite difference replacements at the boundary points involve the points outside the range. These outside points are eliminated using the periodicity conditions, $p_{M+2} = p_2$ and $p_M = p_o$ where p is any of the dependent variables. This system of 3(M + 1) ordinary ordinary differential equations in time are solved by the Trapezoidal rule. Thus, the finite difference method adopted is Crank-Nicolsen scheme.

For each time step, η, $\tilde{V}'_y$ and $\tilde{V}'_z$ are obtained first by the simple explicit scheme and these are iteratively corrected using the semi-implicit scheme. Whenever new values for η, V'_y and V'_z are calculated while advancing the time by $\Delta\tau$ or while iteratively correcting for the same time, $\tilde{v}'_y$ and $\tilde{v}'_z$ are calculated using equations (3.45) and (3.46) followed by the evaluation of v_{om} using (3.11). For the calculation v_{om}, $\langle \eta\eta \rangle$ is needed and is calculated by evaluating $\int_0^{2\pi} \eta^2 \, d\lambda$ by Trapezoidal rule. In the computation presented M = 24 and $\Delta\tau = 1.5 \times 10^{-6}$; $\Delta\lambda = .2618$ ($\approx 2\pi/24$). These values of $\Delta\tau$ and $\Delta\lambda$ are found satisfactory considering the accuracy requirements.

Our aim is to verify the analytical results obtained in sections (3.3) and (3.4) by exactly solving the set of nonlinear basic equations (3.42 through 3.46) numerically. We want to show that the use of nonlinear dispersion relation

vertical electron flux make the perturbation stabilized at some steady amplitude A_o and which might have, in this nonlinear stationary state, the phase velocity given by (3.30). As there are 3M + 3 (= 75) ordinary differential equations (3.42, 3.43 and 3.44) in time and 2M + 2(= 50) algebraic equations (3.45 and 3.46) to be solved and the time step $\Delta\tau$ is so low to satisfy the accuracy requirement, the computational time taken in IBM 360/44 computer becomes fantastically high to establish the solutions of these equations even upto the linear growth time. Therefore, we are compelled to follow an alternative approach given below to verify the results satisfactorily by restricting the solutions of the equations upto $\tau = 1.13 \times 10^{-1}$ (real time $\simeq .5 \times 10^{-5}$ sec).

In this approach, we study the time evolution of an initial density perturbation with amplitude A = .1 and fundamental wavelength $\lambda = 2\pi$, both linearly and nonlinearly. The results are shown in Fig.3.3. The linear evolution of η is shown by the thin solid curve and the nonlinear evolution by the dashed curve. For the latter case, the nonlinear modification of the electron drift v_{om} (eq. 3.11) is taken into account. The thick solid curve represents the initial shape of η at $\tau = 0$. Comparing these curves, it is inferred that in the linear case, the perturbation grows at the linear growth rate, whereas in the nonlinear case, the growth of the perturbation is negligible. This clearly indicates that if we use the nonlinear modification to electron drift and the nonlinear dispersion relation, then a nearly stabilized nonlinear solution is finally obtained

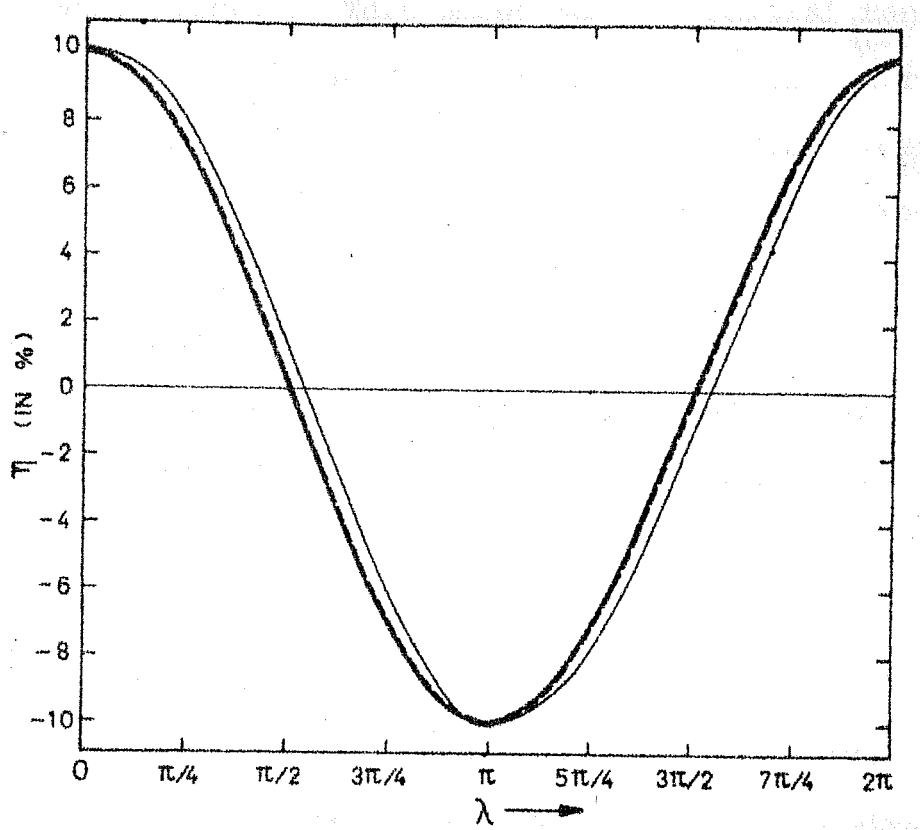


Fig.3.3. Time evolution of an initial density perturbation η with amplitude A = .1 and fundamental wavelength $\lambda = 2\pi$. The linear evolution of η is shown by thin solid curve and the nonlinear evolution by dashed curve, both until $\tau = 1.13 \times 10^{-1}$. The thick solid curve represents the initial shape of η at $\tau = 0$.

initial values of A. In this case it is found that the dashed curve in Fig.3.3 becomes indistinguishable from the initial values (thick curve). This shows that an initial nonlinear perturbation, satisfying the appropriate dispersion relation, persists in its original form. We take this as evidence for the existence of nonlinear stationary solutions of the kind discussed above. Unfortunately, limitations of computational time did not permit us to verify numerically the stability of such nonlinear solutions against slowly varying large amplitude modulational perturbations, although it is highly desirable to do so.

3.7 Discussions and Conclusions:

It is shown that the coherent type I modes observed in the equatorial electrojet can be described by a nonlinear ordinary differential wave equation (3.17). This equation has been solved both analytically and numerically, and harmonic weakly nonlinear stationary waves as its special solutions are obtained, under certain conditions prevailing in the equatorial electrojet. We, therefore, infer that such nonlinear periodic stationary waves might exist in the electrojet and might be responsible for the generation of coherent short wavelength ($\gtrsim$ 1 m) type I irregularities giving rise to type I echoes. The theory predicts that the conditions under which such waves exist, are those for marginally stable state, implying that the type I irregularities are the result of marginally stable nonlinear state, in agreement with the inference drawn from the

orily for some of the observed features of type I irregularities. These features have already been mentioned in sec. 1.31 (a) and are now discussed here below in relevance to the theory presented.

In the linear limit, the earlier results obtained both from kinetic theory (Farley, 1963a,b) and the fluid approach (Buneman, 1963; Rogister and D'Angelo, 1970) are recovered. However, an important difference from earlier linear theories developed within fluid limit, can certainly be noted that the present analysis leads to the wavelength dependent linear dispersion relation (3.20) and the wavelength dependent linear threshold v_c (3.22) for marginally stable waves described by the condition (3.21). This result agrees well with the observations (Cohen and Bowles, 1967; Balsley and Farley, 1971) which indicated that the phase velocity of type I irregularities is, in fact, wavelength dependent and corresponds to marginally stable waves. It is also remarkable to note that these results obtained here within fluid approximation, are similar to those predicted by marginally stability calculations from the kinetic theory(Farley, 1963a,b). It can easily be seen from eq.(3.22) that the threshold v_c is higher for smaller wavelength modes, implying that the strong electrojet current (large electron drift velocity) is required for the generation of shorter wavelength type irregularities, an observational fact.

The present analysis leads to an amplitude dependent

($\gtrsim$ 1 m) type I modes existing in the electrojet. The nonlinear phase velocity thus depends upon both the wavelength (the dependence arising because of the dispersive effects introduced by ion viscosity) and the nonlinear amplitude (the dependence arising due to quasilinear effects). A requirement for steepening of the wave is that its phase velocity must depend in some manner upon local quantities, such as the density or temperature. The amplitude dependence of the phase velocity found here suggests that the waves might steepen in the nonlinear stage, similar to the case of sound waves. The phase velocity of sound wave depends upon the local temperature. In the compressional part of the sound wave, the temperature is higher, and since any local disturbance in this region propagates at a higher phase velocity, the sound wave profile gradually steepens. The waves discussed here are also dispersive and the dispersion resists the steepening of the waves. The amount of steepening will thus depend upon how important the dispersion is. That is, those waves for which the viscosity term k^2/μ is small compared to ν_i, might have appreciable steepening due to nonlinear interactions. As has already been discussed, this term is quite important at least for smaller wavelength, though its effect may be small compared to quasilinear effects. It is thus inferred that this steepening of the waves due to quasilinear effects limits the growth of the initially unstable waves, making it stabilized and in turn, leads to marginally stable

We have shown that in this marginally stable nonlinear state, the nonlinear harmonic stationary type I modes get stabilized at some constant finite nonlinear amplitude A_o nearly equal to 1.38 % and travel with the nonlinear phase velocity u_o defined by (3.30). This implies that type I irregularities occuring in the electrojet propagate with a constant nonlinear amplitude and a nonlinear phase velocity. This is in fair agreement with the observations reported by Prakash et al. (1970, 1971a,b, 1972, 1973) that the short wavelength irregularities which they called as type Ss and identified with type I, are observed having the amplitudes of the order of a few percent (ranging from 0.21 % to 3.44 % with a value of 1.55 % around 104 km). This result is also seen to agree with the magnitude of the amplitudes ($\lesssim$ 3 %) deduced from the backscatter radar measurements (Weinstock, 1968).

We have also shown analytically and later verified numerically that the nonlinear stabilization of nonlinear stationary waves will occur when both the expressions (3.29) and (3.30) for the phase velocity are satisfied. This result suggests two things. Firstly, the quasilinear effects tend to reduce its linear phase velocity (3.20) to a constant nonlinear phase velocity u_o in nonlinear state. This reduction occurs because of the fact that the electron drift velocity v_{om} on which linear phase velocity depends ($v_{om} = v_o$ in linear regime), gets decreased due to increase in turbulent negative vertical electron flux in nonlinear state (Rogister, 1971; Sato, 1972), as discussed in sec.3.2. The nonlinear phase velocity of

marginally stable modes is slightly different from the linear threshold value by an amplitude dependent factor. Looking at the ion equation of motion, it can easily be realized that this effect arises due to the presence of a nonlinear term $(\underline{V}.\underline{\nabla})\underline{V}$, i.e., through a ponderomotive force acting on ions due to quasilinear interactions. As the amplitude of nonlinear modes in marginally stable state remains constant ($\simeq A_o$), the equation (3.30) expresses the remarkable fact that within fluid theory, the marginally stable modes have the threshold phase velocity which is constant and is slightly greater than the ion acoustic velocity, in contrast to the linear result that it is equal to ion acoustic velocity. This conclusion, therefore, appears to account for the observed constant phase velocity of type I irregularities, slightly differing from ion acoustic speed. Secondly, the electron drift velocity v_{om} in the marginal stable state assumes a constant threshold value, $|v_{os}|$ which seems to be appreciably exceeding the ion acoustic velocity, as it is obvious from (3.39). This supports an observational result demonstrated by Cohen (1973) that the electron drift velocity may appreciably exceed the ion sound velocity, when type I irregularities appear. From equation (3.39), one easily observes the wavelength and amplitude dependences of the threshold electron drift velocity, v_{os} for marginally stable nonlinear waves. Thus, the theory predicts that the nonlinear threshold $|v_{os}|$ differs slightly from its linear value by the amplitude dependent term, the effect (as

The numerical solutions of the full nonlinear wave equation (3.17) and the exact set of basic equations (3.1) - (3.4) are found to support many of the analytical results of this theory. We must remark here, however, that the numerical verification of the above results in support of them, could not be done completely and exactly because of lack of availability of computer time. It is, rather, unfortunate that we were compelled to make use of the nonlinear dispersion relation and the quasilinear modification v_{om} which are important only when the nonlinearities start playing role after the linear growth, in finding out the solutions of the exact nonlinear set of basic equations. Furthermore, we could integrate these equations only upto the (real) time $\approx .5 \times 10^{-5}$ sec which is short compared to all time scales of interest (e.g., even much shorter than the linear growth time). Nevertheless, the inferences made by extrapolating the numerical results in Fig.3.3 for larger time, reasonably support the analytical results of our theory. We point out, further that if it were feasible to solve numerically the exact nonlinear set for sufficiently large time, it would have been possible to show clearly first the linear growth and later on, the final nonlinear stable state of the initial small amplitude perturbation. Consequently, this would have provided us with the nonlinear saturation value of the amplitude, A_o, the marginally stable threshold electron drift velocity, v_{os}, the nonlinear phase velocity, u_o and other nonlinear characteristics.

The amplitude dependence of wave frequency and the

type I modes discussed above are found to be stable against slowly varying large amplitude modulational perturbations. We have shown, though not by rigorous treatment, that the large amplitude modulational perturbations to such modes are, however, expected to develop adiabatically into modulational envelope solitons . As mentioned in sec. 1.31 (a), there may already be some evidence to this effect from backscatter observations. (Balsley, 1969a,b, 1973a,b; Farley and Balsley, 1973) that the type I irregularities in the electrojet might travel in the form of fairly discrete wave packets with soliton shaped envelopes.

Unfortunately, limitations of computational time did not permit us to numerically investigate the stability property of nonlinear solutions discussed above, although such a study would be highly desirable. As a result, it could also not be possible to check numerically one of our conclusions, e.g., the conversion of the type I modes into modulational envelope solitons in adiabatically nonstationary case.

In conclusion, the principal results of the theory presented herein, may now be summarized as follows. The author has demonstrated the existence of stationary nonlinear solutions to the equations describing one-dimensional type I irregularities in the equatorial electrojet. The nonlinear phase velocity and threshold electron drift velocity for the marginally stable mode are slightly different from their linear values, the effect arising through ponderomotive force

against slowly varying large amplitude modulational perturbations. However, in the adiabatically nonstationary case, one expects the formation of modulational envelope solitons. Some of the observed features of type I backscatter echoes as well as type S irregularities are consistent with the predictions of the theory presented.

CHAPTER IV

LOW FREQUENCY RAYLEIGH-TAYLOR INSTABILITY AND THE EQUATORIAL SPREAD-F

4.1 Introduction:

The well known phenomenon of equatorial spread-F, which is characterized by blurred or diffused echoes on ionograms (see sec. 1.23(c) for detailed description of spread-F), has been the subject of extensive studies, both observationally and theoretically, over several decades (~ 30 years). The equatorial spread-F, first detected by Booker and Wells (1938), has been attributed to field-aligned electron concentration (density) irregularities occurring in the equatorial F-region. It is, generally, believed to be caused due to partial and multiple reflections or scattering or both of HF radio waves from these irregularities. We now know under what conditions spread-F is likely to occur. It is also well understood how the various radio propagation effects which characterize the spread-F, can arise if irregularities of electron density aligned with earth's magnetic field are present in the ionosphere, but the formation of these irregularities has remained to large extent unexplained (Herman, 1966; Farley et al., 1970; Farley, 1974).

Although a vast amount of data using various techniques has been gathered revealing a wealth of informations about the occurrence, behaviour and properties of equatorial spread-F irregularities, the problem of their generation and of explaining many of their fundamental features has not been yet satis-

made in understanding the basic plasma instability mechanism(s) responsible for their generation. This can be attributed to the bare fact that plasma physics has only recently developed the tools necessary to explain the phenomenon. Though much of spread-F phenomenology can be explained by linear instability theories, there are many observational features, such as their specific stable structures with which they propagate in ionosphere, saturation amplitude, spectral shape, etc., which can not be explained by them and require a satisfactory nonlinear analysis. With this in mind, the author in this chapter has made a modest attempt to investigate into a reasonably satisfactory nonlinear instability theory (nonlinear Rayleigh-Taylor instability) where we have taken into account the finite Larmor radius effects (Rosenbluth et al., 1962) and the complete ion inertia, i.e., convectional motion of ions (suggested by Dungey, 1956) which has been overlooked by all earlier workers, is also included here. The theory so developed could explain, to some extent, their generation and some of the most important basic observed characteristics that have been discussed in the sections 1.23(c) and 1.32.

So far various properties of F-region irregularities have been the subject of both theoretical and experimental investigations by many workers in the recent past, but even then the processes responsible for producing them are not yet completely understood. The difficulty lies in the fact that so

into account simultaneously. Because of this complexity, it seems reasonable to believe that there may be many different physical mechanisms operating individually or simultaneously, which are responsible for the generation of spread-F irregularities observed with a very wide range of scale sizes perpendicular to magnetic field and with a characteristic growth time more than a few seconds to ~ 30 min. Farley et al. (1970) have reviewed most of the theories on the equatorial spread-F that have been advanced in the past and listed the reasons pointing out that none of the existing theories of spread-F could adequately account for all of the observed characteristics. We now review briefly the linear and nonlinear theories of spread-F irregularities in the following where the emphasis will be given mainly to the instability mechanism of our interest (i.e., Rayleigh-Taylor instability).

The most important fact about the equatorial spread-F is that it is a nighttime phenomenon associated with the postsunset rise of the F-layer (Booker and Wells, 1938). This rise of the F-layer is primarily caused by an eastward electric field resulting in an $\underline{E}_0 \times \underline{B}$ vertical drifts of ionization (Rishbeth, 1971), which thus acts as a free energy source for the rise associated with the phenomenon. Farley et al. (1970) have found that correlation of spread-F with the postsunset rise of the F-layer is due to an altitude threshold for spread-F onset, rather than a vertical drift velocity threshold.

most important and obvious source of free energy for driving an instability on the bottomside of the nighttime F-layer is the sharp vertical plasma density gradient. A typical example is shown in Fig.1.5. This, combined with the field-aligned nature of the irregularities, suggests a variety of density gradient-dependent instability mechanisms which require a destabilizing force in addition to the density gradient. The density gradient-driven plasma instabilities which have been proposed, include Hall and Pedersen $\underline{E}_o$ x $\underline{B}$ modes (Reid, 1968; Cunnold, 1969) first investigated by Simon (1963). These are demonstrated physically in sec. 1.4(a) and briefly described in sec. 2.1 (third para). However, the Hall $\underline{E}_o$ x $\underline{B}$ instability which requires a vertical electric field, does not seem to be an efficient process at F-region heights, because the Hall conductivity effectively vanishes there. Though the Pedersen conductivity is non-negligible in the F-region, the Pedersen $\underline{E}_o$ x $\underline{B}$ instability which requires a horizontal eastward electric field, appears to be less suggestive as a mechanism responsible for spread-F formation because the horizontal fields are usually smaller than the vertical fields (Rishbeth, 1971). Moreover, both modes rely on ion-neutral collisions to provide a relative drift between ions and electrons. The high altitude threshold (300-400 km) for spread-F onset (Farley et al., 1970) argues against the dominance of such modes, because collision frequency has negligible effects at such heights. Reid (1968) suggested that the fluctuating electric fields generated by

equipotential magnetic lines to the F-region. However, only, large scale irregularities(> 1 km)could be transported from E- to F-region (Farley et al., 1970). Furthermore, while such a theory may have significance at high latitudes as magnetic field lines become vertical, it is not clear that it is relevant to equatorial regions.

Dungey (1956) was first to suggest that the source of the equatorial F-region irregularities could be a gravitational instability of the underside of the F-layer. At night the gradient in ionization density is often steep, and the layer resembles a slab of inhomogeneous plasma supported against gravity by magnetic field, thus fulfilling broadly the light-fluid (Lower density) supporting heavy-fluid (higher density) description. Such a configuration is well known to be unstable and the instability is called the Rayleigh-Taylor (R-T) instability. Many properties of long wavelength irregularities ($\lambda_\perp >> \rho_i$, ion Larmor radius) below the F-region maximum (where background density gradient, ∇n_o is antiparallel to gravitational acceleration, g) can be explained in terms of this gravitation-induced Rayleigh-Taylor instability (Johnson and Hulburt, 1950; Dungey, 1956; Balsley et al., 1972; Hudson et al., 1973; Hudson and Kennel, 1975a,c). Hudson and Kennel (1974a,b, 1975b, c) have recently proposed that for wavelengths below a few hundred meters (yet $\lambda_\perp >> \rho_i$), some of the observations of the equatorial spread-F irregularities could be explained by the excitation of density gradient-driven collisional drift modes Because the R-T mode has a finite Larmor radius (FLR) cut-off

(stabilized due to FLR effects) at shorter wavelengths (Rosenbluth et al., 1962), whereas the collisional drift modes do not suffer from this problem and are found to be destabilized by FLR effects (Hudson and Kennel, 1974a,b, 1975a,b,c). Hudson et al. (1973) proposed a two-step (multilinear) theory for the formation of short wavelength irregularities ($\lambda_\perp << \rho_i$) in analogy with a similar two-step linear mechanism suggested by by Sudan et al. (1973) for the generation of small scale irregularities in the equatorial E-region. They concluded that the collisionless short wavelength drift modes are linearly excited by the density gradients associated with the collisional R-T modes which grow on the primary long wavelength irregularities (Farley et al., 1970; Balsley et al., 1972). Hudson and Kennel (1975a,b,c) extended the analysis of collisional linear R-T instability to short wavelength collisional R-T drift modes by including ion neutral collisions (Balsley et al., 1972), ion FLR effects (Rosenbluth, et al., 1962) and ion viscous stabilization. It was found that collisions reduce the maximum R-T growth rate and effectively eliminate the collisionless FLR cut-off. They inferred that below the F peak where spread-F predominates, both the drift and R-T modes, growing on the same zero order density gradient, contribute to the total spread-F wavelength spectrum, with the R-T mode dominating at long and the drift mode at short wavelengths above the ion Larmor radius (but closer to it than previous theories).

Very recently, ignoring the equilibrium background

dissipative instability. Chaturvedi and Kaw (1975a) suggested a nonlinear mode-mode coupling approach for the two-step process instead of linear one as used by earlier workers. They pointed out that a short wavelength drift mode can not grow on a long wavelength drift wave because the appropriate mode coupling terms cancel out each other and in a drift wave, the total first order electron diamagnetic drift which would support secondary drift mode, is absent. Their two-step mechanism is, therefore, the excitation of secondary drift waves growing on the density gradients of a large amplitude long wavelength R-T mode. It was here concluded that as the long wavelength irregularities increase in amplitude, the gradient ($\sim \delta n/n\lambda$) associated exceeds a critical value and as a result, the R-T modes become prone to the generation of shorter wavelength drift modes by a collisionless as well as collisional drift instability mechanism on the underside of the equatorial F-region.

In another very recent paper, Chaturvedi and Kaw (1975b) obtained nonlinear steady solutions of the equations describing one-dimensional R-T instability. It is shown here that R-T instability driven modes (fundamental unstable modes) can evolve into coherent, travelling stationary waves having a constant phase velocity, through the nonlinear interactions with the shorter wavelength FLR stable oscillatory modes. The nonlinear interactions then lead to the small real frequency shift of the fundamental and harmonics (both having zero real

phase velocity u to these modes. If u is small compared to the ion diamagnetic drift $V_L (= V_{th}\rho_i/L$, V_{th} is the ion thermal velocity and L the density scale height), then R-T modes evolve into almost sinusoidal solutions. If u becomes comparable to V_L, the solutions assume a strongly non-harmonic profile. Their results could explain some of the observations of the equatorial F-region irregularities (Dyson et al., 1974; Kelley et al., 1975).

So far in all the linear and nonlinear theories of the instabilities developed by earlier workers for the spread-F irregularities, the linear convection part $(\underline{V}_o \cdot \underline{\nabla})\underline{\tilde{V}}$ of the ion inertial term has been neglected (the nonlinear part could be neglected as it is much smaller). However, the convectional motion of the ionization in the equatorial F-region appears to be quite important, since it modifies the diffusion of ionization under gravity significantly (Johnson and Hulburt, 1950; Johnson, 1950; Dungey, 1956) and thus could give an important contribution to the irregularities formation. It was, in fact, first realised by Johnson and Hulburt (1950) and Johnson (1950) that the situation in the equatorial F-region where the diffusion being very slow is unimportant because of $\nu_i << \Omega_i$ and where the ionization is supported by electromagnetic forces, is unstable and that a convective motion of ionization must occur. Assuming the existence of some irregularities in the ionization density, they showed that (a) the current required to support them against gravity will tend to build

ionization density is upward below F_{peak}, a net downward motion of the ionization increases at a fixed point in the region of excess density and so the irregularities are amplified. Although they say that the diffusion under gravity is unaffected by the magnetic field, it is modified by considering a convectional form (Dungey, 1956). Regarding the convective motion as that of a gravity-driven dynamo, Dungey (1956) concluded that Johnson and Hulburt's (1950) suggestion is likely to be important, and showed that the convective diffusion (i.e., convective motion of ionization) would increase any irregularities which may be present. Moreover, the phase velocity of the waves may be comparable with and even smaller than V_L, as has been assumed by Chaturvedi and Kaw (1975b) in order to explain some of the spread-F observations. In spite of this assumption, they did not take into account the convective part $(\underline{V}_o \cdot \nabla)\underline{\tilde{V}}$ along with the term $\partial\underline{\tilde{V}}/\partial t$ in the ion equation of motion (where $V_{oy} = g/\Omega_i + V_L$, the eq.4.11 here), which, we are afraid, will make their conclusions quite inconsistent. We feel that the convective motion $((\underline{V}_o \cdot \nabla)\underline{\tilde{V}})$ might lead to a significant contribution both to the generation of the long wavelength ($> \rho_i$) R-T modes (as first suggested qualitatively by Dungey, 1956) in the F-region and to the stabilization of the modes as will be seen below in the present analysis. Therefore, the convective part of ion inertial term must necessarily be considered in any satisfactory mechanism or theory of equatorial spread-F.

In the present chapter, a nonlinear analysis of the

collisional R-T instability accounting for the FLR effects is presented, which differs from those proposed by Chaturvedi and Kaw (1975b) and earlier workers in the sense that it includes, for the first time, the convective part along with the term $\partial \tilde{\underline{V}}/\partial t$, of ion inertial term, i.e., the complete ion inertia, in ion equation of motion. Having followed a different method from that used by Chaturvedi and Kaw (1975b), the author discusses a special class of coherent, weakly nonlinear R-T modes in the equatorial spread-F region.

The author begins in next section with the basic equations and the assumptions used for the treatment of the present theory and with a brief description of the equilibrium configuration for the equatorial F-region plasma. Having retained the linear convection part $(\underline{V}_o \cdot \nabla)\tilde{\underline{V}}$ of ion inertia, the linear theory is briefly outlined in the third section and an appropriate linear dispersion relation is also obtained which is then compared with one obtained by earlier workers. The fourth section deals with the derivation of an ordinary differential wave equation by reducing one-dimensional set of nonlinear equations describing R-T instability driven modes by making an assumption of ξ $(= ky - \omega t)$ as the only independent variable. Nonlinear solutions to this wave equation, the corresponding dispersion relation and the physical conditions satisfied by these solutions are obtained and discussed in fifth section. Finally, in the last section the results of the theory presented are concluded ~~and in the last section~~

equatorial spread-F irregularities in the ionosphere.

4.2 Basic Equations:

In the F-region, the Debye length is of the order of centimeters which is small compared to the distances of interest. For the wavelength of the perturbations greater than either ion gyroradius or ion mean-free path, the macroscopic fluid equations (valid for perturbations with $k_\perp \rho_i$ and $k_z \lambda_{mfp}^i << 1$) are adequate to describe the F-region plasma. We choose the following rectangular coordinate system appropriate to the equatorial F-region: z-axis points along the direction of earth's magnetic field; y-axis is taken along the west-east direction and x -axis points vertically upwards. The background density gradient is thus along the x-axis and anti-parallel to the acceleration due to gravity $\underline{g}$. In the frame work of a two-fluid theory, the equatorial F-region plasma is, therefore, governed by the continuity and momentum transfer equations for electrons and ions. The governing equations for electrons (4.1 and 4.2) and for ions (4.3 and 4.4) in the neutral rest frame are, therefore, given by

$$\frac{\partial n}{\partial t} + \nabla \cdot (n \underline{v}) = 0 \qquad ..(4.1)$$

$$0 = -\frac{e}{m}\left(\underline{E} + \frac{\underline{v} \times \underline{B}}{c}\right) - \frac{k T_e}{m} \cdot \frac{\nabla n}{n} \qquad ..(4.2)$$

$$\frac{\partial N}{\partial t} + \nabla \cdot (N \cdot \underline{V}) = 0 \qquad ..(4.3)$$

$$\frac{\partial \underline{V}}{\partial t} + (\underline{V} \cdot \nabla)\underline{V} = \frac{e}{M}\left(\underline{E} + \frac{\underline{V} \times \underline{B}}{c}\right) - \nu_i \underline{V} + \underline{g} \qquad ..(4.4)$$

where n and N are the number densities of electrons and ions respectively. $\underline{E} = -\nabla\phi$ is the electric field and ϕ is the electrostatic potential. $\underline{v}$ and $\underline{V}$ represent the electron and ion velocities. m and M refer to the electron and ion masses respectively. μ is the coefficient of ion viscosity and ν_i is the ion-neutral collision frequency. All other symbols have their conventional meanings.

4.21 Assumptions and Approximations Used:

In writing down the above equations and in subsequent discussions, the following assumptions and approximations are made: (i) The electron collision frequency ν_e is neglected, because it is much smaller than electron gyrofrequency $\Omega_e = eB/mc$; (ii) The electron inertia has been ignored, since Ω_e is much larger than the Doppler-shifted wave frequency; (iii) The wave electric field is essentially electrostatic, i.e. $\underline{E} = -\nabla\phi$ (in agreement with observations, Holtet et al., 1975), because the plasma pressure is much smaller than the ambient magnetic energy density and $ck/\omega_{pe} >> 1$ for wavelength of interest (ω_{pe} is electron plasma frequency and k is the wave number); (iv) The ions and electrons are assumed to be isothermal: (v) The ion drag which is unimportant at night (Rishbeth and Garriott, 1969) is neglected; (vi) The recombination is assumed to be negligible which is valid for the processes that occur faster than the several hour time scale of the nighttime F-region; (vii) The waves are assumed to propagate exactly perpendicular to the magnetic field, since these waves

The neutrals can be treated as infinite sink for momentum and energy at oscillation (wave) frequencies exceeding the rate at which ion neutral collisions ν_i transfer momentum and energy to the neutrals (Nicolet, 1953), i.e.,

$$\omega \gg \nu_i \, N / n_n = 4.6 \times 10^{-12} N \qquad ..(4.5)$$

At lower frequencies than ω given by (4.5) a set of fluid equations for neutrals should be included along with the set (4.1) to (4.4). However, in the nighttime F-region the frequencies of interest are generally greater than those given by (4.5). Therefore, the neutrals are considered completely at rest.

As we are interested in long wavelength R-T modes (greater than Debye length and ion Larmor radius ϱ_i), we invoke here quasi-neutrality condition, namely

$$n \approx N \qquad ..(4.6)$$

4.22 Equilibrium Configuration of Equatorial F-region Plasma:

Let us now briefly describe the equilibrium configuration of the equatorial F-region which is going to be perturbed around its equilibrium values. In the presence of collisional transport effects, the sources and sinks are neglected. We will assume that there is no significant effect on the particle motions due to the zero-order d.c. electric field $\underline{E}_0$, i.e., the zero-order drifts of the particles are considered to be negligible compared to other motions. The equations (4.1) to (4.4) in zero-order equilibrium stationary state can then be written as

$$\nabla (n_0 v_0) = 0 \qquad ..(4.7)$$

$$0 = -\frac{e}{m}\left(\frac{\underline{v}_o \times \underline{B}}{c}\right) - v_{TH}^2 \frac{\nabla n_o}{n_o} \qquad ..(4.8)$$

$$\nabla \cdot (n_o \underline{V}_o) = 0 \qquad ..(4.9)$$

$$0 = \frac{e}{M}\left(\frac{\underline{V}_o \times \underline{B}}{c}\right) - \nu_i \underline{V}_o + \underline{g} - V_{TH}^2 \frac{\nabla n_o}{n_o} \qquad ..(4.10)$$

where $v_{TH} = (KT_e/m)^{1/2}$ and $V_{TH} = (KT_i/M)^{1/2}$ are respectively the electron and ion thermal velocities. These equations (4.7) to (4.10) yield the electron and ion zero-order equilibrium drift velocities in the horizontal and vertical directions (neglecting $(\nu_i/\Omega_i)^2$ and ν_i/Ω_i^2, since $\nu_i \ll \Omega_i$ in the F-region) as

$$v_{ox} \approx 0 \quad ; \quad V_{ox} = -(\nu_i/\Omega_i) V_L \qquad ..(4.11)$$

$$v_{oy} = -v_L \quad ; \quad V_{oy} = V_o = \frac{g}{\Omega_i} + V_L \qquad ..(4.12)$$

where $v_L = v_{TH}\,\rho_e/L$ and $V_L = V_{TH}\,\rho_i/L$ are respectively the electron and ion diagmagnetic drifts, $\rho_e = v_{TH}/\Omega_e$ and $\rho_i = V_{TH}/\Omega_i$ being the electron and ion Larmor radii respectively. Thus, in the analysis the FLR effects are introduced through v_L and V_L. Ω_i is the ion gyrofrequency and L is the background density scale height defined by

$$L^{-1} = (1/n_o)\, dn_o/dx \qquad ..(4.13)$$

Equations (4.11) show that while the electron Pedersen diffusion flux is zero (because ν_e being much less than Ω_e ($\nu_e/\Omega_e \ll 10^{-5}$) is neglected), the ion Pedersen diffusion flux is antiparallel to the density gradient. Both the ion collision frequency ν_i and the ion diamagnetic drift velocity V_L ($\nu_i/\Omega_i \ll 10^{-3}$ and V_L is typically $\gtrsim$1 m/sec above 250 km)

ion vertical drift velocity V_{ox} becomes vanishingly small, resulting into the ambipolar diffusion of the particles at greater heights. The ion viscous diffusion flux along the density gradient, which is proportional to $(\nu_i/\Omega_i)\rho_i/L$ (a vanishingly small quantity), is also typically negligible and hence, has not been considered.

In the next section, we briefly describe the linear theory of the Rayleigh-Taylor instability and derive an appropriate dispersion relation for these modes so that a qualitative comparison between the dispersion relations obtained by earlier workers and the present one, can be made.

4.3 Linear Theory:

To establish the notion and the assumptions under which the calculations for obtaining nonlinear solutions of the equations describing R-T modes in the equatorial F-region are performed, we briefly outline the linear instability theory in this section. Now let us define each variable q consisting of two parts as

$$q = q_o + \tilde{q} \qquad ..(4.14)$$

where q_o denotes the equilibrium value and $\tilde{q}$ is the perturbation which we assume to be horizontally propagating low frequency wave of the form $\exp(i(ky - \omega t))$. We neglect, for the time being, both v_L and V_L, i.e., the finite Larmor radius (FLR) corrections which lead to the stabilization effects (Rosenbluth et al., 1962) to be absent. Linearizing eqs. (4.1) to (4.4) and then eliminating all except density variables and using the

$$i u (V_g - u) + \nu_i u/k - i g/k^2 L = 0 \qquad ..(4.15)$$

where u is the phase velocity of the wave equal to ω/k and $V_g = g/\Omega_i$ is the gravitational drift of ions. For simplicity, μ has been neglected and moreover, the term containing μ is much smaller than others in magnitude as discussed in previous section. For the situation when $\nu_i \simeq 0$, this dispersion relation reduces to

$$u (V_g - u) = g/k^2 L \qquad ..(4.16a)$$

or

$$\omega = \frac{k V_g}{2} \pm i \sqrt{g/L - k^2 V_g^2/4} \qquad ..(4.16b)$$

This is essentially the same dispersion relation as obtained by earlier workers, except with the differences (a) that the R-T modes now are not purely growing modes and have the growth rate given by $\omega_i = (g/L)^{1/2} (1-(k V_g)^2/8 gL^{-1})$ (obtained from imaginary part of (4.16) using $g/L >> (kV_g)^2$ valid in spread-F region); (b) that these modes now have the real frequency, i.e., real phase velocity equal to $V_g/2$ (the real part of eq.4.16) which shows that the linear collisionless ($\nu_i = 0$) R-T modes must travel with the constant phase velocity equal to half of the ion gravitational drift velocity $V_g = g/\Omega_i$. These differences arise because we have taken into account here the term $(\underline{V}_o \cdot \underline{\nabla})\underline{\tilde{V}}$ in ion inertial term which was neglected in all previous theories.

It is, therefore, interesting to note that in the linear limit, even if one neglects the FLR stabilization corrections, the dispersion of the waves is such that the modes have the

growth rate by a factor equal to $k^2L^2(g/L)^{3/2}/8\Omega_i^2$ rather than a purely growing term (as obtained in all earlier theories). This gives rise to some contribution to the stabilization of the R-T modes even in the absence of FLR corrections. It is also to be noted, however, that the longer (smaller) wavelength R-T modes will have smaller (higher) frequency shift from zero real frequency and smaller (larger) reduction in the growth rate, in contrast to the earlier linear results of zero real frequency and purely growing R-T modes.

In the collisional limit ($\nu_i \neq 0$), the solutions of the dispersion relations (4.15) are

$$\omega = (kV_g - i\nu_i)/2 \pm \left[(kV_g - i\nu_i)^2 - 4g/L\right]^{1/2}/2 \qquad ..(4.17)$$

For the parameters (either deduced or observed) applicable to the spread-F region (L ≈ 10 to 100 km (Hanson and Sanatini, 1973; Kelley and Carlson,, 1974); $\nu_i \approx 10^{-1} - 10^{-2}$; V_{TH} = 1 km/sec) and for the modes with wavelengths greater than ion Larmor radius ρ_i (≈ 10 meter),

$$\nu_i \gg g/L \,,\; kV_g \text{ or } kV_0 \qquad ..(4.18)$$

Hence, we can expand the radical in (4.17) to obtain its roots as

$$\omega = (kV_g - i\nu_i)/2 \pm \left[(kV_g - i\nu_i)/2 - (g/L)(kV_g + i\nu_i)/(k^2V_g^2 + \nu_i^2)\right] \qquad ..(4.19a)$$

Considering the upper (+) sign, we find that one root is completely damped (with damping rate which is imaginary part

due to collisions, whereas the other root (considering '-' sign) is unstable. The phase velocity and the growth rate of unstable R-T mode are then

$$u = \omega_r / k \approx V_g \cdot g / L \nu_i^2 \qquad ..(4.19b)$$

$$\omega_i = (g/L)\, \nu_i / (k^2 V_g^2 + \nu_i^2) \approx g / \nu_i L \qquad ..(4.19c)$$

where ω_r (frequency) and ω_i (growth rate) are respectively the real and imaginary parts of ω and the inequalities (4.18) have been used. The growth rate, ω_i obtained here agrees with the collisional Rayleigh-Taylor mode growth rate given by Balsley et al. (1972), Hudson and Kennel (1975a,c) and others. Note interestingly, however, that now the modes have a small shift in real frequency ω_r from its zero value as obtained by these authors. This difference arises due to the inclusion in the present theory of the convectional motion of the ions $((\underline{V}_o \cdot \underline{\nabla})\underline{\tilde{V}})$ as suggested by Dungey (1956). It is thus inferred that the collisional R-T modes are also not purely growing modes as these have real phase velocity defined by eq.(4.19b), in contrast to the earlier results of linearly pure growing collisional R-T instability driven modes (Balsley et al., 1972; Hudson and Kennel, 1975a,c). We also find here that in the collisional limit the phase velocity is reduced down from that (eq. 4.16b) obtained in the collisionless limit by a factor $2g/L\nu_i^2$. Note that its magnitude is much smaller at lower altitude F-region where ν_i is large, and becomes equal to half of the ion gravitational drift V_g at higher altitudes where ν_i is negligibly small (collisionless limit). Neverth-

the ion gravitational drift $V_g (\gtrsim 10$ m/sec) in the regions of interest. Chaturvedi and Kaw (1975b) have, however, neglected the term $((\underline{V}_o/k).\nabla)\,\underline{\tilde{V}} = (\nu_o/k)\,\partial\underline{\tilde{V}}/\partial y = (V_g + V_L)\underline{\tilde{V}}$ compared to the term $(1/k)\,\partial\underline{\tilde{V}}/\partial t = u\underline{\tilde{V}}$ in ion equation of motion, which is not justifiable when $u < \nu_o (\nu_o = V_g + V_L)$ as we have seen above. Therefore, their results obtained by neglecting the convective part $(\underline{V}_o.\nabla)\underline{\tilde{V}}$ of ion inertia, do not appear to be consistent with the crucial assumption that $u < V_L$ which they make later for the interpretation of the spread-F observations.

It is also to be noted that the growth rate and the phase velocity of the collisional R-T modes increase with height, because ν_i decreases with altitude. But L which increases with altitude, limits the increase of both the growth rate and the phase velocity. It is thus obvious now that one must include the convection part in ion inertia in a satisfactory theory of spread-F, as the phase velocity of the waves may be comparable with and even smaller than ν_o (low frequency spread-F irregularities) in the region of interest. We shall now use these facts to derive an equation describing coherent nonlinear travelling R-T modes and in turn, to find out the solutions of this equation.

4.4 Wave Equation for Nonlinear R-T Modes:

Substitution of eq.(4.14) into (4.1) - (4.4) and then using (4.7) to (4.10) will give the following set of equations for perturbed quantities.

$$0 = \frac{e}{m}\nabla\tilde{\phi} - \frac{\tilde{\underline{v}}\times\underline{B}}{} - \frac{\nu_{TH}^2}{}\left[\frac{\nabla\tilde{n}}{} - \frac{\tilde{n}}{}\frac{\underline{g}}{}\right] \qquad (4.22)$$

$$\frac{\partial \tilde{n}}{\partial t} + \frac{\partial}{\partial x}(n \tilde{v}_x) + \frac{\partial}{\partial y}(n \tilde{v}_y) + v_{oy} \frac{\partial \tilde{n}}{\partial y} = 0 \qquad ..(4.21)$$

$$\frac{1}{\Omega_i}\left(\frac{\partial}{\partial t} + v_o \frac{\partial}{\partial y}\right) \tilde{\underline{V}} = -\frac{c}{B} \nabla \phi + \frac{\tilde{\underline{V}} \times \underline{B}}{B} - \frac{\nu_i}{\Omega_i} \tilde{\underline{V}} - \frac{V_{Ti}^2}{\Omega_i}\left(\frac{\nabla \tilde{n}}{n} - \frac{\tilde{n}}{nL}\hat{\underline{x}}\right) + \frac{\mu}{\Omega_i} \nabla^2 \tilde{\underline{V}} \qquad ..(4.22)$$

$$\frac{\partial \tilde{n}}{\partial t} + \frac{\partial}{\partial x}(n \tilde{v}_x) + \frac{\partial}{\partial y}(n \tilde{v}_y) + v_{oy} \frac{\partial \tilde{n}}{\partial y} = 0 \qquad ..(4.23)$$

where $\underline{E} = -\nabla \phi$, ϕ being the electrostatic potential perturbation and $\hat{\underline{x}}$ is the unit vector along the x-direction. Combining electron continuity equation (4.21) and equation of motion (4.20), we get

$$\frac{\partial \tilde{n}}{\partial t} - \frac{n_o}{L} \frac{c}{B} \frac{\partial \phi}{\partial y} = 0 \qquad ..(4.24)$$

which shows that the density changes locally because of $\tilde{\underline{E}} \times \underline{B}$ motion of electrons along the density gradient ($\nabla n_o = \frac{n_o}{L}$). Taking x-and y-components of the equation (4.22), the components of ion velocity, $\tilde{v}_x$ and $\tilde{v}_y$ are obtained as

$$\tilde{v}_x = -\frac{c}{B} \frac{\partial \phi}{\partial y} - \frac{L v_L}{n} \frac{\partial \tilde{n}}{\partial y} + \frac{v_L}{\Omega_i} \frac{\partial}{\partial t}\left(\frac{\tilde{n}}{n}\right) \qquad ..(4.25)$$

$$\tilde{v}_y = -\frac{1}{\Omega_i}\left(\frac{\partial}{\partial t} + v_o \frac{\partial}{\partial y} + \nu_i - \mu \frac{\partial^2}{\partial y^2}\right)\left(\frac{c}{B} \frac{\partial \phi}{\partial y} + \frac{L v_L}{n} \frac{\partial \tilde{n}}{\partial y}\right) - v_L \frac{\tilde{n}}{n} \qquad ..(4.26)$$

where in deriving these expressions, such terms which contain the square and the product of ω/Ω_i , k/Ω_i, ν_i/Ω_i and other smaller terms, have been neglected in comparison with other leading terms. The ion continuity equation (4.23) and the equations (4.25) and (4.26) may be combined to yield the equation for density change due to motion of ions as

$$\frac{\partial \tilde{n}}{\partial t} + \frac{n_o v_L}{\Omega_i L} \frac{\partial}{\partial t}\left[\log \frac{n}{n_o} - \frac{\tilde{n}}{n}\right] - \frac{n_o}{L} \frac{c}{B} \frac{\partial \phi}{\partial y} + \frac{g}{\Omega_i} \frac{\partial \tilde{n}}{\partial y}$$

$$+\nu_i \frac{\partial}{\partial y}\left(L V_L \frac{\partial \tilde{n}}{\partial y} + \frac{c}{B} n \frac{\partial \varphi}{\partial y}\right)$$

$$-\frac{\partial}{\partial y}\left\{\left(\frac{c}{B}\frac{\partial \varphi}{\partial y} + \frac{L V_L}{n}\frac{\partial \tilde{n}}{\partial y}\right)\left(\frac{\partial}{\partial t} + V_0 \frac{\partial}{\partial y} - \mu \frac{\partial^2}{\partial y^2}\right) n\right\}\Bigg] = 0 \qquad ..(4.27)$$

In this equation the third term describes the generation of density fluctuation because of $\tilde{E}$ x B effect along the perpendicular density gradient similar to electrons; the fourth term represents the density fluctuation arising because of the d.c. gravitational drift of ions and the last term gives the contribution due to the effects of finite ion inertia, ion collisions and ion viscosity. Combining eq. (4.24) for electrons and eq. (4.27) for ions, we obtain the partial differential equation for the R-T modes.

$$\left(\frac{\partial}{\partial t} + V_0 \frac{\partial}{\partial y} - \mu \frac{\partial^2}{\partial y^2}\right)\left(n \frac{\partial^2 \tilde{n}}{\partial t \partial y} + n_0 V_L \frac{\partial^2 \tilde{n}}{\partial y^2} + \frac{\partial \tilde{n}}{\partial t}\frac{\partial \tilde{n}}{\partial y}\right)$$

$$+\nu_i \frac{\partial}{\partial y}\left(n \frac{\partial \tilde{n}}{\partial t} + n_0 V_L \frac{\partial \tilde{n}}{\partial y}\right) - \frac{\partial}{\partial y}\left[\left(\frac{\partial \tilde{n}}{\partial t}\right)^2 - \frac{n_0 V_L V_0}{n}\left(\frac{\partial \tilde{n}}{\partial y}\right)^2\right.$$

$$\left. + V_0\left(1 + \frac{V_L}{V_0}\frac{n_0}{n}\right)\frac{\partial \tilde{n}}{\partial y}\frac{\partial \tilde{n}}{\partial t} - \mu\left(\frac{\partial \tilde{n}}{\partial t} + \frac{n_0 V_L}{n}\frac{\partial \tilde{n}}{\partial y}\right)\frac{\partial^2 \tilde{n}}{\partial y^2}\right]$$

$$= n_0 \frac{g}{L}\frac{\partial \tilde{n}}{\partial y} + \left(\frac{n_0}{L}\right)^2 V_L \frac{\partial}{\partial t}\left(\log \frac{n}{n_0} - \frac{\tilde{n}}{n}\right) \qquad ..(4.28)$$

Our interest is to look for nonlinear stationary R-T modes by which we mean those waves in which all the oscillating quantities are functions of only s-ut, where s is the

periodic stationary modes, it is therefore, convenient to introduce the phase of the oscillation as

$$\xi = ky - \omega t \qquad ..(4.29)$$

Dividing the equation (4.28) by n_o^2, we thus obtain an ordinary differential equation in the parameter ξ as

$$-(u-V_o)k^2\frac{d}{d\xi}\left[-u(1+\eta)\frac{d^2\eta}{d\xi^2}+V_L\frac{d^2\eta}{d\xi^2}-u\left(\frac{d\eta}{d\xi}\right)^2\right]-\nu_i k\frac{d}{d\xi}\left(u(1+\eta)\frac{d\eta}{d\xi}-V_L\frac{d\eta}{d\xi}\right)+\mu k^3\frac{d}{d\xi}\left[\left(u-\frac{V_L}{1+\eta}\right)\frac{d\eta}{d\xi}\frac{d^2\eta}{d\xi^2}+\frac{d}{d\xi}\left\{u(1+\eta)\frac{d^2\eta}{d\xi^2}-V_L\frac{d^2\eta}{d\xi^2}+u\left(\frac{d\eta}{d\xi}\right)^2\right\}\right]-k^2\frac{d}{d\xi}\left[\left\{u^2-uV_o\left(1+\frac{V_L}{V_o}\frac{1}{1+\eta}\right)+\frac{V_LV_o}{1+\eta}\right\}\left(\frac{d\eta}{d\xi}\right)^2\right]$$

$$=\frac{g}{L}\frac{d\eta}{d\xi}-\frac{uV_L}{L^2}\frac{d}{d\xi}\left(\log(1+\eta)-\frac{\eta}{1+\eta}\right) \qquad ..(4.30)$$

where $\eta = \tilde{n}/n_o$ and $u = \omega/k$. Equation (4.30) after one integration and some algebra yields

$$(u-V_o)\left\{u(1+\eta)-V_L\right\}\frac{d^2\eta}{d\xi^2}+\frac{(u-V_o)V_L}{1+\eta}\left(\frac{d\eta}{d\xi}\right)^2-\frac{\nu_i}{k}\left(u(1+\eta)-V_L\right)\frac{d\eta}{d\xi}-\frac{g}{k^2L}\eta+\mu k\left[\left\{u(1+\eta)-V_L\right\}\frac{d^3\eta}{d\xi^3}+\left(4u-\frac{V_L}{1+\eta}\right)\frac{d\eta}{d\xi}\frac{d^2\eta}{d\xi^2}\right]+\frac{uV_L}{k^2L^2}\left(\log(1+\eta)-\frac{\eta}{1+\eta}\right)=0 \qquad ..(4.31)$$

We will ignore henceforth μ for simplicity and in fact, the ion viscosity term is found to be much smaller in magnitude compared to other terms below the equatorial F-region maximum (see sec. 4.22). Assuming $u < V_o$ in consistent with the inferences drawn in sec. 4.3 and dividing equation (4.31) by $(u - V_o)(u(1 + \eta) - V_L)$, we obtain the nonlinear wave equation for R-T modes as

$$\frac{d^2\eta}{d\xi^2} + \frac{V_L}{(u-V_L)(1+m_o\eta)} \cdot \frac{1}{1+\eta}\left(\frac{d\eta}{d\xi}\right)^2 + \frac{\nu_i}{k(V_o-u)} \cdot \frac{d\eta}{d\xi} +$$

$$+ \frac{g}{k^2L} \frac{1}{(u-V_L)(V_o-u)(1+m_o\eta)} \eta - \frac{u V_L}{k^2L^2(V_o-u)(u-V_L)} \cdot \frac{\log(1+\eta) - \eta/(1+\eta)}{1+m_o\eta} = 0 \quad ..(4.32)$$

where $m_o = u/(u - V_L)$. One can now readily see that the periodic solutions of the equation (4.32) describing R-T modes in the equatorial F-region are possible only when the fourth term is a positive quantity, i.e., $u - V_L > 0$. We further assume that $\eta_L << 1$ (in agreement with observations, Dyson et al., 1974) and then making the expansion of $\log(1+\eta_L)$ in the last term of equation (4.32), the wave equation may be written as

$$\frac{d^2\eta}{d\xi^2} + \frac{V_L}{u-V_L} \cdot \frac{1}{(1+m_o\eta)(1+\eta)} \cdot \left(\frac{d\eta}{d\xi}\right)^2 + \frac{\nu_i}{k(V_o-u)} \cdot \frac{d\eta}{d\xi} + b^2 \frac{\eta}{1+m_o\eta}$$

$$- \frac{m b^2 (1 - \eta/3 + \eta^2/6)\, \eta^2}{(1+m_o\eta)(1+\eta)} = 0 \quad ..(4.33)$$

where $m = u\, V_L/2gL$ and

$$b^2 = \frac{g}{k^2 L (V_o - u)(u - V_L)} \quad ..(4.34)$$

The equation (4.33) is the exact nonlinear wave equation describing the low frequency and long wavelength R-T modes generated on the underside of the F-region maximum of the equatorial ionosphere. In deriving this equation, we have considered the contribution due to FLR corrections as well as due to the linear convection part $(\underline{V}_o \cdot \nabla)\tilde{\underline{V}}$ appearing in the ion motion. The contribution arising because of convection part

done in the present theory) because the phase velocity of modes may be comparable to or even smaller than V_0 defined by eq.(4.12), while all the earlier workers have overlooked this correction. In the next section we will solve this equation (4.33) and obtain the physical conditions and the dispersion relation for stationary periodic R-T type modes.

.5 Nonlinear Solutions of the Wave Equation Describing Nonlinear R-T Modes:

In the case of weakly nonlinear modes for which $\eta \ll 1$ (in agreement with the observations, Dyson et al., 1974), the wave equation (4.33) can be written as (neglecting terms of order higher than η^3)

$$\frac{d^2\eta}{d\xi^2} + \frac{V_L}{(u-V_L)} \cdot \frac{1}{(1+m_0\eta)(1+\eta)} \cdot \left(\frac{d\eta}{d\xi}\right)^2 + \frac{\nu_i}{k(V_0-u)} \cdot \frac{d\eta}{d\xi}$$

$$+ \frac{p^2}{1+m_0\eta} \cdot \eta - \frac{m p^2 (1-\eta/3)}{(1+m_0\eta)(1+\eta)} \cdot \eta^2 = 0 \qquad ..(4.35)$$

In the weakly nonlinear regime, the amplitude and the phase of the wave vary slowly with ξ, therefore we use the method of averaging (Bogoliubov and Mitropolsky, 1961) to solve the equation (4.35). Let the solution be such that

$$\eta = A \cos(p\xi + \Phi) \qquad ..(4.36)$$

where the amplitude A and the phase Φ are slowly varying functions of ξ. Following Bogoliubov and Mitropolsky's (1961) method, we obtain the dependence of A and Φ on ξ as

$$\frac{dA}{d\xi} = -\frac{\nu_i A}{2k(V_0-u)} \cdot \frac{1+m_0 A^2/4}{1+m_0 A^2/2} \qquad ..(4.37)$$

$$\frac{d\Phi}{d\xi} = \frac{1}{2} \cdot \frac{Ap}{1+m_0 A^2/2} \left(1 - \frac{3}{8} m_0 \left(1 - \frac{2V_L}{6 m_0 g L}\right) A\right) \qquad ..(4.38)$$

In nonlinear stationary regime, the amplitude gets

saturated and does not vary with ξ , i.e., the saturated amplitude is given by

$$\frac{dA}{d\xi} = -\frac{\nu_1 A}{2k(V_0-u)}\cdot\left(1+\frac{u}{u-V_L}A^2/4\right)\left(1+\frac{u}{u-V_L}\frac{A^2}{2}\right)^{-1} = 0 \quad ..(4.39)$$

Neglecting the terms of order higher than A^3 in the expansion of $(1 + \frac{u}{u-V_L}\frac{A^2}{2})^{-1}$, this condition (4.39) and the wave equation (4.35) are satisfied by the solution with stationary amplitude (A = constant, say A_0) of the type

$$\eta = A_0 \cos(ky - \omega t + \Phi) \quad ..(4.40)$$

if $\quad p^2 = 1$

i.e., $$(V_0 - u)(u - V_L) = g/k^2 L \quad ..(4.41)$$

and if $u = u_0$ at stationary amplitude A_0, then

$$1 - \frac{u_0}{u_0 - V_L}\cdot\frac{A_0^2}{4} = 0 \quad ..(4.42a)$$

i.e., $$u_0 = V_L\left(1-\frac{A_0^2}{4}\right)^{-1} = V_L\left(1+\frac{A_0^2}{4}\right) \quad ..(4.42b)$$

It is to be noted that the equation (4.38) shows that the phase of the waves Φ changes slowly with ξ in nonlinear state whence the amplitude of the waves(satisfying eq.4.42) becomes stationary and can be found out from the following equation

$$\frac{d\Phi_0}{d\xi} = \frac{p}{2}\cdot\left[1-\frac{3}{8}\cdot\frac{u}{u-V_L}\left(1-\frac{(u-V_L)V_L}{6gL}\right)A_0 - \frac{u}{u-V_L}\cdot\frac{A_0^2}{2}\right]A_0 \quad ..(4.43)$$

where Φ_0 corresponds to the value of Φ in nonlinear regime when the amplitude A attains the constant value A_0. This corresponds to a situation in which coherent, small amplitude, stationary, almost sinusoidal oscillations (eq. 4.40) obeying both the dispersion relation (4.41) and the condition (4.42),

exist in the system which supports R-T instability modes.

It can be noticed from eq.(4.43) that the phase of the waves changes slightly with ξ which indicates that the modes develop finally into slightly distorted sinusoidal shapes rather than pure sinusoidal forms. Such slightly distorted (steepened) wavelike structures have been observed and this result may, therefore, explain some observations of nonsinusoidal steepened wavelike structures of the ionization density irregularities in the equatorial spread-F (Dyson et al., 1974; Kelley et al., 1975). Equation (4.42) shows that the nonlinear phase velocity of the waves which depends upon the nonlinear amplitude A_o, becomes greater than the ion diamagnetic drift velocity V_L by a small factor $V_L A_o^2/4$ (a condition $(u > V_L)$ also to be satisfied for generating sinusoidal oscillations) as the amplitude of the mode increases as a result of the linear growth. This implies that the R-T modes will become stationary (stabilized) only when $u - V_L \approx V_L A_o^2/4$, i.e. $u - V_L > 0$, which is the condition for the periodicity also. Therefore, we infer that nonlinear stationary and harmonic R-T modes will exist in the F-region only when $u - V_L > 0$.

The dispersion relation (4.41) can be solved for u as

$$u = \left(\frac{g}{2\Omega_i} + V_L\right) \pm \left[\left(\frac{g}{2\Omega_i} + V_L\right)^2 - \frac{g}{k^2 L}\right]^{1/2} \qquad ..(4.44a)$$

$$\omega = \left(\frac{kg}{2\Omega_i} + kV_L\right) \pm \left[k^2\left(\frac{g}{2\Omega_i} + V_L\right)^2 - \frac{g}{L}\right]^{1/2} \qquad ..(4.44b)$$

For the modes with wavelengths greater than ρ_i, the second

term for the spread-F region. Hence, the upper (+) sign only will result into the unstable R-T modes which we are interested in, whereas the lower (-) sign will give rise to the damping. Thus the phase velocity $u_o (= \omega_r/k$, ω_r being the real part of eq.4.44) and the growth rate ω_i (the imaginary part of eq.4.44) of the unstable mode are given as

$$u_o = g/2\Omega_i + V_L \qquad ..(4.45)$$

$$\omega_i = \left[g/L - k^2 \left(g/2\Omega_i + V_L \right)^2 \right]^{1/2} \qquad ..(4.46)$$

We have just seen that as the amplitude gets enhanced linearly, the phase velocity u also increases according to eq.(4.42). When u becomes equal to u_o given by eq.(4.45), then a final stationary state is reached in which the amplitude does not increase further and attains a constant value A_o. The Rayleigh-Taylor instability driven modes in nonlinear stationary state must, therefore, satisfy both the expressions (4.42) and (4.44a) or (4.45) for the phase velocity, simultaneously.

It can be immediately noticed from eq.(4.46) that at shorter wavelength the Rayleigh-Taylor mode has a finite cut off which arises because of the combined contributions from the ion convection appearing through V_o (mainly because of the drift due to gravity) and the FLR corrections. We find also that the inclusion of the convective part $(\underline{V}o.\ \nabla)\tilde{\underline{V}}$ in ion inertia adds to the stabilization of the R-T modes in the F-region which is so far known to occur because of the FLR

wavelengths and independent of the background density gradient. The minimum unstable wavelength λ_{min} of the R-T mode to be excited is, therefore, given(by putting $\omega_i = 0$) as

$$\lambda_{min} = \left\{ 2\pi/(g/L)^{1/2} \right\} \left(g/2\Omega_i + V_L \right) \qquad ..(4.47)$$

The FLR stabilization effects depend upon the parameter L through V_L, i.e., the background density gradient ∇n_o (eq.4.46). At shorter wavelengths these effects also are significantly larger and would correspond to a higher λ_{min} if the background density gradient is sharper and vice-versa. It is important to note here that the marginal unstable minimum wavelength is larger by a quantity $\pi\sqrt{gL}/\Omega_i$ than that obtained by earlier workers. This difference may probably be attributed to the convective part of ion inertia which is shown to have significant contribution towards the stabilization and the real phase velocity of the modes. The lower limit of the wavelengths of R-T modes that can be excited by this theory is found to be higher, nevertheless the estimate of the wavelengths seems to agree fairly well with the observed range ($\lesssim$70m-20km) of scale sizes (Calvert and Schmidt, 1964; McClure, 1973; Dyson et al., 1974; Kelley,et al., 1975).

In nonlinear case we, therefore, find that the FLR corrections increase the phase velocity and reduce the linear growth rate further, making the modes more stable. The important role played by the FLR corrections in stabilization of the modes can thus be seen as follows. If we neglect V_L,

equation (4.35) describing R-T modes then reduces to

$$\frac{d\eta}{d\xi^2} + \frac{\nu_i}{k(V_g - u)} \frac{d\eta}{d\xi} + p_o^2 \frac{\eta}{1+\eta} = 0 \qquad ..(4.48)$$

where $V_g = g/\Omega_i$ and $p_o^2 = g/(k^2 L(V_g - u)u)$. For the harmonic solutions of the type $\eta = A \cos(ky - \omega t + \Phi)$, the equation (4.48) yields the dispersion relation

$$p_o^2 = 1, \text{ i.e., } u(V_g - u) = g/k^2 L \qquad ..(4.49)$$

which is essentially the same dispersion relation (4.16) as obtained and discussed earlier in the linear case. It is quite obvious from equation (4.35) that most of the nonlinear effects appear because of FLR corrections. The magnitudes of the different nonlinear terms appearing in wave equation (4.35) can be estimated for the parameters appropriate to the regions of interest. It is found that the leading nonlinear term is one which is proportional to $(dn/d\xi)^2$ and depends upon the ion diamagnetic drift V_L. This clearly shows that the FLR corrections seem to be responsible for giving rise to nonlinearities which, in turn, lead to the stabilization of the R-T modes through the nonlinear interactions of the waves.

Physically, the mechanism of the stabilization of growing R-T modes which evolve into coherent, almost sinusoidal travelling stationary waves in nonlinear regime, may be understood as follows. The fundamental unstable long wavelength R-T modes are first generated, and grow in amplitude. After the growth period when the amplitude becomes sufficiently large,

to the increase in the real frequency of the fundamental modes and their higher harmonics as well as the reduction in the growth rate of these modes due to FLR effects. When the phase velocities of these modes become greater than the ion diamagnetic drift V_L in the nonlinear regime, the nonlinear interactions lead to the dissipation of energy associated with the fundamentals to higher harmonics which grow to finite amplitudes because of nonlinear coupling. As a result, the growing Rayleigh-Taylor modes evolve into coherent, almost harmonic, travelling stationary solutions. However, if the nonlinear coupling is sufficiently strong, it destroys the phase-coherence (as is obvious by eq.4.43 and arguments followed) which the growing modes display when the amplitude is small. This, in turn, distorts the model structure (sinusoidal) as energy is interchanged between fundamentals and harmonics. The overall tendency is for energy to cascade continuously downward from long (hence more unstable) wavelengths (fundamental) into short (less unstable or even marginally stable) wavelength dissipation regime.

4.6 Discussions of Results and Their Relevance to the Observations of Spread-F Irregularities:

We have shown that the Rayleigh-Taylor instability driven modes can evolve into coherent, nonlinear, travelling, stationary waves having a constant phase velocity, through the nonlinear interactions with the higher harmonics generated by the fundamental unstable R-T modes. It is, particularly,

neglects the FLR corrections, the dispersion of the waves is such that the modes have real constant phase velocity and there is a reduction in the linear growth rate. These results appear to modify the results of the linear theory developed by all earlier workers that the modes have almost zero real frequency and that they are purely growing modes. This discrepancy arises because of the fact that they did not take into account the convection part $(\underline{V}_o \cdot \nabla)\underline{\tilde{V}}$ which is important to include for the waves having phase velocities comparable to or less than V_o.

We find from the linear theory predictions that the collisional long wavelength R-T mode (growth rate$=g/L\nu_i$) is altitude dependent and is smaller at lower altitudes where ν_i is higher. The observations (Farley et al., 1970; Kelley and Carlson, 1974) show that the unstable region occurs on the sharp plasma density gradient ($L \simeq 20$ km) at the bottom of the F-layer between 300 - 400 km region. It was also observed that the equilibrium F-layer preceding spread-F onset, has shifted downwards to a stable configuration for an increased ν_i, in agreement with a theoretical decreased growth rate of R-T mode (stable system). This downward drift is unusual near spread-F onset (contrary to the well known observation of spread-F associated with the postsunset rise of the F-layer), but demonstrates that it is not usual drift itself which is responsible for spread-F instability. Thus, we concur with Farley et al. (1970) that it is altitude threshold which is

plasma density and sharper gradient at night. The altitude threshold of spread-F can thus be qualitatively explained by the fact that the ion neutral collisions ν_i decrease the R-T mode growth rate, while lower plasma density and sharper density gradient favour it.

The weak nonlinearity ($\eta << 1$) considered in the system is found to enhance the phase velocity of the modes and to be responsible for the further reduction in the growth rate, both effects arising due to FLR corrections, and thereby making the phase velocity u greater than V_L. For such situation when u becomes greater than V_L, it is shown that the coherent, almost sinusoidal, travelling stationary solutions of the equations describing the R-T instability driven modes are found to exist in the equatorial F-region. It is clearly demonstrated that the neglect of FLR corrections (i.e., neglecting V_L) leads to the disappearance of important leading nonlinearities proportional to $(d\eta/d\xi)^2$ in the system and in turn, to the increased growth of the perturbations. This clearly indicates that an important role is played by the FLR corrections and that they appear to be the main cause of creating nonlinearities in the system which are responsible for the stabilization of the R-T modes, through the nonlinear interactions of the waves. Physically, therefore the mechanism of the stabilization of these modes seems to be nonlinear coupling between the growing fundamental modes and their higher harmonics, which gives rise to the dissipation of energy associated with the fundamentals (long wavelengths) to higher harmonics (short wavelengths) which grow to finite

It appears quite certain now that the Rayleigh-Taylor instability must be the main source of the irregularities of large scale sizes ($> \rho_i$) in the equatorial spread-F (Balsley et al., 1972; Hudson et al., 1973; Chaturvedi and Kaw, 1975a,b; Hudson and Kennel, 1975a,c). As is obvious from eq. (4.44), this mechanism has a cut-off at shorter wavelengths because of finite Larmor stabilization effects and the drift of ions due to gravity, and seems to be operative only below the F_{peak} where the background density increases upwards, i.e., $L > 0$ vertically upwards and is antiparallel to the gravity $\underline{g}$.

The recent satellite observations (Calvert and Schmidt, 1964; McClure, 1973; Dyson et al., 1974) do indeed provide the experimental evidence for such nonlinear travelling wave-like structures of the equatorial spread-F irregularities over a large number of scale sizes ($\lesssim$ 70 meter to 20 km). They have reported observations below and above (upto an altitude of 1000 km) F_{peak} respectively at equatorial and high latitudes. Our discussions here are confined mainly to the equatorial observations. A rough numerical estimate made for parameters appropriate to the equatorial F-region of wavelengths (eq.4.47) excited suggests that the range of scale sizes observed (Calvert and Schmidt, 1964; McClure 1973; Dyson et al., 1974) corresponds to the instability mechanism discussed in this chapter. This measured range of scale sizes is less than 70 m to 20 km. Dyson et al. (1974) also observe that at times the power spectra of equatorial spread-F

a limited scale size band and that the wave form of the irregularities is composed of a fundamental plus harmonics. This limited scale size range turns out to be the fundamental and its first harmonics. The scale size of the fundamental is around 7.5 km which seems to agree well with the typical wavelength of a R-T mode strongly excited in the equatorial F-region. It is presumably at this scale size that the dissipation of energy associated with the fundamental (long wavelengh mode) to the higher harmonics (short wavelengths) occurs due to nonlinear interactions between the fundamentals and the harmonics when the amplitude of the fundamentals become sufficiently large after the growth period and thereby generating smaller and smaller irregularities with scale sizes down to 70 m or even less at some finite amplitude satisfying the relation (4.42). Since the smaller wavelength modes have, as has been discussed, finite cut-off in growth, they are stabilized at some finite amplitude. But it is predicted by the present theory that such nonlinear structures must travel with the phase velocity u_o given by (4.42) on which there are, to our knowledge, no observations so far. However, the R-T mode generally grows faster (large growth rate) at longer wavelength on the bottom side when the stabilization effects are not significant (spread-F spectrum peaks at longer wavelength, as observed), so we have given careful consideration to the stabilization effects which are important at shorter wavelengths.

observations also (Kelley and Carlson, 1974 ; Kelley et al., 1975). These authors reported that the spread-F irregularities following the onset, developed into coherent, steepened structures with asymmetric slopes on the two sides in a time period of approximately 30 minutes. The result obtained here that in the nonlinear state, the modes evolve finally into coherent, travelling distorted sinusoidal shapes with a symmetrical steepened profile rather than pure sinusoidal forms (as is evident from eq.4.43), appears to show a good agreement with these observations (Kelley and Carlson, 1974; Kelley et al., 1975). The typical growth time of approximately 10^3 secs. for R-T modes estimated in the F-region, also seems to agree well with the observed growth time of the irregularities. The observed asymmetry may be due to the presence of a westward-pointing background density gradient which is believed to exist in the medium at evening hours and even at later times (Farley et al., 1970). The superposition of this gradient on the symmetric steepened wave profile would then lead to an observed asymmetric steepening on the eastward edge (Chaturvedi and Kaw, 1975b). A precise agreement between the theoretical and experimental values and results is not to be expected because all the parameters vary in the ionosphere from day to day in a complex way, and the exact values of these parameters on the day of the irregularity observations are uncertain.

The stabilization at shorter wavelengths depends upon the background density gradient (appearing through V_+) and

and vice versa. It is well known that the gradient varies from day to day and the spread-F seems to be stronger on the day when the gradient is weaker, i.e., the ion diamagnetic drift V_L is smaller (Kelley and Carlson, 1974). This supports the Rayleigh-Taylor instability model for longer wavelengths spread-F irregularities at equatorial latitudes and describes that the FLR limit on $\lambda_{y_{min}}$ obtained by Hudson and Kennel (1974b, 1975a,c) for R-T instability is not unique and can vary from day to day. Also the fact that such nonlinear structures are observed only in the equatorial spread-F region is of considerable significance, since it ties up well with the view that R-T instability is the main source of irregularities at these latitudes, whereas a different mechanism (Perkins, 1973) seems to operate for the generation of the spread-F irregularities at higher latitudes (Calvert and Schmidt, 1964; McClure, 1973; Dyson et al., 1974).

So far we have not mentioned anything about the irregularities observations at high altitude regions ($\sim$700 - 1000 kms) by topside sounders at wavelengths of $\sim$ 100 m to 20 km (Calvert and Schmidt, 1964; Dyson et al., 1974) and by radar backscatter at the wavelengths of $\sim$ 3 m (Farley et al., 1970; Woodman, 1973). It is certainly quite obvious now that the mechanism responsible for the production of both these larger and smaller scale irregularities is not the Rayleigh-Taylor instability because the background density gradient ∇n_o and the acceleration due to gravity $\underline{g}$ point in the same direction at higher altitudes above $F_{\ldots}$. However, the linear theory

of the drift mode instability proposed by Hudson and Kennel (1974a,b, 1975b,c) which can grow independent of the sign of $\underline{g} \cdot \nabla n_o$, in contrast to the R-T mode which requires that $\underline{g}$ be antiparallel to ∇n_o, could account for the occurrence of spread-F on the topside of the F-layer. Though Chaturvedi and Kaw (1975a) have suggested the two-step process (proposed by them for the equatorial regions below F_{peak}) as the amplitude limiting mechanism for these irregularities, the instability mechanism responsible for their generation and accounting for their observed features satisfactorily at such altitudes and high latitude F-regions remains unidentified yet. This, therefore, remains as on open question to be attempted at further.

4.7 Conclusions:

On the basis of the method of averaging by Bogoliubov and Mitropolsky (1961), we have demonstrated the existence of coherent, nonlinear, almost sinusoidal, travelling stationary solutions to the equations describing the long wavelength ($> \rho_i$) Rayleigh-Taylor modes in the equatorial spread-F region. We have also shown that the linearly unstable R-T modes can finally evolve into coherent, travelling, stationary distorted wave structures, with a symmetric steepened profile in the nonlinear state when the phase velocity of the waves become greater than the ion diamagnetic drift. The FRL corrections are found to give rise to main nonlinear term in the wave equation for R-T modes and thus seem to be mainly responsible

for the stabilization of the R-T modes, through the nonlinear interactions of the waves as discussed. In addition to the FLR corrections, the convective part(which includes the zero order ion gravitational drift along with the ion diamagnetic drift) of the ion inertia is also found to have an important contribution in giving rise to the modes a larger real phase velocity such that u becomes greater than V_L and in diminishing the growth rates of the modes further. This, therefore, helps significantly in the stabilization of the R-T modes.

The results of earlier theories in the linear limit are also modified here by the present analysis in the sense that now the R-T modes are not purely growing modes, but these travel with a constant phase velocity and have reduced growth rates, the reduction being more (large cut-off) for shorter wavelength R-T modes.

Here a reasonably good agreement is established between our theoretical results and many of the recent observations of the equatorial spread-F region irregularities (Dyson et al., 1974; Kelley and Carlson, 1974; Kelley et al., 1975), and some of their observed features are satisfactorily explained by our theory.

CHAPTER V

SUMMARY, LIMITATIONS AND SCOPE FOR FURTHER WORK

Experimental studies of the ionospheric E-and F-regions, employing a wide variety of ground based and space techniques, have revealed the presence of an assortment of field-aligned ionization density irregularities under various circumstances and over a wide range of wavelengths. These observations have shown several types of irregularities of various scale sizes, shapes and spectral characteristics which mostly depend upon the ionospheric plasma parameters, such as electron density, electric fields, plasma streaming velocity, etc.. As has already been discussed, most of the irregularities are generated in the equatorial ionospheric regions where the electric and magnetic fields and the electron density gradients are most suited for the creation of these irregularities. The equatorial ionospheric phenomena, such as E_{sq}, spread-F, etc., are familiar manifestations of these irregularities.

The prime goal of the investigation presented in this thesis has been to carry out a detailed theoretical study relevant to these irregularities. The ionospheric plasma can become unstable against self excitation of a large variety of waves and natural modes of oscillations. Because of highly complex nature of ionospheric plasma, it is most likely that there are many different plasma instability mechanisms which may be operating at a time individually or simultaneously so as to give rise to the occurrence of the irregularities

5.1 A Synoptic View (Summary) of the Work Done:

An attempt has been made in the preceding chapters to present the theoretical treatment, in both linear and non-linear regimes, of three kinds of low frequency ($\omega \lesssim \Omega_i$) electrostatic plasma instabilities, namely (1) the cross-field ($\underline{E} \times \underline{B}$) or gradient-drift instability; (2) two-stream instability; and (3) gravitation-induced Rayleigh-Taylor instability. The first two (discussed in Chapter II and III respectively) are capable of explaining successfully the generation and most of the features of irregularities observed during both day and night time in E-region, particularly in irregularity-type sporadic E-layers, while the third one (developed in Chapter IV) appears to be responsible for the formation of equatorial spread-F irregularities with satisfactory explanation of some of their important basic features.

In order to establish the definiteness of our analytical results which are obtained with some approximations, we have solved numerically the exact set of nonlinear basic equations describing the irregularities in equatorial E-region plasma. It is found that there is a reasonably good agreement between the numerical and analytical results. In order to apply the theoretical results to the observations, the dispersion relations obtained for different physical situations have also been solved numerically by considering the appropriate values of ionospheric parameters observed or estimated. A fairly good agreement between the computed and experimental results

In conclusion , we now summarize,in the following,the principal results of the investigations made in the thesis.

In Chapter II, the author has treated the two-dimensional linear theory of resistive type gradient drift (or $\underline{E} \times \underline{B}$) instability in an inhomogeneous weakly ionized plasma immersed in crossed electric and magnetic fields. It has been shown that this instability appears to be responsible for the creation of the field-aligned irregularities in equatorial E-region, if the magnitudes and the directions of applied electric fields are appropriately considered and the background electron density and temperature profiles are properly chosen.

The mechanism seems to be quite capable of generating larger as well as smaller scale sizes irregularities (types II, L, Mc and Sc) propagating both in horizontal and vertical directions in 90-130 km region and of accounting for many of their features satisfactorily. The scale sizes range from a few meters ($\geq$ 14 m) to a few kms ($<$ 3 km), which agree fairly well with the observed values of scale sizes of type L, Mc and Sc irregularities. The theory discussed is likely to be more competent in the regions of electrojet where there are pronounced valleys (93-105 kms and 115-130 kms) in the nighttime electron density profile observed. The intense growing irregularities are predicted to develop in the region of 93-120 kms because the growth rates in the upper valley (115-130 kms) are smaller than those in the lower valley

The theory of the gradient drift instability predicts that the vertical polarization electric field plays an important role in the formation of smaller scale and fastest growing (intense) irregularities. The characteristics of the irregularities are such that the growth rate is proportional to the square of the ratio K_h of Hall to Pedersen conductivities which is maximum around 100 km (the region of intense electrojet currents), whereas the scale sizes show the contrary behaviour, varying inversely with $K_o^{1/2}$. Thus we conclude that smaller scale and fastest growing irregularities are formed within the strongest electrojet region, inferring that strong echoes (type II) are observed from the region centred around 100 km. The theory predicts further that in the vertical direction, the irregularities are seen to be produced only for the case when the amplitudes of perturbations are assumed to be function of altitude, as they are found observationally. We, therefore, suggest that the altitude dependence of perturbation amplitude must be taken into account for any realistic and complete theory.

We have shown that the characteristics of the irregularities depend upon both the electric field and the ambient electron density in such a way that the growth rate is enhanced with these parameters, while scale sizes are diminished. It has been, qualitatively, inferred that the type II echo power is proportional to square of the type II irregularity drift velocity. The E-region irregularities are found to have layered structured with many thin layers in the

regions of their occurrence. It has been suggested that a marked splitting (bifurcation) of the echoing region (corresponding to type II irregularities observed by Balsley, 1969b) in the electrojet may be caused, at least at night, by the irregularities produced in two different height regions.

In the third chapter, the author has discussed a special class of coherent weakly nonlinear type I modes excited by the resistive type two-stream instability in the equatorial electrojet. Having retained the quasilinear modification of the vertical polarization electric field (quasilinear effects, modifying the electron streaming drift that drives the instability) and ion viscous effects giving rise to the dispersion of the waves, it has been demonstrated that in the weakly nonlinear limit, almost harmonic nonlinear stationary waves might exist in the electrojet. These waves might be responsible for the coherent short wavelength ($\gtrsim 1$ m) type I irregularities giving rise to type I echoes. The theory predicts that the conditions under which such waves exist are those for marginally stable state, implying that the type I irregularities are the result of marginally stable nonlinear state, in agreement with the inferences drawn from the observations.

An important result was obtained that the linear dispersion relation and the linear threshold electron streaming drift, obtained within fluid limit, for marginally unstable type I modes are found to be wavelength dependent, which

1967; Balsley and Farley, 1971). It is also remarkable to note that the results predicted by the present theory within fluid approximations, were found similar to those predicted by marginal stability calculations from the kinetic theory (Farley, 1963a,b).

The dispersion relation derived for nonlinear type I modes suggests that the nonlinear phase velocity depends upon both the wavelength and the amplitude of the wave. We have shown that within fluid theory, the marginally stable nonlinear modes have the threshold phase velocity which is constant and slightly greater (by a factor depending upon the nonlinear amplitude which remains constant in nonlinear state) than the ion acoustic velocity (an observational fact), in contrast to the linear result that it is equal to ion acoustic velocity. The nonlinear threshold electron drift velocity was also found to differ slightly from its linear value by the nonlinear amplitude dependent term, the effect arising through ponderomotive force on ions.

The amplitude dependence of wave frequency and the wave dispersion are such that the coherent nonlinear stationary type I modes discussed, were found to be stable against slowly varying, large amplitude, long wavelength, modulational perturbations. It has been shown, further, that such a modulational perturbation to the nonlinear harmonic stationary modes has a tendency to develop, adiabatically, into modulational envelope solitons. This result led us to speculate

the form of fairly discrete wave-packets with soliton shaped envelopes, in support of the observational evidence from VHF radar backscatter measurements. Unfortunately, there are not many observations of such nonlinear characteristics, but many become possible in future. It would be possible to test this idea more convincingly if more observations are available.

It has become quite apparent now that the two instability mechanisms that we have discussed in Chapter II and III, could be responsible for the formation of the observed intense growing irregularities with smaller wavelengths in the electrojet region around 100 km, the region of strong electrojet currents. These irregularities can, therefore, give rise to the enhanced radio-wave scattering in the equatorial region, commonly called the equatorial sporadic E-layer, E_{sq}. Matsushita's (1951) suggestion that the occurrence of E_{sq} is predominent in the equatorial electrojet, is also well supported by the present models of these two instability mechanisms.

During the period when the magnetic field suddenly decreases below the nighttime mean value, the E_{sq} was observed to disappear. These observations are, however, made during the daytime when the density profile shows only the positive gradients. It was suggested (Rastogi et al., 1971) that the disappearance of E_{sq} is due to the temporary reversal of equatorial electrojet currents. This is supported by the present theory of the gradient drift instability, because if sudden decrease in the magnetic field can be attributed to the sudden reversal of electrojet currents which may be

caused due to the temporary reversal of the electric fields satisfying now the nighttime conditions, then the criteria of the occurrence of the instability that the product of electric field and the density gradient must be positive, will not be valid because a density gradient of opposite direction does not exist in the daytime and hence no irregularities could be formed.

In Chapter IV, we carried out the nonlinear analysis of the one-dimensional gravitation-induced Rayleigh-Taylor instability driven modes which might be produced in the nighttime equatorial spread-F region. Having included in the instability theory the linear convection part $(\underline{V}.\ \nabla)\tilde{\underline{V}}$ of ion inertia, ion neutral collisions and finite Larmor radius effects, we have demonstrated the existence of coherent, nonlinear, almost sinusoidal, travelling stationary solutions to the equations describing the long wavelength ($> \rho_i$) R-T modes in the equatorial F-region. We have shown, further, that linearly unstable R-T modes can finally evolve into coherent, travelling stationary distorted (rather than pure sinusoidal) wave structures through the nonlinear interactions arising mainly due to FLR effects, with a symmetric steepened profile in the nonlinear state when the phase velocity of the waves becomes greater than ion diamagnetic drift.

In the linear limit, our analysis was found to greatly modify the results of the linear theory developed by earlier workers in the sense that now R-T modes are not purely growing

have reduced growth rates, the reduction being more (large cut-off) for shorter wavelength R-T modes. This contrasts the earlier result that the modes have almost zero real frequency and are purely growing in nature.

The FLR corrections were found to result into the main leading nonlinearities in the wave equation describing R-T modes, which implies that the FLR corrections are mainly responsible for the nonlinear interactions leading to the stabilization of the modes. In addition to the FLR corrections, the convective part of ion inertia was also seen to provide a significant contribution to give rise to the modes a larger real phase velocity and to diminish the growth rate further.

The instability mechanisms which are discussed above, seem to be in reasonably good agreement with the HF and VHF backscatter radar and in-situ rocket and satellite observations of the equatorial ionization density irregularities.

Although more accurate theoretical and numerical calculations of the instabilities are needed before deviation of observations from theoretical results can be attributed to errors in the theory, the results of present analyses could have some general plasma physics significance. Also our results could be of some importance to have a proper selection of MUF and angles of transmission of radio waves in HF communication via equatorial ionosphere.

5.2 Limitations and Scope for Further Studies:

Although we have discussed some aspects of various

dispersion characteristics, a rigourous treatment of the instabilities as the mechanisms for their formation, is required so as to have a closer and better agreement between the threoretical results and the observations.

We have confined ourselves, for simplicity, to the discussions of the generation of either purely horizontally or vertically propagating irregularities. It is highly desirable to include both the propagation directions together (oblique angle propagation) in a complete theory so as to account simultaneously for both the horizontally and vertically observed structures of the irregularities. This is a problem for further study.

While we have neglected the explicit dependence of ionospheric parameters (e.g., electric fields, temperatures, collision frequencies, conductivities, etc.) with altitude, our results suggest that the irregularity formation is largely dependent upon the variation with altitude of these parameters. Hence, the variation of these parameters with altitude, i.e., their vertical gradients which might play the significant role, must be explicitely included while making an extension of the theories developed here.

We have assumed the ions and electrons to be isothermal. The temperature of electrons in ionosphere, particularly in F-region where their collision frequencies are negligibly small, is influenced by thermal conductions, and under certain circumstances, by Joule heating and the thermoelectric effects.

electric field in the ionosphere. Moreover, at shorter wavelengths of the order of a few meters the electrons become less isothermal and more adiabatic violating the assumption of electrons being isothermal, whereas the ions remain isothermal because of higher collisions. An extension to the studies made here can, therefore, be carried out by taking into account the thermal gradients affecting the current flow conductivity and the adiabatic pressure law for electrons instead of isothermal limit.

Whether or not the density gradients can be neglected in the nonlinear theory of two-stream instability is less clear, even then these must be included, at least for the conditions of nighttime electrojet where they are much steeper and highly variable.

Since the modes having wave number parallel to magnetic field are of different physical nature(for example, these effectively change the electron collision frequency and are reactive or resistive-inductive rather than purely resistive modes), the present analyses of gradient drift as well as two-stream instability need to be reexamined by considering finite $k_{||}$. (These finite $k_{||}$ modes may not be important in F-regions, since they are highly damped due to large diffusion). This along with a stabilization mechanism different from the one stabilizing the purely resistive $k_{||} = 0$ modes is the problem for future work.

For VHF radar observations (using the signal frequency

at perpendicular wavelengths as short as 3 m or less, the validity of fluid equations is questionable. However, for such irregularities the use of fluid theory in the electrojet may be permissible, but in the F-region it is not valid since k^{-1} is comparable with or less than the ion Larmor radius or ion mean-free path. Moreover, high frequency (short wavelength) instabilities tend to have a more 'fine-grained' nature and can thus lead to the more detailed properties of the modes than low frequency instabilities. Hence, a kinetic theory which we believe, will be more appropriate to be dealt with for explaining the fundamental nature of such short wavelength irregularities, more clearly.

We have neglected the ion viscous effects in the investigation of R-T modes in the spread-F region. Ion viscosity only affects transport when there exists a spatial gradient. For $kL >> 1$, the important spatial gradient is the perpendicular wavelength. In a plasma where $\nu_{ii} >> \nu_{in}$, such as the nighttime equatorial F-region, ion viscosity will dominate ion neutral collisions in determining the Rayleigh-Taylor growth rate at short perpendicular wavelengths. Inclusion of ion viscous effects in the present theory would be a further extension of the study made here.

In the present investigation of the R-T instability, no attempt has been made to explain high latitude spread-F. The lower latitude boundary of in-situ density and potential fluctuation measurements, which extends into the midlatitude

that the convection electric fields which are present in that region, may be important. Inclusion of a zero order electric field along with the gravity as the destabilizing forces for the R-T modes should be a straightforward extension of our investigation of the Rayleigh-Taylor instability theory.

BIBLIOGRAPHY

Aarons, J., J.P. Mullen and H.E. Whitney, Paper presented at First Lloyd Berkner Symposium, AGU, Univ. of Texas, Dallas, Texas, 1973.

Aono, Y., K. Hirao and S. Miyazaki, J. Radio Res. Lab., Japan, 9, 407-419, 1962.

Baker, W.G., Phil. Trans. Roy. Soc., A246, 295-305, 1953.

Baker, W.G. and D.F. Martyn, Phil. Trans. Roy. Soc., A246, 281-294, 1953.

Balsley, B.B., J. Geophys. Res., 70, 3175-3182, 1965.

Balsley, B.B., Ann. Geophys., 22, 460-462, 1966.

Balsley, B.B., Ph.D. Thesis, Inst. Environ. Res. Tech. Memorandum ITSA 89, Boulder, Colorado, 1967.

Balsley, B.B., J. Geophys. Res., 74, 1213-1217, 1969a.

Balsley, B.B., J. Geophys. Res., 74, 2333-2347, 1969b.

Balsley, B.B., J. Geophys. Res., 75, 4369-4371, 1970.

Balsley, B.B., J. Atmos. Terr. Phys., 35, 1035-1044, 1973a; Also A review paper presented at First Lloyd Berkner Symposium, AGU, Univ. of Texas, Dallas, Texas, 1973a.

Balsley, B.B., Private Communication, 1973b.

Balsley, B.B., and D.T. Farley, J. Geophys. Res., 76, 8341-8351, 1971.

Balsley, B.B. and D.T. Farley, J. Geophys. Res., 78, 7174-7179, 1973.

Balsley, B.B. and G. Haerendel, Proc. Fourth Int. Symposium on Equatorial Aeronomy, Ed. by E. Oni, Dept. of Phys., Univ. of Ibadan, Ibadan, p.705-707, 1972.

Balsley, B.B. and R.F. Woodman, J. Atmos. Terr. Phys., 31, 865-867, 1969.

Balsley, B.B. and R.F. Woodman, World Data Centre A, Upper Atmos. Geophys., Rept. UAG-17, 1971.

Balsley, B.B., G. Haerendel and R.A. Greenwald, J. Geophys.Res., 77, 5625, 1972.

Berkner, L.V. and H.W. Wells, Terr. Magn. Atmos. Elec., 39, 215-230, 1934.

Berkner, L.V. and H.W. Wells, Terr. Magn. Atmos. Elec., 42, 73-76, 1937.

Bogoliubov, N.N. and Y.A. Mitropolsky, 'Assymptotic methods in theory of nonlinear oscillations (English Translation)', Hindustan Publishing Corpn., Delhi - 6 (India), p.51-54, 1961.

Bohm, D. and E.P. Gross, Phys. Rev., 75, 1851, 1949; Ibid, 75, 1864, 1949.

Booker, H.G. and H.W. Wells, Terr. Magn. Atmos. Elec., 43, 249-256, 1938.

Bourdeau, R.E., Space Res., 5, 77-90, 1964.

Bowles, K.L. and R. Cohen, N.B.S. Equatorial Region VHF Scatter Research Prog. for the I.G.Y., QST, 41, 11-15, 1957.

Bowles, K.L. and R. Cohen, 'Ionospheric Sporadic-E', Ed. by E.K. Smith and S. Matsushita, Pergamon, London, 51-57, 1962.

Bowles, K.L., R. Cohen, R. Ochs and B.B. Balsley, J. Geophys. Res., 65, 1853-1855, 1960.

Bowles, K.L., B.B. Balsley and R. Cohen, J. Geophys. Res., 68, 2488-2501, 1963.

Brace, L.H., N.W. Spencer and G.R. Carignan, J. Geophys. Res., 68, 5397-5412, 1963.

Brace, L.H., N.W. Spencer and A. Dalgarno, Planet. Space Sci., 13, 647-660, 1965.

Buneman, O., Phys. Rev., 115, 503, 1959.

Buneman, O., Phys. Rev. Lett., 10, 285-287, 1963.

Calvert, W. and R. Cohen, J. Geophys. Res., 66, 3125-3140, 1961.

Calvert, W. and C.W. Schmidt, J. Geophys. Res., 69, 1839-1850, 1964.

Chandrasekhar, S., 'Hydrodynamics and Hydromagnetic Stability', Oxford University Press, London, 1961.

Chaturvedi, P.K. and P.K. Kaw, Preprint, 1975a; to appear in J. Geophys. Res., 1976.

Chaturvedi, P.K. and P.K. Kaw, Geophys. Res. Lett., 2, 381 and 499, 1975b.

Chapman, S., Arch. Meterol. Geophys. Bioklimatol., Ser.A4, 368-390, 1951.

Chapman, S., Nuovo Cimento, Ser.10 (Suppl.4), 1385-1412, 1956.

Chapman, S. and J. Bartels, 'Geomagnetism', Oxford University Press, 1940.

Chen, F.F. and A.W. Cooper, Phys. Rev. Lett., 9, 333-335, 1962.

Chimonas, G., J. Geophys. Res., 74, 4091, 1959.

CIRA, Cospar International Reference Atmosphere, North Holland Pub. Co., Amsterdam, 1969.

Clemesha, B.R., J. Atmos. Terr. Phys., 26, 91-112, 1964.

Clemesha, B.R. and R.W.H. Wright, 'Spread-F and Its Effects Upon Radiowave Propagation and Communication', Ed. by

Clemmov, P.C. and M.A. Johnson, J. Atmos. Terr., 16, 21, 1959.

Cohen, R., J. Geophys. Res., 78, 2222-2231, 1973.

Cohen, R. and K.L. Bowles, J. Geophys. Res., 66, 1081-1106, 1961.

Cohen, R. and K.L. Bowles, J. Res. NBS, 67D, 459-480, 1963a.

Cohen, R. and K.L. Bowles, J. Geophys. Res., 68, 2503-2525, 1963b.

Cohen, R. and K.L. Bowles, J. Geophys. Res., 72, 885-893, 1967.

Cohen, R., K.L. Bowles and W. Calvert, J. Geophys. Res., 67, 965, 1962.

Cole, K.D., A review paper presented at First Lloyd Berkner Symposium, AGU, Univ. of Texas, Dallas, Texas, 1973.

Cowling, T.G., Monthly Notices, Roy. Astron. Soc., 93, 90-98, 1932.

Cowling, T.G. and R. Borger, Nature, 162, 142-143, 1948.

Cunnold, D.M., J. Geophys. Res., 74, 5709-5720, 1969.

D'Angelo, N., 'Low-Frequency Waves and Irregularities in the Ionosphere', D. Reidel Pub. Co., Dordrecht-Holland, 1969.

D'Angelo, N., H.L. Pecseli and P.I. Petersen, J. Geophys. Res., 79, 4747-4751, 1974.

D'Angelo, N., H.L. Pecseli and P.I. Petersen, J. Geophys. Res., 80, 1854-1855, 1975.

Dalgarno, A., M.B. McElroy and R.J. Moffet, Planet. Space Sci., 11, 463-489, 1963.

Davis, J.R., J. Geophys. Res., 76, 5292, 1971.

Davis, J.R. and E.L. Althouse, Proc. Upper Atmos. Currents and Electric Fields Symposium, Ed. by W.H. Campbell and S. Matsushita, ESSA Tech. Memorandum, ERLTM-ESL-12, Earth Sciences Laboratories, Boulder, Colorado, pp.262-277, 1970.

Davis, J.R. and J.C. Moore, J. Geophys. Res., 75, 171-182, 1970.

Dougherty, J.P. and D.T. Farley, J. Geophys. Res., 72, 895-901, 1967.

Dungey, J.W., J. Atmos. Terr. Phys., 9, 304-310, 1956.

Dupree, T.H., Phys. Fluids, 9, 1773, 1966.

Dupree, T.H., Phys. Fluids, 10, 1049, 1967.

Dupree, T.H., Phys. Fluids, 11, 2680, 1968.

Dyson, P.L., J. Geophys. Res., 76, 4689, 1971.

Dyson, P.L., paper presented at First Lloyd Berkner Symposium, AGU, Univ. of Texas, Dallas, Texas, 1973.

Dyson, P.L., J.P. McClure and W.B. Hanson, J. Geophys. Res., 79, 1497-1502, 1974.

Farley, D.T., Phys. Rev. Lett., 10, 279-282, 1963a.

Farley, D.T., J. Geophys. Res., 68, 6083-6097, 1963b.

Farley, D.T., 'Methods of Experimental Physics', 9B,- Plasma Physics, Ed. by R.H. Lovberg and H.R. Griem, Academic, New York, 1971.

Farley, D.T., Revs. Geophys. Space Sci., 12, 285-289, 1974.

Farley, D.T. and B.B. Balsley, Trans. Amer. Geophys. Union, 53, 457, 1972.

Farley, D.T. and B.B. Balsley, J. Geophys. Res., 78, 227-239, 1973.

Farley, D.T. and B.G. Fejer, J. Geophys. Res., 80, 3087-3090, 1975.

Farley, D.T., B.B. Balsley, R.F. Woodman and J.P. McClure, J. Geophys. Res., 75, 7199-7216, 1970.

Fejer, J.A., Proc. Roy. Soc., A220, 455, 1953.

Fejer, J.A., J. Geophys. Res., 64, 2217-2218, 1959.

Fejer, B.G., B.B. Balsley, D.T. Farley and R.F. Woodman, Paper presented at First Lloyd Berkner Symposium, AGU, Univ. of Texas, Dallas, Texas, 1973.

Fejer, B.G., D.T. Farley, B.B. Balsley and R.F. Woodman, J. Geophys. Res., 80, 1307-1312, 1975a.

Fejer, B.G., D.T. Farley, B.B. Balsley and R.F. Woodman, J. Geophys. Res., 80, 1313-1324, 1975b.

Geisler, J.E. and S.A. Bowhill, J. Atmos. Terr. Phys., 27, 457-474, 1965.

Greenwald, R.A., J. Geophys. Res., 79, 4807-4810, 1974.

Greenwald, R.A., W.L. Eckland and B.B. Balsley, J. Geophys. Res., 80, 131-139, 1975.

Gouin, P. and P.N. Mayaud, Ann. Geophys., 23, 41, 1967.

Gupta, S.P., Ph.D. Thesis, Physical Research Laboratory, Ahmedabad - 9, India, 1970.

Haerendel, G., R. Lust, F. Melzner, H. Neuss, E. Rieger, R. Raghavarao, M.S. Narayanan, P.D. Bhavsar, MPI-Report, 1970; Presented at the International Symposium on 'Solar Terr. Physics', Leningrad, MPI/PAE-Extraterr.44/70, 1970.

Hanson, W.B., Space Res., 3, 282-302, 1962.

Hanson, W.B. and F.S. Johnson, Mem. Soc. Roy. Sci. Liege, 4, 390-424, 1961.

Hanson, W.B. and S. Sanatani, J. Geophys. Res., 78, 1167, 1973.

Hanson, W.B., D.L. Sterling and R.F. Woodman, J. Geophys. Res., 77, 5530, 1972.

Hanson, W.B., J.P. McClure and D.L. Sterling, J. Geophys. Res., 78, 2353-2356, 1973.

Herman, J.R. Rev. Geophys., 4, 255-299, 1966.

Hines, C.O., I. Paghis, T.R. Hartz and J.A. Fejer, 'Physics of the Earth's Upper Atmosphere', Prentice-Hall, Inc. (USA), 1965.

Hoh, F.C., Phys. Fluids, 6, 1184-1191, 1963.

Holtet, J.A., N.C. Maynard, and J.P. Heppner, Trans. Amer. Union (AGU), 56, 418,1975.

Hooper, E.B., Jr., Phys. Fluids, 13, 96, 1970.

Hooper, E.B., Jr. and S.M. Girvin, J. Appl. Phys., 42, 4832, 1971.

Hooper, E.B., and J.C.G. Walker, J. Atmos, Terr. Phys., 33, 1441-1455, 1971.

Huang, C., J. Geophys. Res. 75, 4833-4841, 1970.

Hudson, M.K., Ph.D. Thesis, Dept. of Phys., Univ. of California, Los Angeles, California, 1974a; UCLA-Rept. PPG-179, 1974a.

Hudson, M.K. and C.F. Kennel, UCLA-Rept. PPG-201, 1974b.

Hudson, M.K. and C.F. Kennel, J. Plasma Phys., 14, 121, 1975a.

Hudson, M.K. and C.F. Kennel, J. Plasma Phys., 14, 135, 1975b.

Hudson, M.K. and C.F. Kennel, J. Geophys. Res., 80, 4581, 1975c.

Jain, R.K. and A.C. Das, Indian J. Pure and Appl. Phys., 9, 618-625, 1971.

John, P.I. and Y.C. Saxena, Ind. J. Radio Space Phys., 4, 267, 1975a.

John, P.I. and Y.C. Saxena, Geophys. Res. Lett., 2, 251, 1975b.

John, P.I. and Y.C. Saxena, Preprint, 1976; To appear in Phys. Lett., 1976a.

John, P.I. and Y.C. Saxena, Paper presented at Symp. on Solar Planet. Phys. held at Physical Research Laboratory, Ahmedabad - 380009, India, 1976b.

Johnson, M.H., Proc. Conf. Ionosph. Phys., Penn. State, paper J., 1950.

Johnson, M.H. and E.O. Hulburt, Phys. Rev., 79, 802, 1950.

Kadomtsev, B.B. and A.V. Nedospasov, Plasma Phys., C1, 230, 1960.

Kamenetskaya, G. Kh., Geomagn. Aeron., 11, 71, 1971.

Karpman, V.I. and E.M. Krushkal, (Eng. Trans.) Sov. Phys., JETP (USA), 28, 277-281, 1969.

Kato, S., Radio Science, 7, 417-423, 1972.

Kato, S. and Y. Hirata, Rep. Ionosp. Space Res., Japan, 21, 85,1967.

Kaw, P.K., J. Geophys. Res., 77, 1323-1326, 1972.

Kelleher, R.F. and J. Rottger, Proc. Fourth Int. Symp. on Equatorial Aeron., Ed. by E. Oni, Dept. of Phys.,Univ. of Ibadan, Ibadan, 1972; Also published in J. Atmos. Terr. Phys., 35, 1207-1211, 1973.

Kelleher, R.F. and N.J. Skinner, Ann. Geophys., 27, 195-200, 1971.

Kelley, M.C., A review paper presented at First Lloyd Berkner Symp., AGU, Univ. of Texas, Dallas, Texas, 1973.

Kelley, M.C., and C.W. Carlson, Trans. Amer. Geophys. Union, 55, 381, 1974.

Kelley, M.C. and F.S. Mozer, J. Geophys. Res., 77, 4183, 1972.

Kelley, M.C., G. Haerendel, B. Hausler, H. Kappler, J. Rieger, A. Valenzuela,C. Carlson, R. Torbert, B. Balsley and W. Ecklund, Univ. of California Preprint, In Press, J. Geophys. Res., 1975.

Kent, G.S., Rev. Geophys. Space Phys., 8, 229-288, 1970.

Kent, G.S. and R.W.H. Wright, J. Atmos. Terr. Phys., 30, 657, 1968.

Kim, J.J. and Simon, A., Phys. Fluids, 12, 895-900, 1969.

King, G.A.M., J. Atmos. Terr. Phys., 32, 209-231, 1970.

Knox, F.B., J. Atmos. Terr. Phys., 26, 239-249, 1964.

Knox, F.B., J. Atmos. Terr. Phys., 36, 747-764, 1972.

Koster, J.R., J. Geophys. Res., 68, 2579-2590, 1968.

Krall, N.A. and P.C. Liewer, Phys. Rev., A4, 2094, 1971.

Krishnamurthy, B.V. and B.R. Rao, J. Atmos. Terr. Phys., 26, 783-784, 1964.

Krishnamurthy, B.V. and K. Sengupta, Planet. Space Sci., 20, 371, 1972.

Langmuir, I., Phys. Rev., 26, 585, 1925.

Lee, K. and C.F. Kennel, J. Geophys. Res., 78, 4619, 1973a.

Lee, K. and C.F. Kennel, Planet. Space Sci., 21, 1339, 1973b.

Lee, K., C.F. Kennel and F.V. Coroniti, J. Geophys. Res., 79, 249-266, 1974.

Lee, K., C.F. Kennel and J.M. Kindel, Radio Sci., 6, 209-214, 1971.

Lighthill, M.J., Proc. Roy. Soc., London, A299, 28-53, 1967.

Linson, L.M., Proc. Upper. Atmos. Currents and Electric Fields Symp., Ed. by W.H. Campbell and S. Matsushita, ESSA Tech. Memorandum, ERLTM-ESL-12, Earth Sciences Laboratories,

Linson, L.M. and J.B. Workman, J. Geophys. Res., 75,3211, 1970.

Maeda, H., J. Geomag. Geoelectricity, 9, 75-85, 1955.

Maeda, K., T. Tsuda, and H. Maeda, Rep. Ionosp. Space Res. Japan, 17, 147-159, 1963a.

Maeda, K., T. Tsuda and H. Maeda, Phys. Rev. Lett., 11, 406-407, 1963b.

Martyn, D.F., Prof. Roy. Soc. (London), A190, 273, 1947.

Martyn, D.F., Proc. Inst. Radio. Engrs. (NY), 47, 147, 1959; also Nature, 183, 1382, 1959.

Matsushita, S., J. Geomag. Geoelec., 3, 44-46, 1951.

Matsushita, S., J. Atmos. Terr. Phys., 10, 163, 1957.

Matsushita, S., Radio Science, 4, 771, 1969.

McBride, J.B., E. Ott, J.B. Boris, and J.H. Orens, Phys. Fluids, 15, 2367, 1972.

McClure, J.P., Paper presented at First Lloyd Berkner Symp., AGU, Univ. of Texas, Dallas, Texas, 1973.

McClure, J.P. and W.B. Hanson, J. Geophys. Res., 78, 7431, 1973.

McClure, J.P. and R.F. Woodman, J. Geophys. Res., 77, 5617-5621, 1972.

McDonald, B.E., T.P. Coeffy, S.L. Ossakow and R.N. Sudan, J. Geophys. Res., 79, 2551-2554, 1974.

McDonald, B.E., T.P. Coeffy, S.L. Ossakow and R.N. Sudan, Radio Sci., 10, 247-254, 1975.

Morse, D.L., Phys. Fluids, 8, 1339, 1965.

Nagy, A.F., L.H. Brace, G.R. Carignan and M. Kennel, J.Geophys. Res., 68, 6401-6412, 1963.

Nicolet, M., J. Atmos.Terr. Phys., 3, 200-211, 1953.

Nielson, D.L., and M. Crochet, A Review: Proc. Fourth Inter.Symp. on Equatorial Aeron., Ed. by E. Oni, Dept. of Phys., Univ. of Ibadan, Ibadan, pp.477-532, 1972.

Ogawa, T, Ph.D Thesis, Dept. of Electronics, Kyoto Univ., Kyoto, Japan, 1972.

Ogawa, T. and T. Sato, Planet. Space Sci., 19, 1393, 1971.

Oksman, J., Ann. Geophys., 30, 285-290, 1974.

Ossakow, S.L., Rept. NRL (USA), pp.1-19, 1974.

Ossakow, S.L., K. Papadopoulos, J. Orens and T. Coeffy, J. Geophys. Res., 80, 141-148, 1975.

Ott, E. and D.T. Farley, J. Geophys. Res., 79, 2469-2472, 1974.

Perkins, F., J. Geophys. Res., 78, 218, 1973.

Pitteway, M. and R. Cohen, J. Geophys. Res., 66, 3141-3156, 1961.

Prakash, S., A review paper presented at First Lloyd Berkner

Prakas, S. and B.H. Subbaraya, Rev. Scient. Instrum., 38, 1132, 1967.

Prakash, S., B.H. Subbaraya and S.P. Gupta, J. Atmos. Terr. Phys., 30, 1193, 1968.

Prakash, S., S.P. Gupta and B.H. Subbaraya, Radio Sci., 4, 791-796, 1969.

Prakash, S., S.P. Gupta and B.H. Subbaraya, Planet. Space Sci., 18, 1307-1318, 1970.

Prakash, S., S.P. Gupta and B.H. Subbaraya, Space Res., 11, 1139-1145, 1971a.

Prakash, S., S.P. Gupta and B.H. Subbaraya, Nature (Phys. Sci.), 230, 170-171, 1971b.

Prakash, S., B.H. Subbaraya and S.P. Gupta, Indian J. Radio Space Phys., 1, 72-80, 1972.

Prakash, S., S.P. Gupta, B.H. Subbaraya, H.S.S. Sinha and C.L. Jain, A review paper presented at First Lloyd Berkner Symposium, AGU, Univ. of Texas, Dallas, Texas, 1973.

Raghavarao, R. B.G. Anandarao and J.N. Desai, Paper presented at Symposium on Solar Planet. Phys. held at Physical Research Laboratory, Ahmedabad 380009, India, 1976.

Rao, P.B. and W.H. Russel, Radio Sci., 6, 221-232, 1971.

Rastogi, R.G., A review presented at First Llyod Berkner Symposium, AGU, Univ. of Texas, Dallas, Texas, 1973.

Rastogi, R.G., H. Chandra and S.C. Chakravarty, Proc. Indian Acad. Sci., 74A, 62, 1971.

Rayleigh, B.J.W.S., Phil. Magn., 32, 529, 1916.

Reid, G.C., J. Geophys. Res., 73, 1627-1640, 1968.

Reid, G.C., Planet Space Sci., 18, 1105, 1970.

Richmond, A.D., J. Atmos. Terr. Phys., 35, 1105-1118, 1973.

Rieger, E., 'Low-Frequency Waves and Irregularities in the Ionosphere', Ed. by N. D'Angleo, D. Reidel Pub. Co., Dordrecht-Holland, pp.218, 1969.

Rieger, E., Gerlands Beitr. Geophysk. Leipzig, 80, 243, 1971.

Rishbeth, H. and O.K. Garriott, 'Introduction to Ionospheric Physics', Academic Press (Inter. Geophys. Ser. 14), N.Y., 1969.

Rishbeth, H., Planet. Space Sci., 19, 357, 1971.

Rogister, A., J. Geophys. Res., 76, 7754-7760, 1971.

Rogister, A., J. Geophys. Res., 77, 2975-2981, 1972.

Rogister, A. and N. D'Angelo, J. Geophys., Res., 75, 3879-3887, 1970.

Rogister, A. and N. D'Angelo, J. Geophys. Res., 77, 6298-6299, 1972.

Rogister, A. and E. Jamin, J. Geophys. Res., 80, 1820-1828, 1975.

Rognlien, T.D. and J. Weinstock, J. Geophys. Res., 78, 6808-6810, 1973.

Rognlien, T.D. and J.Weinstock, J. Geophys. Res., 79, 4733-4746, 1974a.

Rognlien, T.D. and J. Weinstock, Bull. Amer. Phys. Soc., 19, 895, 1974b.

Rognlien, T.D. and J. Weinstock, Radio Sci., 10, 239-246, 1975.

Rosenbluth, M.N. and C.L. Longmire, Ann. Phys., 1, 120, 1957.

Rosenbluth, M.N., N. Krall and N. Rostokev, Nucl. Fus. Suppl., 1, 143, 1962.

Rottger, J., Paper presented at Fourth Inter. Symp. on Equatorial Aeron., Ed. by E. Oni, University of Ibadan, Ibadan, pp.552-564, 1972.

Rudakov, L.I. and R.Z. Sagdeev, Sov. Phys. - Doklady (USA), 6, 415-417, 1961.

Sagalyn, R.C., M. Smiddy and Y.N. Bhargwa, Space Res., 5, 189-206, 1964.

Sastry, T.S.G., Space Res., 10, 778, 1970.

Sato, T., J. Geophys. Res., 73, 2941, 1968.

Sato, T., Phys. Fluids, 14, 2426-2435, 1971.

Sato, T., Phys. Rev. Lett., 28, 732-734, 1972.

Sato, T., J. Geophys. Res., 78, 2232-2243, 1973.

Sato, T., Phys. Fluids, 17, 621-627, 1974.

Sato, T. and T. Ogawa, Phys. Fluids, 17, 628-633, 1974.

Sato, T. and T. Tsuda, Phys. Fluids, 10, 1262-1268, 1967.

Sato, T. and T. Tsuda, Radio Sci., 7, 429-432, 1972.

Sato, T., T. Tsuda and K.T. Maeda, Radio Sci., 3, 529-534, 1968.

Sato, T., T. Ogawa and Y. Matsuda, Phys. Fluids, 15, 1926-1930, 1972.

Saxena, Y.C. and P.I. John, Geophys. Res. Lett., 2, 492-495, 1975.

Schmidt, M.J. and S.P. Gary, J. Geophys. Res., 78, 8261, 1973.

Simon, A., Phys. Fluids, 6, 382-388, 1963.

Simon, A., J. Geophys. Res., 75, 6287-6294, 1970.

Singer, S.F., E. Maple and W.A. Bowen, J. Geophys. Res., 56,

Skadron, G. and J. Weinstock, J. Geophys. Res., 74, 5113, 1969.

Skinner, N.J. and R.F. Kelheher, Ann. Geophys., 27, 181-194, 1971.

Sleeper, A.M. and A. Simon, Phys. Fluids, 13, 2257-2765, 1970.

Sleeper, A.M. and J. Weinstock, Phys. Fluids, 15, 1507-1514, 1972.

Sleeper, A.M. and J. Weinstock, Paper presented at First Lloyd Berkner Symp., AGU, Univ. of Texas, Dallas, Texas, 1973.

Southworth, M.P., J. Geophys. Res., 65, 601, 1960.

Spencer, M., Proc. Phys. Soc., B68, Pt.8, 493-503, 1955.

Spencer, N.W., L.H. Brace, G.R. Carignan, D.R. Taesch and H. Niewmann, J. Geophys. Res., 70, 2665-2698, 1965.

Subbaraya, B.H., P. Murlikrishna, T.S.G. Sastry and S. Prakash, Planet Space Sci., 20, 47-52, 1972.

Subbaraya, B.H., S. Prakash, S.P. Gupta and H.S.S. Sinha, Preprint, 1973; Planet Space Sci., 22, 180-181, 1974.

Sudan, R.N., J. Akinrimisi and D.T. Farley, J. Geophys. Res., 78, 240-248, 1973.

Sugiura, M. and J.C. Cain, J. Geophys. Res., 71, 1869-1877, 1966.

Sugiura, M. and D.J. Poros, J. Geophys. Res., 74, 4025-4035, 1969.

Tserkovnikov, Yu. A., J. Exp. Terr. Phys., 5, 58, 1957.

Tsuda, T., A review paper presented at First Lloyd Berkner Symposium, AGU, Univ. of Texas, Dallas, Texas, 1973.

Tsuda, T. and T. Sato, Phys. Fluids, 11, 677-678, 1968.

Tsuda, T., T. Sato and K. Maeda, Radio Sci., 1, 212-225, 1966.

Tsuda, T., T. Sato and S. Matsushita, J. Geophys. Res., 74, 2923-2932, 1969.

Untiedt, J., J. Geophys. Res., 72, 5799-5810, 1970.

Unwin, R.S. and W.J. Baggaley, Ann. Geophys., 28, 111-127, 1972.

Unwin, R.S. and F.B. Knox, J. Atmos. Terr. Phys., 30, 25-46, 1968.

Unwin, R.S. and F.B. Knox, Proc. Upper Atmos. Currents and Electric Fields Symp., ESSA Tech. Mem., ERLTM-12, Earth Sci. Lab., Boulder, Colorado, pp.172-180, 1970.

Unwin, R.S. and F.B. Knox, Radio Sci., 6, 1061-1077, 1971.

Valenzuela, A., H. Kappler, G. Haerendel, H. Foppl, H. Hippmann and R.F. Woodman, Paper presented at First Lloyd Berkner Symp., AGU, Univ. of Texas, Dallas, Texas, 1973.

Waldteufel, P., Ann. Geophys., 21, 579, 1965.

Weinstock, J., Phys. Fluids, 11, 1977-1981, 1968.

Weinstock, J., Phys. Fluids, 12, 1045, 1969.

Weinstock, J., Phys. Fluids, 13, 2308, 1970.

Weinstock, J., J. Geophys. Res., 78, 772, 1973.

Weinstock, J. and T.D. Rognlien, Radio Sci., 10, 231-237, 1975.

Weinstock, J. and A.M. Sleeper, J. Geophys. Res., 77, 3621-3624, 1972.

Weinstock, J. and A.M. Sleeper, Paper presented at First Lloyd Berkner Symp., AGU, Univ. of Texas, Dallas, Texas, 1973.

Weinstock, J. and R.H. Williams, Phys. Fluids, 14, 1472-1480, 1971.

Wernik, A.W. and C.H. Liu, Paper presented at First Lloyd Berkner Symp., AGU, Univ. of Texas, Dallas, Texas, 1973.

Wescott, E.M., J.P. Heppner, J.D. Slolarik, T. Hallinan, T.N. Davis, G.J. Romick, Trans. Amer. Geophys. Union, 50, 281, 1969.

Whitehead, J.D., J. Atmos. Terr. Phys., 29,1285-1297, 1967.

Whitehead, J.D., J. Atmos. Terr. Phys., 30, 1563-1570, 1968.

Whitehead, J.D., Rev. Geophys. Space Phys., 8, 65-144, 1970a.

Whitehead, J.D., J. Atmos. Terr. Phys., 32, 1283-1304, 1970b.

Whitehead, J.D., Geophys. Res., 76, 3116-3126, 1971.

Williams, R.H. and J. Weinstock, J. Geophys. Res., 75, 7217, 1970

Woodman, R.F., J. Geophys. Res., 75, 6249-6259, 1970.

Woodman, R.F., A review paper presented at First Lloyd Berkner Symp., AGU, Univ. of Texas, Dallas, Texas, 1973.

Woodman, R.F. and J. Pomalaza, Paper presented at Fourth Inter. Conf. on Equatorial Aeron., Ed. by E. Oni, Deptt. of Phys., Univ. of Ibadan, Ibadan, pp.696-698, 1972.

Yerukhimov, L.M., Geomag. Aeron. (Eng. Trans.), 2, 527-574, 1962.

Zmuda, A.J., J. Geophys. Res., 65, 2247-2253, 1960.